

Mechanisms Underlying Longevity Regulation and Extension by Genetic, Dietary and
Pharmacological Interventions in the Yeast *Saccharomyces Cerevisiae*

Pavlo Kyryakov

A Thesis

in

The Department

of

Biology

Presented in Partial Fulfillment of the Requirements

For the Degree of Doctor of Philosophy at

Concordia University

Montreal, Quebec, Canada

June 2012

© Pavlo Kyryakov

**CONCORDIA UNIVERSITY
SCHOOL OF GRADUATE STUDIES**

This is to certify that the thesis prepared

By: Pavlo Kyryakov

Entitled: Mechanisms Underlying Longevity Regulation and Extension

by Genetic, Dietary and Pharmacological Interventions in the

Yeast Saccharomyces Cerevisiae

and submitted in partial fulfillment of the requirements for the degree of

complies with the regulations of the University and meets the accepted standards with respect to originality and quality.

Signed by the final examining committee:

<u>Dr. A. Chapman</u>	Chair
<u>Dr. N. Braverman</u>	External Examiner
<u>Dr. A. English</u>	External to Program
<u>Dr. R. Storms</u>	Examiner
<u>Dr. P. Gulick</u>	Examiner
<u>Dr. V. Titorenko</u>	Thesis Supervisor

Approved by

Chair of Department or Graduate Program Director

Dean of Faculty

ABSTRACT

Mechanisms Underlying Longevity Regulation and Extension by Genetic, Dietary and Pharmacological Interventions in the Yeast *Saccharomyces Cerevisiae*

Pavlo Kyryakov, Ph.D.

Concordia University, 2012

This thesis describes studies in which the yeast *Saccharomyces cerevisiae* was used as a model organism for unveiling the mechanisms underlying longevity regulation and extension by genetic, dietary and pharmacological interventions. We found that a diet known as caloric restriction (CR) modulates oxidation-reduction processes and reactive oxygen species (ROS) production in yeast mitochondria, reduces the frequency of mitochondrial DNA (mtDNA) mutations, and alters the abundance and mtDNA-binding activity of mitochondrial nucleoid-associated proteins. Our findings provide evidence that these mitochondrial processes play essential roles in regulating longevity of chronologically active yeast by defining their viability following cell entry into a quiescent state. Based on these findings, we propose a hypothesis that ROS, which are mostly generated as by-products of mitochondrial respiration, play a dual role in regulating longevity of chronologically aging yeast. On the one hand, if yeast mitochondria are unable (due to a dietary regimen) to maintain ROS concentration below a toxic threshold, ROS promote aging by oxidatively damaging certain mitochondrial proteins and mtDNA. On the other hand, if yeast mitochondria can (due to a dietary regimen) maintain ROS concentration at a certain “optimal” level, ROS delay

chronological aging. We propose that this “optimal” level of ROS is insufficient to damage cellular macromolecules but can activate certain signaling networks that extend lifespan by increasing the abundance or activity of stress-protecting and other anti-aging proteins. In addition, studies presented in this thesis imply that mtDNA mutations do not contribute to longevity regulation in yeast grown under non-CR conditions but make important contribution to longevity regulation in yeast placed on a CR diet. The nonreducing disaccharide trehalose has been long considered only as a reserve carbohydrate. However, recent studies in yeast suggested that this osmolyte can protect cells and cellular proteins from oxidative damage elicited by exogenously added ROS. Trehalose has been also shown to affect stability, folding and aggregation of bacterial and firefly proteins heterologously expressed in heat-shocked yeast cells. Our investigation of how a lifespan-extending CR diet alters the metabolic history of chronologically aging yeast suggested that their longevity is programmed by the level of metabolic capacity - including trehalose biosynthesis and degradation - that yeast cells developed prior to entry into quiescence. To investigate whether trehalose homeostasis in chronologically aging yeast may play a role in longevity extension by CR, we examined how single-gene-deletion mutations affecting trehalose biosynthesis and degradation impact 1) the age-related dynamics of changes in trehalose concentration; 2) yeast chronological lifespan under CR conditions; 3) the chronology of oxidative protein damage, intracellular ROS level and protein aggregation; and 4) the timeline of thermal inactivation of a protein in heat-shocked yeast cells and its subsequent reactivation in yeast returned to low temperature. Our data imply that CR extends yeast chronological lifespan by altering a pattern of age-related changes in trehalose concentration.

Acknowledgements

I am grateful to my supervisor, Dr. Vladimir Titorenko, for his guidance and support during the years I spent in his laboratory. I would like to thank the members of my committee, Dr. Patrick Gulick and Dr. Reginald Storms, for their valuable suggestions during the course of my graduate research and studies.

Many thanks to all of my current and former lab-mates Adam Beach, Tatiana Boukh-Viner, Simon Bourque, Michelle Tali Burstein, Subrata Chowdhury, Asya Glebov, Tong Guo, Christopher Gregg, Tatiana Iouk, Olivia Koupaki, Oleh Petriv, Vincent Richard, Bahador Abadi, Daniel Aguirre, Zineea Ahmed, Riad Akkari, Alex Alexandrian, Samira Ansary, Sadaf Anwar, Mohammad Sharif Askari, Zeinab Aziz, Kabongo Balufu, Alpana Bangur, Farhana Banu, Quesny Jean Baptiste, Carmen Bayly, Gabriella Bazdikian, Guillaume Beaudoin, Matthieu Bedard, Moria Belanger, Adrian Buensuceso, Stephanie Bramwell, Aman Brar, Andre Cerracchio, Andrew Chang, Steve Chausse, Eileen Colella, Thaisa Cotton, David Cyr, Julie Cyr, Mark Dass, Rosa De Fenza, Gabrielle Depres, Cassandra Di Tomasso, Ozlem Doygun, Supria Mohan Dubey, Lucia Farisello, Fernando Fiscina, Victor Germanov, Colin Goldfinch, Alejandra Gomez Perez, Alexandra Greco, Sandra Haile, Karen Hung Yeung San, Saeeda Hasan, Ahmed Hossain, Mara Inniss, Chidiebere Michael Iro, Mylène Juneau, Wael Kalaji, Narges Kalantari, Simin Kargari, Mulanda Kayembe, Sukhdeep Kenth, Hyun Young Kim, Petko Komsalov, Shogher Kouyoumjian, Karine Lalonde, Melanie Larche, Clemence Larroche, Jeffrey MacKenzie Lee, Sabrina Lo, Michael A. London, Samira Lorne, Lawrence Ma, Gayane Machkalyan, Lydia Makoroka, Naveed Malik, Cynthia Mancinelli, Patrick Marcoux, Haider Mashhedi, Dale Mc Naught, Hannah Meltzer, Svetlana Milijevic,

Gianni Montanaro, Janine Morcos, Ramandeep Mudhar, Rasesh Nagar, Andrew Naimi, Parisa Namitabar, Florentina Negoita, Phuong Nguyen, Yves Nimbona, Mehdi Noei, Reza Noei, Jordan O’Byrne, Derek O’Flaherty, Aloysius Oluoha, David Papadopoli, Christian Parent-Robitaille, Bhavini Patel, Mital Patel, Sabrina Piccioni, Premala Premanathan, Peter Quashie, Nishant Ramlal, Sonia Rampersad, Savitri Rampersad, Parvin Ranjbar, Joel Richard, Stephanie Russo, Tarek Sabri, Abdelhak Saddiki, Mohammad Hassan Salah, Karen Hung Yeung San, Eric Scazzosi, Sandra Scharaw, Christine Schäfers, Elyse Schmidt, Nadia Sheikh, Arash B. Shokouhi, Cristina Sison, Jerani Sivayogan, Rhoda Sollazzo, Jonathan Solomon, Saamala Subramaniam, Nader Toban, Victor Uscatescu, Andrew Victor, Lisiana Vigliotti, Laura Whelton and Vivianne Wong for their friendship and support.

I am grateful to my family, parents and friends for their invaluable support.

Table of Contents

List of Figures and Tables

List of Abbreviations

1	Introduction	1
1.1	Yeast as a model organism for elucidating the molecular and cellular mechanisms underlying aging of multicellular eukaryotes	1
1.2	Longevity is regulated by a limited number of “master regulator” proteins that in organisms across phyla orchestrate numerous longevity-defining cellular processes in space and time	2
1.3	Effect of dietary regimens on longevity	4
1.4	Mitochondria and reactive oxygen species (ROS) in aging	5
1.5	A modular network regulates longevity of chronologically aging yeast	12
1.6	Five groups of novel anti-aging small molecules greatly extend longevity of chronologically aging yeast	19
1.7	Autophagy and aging	21
1.8	Thesis outline and contributions of colleagues	28
2	Caloric restriction modulates oxidation-reduction processes and ROS production in yeast mitochondria, reduces the frequency of mitochondrial DNA (mtDNA) mutations, and alters the abundance and mtDNA-binding activity of mitochondrial nucleoid-associated proteins	39
2.1	Abstract	39
2.2	Introduction	40
2.3	Materials and Methods	44
2.4	Results	52
2.4.1	In chronologically aging yeast, CR modulates oxidation-reduction processes in mitochondria and alters the age-related dynamics of mitochondrially produced ROS	52
2.4.2	CR influences the frequency of mitochondrial DNA (mtDNA) mutations and modulates the abundance and mtDNA-binding	

	activity of mitochondrial nucleoid-associated proteins	55
2.5	Discussion	58
2.6	Conclusions	60
3	Caloric restriction extends yeast chronological lifespan by altering a pattern of age-related changes in trehalose concentration	62
3.1	Abstract	62
3.2	Introduction	63
3.3	Materials and Methods	64
3.4	Results	69
3.4.1	Lifespan extension by CR requires a specific pattern of age-related changes in trehalose concentration	69
3.4.2	Mutations that increase trehalose concentration prior to entry into quiescence reduce oxidative damage to cellular proteins throughout lifespan, irrespective of their effects on longevity	72
3.4.3	A pattern of age-related changes in trehalose concentration defines the dynamics of protein aggregation throughout lifespan	75
3.4.4	Trehalose concentration in yeast cells defines the sensitivity of an endogenous enzyme to thermal inactivation and the extent of its subsequent reactivation at low temperature	78
3.5	Discussion	81
3.6	Conclusions	88
4	A proper balance between the biosynthesis and degradation of glycogen is obligatory for lifespan extension by CR	90
4.1	Abstract	90
4.2	Introduction	90
4.3	Materials and Methods	91
4.4	Results	96
4.4.1	CR remodels glycogen metabolism	96

4.4.2	The maintenance of a proper balance between the biosynthesis and degradation of glycogen is mandatory for lifespan extension by CR	96
4.5	Discussion	98
4.6	Conclusions	99
5	Caloric restriction (CR) extends yeast chronological lifespan by reducing ethanol concentration	100
5.1	Abstract	100
5.2	Introduction	101
5.3	Materials and Methods	102
5.4	Results	108
5.4.1	Concentration of ethanol is one of the key factors influencing chronological aging	108
5.4.2	Ethanol remodels metabolism of trehalose, glycogen and several lipid species in chronologically aging yeast	110
5.4.3	Ethanol decelerates fatty acid oxidation in peroxisomes of chronologically aging yeast	112
5.5	Discussion	116
5.6	Conclusions	120
6	Lithocholic acid (LCA), a novel anti-aging compound, alters mitochondrial structure and function, reduces cell susceptibility to mitochondria-controlled apoptosis, and increases cell resistance to oxidative and thermal stresses	121
6.1	Abstract	121
6.2	Introduction	122
6.3	Materials and Methods	125
6.4	Results	133
6.4.1	The <i>pex5Δ</i> mutation causes the profound changes in mitochondrial structure and function, cell susceptibility to mitochondria-controlled apoptosis, and resistance to oxidative, thermal and osmotic stresses	133

6.4.2	LCA, a novel anti-aging compound, extends longevity of chronologically aging yeast by altering mitochondrial structure and function, reducing cell susceptibility to mitochondria-controlled apoptosis, and increasing cell resistance to oxidative and thermal stresses	137
6.5	Discussion	140
6.6	Conclusions	141
7	Lithocholic acid (LCA), a novel anti-aging compound, extends longevity of chronologically aging yeast only if added at certain critical periods of their lifespan	143
7.1	Abstract	143
7.2	Introduction	144
7.3	Materials and Methods	155
7.4	Results	161
7.4.1	LCA delays chronological aging of yeast grown under CR or non-CR conditions only if added at certain critical periods of their lifespan	161
7.4.2	The ways through which LCA could differentially influence longevity if added to CR yeast at different periods of their lifespan	166
7.4.3	LCA makes yeast cells resistant to mitochondria-controlled apoptotic death, a pro-aging process, only if added at periods 1, 2 or 3 of their chronological lifespan	168
7.4.4	LCA differentially influences the susceptibility of chronologically aging yeast to palmitoleic acid-induced necrotic cell death, a pro-aging process, if added at different periods of their lifespan	171
7.4.5	In chronologically aging yeast, LCA differentially influences the anti-aging processes of nuclear and mitochondrial genomes maintenance if added at different periods of their lifespan	174
7.4.6	In chronologically aging yeast, LCA differentially influences the anti-aging processes of development of resistance to chronic (long-term) oxidative, thermal and osmotic stresses if added at	

	different periods of their lifespan	179
7.5	Discussion	187
7.6	Conclusions	191
8	Mitophagy is a longevity assurance process that in yeast sustains functional mitochondria and protects cells from apoptotic and necrosis-like “lipoptotic” modes of cell death	193
8.1	Abstract	193
8.2	Introduction	194
8.3	Materials and Methods	195
8.4	Results	200
8.4.1	Mitophagy is a longevity assurance process	200
8.4.2	Mitophagy is required for longevity extension by an anti-aging compound	201
8.4.3	Mitophagy is essential for maintaining functional mitochondria	202
8.4.4	Mitophagy protects yeast cells from mitochondria-controlled apoptotic death caused by exogenous hydrogen peroxide	207
8.4.5	Mitophagy protects yeast from a mode of cell death triggered by exposure to palmitoleic fatty acid	210
8.4.6	Microscopical analyses confirm the essential role of mitophagy in protecting yeast from mitochondria-controlled apoptotic cell death	213
8.4.7	EM analysis implies that exogenous palmitoleic fatty acid triggers a necrosis-like “lipoptotic” cell death and confirms the essential role of mitophagy in protecting yeast from this previously unknown mode of death	215
8.5	Discussion	227
8.6	Conclusions	228
9	Conclusions and suggestions for future work	229
9.1	General conclusions	229
9.1.1	Caloric restriction (CR) modulates oxidation-reduction processes	

	and ROS production in yeast mitochondria, reduces the frequency of mitochondrial DNA (mtDNA) mutations, and alters the abundance and mtDNA-binding activity of mitochondrial nucleoid-associated proteins	229
9.1.2	CR extends yeast chronological lifespan by altering a pattern of age-related changes in trehalose concentration	230
9.1.3	A proper balance between the biosynthesis and degradation of glycogen is obligatory for lifespan extension by CR	231
9.1.4	CR extends yeast chronological lifespan by reducing ethanol concentration	232
9.1.5	LCA, a novel anti-aging compound, alters mitochondrial structure and function, reduces cell susceptibility to mitochondria-controlled apoptosis, and increases cell resistance to oxidative and thermal stresses	233
9.1.6	LCA extends longevity of chronologically aging yeast only if added at certain critical periods of their lifespan	234
9.1.7	Mitophagy is a longevity assurance process that in yeast sustains functional mitochondria and protects cells from apoptotic and necrosis-like “lipoptotic” modes of cell death	235
9.2	Suggestions for future work	236
10	References	241
11	List of my publications and manuscripts in preparation	305

List of Figures and Tables

Figure 1.1	ROS are generated by numerous enzymes in multiple compartments within the cell, mostly (~ 90%) within mitochondria	7
Figure 1.2	Detoxification of ROS occurs in antioxidant scavenger reactions confined to various cellular compartments	8

Figure 1.3	High levels of ROS cause oxidative damage to various cellular constituents	9
Figure 1.4	The sub-lethal concentrations of ROS promote a number of processes related to the protection of the cellular macromolecules from oxidative damage	10
Figure 1.5	A delicate balance between mitochondrial fission and fusion controls the intrinsic pathway of apoptosis and numerous other vital processes in a cell	11
Figure 1.6	A strategy that we developed for elucidating the mechanisms underlying longevity regulation in yeast	15
Figure 1.7	A modular network regulates longevity of chronologically aging yeast	16
Figure 1.8	A model for the spatiotemporal dynamics of the longevity network operating in chronologically aging yeast	18
Figure 1.9	Three fundamentally different modes of autophagy are macroautophagy, microautophagy and chaperone-mediated autophagy	21
Figure 1.10	Macroautophagy is the major mode of autophagy involving the sequestration of organelles and cytosolic proteins by double-membrane vesicles (called autophagosomes) and their delivery to the lysosome/vacuole	22
Figure 1.11	The macroautophagy pathways include non-selective macroautophagy, mitophagy (a cargo-specific, selective pathway), macropexophagy (a cargo-specific, selective pathway), and cytoplasm-to-vacuole [Cvt] (a biosynthetic pathway)	23
Figure 1.12	Macroautophagy plays an essential role in longevity regulation and has been implicated in the incidence of diverse age-related pathologies, including neurodegeneration and cancer	24
Figure 1.13	The molecular machinery of yeast macroautophagy and its regulation by longevity signaling pathways and anti-aging compounds	27
Figure 2.1	CR extends the chronological lifespan of yeast	41
Figure 2.2	CR alters the abundance of a distinct set of proteins in mitochondria	

	of chronologically aging yeast	43
Figure 2.3	CR influences oxidation-reduction processes in mitochondria and modulates the level of mitochondrially produced ROS	54
Figure 2.4	CR modulates the frequency of mtDNA mutations and influences the efficiency of aconitase binding to mtDNA	56
Figure 3.1	The chronological lifespan of yeast grown under CR conditions can be extended by mutations that simultaneously increase trehalose concentration prior to quiescence and reduce trehalose concentration following entry into a quiescent state	70
Figure 3.2	Although mutations that in yeast grown under CR conditions increase trehalose concentration prior to entry into quiescence do not alter ROS levels, they reduce oxidative damage to cellular proteins throughout lifespan	74
Figure 3.3	In yeast grown under CR conditions, a pattern of age-related changes in trehalose concentration defines the dynamics of protein aggregation throughout lifespan	77
Figure 3.4	In yeast grown under CR conditions, trehalose concentration defines the sensitivity of hexokinase, an endogenous enzyme, to thermal inactivation and the extent of its subsequent reactivation at low temperature	80
Figure 3.5	A model for molecular mechanisms underlying the essential role of trehalose in defining yeast longevity by modulating cellular proteostasis throughout lifespan	83
Figure 4.1	In chronologically aging yeast cells, CR alters the abundance of proteins that function in carbohydrate and lipid metabolism, stress protection, ROS detoxification, and essential processes confined to mitochondria	92
Figure 4.2	CR remodels glycogen metabolism	95
Figure 4.3	CR extends lifespan in part by maintaining a proper balance between the biosynthesis and degradation of glycogen	97
Figure 5.1	CR accelerates ethanol catabolism	109

Figure 5.2	Ethanol is one of the key factors regulating longevity	111
Figure 5.3	In chronologically aging yeast, ethanol modulates the dynamics of trehalose, glycogen, neutral lipids, FFA and DAG	113
Figure 5.4	Ethanol suppresses the synthesis of Fox1p, Fox2p and Fox3p, all of which are the core enzymes of peroxisomal fatty acid β -oxidation	115
Figure 5.5	A possible mechanism linking longevity and lipid dynamics in the endoplasmic reticulum (ER), lipid bodies (LBs) and peroxisomes of yeast placed on a calorie-rich diet	117
Figure 6.1	The <i>pex5Δ</i> mutation alters mitochondrial morphology and functions in CR yeast	135
Figure 6.2	The <i>pex5Δ</i> mutation reduces the resistance of CR yeast to stresses, sensitizes them to exogenously induced apoptosis and elevates the frequencies of mutations in their mitochondrial and nuclear DNA	137
Figure 6.3	In reproductively mature WT yeast that entered the non-proliferative stationary phase under CR, LCA modulates mitochondrial morphology and functions, enhances stress resistance, attenuates mitochondria-controlled apoptosis, and increases stability of nuclear and mitochondrial DNA	139
Figure 7.1	A concept for a stepwise development of a longevity network configuration at a series of checkpoints	147
Table 7.1	Known anti-aging compounds, their abilities to increase life span in different organisms (under caloric or dietary restriction [CR or DR, respectively], on a standard diet or fed a high-calorie diet), and the mechanisms of their anti-aging action	149
Figure 7.2	In yeast grown under CR conditions on 0.2% glucose, there are two critical periods when the addition of LCA to growth medium can extend longevity	162
Figure 7.3	In yeast grown under non-CR conditions on 2% glucose, there is only one critical period when the addition of LCA to growth medium can extend longevity	163

Figure 7.4	In yeast grown under CR conditions on 0.2% glucose, there are two critical periods when the addition of LCA to growth medium can extend longevity	164
Figure 7.5	There are several ways through which LCA could differentially influence some anti- and pro-aging processes if it is added at different checkpoints of the chronological lifespan of yeast	167
Figure 7.6	LCA makes yeast cells resistant to mitochondria-controlled apoptotic death, a pro-aging process, only if added at periods 1, 2 or 3 of their chronological lifespan	169
Figure 7.7	LCA differentially influences the susceptibility of chronologically aging yeast to palmitoleic acid-induced necrotic cell death, a pro-aging process, if added at different periods of their lifespan	172
Figure 7.8	LCA differentially influences the maintenance of nDNA integrity, an essential anti-aging process, if added at different periods of yeast lifespan	175
Figure 7.9	LCA differentially influences the maintenance of mtDNA integrity, an essential anti-aging process, if added at different periods of yeast lifespan	177
Figure 7.10	LCA differentially influences the maintenance of mtDNA integrity, an essential anti-aging process, if added at different periods of yeast lifespan	178
Figure 7.11	Effect of LCA added at different periods of yeast chronological lifespan on cell growth under non-stressful conditions	180
Figure 7.12	Effect of LCA added at different periods of chronological lifespan on the ability of yeast to resist chronic oxidative stress	181
Figure 7.13	LCA differentially influences the anti-aging process of development of resistance to chronic oxidative stress if added at different periods of yeast chronological lifespan	182
Figure 7.14	Effect of LCA added at different periods of chronological lifespan on the ability of yeast to resist chronic thermal stress	183
Figure 7.15	LCA differentially influences the anti-aging process of development	

	of resistance to chronic thermal stress if added at different periods of yeast chronological lifespan	184
Figure 7.16	Effect of LCA added at different periods of chronological lifespan on the ability of yeast to resist chronic osmotic stress	185
Figure 7.17	LCA differentially influences the anti-aging process of development of resistance to chronic osmotic stress if added at different periods of yeast chronological lifespan	186
Figure 7.18	A mechanism linking the ability of LCA to delay chronological aging of CR yeast only if added at certain critical periods (checkpoints) of their lifespan to the differential effects of this natural anti-aging compound on certain anti- and pro-aging processes at different checkpoints	189
Figure 8.1	Under CR conditions, the <i>atg32Δ</i> -dependent mutational block of mitophagy substantially shortens both the mean and maximum chronological life spans (CLS) of yeast	201
Figure 8.2	Under CR conditions, the <i>atg32Δ</i> -dependent mutational block of mitophagy abolishes the ability of LCA to increase both the mean and maximum chronological lifespans (CLS) of yeast	203
Figure 8.3	Under CR conditions, the <i>atg32Δ</i> -dependent mutational block of mitophagy leads to accumulation of dysfunctional mitochondria displaying reduced respiration	205
Figure 8.4	Under CR conditions, the <i>atg32Δ</i> -dependent mutational block of mitophagy abolishes the ability of LCA to cause longevity-increasing changes in mitochondrial respiration	207
Figure 8.5	Under CR conditions, the <i>atg32Δ</i> mutation significantly enhances susceptibility of yeast to apoptotic cell death triggered by a brief exposure to exogenous hydrogen peroxide	208
Figure 8.6	Under non-CR conditions, the <i>atg32Δ</i> mutation significantly enhances susceptibility of yeast to apoptotic cell death triggered by a brief exposure to exogenous hydrogen peroxide	209

Figure 8.7	Under CR conditions, the <i>atg32Δ</i> mutation significantly enhances susceptibility of yeast to apoptotic cell death triggered by a brief exposure to exogenous palmitoleic fatty acid	211
Figure 8.8	Under non-CR conditions, the <i>atg32Δ</i> mutation significantly enhances susceptibility of yeast to apoptotic cell death triggered by a brief exposure to exogenous palmitoleic fatty acid	212
Figure 8.9	Under CR conditions, the <i>atg32Δ</i> mutation significantly increases the percentage of cells exhibiting nuclear fragmentation, a characteristic marker of the mitochondria-controlled apoptotic mode of cell death	214
Figure 8.10	Unlike significant portions of briefly exposed to exogenous hydrogen peroxide wild-type (WT) and <i>atg32Δ</i> cells that display nuclear fragmentation, only minor fractions of WT and <i>atg32Δ</i> cells briefly treated with various concentrations of palmitoleic acid exhibit this hallmark event of apoptotic cell death	216
Figure 8.11	Under CR conditions, wild-type and <i>atg32Δ</i> cells briefly treated with various concentrations of palmitoleic acid do not exhibit such hallmark event of necrotic cell death as plasma membrane rupture	217
Figure 8.12	Under CR conditions, wild-type cells briefly treated with various concentrations of palmitoleic acid (PA) exhibit excessive accumulation of lipid droplets, and the <i>atg32Δ</i> mutation significantly reduces the fraction of cells that display this feature following PA treatment	219
Figure 8.13	Under CR conditions, wild-type (WT) cells briefly treated with various concentrations of palmitoleic acid (PA) exhibit an irregularly shaped nucleus, and the <i>atg32Δ</i> mutation significantly reduces the fraction of cells that display this feature following PA treatment	220
Figure 8.14	Under CR conditions, a short-term exposure of wild-type strain to various concentrations of palmitoleic acid (PA) reduces the fraction of cells that contain vacuoles, and the <i>atg32Δ</i> mutation further decreases the portion of such cells following PA treatment	221

- Figure 8.15 Under CR conditions, a short-term exposure of wild-type strain to various concentrations of palmitoleic acid (PA) reduces the fraction of cells that contain the nucleus, and the *atg32Δ* mutation further decreases the portion of such cells following PA treatment 222
- Figure 8.16 Under CR conditions, a short-term exposure of wild-type strain to various concentrations of palmitoleic acid (PA) reduces the fraction of cells that contain the ER, and the *atg32Δ* mutation further decreases the portion of such cells following PA treatment 223
- Figure 8.17 Under CR conditions, a short-term exposure of wild-type strain to various concentrations of palmitoleic acid (PA) reduces the fraction of cells that contain mitochondria, and the *atg32Δ* mutation further decreases the portion of such cells following PA treatment 224
- Figure 8.18 Under CR conditions, a short-term exposure of wild-type strain to various concentrations of palmitoleic acid (PA) increases the fraction of cells lacking all organelles, and the *atg32Δ* mutation further decreases the portion of such cells following PA treatment 225

List of Abbreviations

ACO, aconitase; AMPK/TOR, AMP-activated protein kinase/target of rapamycin; cAMP/PKA, cAMP/protein kinase A; C/EBP α , CCAAT/enhancer-binding protein; CCO, cytochrome c oxidase; CFU, colony forming units; CNS, central nervous system; CL, cardiolipin; CLS, chronological life span; CR, caloric restriction; DAG, diacylglycerols; DHAP, dihydroxyacetone phosphate; DHR, dihydrorhodamine 123; DR, dietary restriction; EE, ergosteryl esters; ESI/MS, electrospray ionization mass spectrometry; ER, endoplasmic reticulum; ERG, ergosterol; FA-CoA, CoA esters of fatty acids; FFA, free fatty acids; FoxO, Forkhead box type O; GC/MS, gas chromatography followed by mass spectrometry; HPLC, high performance liquid chromatography; IGF-1, insulin/insulin-like growth factor 1; LBs, lipid bodies; LCA, lithocholic acid; LOD, limit of detection; LOQ, limit of quantitation; LPA, lysophosphatidic acid; MCA, metabolic control analysis; NB, neuroblastoma; PA, phosphatidic acid; PC, phosphatidylcholine; PE, phosphatidylethanolamine; PI, phosphatidylinositol; PI3K, phosphatidylinositol-3-kinase;

PKC, protein kinase C; PMBC, peripheral blood mononuclear cells; rDNA, ribosomal DNA; ROS, reactive oxygen species; RLS, replicative life span; SD, standard deviation; SDH, succinate dehydrogenase; TAG, triacylglycerols; TLC, thin-layer chromatography; TORC1, TOR complex 1; WAT, white adipose tissue.

1 Introduction

1.1 Yeast as a model organism for elucidating the molecular and cellular mechanisms underlying aging of multicellular eukaryotes

At the organismal level, aging is a complex biological process of the progressive decline in the ability of an organism to resist stress, damage and disease [1 - 7].

Demographically, aging manifests itself as an exponential increase in mortality rate with the age of the cohort [1, 4, 8, 9 - 12]. Because longevity signaling pathways and mechanisms underlying their modulation by genetic, dietary and pharmacological interventions are known to be conserved from yeast to humans, the budding yeast *Saccharomyces cerevisiae* is a valuable model organism in aging research [13 - 20].

Aging of *S. cerevisiae*, a unicellular eukaryote amenable to comprehensive biochemical, genetic, cell biological, chemical biological and system biological analyses, can be measured in two different ways. Replicative aging is defined by the maximum number of daughter cells that a mother yeast cell can produce before senescence; it may serve as a model for studying aging of mitotically active cells in a multicellular eukaryotic organism [15, 21]. In contrast, chronological aging is measured by the length of time a yeast cell remains viable following entry into a non-proliferative state; it has been suggested to model aging of non-dividing (“post-mitotic”) cells in a multicellular eukaryotic organism [13, 15, 22]. A simple clonogenic assay is used to monitor the chronological aging of yeast. This assay measures the percentage of yeast cells that remain viable at different time points following the entry of a cell population into the non-proliferative stationary phase [15, 22]. Both the replicative and chronological aging of yeast can be slowed down

by caloric restriction (CR), a low-calorie dietary regimen known to extend lifespan and postpone age-related disease in a wide spectrum of organisms [16, 22 - 26]. In yeast, a CR diet can be imposed by reducing the initial glucose concentration in a growth medium from 2% to 0.5% or lower [15, 16, 27]. The use of yeast as an advantageous model organism in aging research has already greatly contributed to the current understanding of the molecular and cellular mechanisms underlying longevity regulation in evolutionarily distant eukaryotic organisms. Specifically, studies in yeast enabled: 1) to reveal for the first time numerous longevity genes, all of which have been later implicated in regulating longevity of multicellular eukaryotic organisms; 2) establish the chemical nature of molecular damage that causes aging and accelerates the onset of age-related diseases across evolutionary spectra of species; and 3) identify several longevity-extending small molecules, all of which have been later shown to decelerate aging, improve health, attenuate age-related pathologies and slow down the onset of age-related diseases in eukaryotic organisms across phyla [9, 13, 15, 16, 21, 24, 25, 28].

This thesis describes studies in which the yeast *S. cerevisiae* was used as a model organism for unveiling the molecular and cellular mechanisms underlying longevity regulation and extension by genetic, dietary and pharmacological interventions.

1.2 Longevity is regulated by a limited number of “master regulator” proteins that in organisms across phyla orchestrate numerous longevity-defining cellular processes in space and time

Growing evidence supports the view that the fundamental mechanisms of aging have been conserved through the evolution process [2, 3, 8, 11, 16 - 20]. The

identification of single-gene mutations that extend lifespan in yeast, worms, flies and mice revealed numerous proteins whose relative abundances define longevity of an organism. These proteins have been implicated in a number of cellular processes including cell cycle, cell growth, stress response, protein folding, apoptosis, autophagy, proteasomal protein degradation, actin organization, signal transduction, nuclear DNA replication, chromatin assembly and maintenance, ribosome biogenesis and translation, lipid and carbohydrate metabolism, oxidative metabolism in mitochondria, NAD⁺ homeostasis, amino acid biosynthesis and degradation, and ammonium and amino acid uptake [2, 3, 7, 9, 14, 17 - 21, 27 - 36]. The spatiotemporal organization of all these numerous cellular processes and their functional states are governed by a limited number of so-called master regulators of longevity. These master regulators are evolutionarily conserved and include the following proteins: 1) sirtuins, a family of NAD⁺-dependent protein deacetylases and ADP ribosylases, in yeast, worms, flies and mammals [3, 13, 17, 18, 29, 30, 33, 34, 37, 38]; 2) nutrient- or insulin/IGF-1-like signaling pathways in evolutionarily distant organisms [3, 19, 20, 33, 35, 36, 39]; 3) nutrient-responsive protein kinases TORC1, Sch9p and PKA in yeast, worms, flies and mammals [3, 16, 27, 36, 37, 39, 40]; 4) the transcriptional factors Msn2p, Msn4p and Rim15p, whose ability to activate expression of numerous stress-response genes in yeast is modulated by TORC1, Sch9p and PKA [3, 21, 27, 40]; 5) the transcriptional factors Rtg1p and Rtg3p that in yeast are modulated by a mitochondrion-to-nucleus signal transduction pathway required for the maintenance of glutamate homeostasis [41 - 44]; 6) the transcription factor DAF-16, whose ability to activate expression of numerous genes in worms is under the control of the insulin/IGF-1 signaling (IIS) pathway and several IIS-independent mechanisms [3,

4, 17, 18, 20, 33-36, 39]; 7) the diet-restriction-specific transcription factor PHA-4 in worms [3, 9, 30, 33, 36, 45]; and 8) some members of the FOXO family of forkhead transcription factors that in flies and mammals activate expression of a number of genes [2 - 4, 9, 30, 33, 36, 46].

One of the major objectives of this thesis was to identify previously unknown longevity-defining processes in chronologically aging yeast. Studies described in this thesis led to the establishment of molecular and cellular mechanisms underlying regulation of these novel longevity-defining processes and their integration into a network of currently known pro-aging and anti-aging processes.

1.3 Effect of dietary regimens on longevity

Most of the genetic manipulations that extend lifespan in organisms across phyla (see above) have been shown to cause major side effects, including irreversible developmental or reproductive defects [3, 11, 17 - 19, 24, 30, 33 - 35]. An alternative way in which lifespan has been shown to be lengthened in various organisms is to impose a caloric restriction (CR) diet, which refers to a dietary regimen low in calories without undernutrition [3, 7, 9, 23 - 26, 47 - 53]. It is well established that CR significantly extends lifespan of a remarkable range of organisms, including yeast, rotifers, spiders, worms, fish, mice, rats, and nonhuman primates [3, 9, 47 - 49, 54 - 57]. This longevity results from the limitation of total calories derived from carbohydrates, fats, or proteins to a level 25% - 60% below that of control animals fed *ad libitum* [47, 54, 55]. In addition to its effect on lifespan *per se*, the CR dietary regimen delays most diseases of aging including cancer, atherosclerosis, type II diabetes and neurodegeneration [3, 7, 9, 24 - 26,

49, 55 - 58]. In fact, it has been shown that CR reduces age-associated neuronal loss in most mouse models of neurodegenerative disorders such as Parkinson's disease [9, 59] or Alzheimer's disease [9, 60]. The CR dietary regimen also prevents age-associated declines in psychomotor and spatial memory tasks [61], alleviates loss of dendritic spines necessary for learning [62], and improves the brain's plasticity and ability for self-repair [63].

In yeast, a CR dietary regimen can be imposed in yeast by reducing the glucose concentration in the complete YEPD (yeast extract, peptone, dextrose) medium from the usual 2% to 0.5% [64] or to 0.2% (this study; [32]). Because cells continue to feed on yeast extract plus peptone, which are rich in amino acids, nucleotides, and vitamins, the growth rate remains rapid as glucose levels are lowered. Thus, the reduction in glucose from 2% to 0.5% or to 0.2% could impose a state of partial energy (ATP) limitation. Other dietary restriction protocols, in particular those that limit amino acids and other nutrients [65, 66], have been shown to drastically reduce the growth rate and may make it more difficult to impose energy limitation.

One of the objectives of this thesis was to gain new insight into the molecular mechanisms by which CR extends longevity of chronologically aging yeast. Studies described in this thesis revealed that the low-calorie diet delays aging in yeast by altering a pattern of age-related changes in trehalose and glycogen concentration.

1.4 Mitochondria and reactive oxygen species (ROS) in aging

Even though benefits of CR have been known for many years, the molecular and cellular mechanisms that underly its longevity-extending effect remain unclear. The

complexity of these mechanisms lies in multiple effects including metabolic, neuroendocrine and apoptotic changes, which vary in intensity and exhibit striking differences among various cells, tissues, organs and organisms [3, 9, 11, 24, 26, 49, 57, 67]. The generally (until recently) accepted “free radical theory” of aging postulates that aging is caused by cumulative oxidative damage generated by reactive oxygen species (ROS) produced during respiration [68, 69]. Indeed, oxidative damage to DNA, RNA, proteins and lipids is known to progress and accumulate with aging [70 - 73]. This damage may limit lifespan. In fact, overexpression of the enzyme superoxide dismutase (SOD), which reduces ROS, extends lifespan in *Drosophila* [74] and in chronologically aging yeast reached quiescence [75].

ROS are generated in multiple compartments and by multiple enzymes within the cell. Although the vast majority (estimated at approximately 90%) of these harmful compounds is produced in mitochondria (Figure 1.1) [76 - 79], ROS are also generated by NADP/H oxidases and phagocytic oxidases in the plasma membrane [76 - 79], in several oxidative reactions that are catalyzed by amino acid oxidases, cyclooxygenases, lipid oxygenase and xanthine oxidase in the cytosol [76 - 79], and during lipid metabolism in peroxisomes [44, 80, 81]. The steady-state level of ROS within the cell is the result of a delicate balance that exists between the rates of ROS formation and of their detoxification in antioxidant scavenger reactions taking place in various cellular locations. The CuZnSOD (SOD1) subform of superoxide dismutase in the cytosol and the MnSOD (SOD2) subform of this enzyme in the mitochondrion convert superoxide radicals to a less toxic and more stable compound, namely hydrogen peroxide (Figure 1.2) [76 - 79]. The subsequent detoxification of hydrogen peroxide depends on the

following enzymes (Figure 1.2) [76 - 79]: 1) glutathione peroxidases in the cytosol, mitochondria and peroxisomes; 2) catalases in the cytosol, mitochondria and peroxisomes; and 3) peroxiredoxins in the cytosol, mitochondria and peroxisomes.

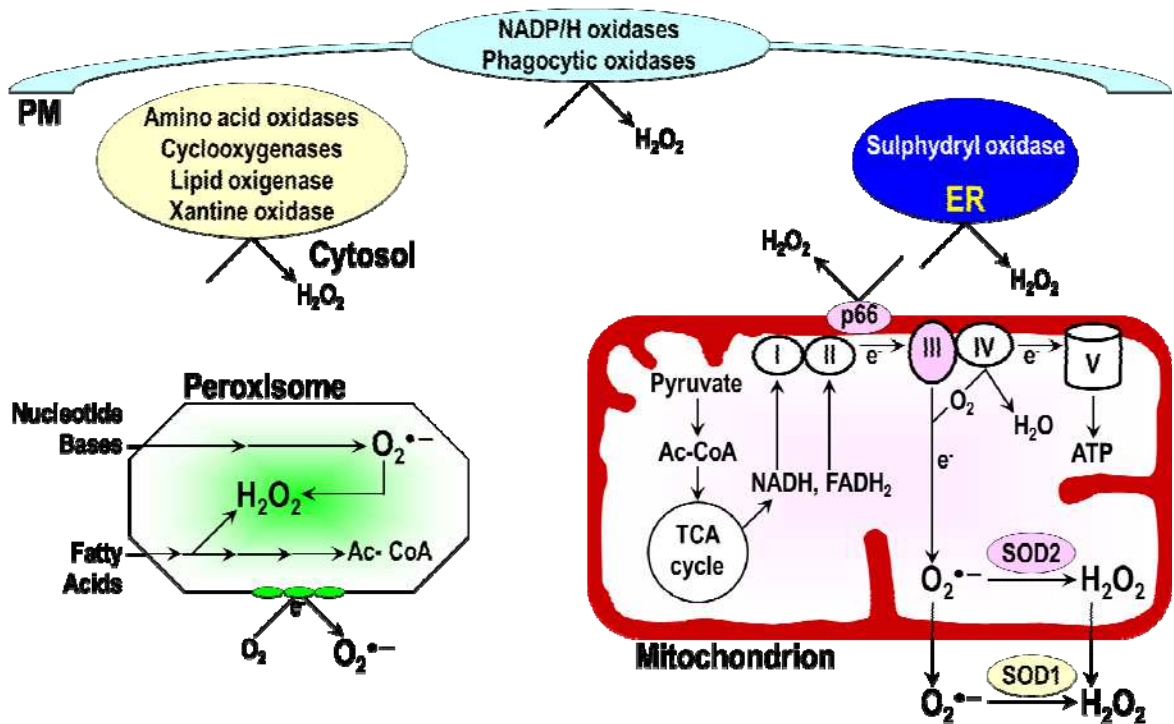


Figure 1.1. ROS are generated by numerous enzymes in multiple compartments within the cell, mostly (~ 90%) within mitochondria.

Most of the known targets for the oxidative damage by ROS are mitochondrial proteins, DNA and lipids, including (Figure 1.3) [44, 76 - 79]: 1) aconitase, a [4Fe-4S] cluster enzyme of the tricarboxylic acid (TCA) cycle; 2) Lys4p, a [4Fe-4S] cluster enzyme of lysine biosynthesis that takes place in the mitochondrion; 3) succinate dehydrogenase (SDH), a [3Fe-3S] cluster- and heme-containing enzyme of the TCA that also functions as complex II of the electron transfer chain (ETC) in the mitochondrial

membrane; 4) cytochrome c, a heme-containing mobile component of the mitochondrial ETC; 5) cytochrome c oxidase, a heme-containing complex IV of the mitochondrial ETC; 6) the mitochondrial DNA (mtDNA) nucleoid that, in contrast to chromatin in the nucleus, lacks histones; and 7) saturated fatty acids of membrane lipids.

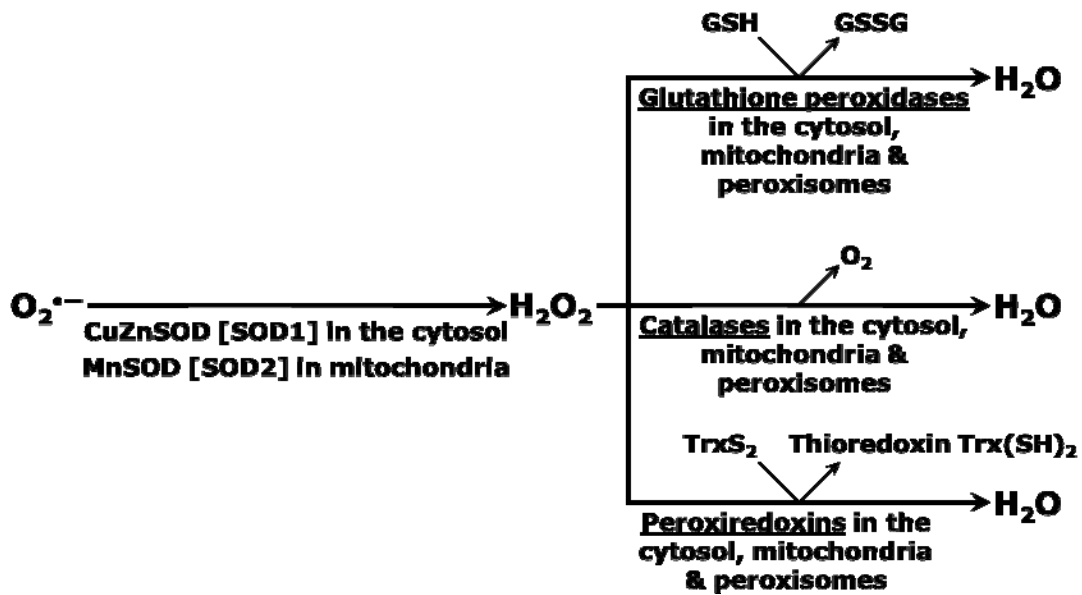


Figure 1.2. Detoxification of ROS occurs in antioxidant scavenger reactions confined to various cellular compartments.

While high intracellular and intraorganellar levels of ROS tend to cause oxidative damage to various cellular constituents, the low concentrations of these highly reactive chemical compounds promote a number of processes related to the protection of the cellular macromolecules from oxidative damage (Figure 1.4) [36, 44, 80 - 93]. In addition, the low intracellular and intraorganellar concentrations of ROS activate protein machinery that protects the cell from apoptosis, one of the forms of programmed cell death [44, 82 - 89, 91 - 93]. Such a protective function of ROS is initiated by ROS sensors present in the mitochondrion (*i.e.*, protein kinases PKD1, PKC δ , Src, Abl, PI3

kinase and Akt), plasma membrane (*i.e.*, the Ras protein), and cytosol (*i.e.*, the PNC1 protein) (Figure 1.4) [44, 76 - 79, 82 - 87, 91 - 93]. Some of these ROS sensors in the cytosol and mitochondrion interact with the cytosol-to-nucleus and mitochondrion-to-nucleus shuttling proteins (*i.e.*, p32 and Hsp27p, respectively), thereby promoting their relocation to the nucleus (Figure 1.4) [76 - 79, 84 - 87, 91 - 93]. In the nucleus, these two shuttling proteins activate a distinct group of transcriptional factors and cofactors (*i.e.*, SIRT1, FOXO3, p53, NF- κ B, DET1 and COP1), all of which function as global transcriptional activators of genes encoding oxidative stress-response and anti-apoptotic proteins (Figure 1.4) [76 - 79, 84, 86, 87, 91 - 93]. Moreover, some of the ROS sensors in the cytosol and mitochondrion phosphorylate and inactivate the pro-apoptotic factors Bad and JNK, thereby delaying the intrinsic, mitochondria-dependent apoptotic pathway of programmed cell death (Figure 1.4) [77 - 79, 85, 87, 91 - 93].

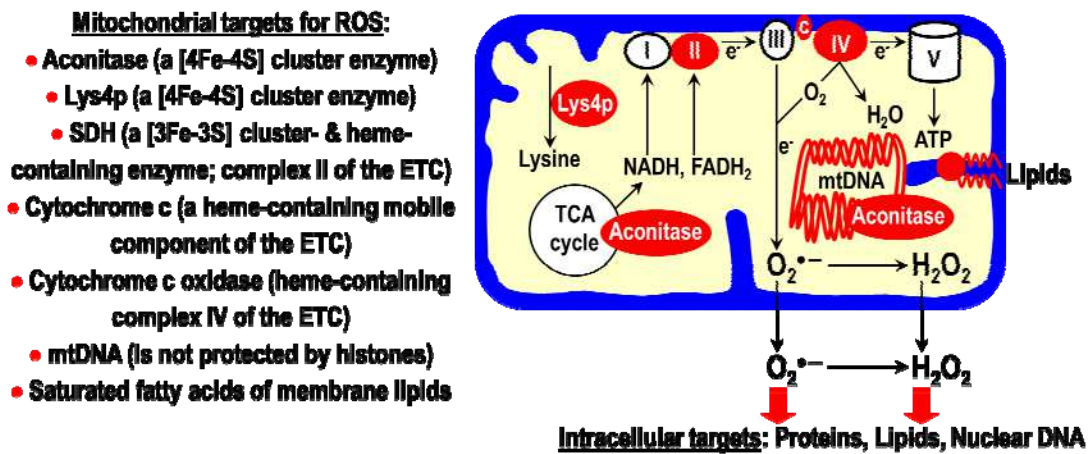


Figure 1.3. High levels of ROS cause oxidative damage to various cellular constituents. Most of the known targets for the oxidative damage by ROS are mitochondrial proteins, DNA and lipids.

The mitochondria-controlled, ROS-modulated intrinsic pathway of apoptosis also

depends on the delicate balance between mitochondrial fission and fusion (Figure 1.5) [94 - 98]. Mitochondrial fusion maintains a tubular mitochondrial network, thereby: 1) facilitating transfer of the mitochondrial membrane potential (*i.e.*, energy) from O₂-rich to O₂-poor cellular regions; 2) complementing mtDNA mutations that accumulate with aging; and 3) hampering the intrinsic pathway of apoptosis (Figure 1.5) [94 - 99]. On the other hand, mitochondrial fission breaks down the mitochondrial network, thereby: 1) ensuring inheritance of mitochondria by newly formed daughter cells; 2) causing respiratory defects; 3) leading to loss or mutation of mtDNA that remains uncomplemented; and 4) promoting the intrinsic pathway of apoptosis (Figure 1.5) [94 - 99].

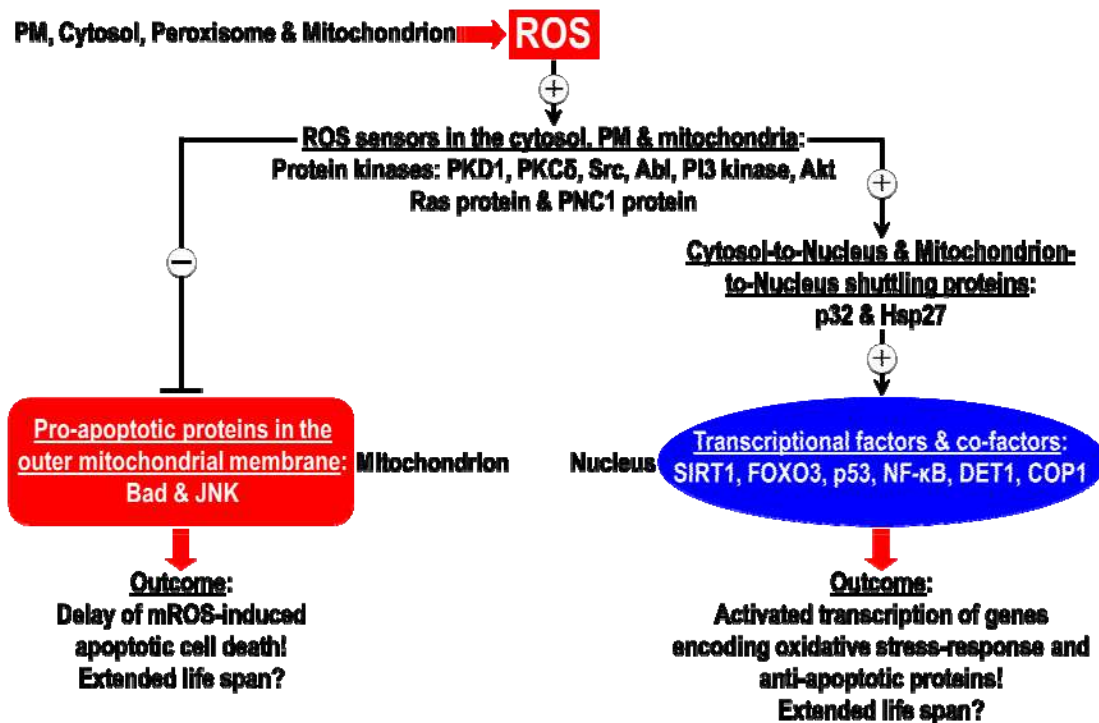
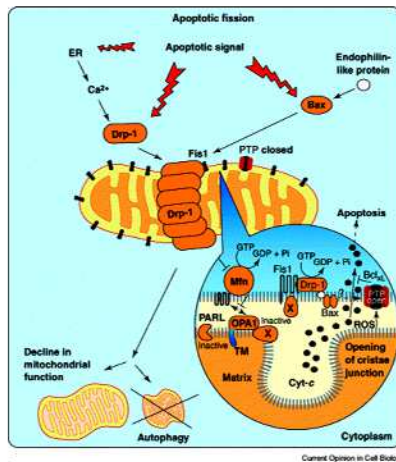


Figure 1.4. The sub-lethal concentrations of ROS promote a number of processes related to the protection of the cellular macromolecules from oxidative damage.

Numerous recent findings have implicated the intrinsic, mitochondria-dependent apoptotic pathway of programmed cell death in aging of evolutionary distant organisms. Apoptosis has been well known for its fundamental role in human development and physiology [100]. The apoptotic pathway of programmed cell death also exists in other mammals and multicellular organisms [101].

Mitochondrial fusion maintains a tubular mitochondrial network, thereby:

- Facilitating transfer of the mitochondrial membrane potential (i.e., energy) from O_2 -rich to O_2 -poor cellular regions
- Complementing mtDNA mutations that accumulate with aging
- Hampering the intrinsic pathway of apoptosis



Mitochondrial fission breaks down the mitochondrial network, thereby:

- Ensuring inheritance of mitochondria by newly formed daughter cells
- Causing respiratory defects
- Leading to loss or mutation of mtDNA that remains uncomplemented
- Promoting the intrinsic pathway of apoptosis

Figure 1.5. A delicate balance between mitochondrial fission and fusion controls the intrinsic pathway of apoptosis and numerous other vital processes in a cell.

Until recently, it has been unknown whether apoptosis exists in unicellular organisms (such as yeast), and if it did what role it may serve. Recent data provided evidence that yeast cells can undergo apoptosis by showing characteristic apoptotic markers: DNA cleavage, chromatin condensation, externalization of phosphatidylserine to the outer leaflet of the plasma membrane, and cytochrome c release from the mitochondria [102]. The first proof for an apoptotic process operating in yeast cells came from the study that revealed an apoptotic phenotype caused by a mutation in the *CDC48*

gene [103]. ROS have been implicated as central regulators of yeast apoptosis, which leads to even more similarity towards apoptosis in metazoan organisms [104]. Recent discovery of several yeast orthologues of mammalian apoptotic regulators provided the final proof that yeast and metazoan apoptosis are two versions of the same cellular program. These key apoptotic regulators in yeast cells include: 1) the yeast metacaspase Yca1p [103]; 2) an HtrA2/Omi-like protein, the yeast apoptotic serine protease Nma111p [105]; 3) the yeast apoptosis inducing factor Aif1p [106]; 4) the yeast histone chaperone Asf1p [107]; and 5) the yeast mitochondrial fission protein Drp1p [108]. Recent finding that aged yeast cells die exhibiting markers of apoptosis [109] suggested that apoptosis plays a pivotal role in aging of this unicellular eukaryotic organism.

One of the major objectives of this thesis was to provide deep mechanistic insight into the essential roles for mitochondrial morphology, mitochondria-generated ROS and mitochondria-controlled apoptosis in defining longevity of chronologically aging yeast.

1.5 A modular network regulates longevity of chronologically aging yeast

One way to look at the complexity of the aging process, in which a limited number of master regulators orchestrate numerous cellular processes in space and time (see above) [3, 4, 6, 17, 31, 33, 36], is to consider each of these processes as a functional module integrated with other modules into a longevity network [1, 6, 8, 31, 32]. The synergistic action of individual modules could establish the rate of aging. Furthermore, the relative impact of each module on the rate of aging in a particular organism or cell type could differ at various stages of its lifetime and could also vary in different organisms and cell types [1, 6, 8, 31, 32]. In this conceptual framework, the longevity

network could progress through a series of checkpoints. At each of these checkpoints, a distinct set of master regulators senses the functional states of critical modules comprising the network. Based on this information and considering the input of some environmental cues (such as dietary intake, environmental stresses, endocrine factors etc.), master regulators modulate certain processes within monitored modules in order to limit the age-related accumulation of molecular and cellular damage [31, 32]. The resulting changes in the dynamics of individual modules comprising the network and in its general configuration are critically important for specifying the rate of aging during late adulthood.

Recent studies in our laboratory not only provided evidence for the existence of a modular network regulating longevity of chronologically aging yeast but also revealed the spatio-temporal dynamics of this network and its remodeling under longevity-extending CR conditions [32, 40, 44, 110]. To study the effect of CR on the chronological lifespan of yeast, we incubated the wild-type strain BY4742 in rich YP medium initially containing 0.2%, 0.5%, 1% or 2% glucose. YP medium was chosen for chronological aging studies because, in contrast to a synthetic medium, it is rich in amino acids, nucleotides, vitamins and other nutrients. We therefore expected that the reduction of glucose concentration in YP medium would lower the number of available calories without compromising the supply of essential nutrients [32], thereby modeling a traditional CR dietary regimen established in experiments with laboratory rodents [25, 26]. An equally important reason for choosing rich YP medium for chronological aging studies was that the recent isolation of quiescent and nonquiescent cells from yeast stationary-phase cultures grown in this medium provided a novel, valuable system for

elucidating the mechanisms linking chronological aging to quiescence, the mitotic cell cycle and apoptosis [111, 112]. Our choice of the strain BY4742 was based on its relatively short chronological lifespan [113], thereby offering considerable time savings for chronological aging studies of yeast cultivated in rich YP medium. Importantly, this yeast strain serves as one of the two haploid genetic backgrounds of the widely used Yeast Knock-Out Collection available from Open Biosystems. We found that CR cells of wild-type grown on 0.2% or 0.5% glucose lived significantly longer than wild-type cells grown under non-CR conditions on 1% or 2% glucose [32, 40]. Importantly, ATP levels and the dynamics of their change during chronological aging were very similar for CR and non-CR yeast [32]. Thus, CR yeast are not starving. Based on this important conclusion, we suggested that: 1) CR yeast remodel their metabolism in order to match the level of ATP produced in non-CR yeast; and 2) such specific remodeling of metabolism in CR yeast prolongs their lifespan [32]. To define a specific pattern of metabolism that is responsible for the anti-aging effect of CR and to establish the mechanisms underlying such effect, we routinely monitor the age-dependent dynamics of proteomes, lipidomes and metabolomes in wild-type and numerous long- and short-lived mutant strains of yeast [32, 40, 44, 110, 114]. In our research on aging, we also assess the effect of a CR diet and various single-gene-deletion mutations on the age-related alterations in cell ultrastructure, stability of nuclear genome, telomere length, carbohydrate and lipid metabolism, concentration of ROS, mitochondrial morphology, essential processes in mitochondria, mitochondrial membrane lipids, frequency of mitochondrial DNA (mtDNA) mutations, composition of mitochondrial nucleoid, susceptibility to exogenously induced apoptosis, and stress resistance [32, 40, 44, 110,

114]. A strategy that we developed for elucidating the mechanisms of longevity regulation in yeast is outlined in Figure 1.6.

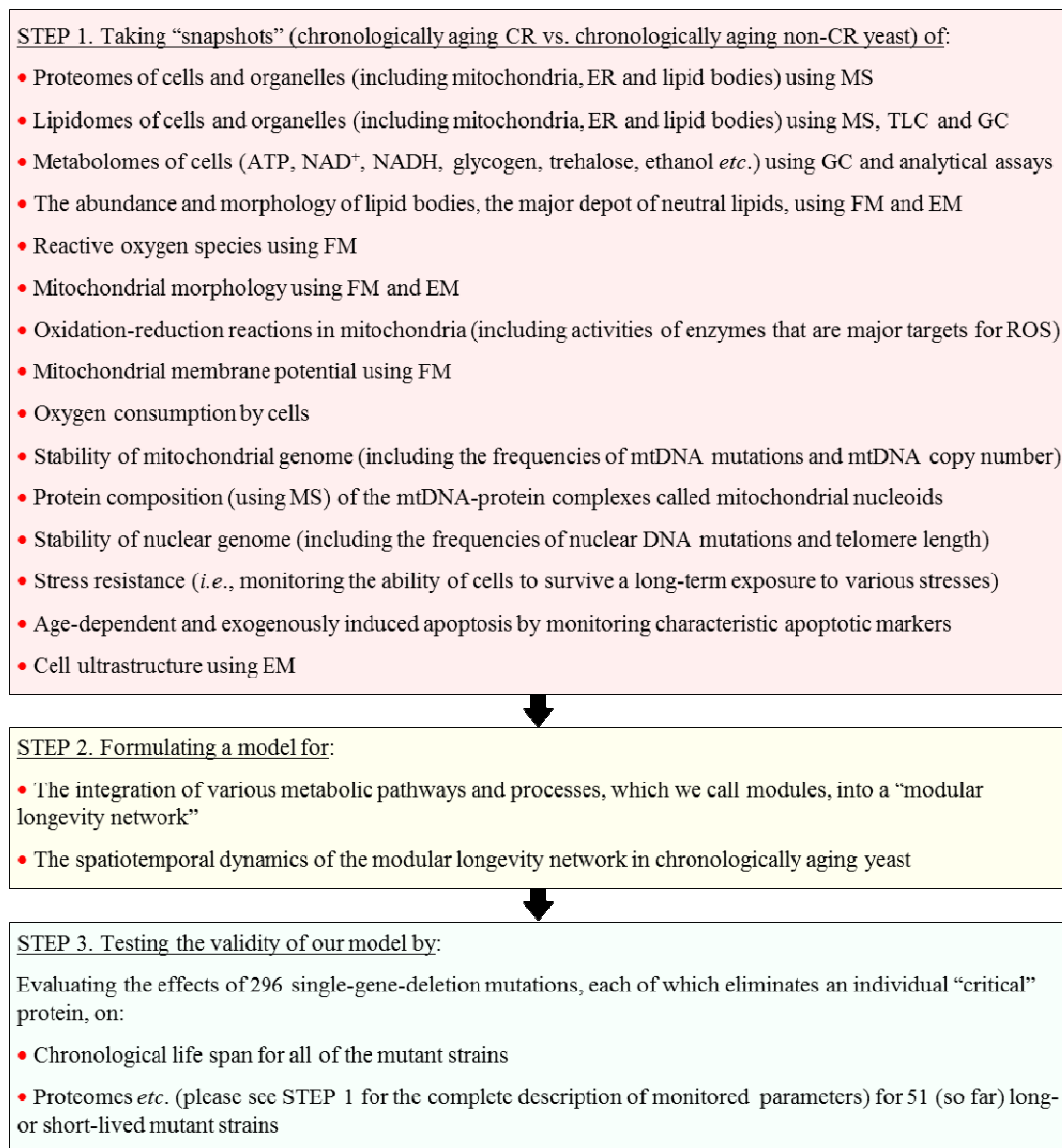


Figure 1.6. A strategy that we developed for elucidating the mechanisms underlying longevity regulation in yeast. *Abbreviations:* CR, calorie restriction; EM, electron microscopy; ER, endoplasmic reticulum; FM, fluorescence microscopy; GC, gas chromatography; MS, mass spectrometry; mtDNA, mitochondrial DNA; ROS, reactive oxygen species; TLC, thin-layer chromatography.

Using this strategy, we provided evidence that, before yeast enter the non-

proliferative stationary (ST) phase, they establish a diet- and genotype-specific pattern of metabolism and organelle dynamics during the preceding diauxic (D) and post-diauxic (PD) growth phases [32, 40, 44, 110, 114]. Our findings imply that, by designing such specific pattern prior to entry into a non-proliferative state, yeast define their long-term viability. We therefore concluded that yeast longevity is programmed by the level of metabolic capacity and organelle organization they reached prior to reproductive maturation [32, 40, 44, 110, 114]. We found that yeast reach such a level by establishing a diet- and genotype-specific configuration of what we call “a modular longevity network” [32, 114] (Figure 1.7).

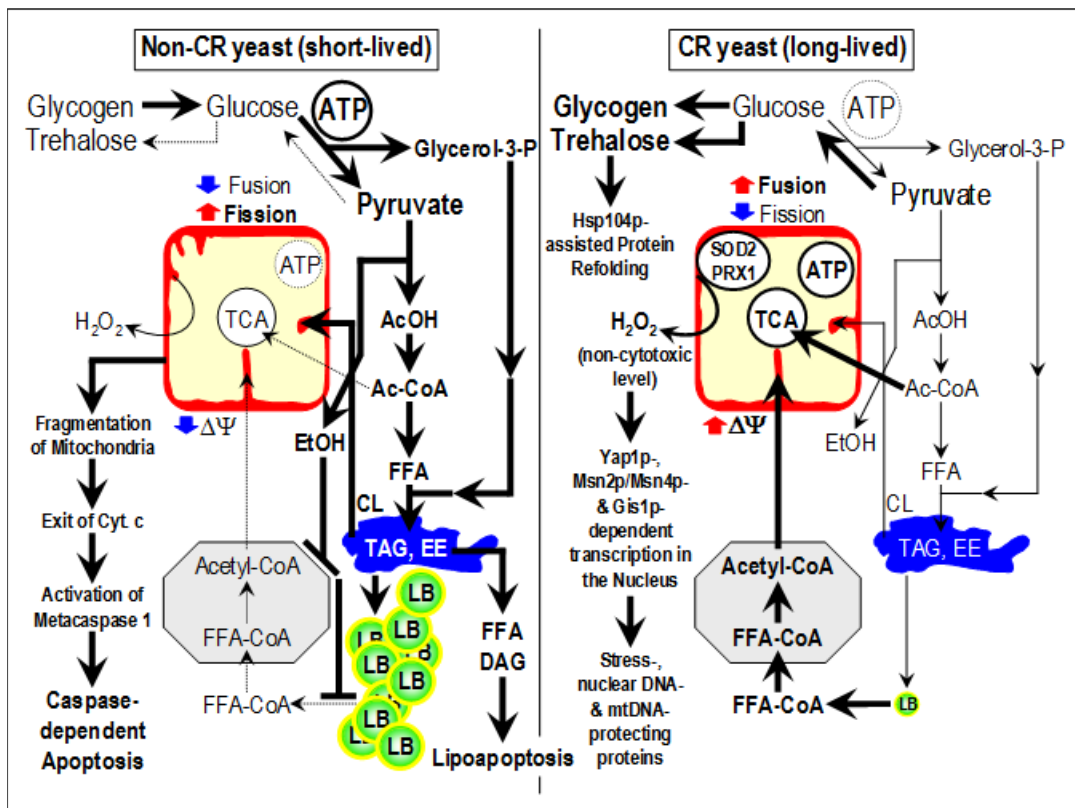


Figure 1.7. A modular network regulates longevity of chronologically aging yeast. The network integrates a number of cellular processes, which we call modules (see this thesis and [32] for detailed description of individual modules). CR and non-CR yeast establish different configurations of the longevity network by altering the dynamics of individual modules that comprise the network. During diauxic (D) and

post-diauxic (PD) phases, yeast establish a particular configuration of their longevity network by setting up the rates of the processes that take place within each of the network's modules. Different configurations of the network designed during D and PD phases define different rates of survival during the non-proliferative stationary (ST) phase. The different network's configurations established by CR and non-CR yeast entering ST phase are shown. *Note:* The thickness of arrows correlates with the rates of the processes taking place within each of the network's modules. The metabolites accumulated in bulk quantities and the processes accelerated to the highest extent are shown in bold. *Abbreviations:* Ac-CoA, acetyl-CoA; AcOH, acetic acid; CL, cardiolipins; CR, calorie restriction; DAG, diacylglycerols; EE, ethyl esters; ER, endoplasmic reticulum; EtOH, ethanol; FA-CoA, CoA esters of fatty acids; FFA, free fatty acids; LB, lipid bodies; PL, phospholipids; Prx1p, peroxiredoxin; Sod2, superoxide dismutase; TAG, triacylglycerols; TCA, the tricarboxylic acid cycle in mitochondria; $\Delta\Psi$, the mitochondrial membrane potential.

Based on such analysis of the spatiotemporal dynamics of the network, we proposed that it integrates modules operating in 1) trehalose and glycogen metabolism; 2) glycolysis, glucose fermentation to ethanol, and gluconeogenesis; 3) lipid metabolism in the endoplasmic reticulum (ER), lipid bodies and peroxisomes; 4) various routes of interorganellar metabolic flow; 5) essential oxidation-reduction reactions in mitochondria; 6) maintenance of ROS homeostasis; 7) protection of mtDNA from oxidative damage; 8) maintenance of a tubular mitochondrial network; and 9) mitochondria-controlled apoptosis (Figure 1.7) [32, 40, 44, 110, 114]. By evaluating how various interventions alter the functional state of the network's modules and affect lifespan, we inferred the logistics of integrating individual modules into the network and suggested a model for the spatiotemporal dynamics of the longevity network operating in chronologically aging yeast (Figure 1.8). This model envisions that 1) yeast establish a diet- and genotype-specific configuration of the network by setting up the rates of the

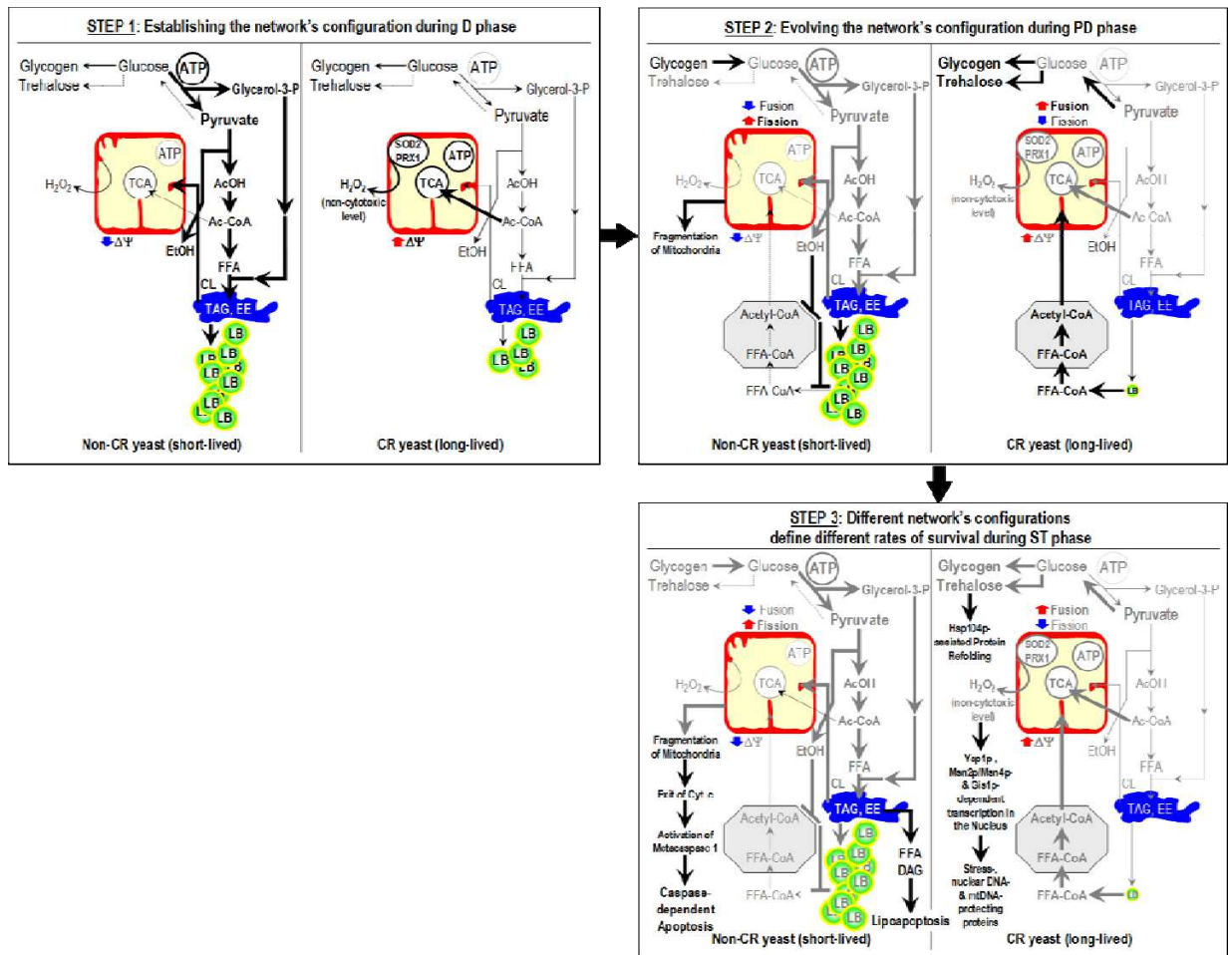


Figure 1.8. A model for the spatiotemporal dynamics of the longevity network operating in chronologically aging yeast. The specific configurations of the longevity network that have been differently designed by CR and non-CR yeast during diauxic (D) phase and that have differently evolved in these yeast during the subsequent post-diauxic (PD) phase, result in establishing different rates of survival during the non-proliferative stationary (ST) phase. Thus, by designing a specific configuration of the modular longevity network prior to reproductive maturation, yeast define their chronological life span. *Note:* The thickness of arrows correlates with the rates of the processes taking place within each of the network's modules. The metabolites accumulated in bulk quantities and the processes accelerated to the highest extent are shown in bold. The metabolites produced and the processes occurred during the step of the aging process preceding the step that is displayed are shown in gray colour. T bars denote inhibition of the process. *Abbreviations:* Ac-CoA, acetyl-CoA; AcOH, acetic acid; CL, cardiolipins; CR, calorie restriction; DAG, diacylglycerols; EE, ethyl esters; ER, endoplasmic reticulum; EtOH, ethanol; FA-CoA,

CoA esters of fatty acids; FFA, free fatty acids; LB, lipid bodies; PL, phospholipids; Prx1p, peroxiredoxin; Sod2, superoxide dismutase; TAG, triacylglycerols; TCA, the tricarboxylic acid cycle in mitochondria; $\Psi\Delta$, the mitochondrial membrane potential.

processes taking place within each of its modules; 2) the establishment of a network's configuration occurs before yeast enter a non-proliferative state; and 3) different network's configurations established prior to entry into a non-proliferative state define different rates of survival following such entry [32, 40, 44, 110, 114]. Thus, by designing a specific configuration of the modular longevity network prior to reproductive maturation, yeast define their chronological lifespan. We therefore concluded that the chronological aging of yeast is an ontogenetic program that progresses through at least two checkpoints before yeast enter the non-proliferative ST phase (Figure 1.8) [32, 44].

One of the major objectives of this thesis was to elucidate the molecular and cellular mechanisms by which several modules of the longevity network depicted in Figures 1.7 and 1.8 control the aging process in yeast.

1.6 Five groups of novel anti-aging small molecules greatly extend longevity of chronologically aging yeast

In the model for the modular longevity network operating in chronologically yeast (Figures 1.7 and 1.8) [32, 44], lipid metabolism in the ER, peroxisomes and lipid bodies regulates longevity. Our laboratory provided evidence that the specific remodeling of lipid metabolism in CR yeast extends their lifespan by delaying lipoapoptosis (a lipid-induced form of cell death) and by modulating some apoptosis- and stress response-related processes in mitochondria (Figures 1.7 and 1.8) [32, 40, 44, 110, 114]. One of the

objectives of the research on mechanisms of longevity regulation in our laboratory is to identify chemical compounds that, by targeting longevity-defining cellular processes that integrate lipid metabolism and mitochondria-confined modules into the longevity network, can extend yeast lifespan. Our recent high-throughput chemical genetic screen of several commercially available compound libraries identified 24 compounds that greatly extend yeast chronological lifespan and belong to 5 chemically distinct groups [32]. Importantly, all of the compounds that we identified are structurally distinct from resveratrol, a constituent of red wine that extends the replicative lifespan of yeast [115] and the chronological lifespans of worms, flies and fishes [116 - 121] by activating so-called sirtuins of the Sir2p protein family. Furthermore, all these compounds are structurally unrelated to several other small molecules that, similar to resveratrol, activate the sirtuin SIRT1, improve health and survival, and delay the onset of age-related diseases in rodent models [122 - 124]. Thus, it is conceivable that the novel anti-aging compounds that we identified target longevity-related cellular processes that are not modulated by resveratrol and other known activators of sirtuins.

The novel anti-aging small molecules that we identified can be used as research tools for studying mechanisms of longevity and as pharmaceutical agents for aging and age-related disorders. Recent studies in our laboratory revealed that at least one of them, a bile lithocholic acid (LCA), is also a potent and selective anti-tumor agent in cultured human neuroblastoma, glioma and breast cancer cells [125]. One of the objectives of this thesis was to establish the molecular and cellular mechanisms through which LCA extends yeast longevity by modulating age-related changes in mitochondrial morphology, mitochondrially-generated ROS and mitochondria-controlled apoptosis.

1.7 Autophagy and aging

Autophagy is a cellular process in which damaged and dysfunctional organelles or portions of cytoplasm are sequestered for degradation in lysosomes of mammalian cells or vacuoles of yeast cells [126]. Autophagic degradation is an essential cytoprotective mechanism that is vital for cell resistance to various stresses and mandatory for proper turnover of cellular organelles and macromolecules. Importantly, autophagy has been shown to be induced under longevity-extending CR conditions [127].

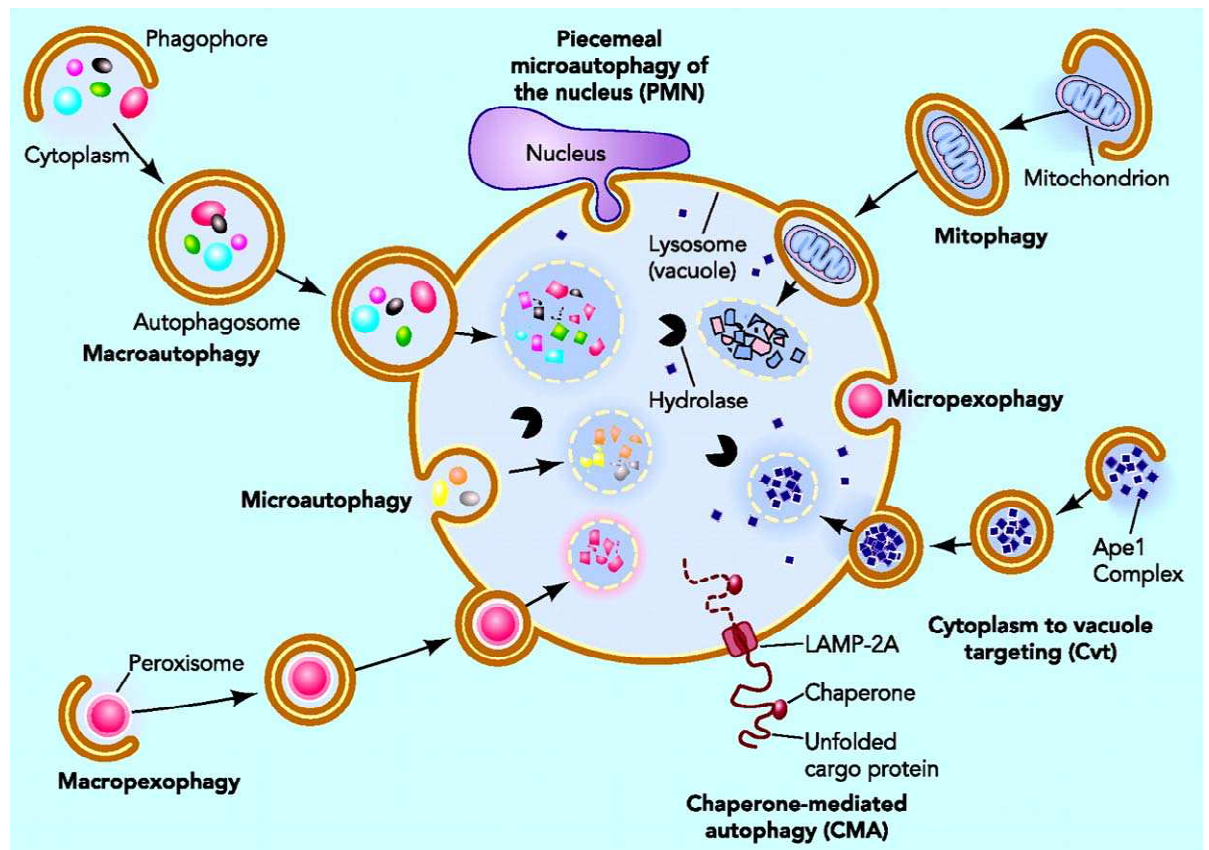


Figure 1.9. Three fundamentally different modes of autophagy are macroautophagy, microautophagy and chaperone-mediated autophagy. From: Yen and Klionsky (2008). *Physiology* 23:248-262.

Three major modes of autophagy are known as macroautophagy, microautophagy and chaperone-mediated autophagy; each of them is known to have a distinct cellular function and underlying mechanism (Figure 1.9). Macroautophagy involves the sequestration of cellular components into double-membrane vesicles called autophagosomes and the subsequent targeting of these vesicles to lysosomes (vacuoles in yeast), where their entire content is degraded by proteases, lipases, nucleases and glucosidases [128]. In a so-called non-selective macroautophagy pathway, an organelle or a portion of cytoplasm is first sequestered by a double membrane into a structure called autophagosome and then targeted for degradation in the lysosome/vacuole (Figures 1.10 and 1.11). In contrast,

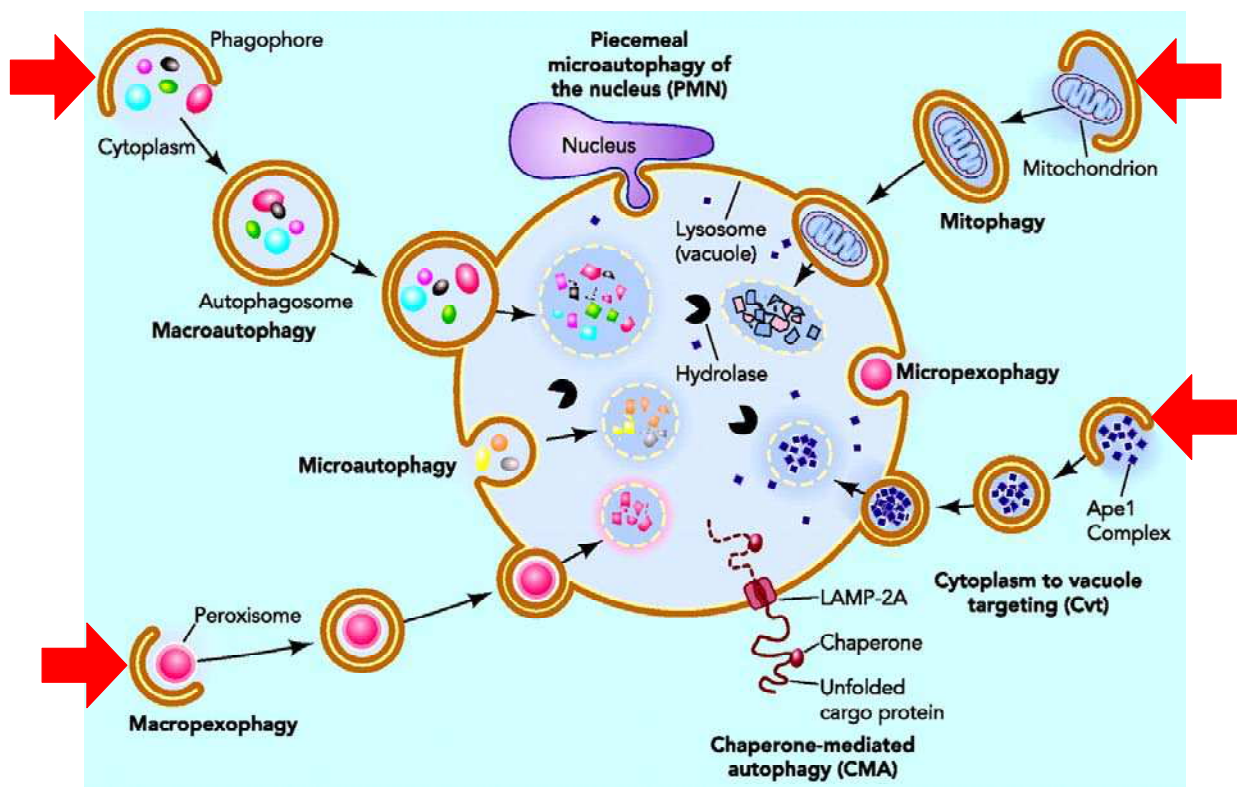


Figure 1.10. Macroautophagy is the major mode of autophagy involving the sequestration of organelles and cytosolic proteins by double-membrane vesicles (called autophagosomes) and their delivery to the lysosome/vacuole. From: Yen and Klionsky (2008). *Physiology* 23:248-262.

selective macroautophagy targets specific organelles or cellular components such as mitochondria (mitophagy), peroxisomes (macropexophagy) and endoplasmic reticulum (reticulophagy) (Figures 1.10 and 1.11) [126]. In either of these pathways, the underlying mechanisms are similar; they are initiated by pre-vesicle formation (phagophore nucleation) and expansion and are followed by vesicle completion (fusion of phagophore ends) around a cellular component or cytosolic fraction [126, 128]. This process is completed by the targeting of the autophagosome to a lysosome/vacuole, with which the autophagosome then fuses to form an autolysosome - thus releasing its contents for degradation and recycling [126, 128].

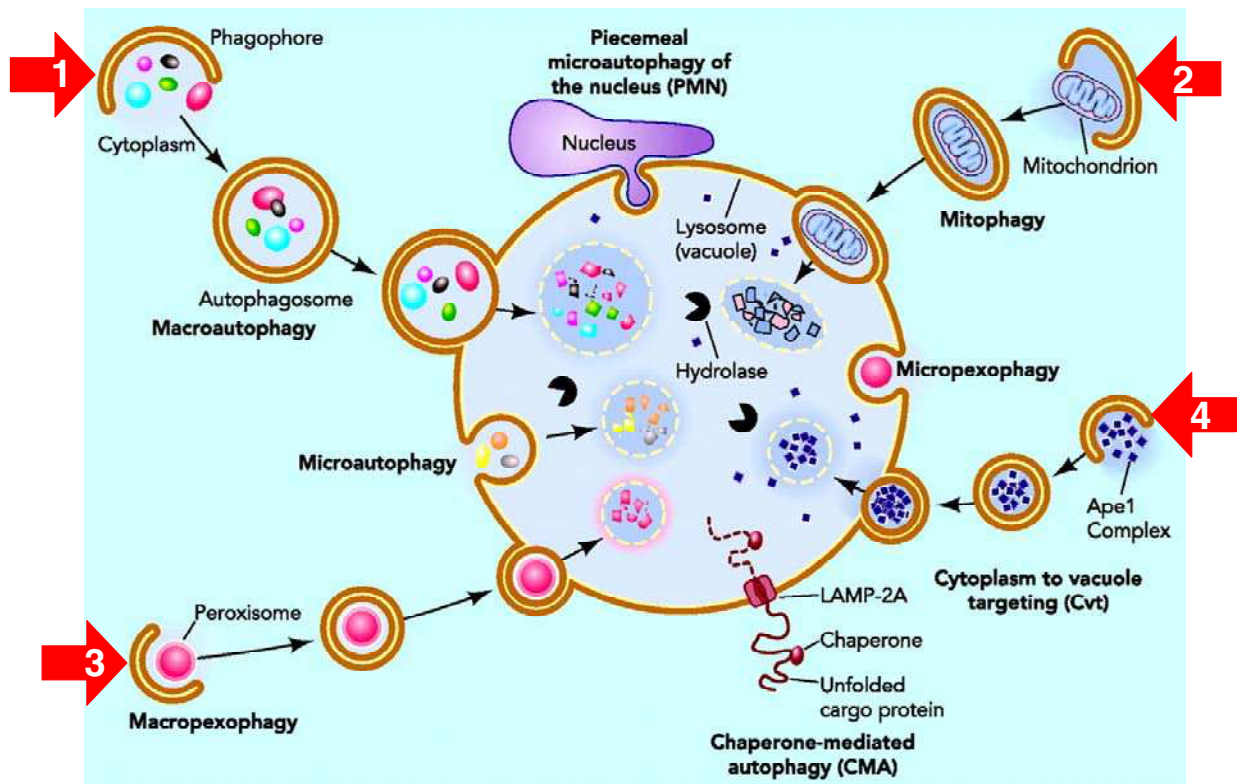


Figure 1.11. The macroautophagy pathways include 1) non-selective macroautophagy; 2) mitophagy (a cargo-specific, selective pathway); 3) macropexophagy (a cargo-specific, selective pathway); and 4)

cytoplasm-to-vacuole [Cvt] (a biosynthetic pathway). From: Yen and Klionsky (2008). *Physiology* 23:248-262.

The recycling of dysfunctional organelles, misfolded proteins and other by-products of cellular aging by macroautophagy is highly beneficial to survival.

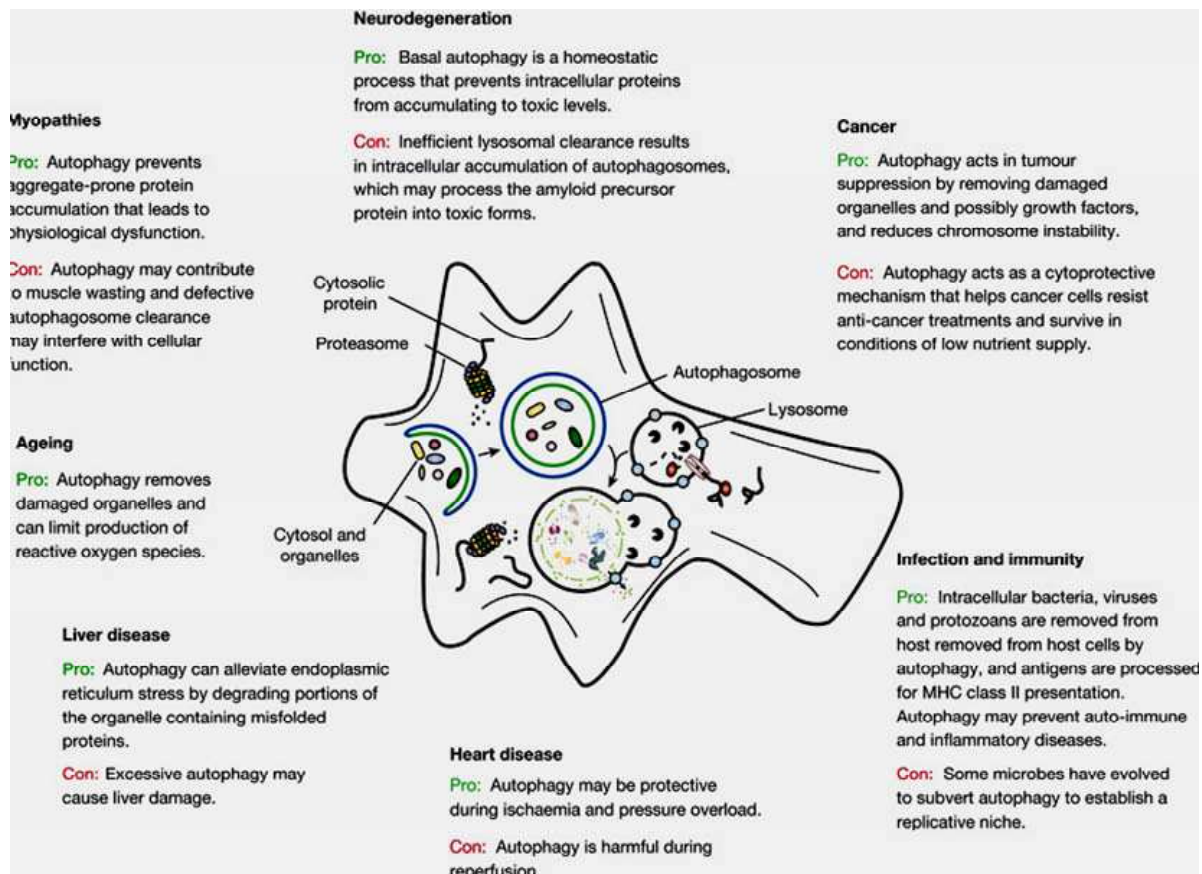


Figure 1.12. Macroautophagy plays an essential role in longevity regulation and has been implicated in the incidence of diverse age-related pathologies, including neurodegeneration and cancer. From: Mizushima et al (2008). *Nature* 451:1069-1075.

Macroautophagy also plays a role in resisting starvation by providing cells with the

metabolic precursors and biosynthetic components when their environmental availability is low [129]. Gradual age-related reduction of autophagy efficacy results in the accumulation of dysfunctional organelles and other by-products of cellular aging [126], and has been implicated in the incidence of diverse age-related pathologies - including cancer, neurodegenerative diseases, infections and heart attacks [130] (Figure 1.12). Due to its important cytoprotective and organelle-renewing functions, macroautophagy is vital for longevity in non-dividing cells such as neurons, monocytes and liver cells [126, 128, 129]. Indeed, the nervous-tissue specific knockout of autophagy related genes (*Atg*) in mice has been shown to cause motor deficits and abnormal reflexes [129]. Furthermore, macroautophagy is necessary for the clearance of protein aggregates associated with neurodegenerative conditions, such as Parkinson, Alzheimer and Huntingdon diseases [126, 128 - 130].

Because of their essential roles in mitigating the effects of disease, infection and aging, the regulatory pathways of autophagy are promising targets for the development of new therapeutic compounds [126, 128, 129]. Autophagy is known to be governed by several conserved autophagy-related (*Atg*) genes. The products of these genes are regulated transcriptionally and post-transcriptionally by a nutrient-sensing signaling network that has been implicated in longevity regulation in organism across phyla [126, 130]. In yeast, this network is centered on the target of rapamycin complex 1 (TOR1), which has been shown to phosphorylate Atg1p, Atg13p and Atg17p that compose a macroautophagy induction protein complex [126, 128, 129]. This protein complex has been shown to drive the assembly of a pre-autophagosome structure (PAS). Phosphorylation of Atg13p by TOR1 is thought to inhibit the formation of the complex

and subsequent macroautophagy induction, thereby suppressing macroautophagy [131]. This complex is also a target of the cAMP/PKA pathway [130]. In a mechanism independent or parallel to TOR1, protein kinase A (PKA) inhibits the formation of the macroautophagy induction protein complex (Atg1p/Atg13p/Atg17p) by phosphorylating Atg1p and Atg13p [128, 130, 132]. Thus, the induction of macroautophagy in yeast is driven by a concerted action of the TOR1 and PKA signaling pathways of longevity regulation [132].

Atg1p, a key component of the macroautophagy pathway, is a serine-threonine kinase highly conserved in eukaryotes [126, 128, 130]. In response to conditions that induce autophagy, Atg1p is initially recruited by adaptor proteins to the PAS, and then activated by associating with Atg13p (Figure 1.13) [133, 134]. Although only some of its cellular protein targets have been identified, Atg1 has been shown to play a pivotal role in macroautophagy [135]. Indeed, the *atg1* mutant yeast strain is known to be deficient in the formation of autophagosomes as well as in several downstream steps in macroautophagy [126, 128, 130]. The human homologs of yeast Atg1p, ULK1 and ULK2, are upregulated at the transcription level by the tumor suppressor p53 in response to DNA damage. As such, a number of human cancers are associated with ULK1/2 suppression [136].

Atg 11p, on the other hand, is necessary only for the selective pathways of macroautophagy operating in yeast cells (Figure 1.13). It is an adaptor protein that interacts with Atg1p and several other autophagy-related proteins [128 - 130]. The localization of Atg1p, Atg8p and several other selective autophagy factors to the pre-autophagosome structure has been shown to be dependent on Atg11p [137]. Atg11p has

been hypothesized to function similar to myosins, namely by guiding the associated autophagosomes on an actin filament [138]. This hypothesis is based on structural similarities between myosin motor proteins and Atg11p and on the demonstrated involvement of the actin cytoskeleton in selective macroautophagy, but not non-selective macroautophagy [138, 139].

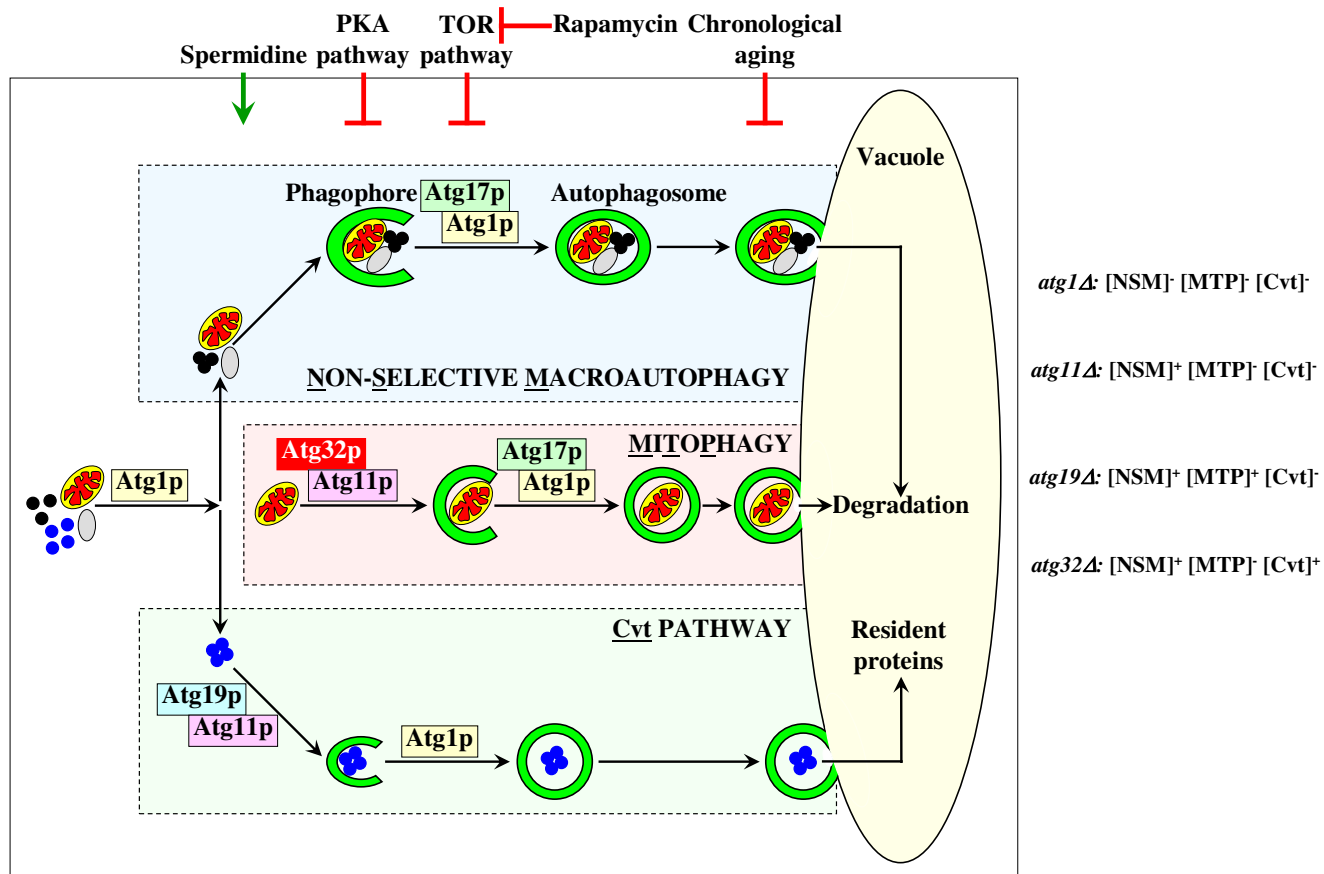


Figure 1.13. The molecular machinery of yeast macroautophagy and its regulation by longevity signaling pathways and anti-aging compounds.

One of the major objectives of this thesis was to explore the involvement of mitophagy, a selective pathway of autophagic degradation aimed at dysfunctional mitochondria, in regulating yeast longevity, maintaining functional mitochondria and

protecting yeast from apoptotic and a recently discovered by our laboratory necrosis-like “lipoptotic” modes of age-related cell death.

1.8 Thesis outline and contributions of colleagues

Chapter 2 of my thesis outlines the spectrum of mitochondria-confined processes affected by CR. We found that CR modulates oxidation-reduction processes and ROS production in yeast mitochondria, reduces the frequency of mtDNA mutations, and alters the abundance and mtDNA-binding activity of mitochondrial nucleoid-associated proteins. Findings described in Chapter 2 provide evidence that these mitochondrial processes play essential roles in regulating longevity of chronologically active yeast by defining their viability following cell entry into a quiescent state. Based on these findings, we propose a hypothesis that ROS, which are mostly generated as by-products of mitochondrial respiration, play a dual role in regulating longevity of chronologically aging yeast. On the one hand, if yeast mitochondria are unable (due to a dietary regimen) to maintain ROS concentration below a toxic threshold, ROS promote aging by oxidatively damaging certain mitochondrial proteins and mtDNA. On the other hand, if yeast mitochondria can (due to a dietary regimen) maintain ROS concentration at a certain “optimal” level, ROS delay chronological aging. We propose that this “optimal” level of ROS is insufficient to damage cellular macromolecules but can activate certain signaling networks that extend lifespan by increasing the abundance or activity of stress-protecting and other anti-aging proteins. In addition, studies presented in Chapter 2 imply that mtDNA mutations do not contribute to longevity regulation in yeast grown under non-CR conditions but make important contribution to longevity regulation in yeast

placed on a CR diet.

Chapter 3 of my thesis describes the results of our examination of how single-gene-deletion mutations affecting trehalose biosynthesis and degradation impact 1) the age-related dynamics of changes in trehalose concentration; 2) yeast chronological lifespan under CR conditions; 3) the chronology of oxidative protein damage, intracellular ROS level and protein aggregation; and 4) the timeline of thermal inactivation of a protein in heat-shocked yeast cells and its subsequent reactivation in yeast returned to low temperature. Findings described in Chapter 3 provide evidence that CR extends yeast chronological lifespan in part by altering a pattern of age-related changes in trehalose concentration. We outline a model for molecular mechanisms underlying the essential role of trehalose in defining yeast longevity by modulating protein folding, misfolding, unfolding, refolding, oxidative damage, solubility and aggregation throughout lifespan.

Chapter 4 of my thesis describes the results of our evaluation of a potential role for glycogen metabolism in lifespan extension by CR. To attain this objective, in studies described in this chapter we monitored the dynamics of age-related changes in its intracellular level. We also assessed how various single-gene-deletion mutations that differently alter glycogen concentrations in pre-quiescent and quiescent yeast cells affect longevity of chronologically aging yeast under CR conditions. Our findings provide evidence that the maintenance of a proper balance between the biosynthesis and degradation of glycogen is mandatory for lifespan extension by CR.

Chapter 5 of my thesis describes the results of our evaluation of a role for ethanol metabolism in lifespan extension by CR. To attain this objective, in studies described in this chapter we monitored the dynamics of age-related changes in ethanol concentration

in chronologically aging yeast cultured under CR and non-CR conditions. We also assessed how single-gene-deletion mutations eliminating Adh1p (an enzyme that is required for ethanol synthesis) or Adh2p (an enzyme that catalyzes ethanol degradation) affect longevity of chronologically aging yeast under CR and non-CR conditions. Furthermore, we examined the effects of the *adh1Δ* and *adh2Δ* mutations on the intracellular levels of trehalose, glycogen, neutral lipids, free fatty acids (FFA) and diacylglycerols (DAG) in chronologically aging yeast under non-CR conditions. Moreover, we monitored how single-gene-deletion mutations eliminating Adh1p or Adh2p influence the abundance of Fox1p, Fox2p and Fox3p, all of which are the core enzymes of fatty acid β -oxidation in peroxisomes. Our findings provide evidence that ethanol accumulated in yeast placed on a calorie-rich diet represses the synthesis of Fox1p, Fox2p and Fox3p, thereby suppressing peroxisomal oxidation of FFA that originate from triacylglycerols synthesized in the endoplasmic reticulum (ER) and deposited within LBs. The resulting build-up of arrays of FFA (so-called gnarls) within LBs of non-CR yeast initiates several negative feedback loops regulating the metabolism of triacylglycerols. Due to the action of these negative feedback loops, chronologically aging non-CR yeast not only amass triacylglycerols in LBs but also accumulate DAG and FFA in the ER. The resulting remodeling of lipid dynamics in chronologically aging non-CR yeast shortens their lifespan by causing their premature death due to 1) necrosis triggered by the inability of their peroxisomes to oxidize FFA; 2) lipoapoptosis initiated in response to the accumulation of DAG and FFA; and 3) the DAG-induced reorganization of the protein kinase C-dependent signal transduction network affecting multiple longevity-related cellular targets.

Chapter 6 of my thesis describes studies that ultimately led us to the identification of small molecules increasing the chronological lifespan of yeast under CR conditions by targeting lipid metabolism and modulating “housekeeping” longevity assurance pathways. We predicted that such housekeeping pathways 1) modulate longevity irrespective of the organismal and intracellular nutrient and energy status; and 2) do not overlap (or only partially overlap) with the “adaptable” longevity pathways that are under the stringent control of calorie and/or nutrient availability. In studies presented in this chapter of my thesis, we found that in yeast grown under CR conditions the *pex5Δ* mutation not only remodels lipid metabolism but also causes the profound changes in longevity-defining processes in mitochondria, resistance to chronic (long-term) stresses, susceptibility to mitochondria-controlled apoptosis, and frequencies of mutations in mitochondrial and nuclear DNA. We therefore chose the single-gene-deletion mutant strain *pex5Δ* as a short-lived strain for carrying out a chemical genetic screen aimed at the identification of novel anti-aging compounds targeting housekeeping longevity assurance pathways. By screening the total of approximately 19,000 representative compounds from seven commercial libraries, our laboratory recently identified 24 small molecules that greatly extend the chronological lifespan of *pex5Δ* under CR conditions and belong to 5 chemical groups. One of these groups consisted of 6 bile acids, including lithocholic acid (LCA). Findings presented in this chapter of my thesis imply that LCA, a bile acid, modulates housekeeping longevity assurance pathways by 1) attenuating the pro-aging process of mitochondrial fragmentation, a hallmark event of age-related cell death; 2) altering oxidation-reduction processes in mitochondria - such as oxygen consumption, the maintenance of membrane potential and ROS production - known to be essential for

longevity regulation; 3) enhancing cell resistance to oxidative and thermal stresses, thereby activating the anti-aging process of stress response; 4) suppressing the pro-aging process of mitochondria-controlled apoptosis; and 5) enhancing stability of nuclear and mitochondrial DNA, thus activating the anti-aging process of genome maintenance. The observed pleiotropic effect of LCA on a compendium of housekeeping longevity assurance processes implies that this bile acid is a multi-target life-extending compound that increases chronological lifespan in yeast by modulating a network of the highly integrated cellular events that are not controlled by the adaptable AMP-activated protein kinase/target of rapamycin (AMPK/TOR) and cAMP/protein kinase A (cAMP/PKA) pathways.

Chapter 7 of my thesis describes studies that provided evidence for the existence of two critical periods when the addition of LCA to yeast grown under CR conditions on 0.2% glucose can increase both their mean and maximum chronological lifespans. One of these two critical periods includes logarithmic and diauxic growth phases, whereas the other period exists in the early stationary (ST) phase of growth. In contrast, LCA does not cause a significant extension of the mean or maximum chronological lifespan of CR yeast if it is added in post-diauxic or late ST growth phases. Because aging of multicellular and unicellular eukaryotic organisms affects numerous anti- and pro-aging processes within cells [2, 3, 7, 9, 14, 17 - 21, 27 - 36], we hypothesized that the observed ability of LCA to delay chronological aging of yeast grown under CR conditions only if added at certain critical periods (checkpoints) of their lifespan could be due to its differential effects on certain anti- and pro-aging processes at different checkpoints. To test the validity of our hypothesis, in studies described in this chapter of my thesis we examined how the

addition of LCA at different periods of chronological lifespan in yeast grown under CR conditions influences anti- and pro-aging processes taking place during each of these periods. Our empirical validation of this hypothesis suggests a mechanism linking the ability of LCA to delay chronological aging of yeast only if added at certain periods (checkpoints) of their lifespan to the differential effects of this natural anti-aging compound on certain anti- and pro-aging processes at each of these checkpoints.

Chapter 8 of my thesis describes studies aimed at exploring possible roles of mitophagy - a selective macroautophagic removal of dysfunctional mitochondria - in regulating yeast longevity, maintaining functional mitochondria, and protecting yeast from apoptotic and a recently discovered by our laboratory necrosis-like “lipoptotic” modes of age-related cell death. We used a combination of functional genetic, chemical biological, cell biological and electron microscopical analyses to carry out comparative analyses of the single-gene-deletion mutant strain *atg32Δ*, which is impaired only in the mitophagic pathway of selective macroautophagy, and wild-type (WT) strain. *atg32Δ* is known to lack a mitochondrial outer membrane protein Atg32p whose binding to an adaptor protein Atg11p drives the recruitment of mitochondria to the phagophore assembly site, thereby initiating the mitophagy process. Our findings provide the first comprehensive evidence that mitophagy defines yeast longevity, facilitates yeast chronological lifespan extension by a recently discovered anti-aging natural compound, sustains functional mitochondria, and protects yeast from apoptotic and necrosis-like “lipoptotic” forms of cell death.

Most of the findings described in Chapter 2 have been published in *Experimental Gerontology* [Goldberg, A.A.*, Bourque, S.D.*, Kyryakov, P.*, Gregg, C., Boukh-Viner,

T., Beach, A., Burstein, M.T., Machkalyan, G., Richard, V., Rampersad, S., Cyr, D., Milijevic, S. and Titorenko, V.I. (2009). Effect of calorie restriction on the metabolic history of chronologically aging yeast. *Exp. Gerontol.* 44:555-571; * *Equally contributed first co-authors*] and in *The Biochemical Society Transactions* [Goldberg, A.A.*, Bourque, S.D.*, Kyryakov, P.*, Boukh-Viner, T., Gregg, C., Beach, A., Burstein, M.T., Machkalyan, G., Richard, V., Rampersad, S. and Titorenko, V.I. (2009). A novel function of lipid droplets in regulating longevity. *Biochem. Soc. Trans.* 37:1050-1055; * *Equally contributed first co-authors*]. I carried out and supervised more than 30% of all of the work described in each of these publications and prepared the first draft of sections relevant to my work. I am an equally contributed first co-author on both these publications. Dr. V. Titorenko provided intellectual leadership of these projects and edited both manuscripts.

All findings described in Chapter 3 have been published in *Frontiers in Physiology* [Kyryakov, P., Beach, A., Richard, V.R., Burstein, M.T., Leonov, A., Levy, S., and Titorenko, V.I. (2012). Caloric restriction extends yeast chronological lifespan by altering a pattern of age-related changes in trehalose concentration. *Front. Physiol.*; in press]. I carried out and supervised more than 50% of the work described in this publication and prepared the first draft of the entire manuscript. Dr. V. Titorenko provided intellectual leadership of these projects and edited both manuscripts.

Some of the findings described in Chapter 4 have been published in *Experimental Gerontology* [Goldberg, A.A.*, Bourque, S.D.*, Kyryakov, P.*, Gregg, C., Boukh-Viner, T., Beach, A., Burstein, M.T., Machkalyan, G., Richard, V., Rampersad, S., Cyr, D., Milijevic, S. and Titorenko, V.I. (2009). Effect of calorie restriction on the metabolic

history of chronologically aging yeast. *Exp. Gerontol.* 44:555-571; * *Equally contributed first co-authors*]. I carried out and supervised more than 30% of the work described in this publication and prepared the first draft of sections relevant to my work. I am an equally contributed first co-author on this publication. Dr. V. Titorenko provided intellectual leadership of this project and edited the manuscript. Furthermore, some of the findings described in Chapter 4 are presented in the manuscript of a paper [Kyryakov, P., Beach, A., Burstein, M.T., Richard, V.R. and Titorenko, V.I. The maintenance of a proper balance between the biosynthesis and degradation of glycogen in chronologically aging yeast is mandatory for lifespan extension by caloric restriction] that is currently in preparation for submission to *Aging Cell*. I expect this manuscript to be submitted for publication in September or October 2012. I carried out and supervised more than 60% of the work described in this publication and prepared the first draft of sections relevant to my work. Dr. V. Titorenko provided intellectual leadership of this project and will be editing the first draft of the manuscript.

Some of the findings described in Chapter 5 have been published in *Experimental Gerontology* [Goldberg, A.A.*, Bourque, S.D.*, Kyryakov, P.*, Gregg, C., Boukh-Viner, T., Beach, A., Burstein, M.T., Machkalyan, G., Richard, V., Rampersad, S., Cyr, D., Milijevic, S. and Titorenko, V.I. (2009). Effect of calorie restriction on the metabolic history of chronologically aging yeast. *Exp. Gerontol.* 44:555-571; * *Equally contributed first co-authors*] and in *The Biochemical Society Transactions* [Goldberg, A.A.*, Bourque, S.D.*, Kyryakov, P.*, Boukh-Viner, T., Gregg, C., Beach, A., Burstein, M.T., Machkalyan, G., Richard, V., Rampersad, S. and Titorenko, V.I. (2009). A novel function of lipid droplets in regulating longevity. *Biochem. Soc. Trans.* 37:1050-1055; * *Equally*

contributed first co-authors]. I carried out and supervised more than 30% of all of the work described in each of these publications and prepared the first draft of sections relevant to my work. I am an equally contributed first co-author on both these publications. Dr. V. Titorenko provided intellectual leadership of these projects and edited both manuscripts. Furthermore, some of the findings described in Chapter 5 are presented in the manuscript of a paper [Kyryakov, P., Beach, A., Burstein, M.T., Richard, V.R. and Titorenko, V.I. Lipid droplets function as a hub in a regulatory network that defines the chronological lifespan of yeast by modulating lipid metabolism in the endoplasmic reticulum and peroxisomes] that is currently in preparation for submission to *Cell Metabolism*. I expect this manuscript to be submitted for publication in October or November 2012. I carried out and supervised more than 40% of the work described in this publication and prepared the first draft of sections relevant to my work. Dr. V. Titorenko provided intellectual leadership of this project and will be editing the first draft of the manuscript.

Most of the findings described in Chapter 6 have been published in *Aging* [Goldberg, A.A.*, Richard, V.R.*, Kyryakov, P.*, Bourque, S.D.*, Beach, A., Burstein, M.T., Glebov, A., Koupaki, O., Boukh-Viner, T., Gregg, C., Juneau, M., English, A.M., Thomas, D.Y., and Titorenko, V.I. (2010). Chemical genetic screen identifies lithocholic acid as an anti-aging compound that extends yeast chronological life span in a TOR-independent manner, by modulating housekeeping longevity assurance processes. *Aging* 2:393-414; * *Equally contributed first co-authors*]. I carried out and supervised about 25% of the work described in this publication and prepared the first draft of sections relevant to my work. I am an equally contributed first co-author on this publication. Dr.

V. Titorenko provided intellectual leadership of this project and edited the manuscript. Furthermore, some of the findings described in Chapter 6 are presented in the manuscript of a paper [Kyryakov, P., Beach, A., Burstein, M.T., Richard, V.R. and Titorenko, V.I. Lipid droplets function as a hub in a regulatory network that defines the chronological lifespan of yeast by modulating lipid metabolism in the endoplasmic reticulum and peroxisomes] that is currently in preparation for submission to *Cell Metabolism*. I expect this manuscript to be submitted for publication in October or November 2012. I carried out and supervised more than 40% of the work described in this publication and prepared the first draft of sections relevant to my work. Dr. V. Titorenko provided intellectual leadership of this project and will be editing the first draft of the manuscript.

All findings described in Chapter 7 are presented in the manuscript of a paper [Kyryakov, P., Beach, A., Burstein, M.T., Richard, V.R., Gomez-Perez, A. and Titorenko, V.I. Lithocholic acid, a natural anti-aging compound, extends longevity of chronologically aging yeast only if added at certain critical periods of their lifespan] that is currently in preparation for submission to *Cell Cycle*. I expect this manuscript to be submitted for publication in August 2012. I carried out and supervised more than 50% of the work described in this publication and prepared the first draft of sections relevant to my work. Dr. V. Titorenko provided intellectual leadership of this project and is currently editing the first draft of the manuscript.

All findings described in Chapter 8 are presented in the manuscripts of two papers [1. Kyryakov, P., Gomez-Perez, A., Koupaki, O., Beach, A., Burstein, M.T., Richard, V.R., Leonov, A. and Titorenko, V.I. Mitophagy is a longevity assurance process that in chronologically aging yeast sustains functional mitochondria and maintains lipid

homeostasis. 2. Kyryakov, P., Sheibani, S., Mattie, S., Gomez-Perez, A., Beach, A., Burstein, M.T., Richard, V.R., Leonov, A., Vali, H. and Titorenko, V.I. Mitophagy protects yeast from a necrosis-like “lipoptotic” mode of cell death triggered by exposure to palmitoleic fatty acid] that are currently in preparation for submission to *Autophagy* and *Cell Death and Differentiation*, respectively. I expect these manuscripts to be submitted for publication in August 2012 and October 2012, respectively. I carried out and supervised more than 50% of the work described in each of these two manuscripts and prepared the first drafts of sections relevant to my work. Dr. V. Titorenko provided intellectual leadership of this project and is currently editing the first drafts of the manuscripts.

All abbreviations, citations, and the numbering of figures and tables that have been used in the published papers and in the manuscripts in preparation have been changed to the format of this thesis.

2 Caloric restriction (CR) modulates oxidation-reduction processes and ROS production in yeast mitochondria, reduces the frequency of mitochondrial DNA (mtDNA) mutations, and alters the abundance and mtDNA-binding activity of mitochondrial nucleoid-associated proteins

2.1 Abstract

To make a first step towards the use of high-throughput empirical data on cell metabolic history of chronologically aging yeast for defining the molecular causes of cellular aging, we recently conducted the mass spectrometry-based identification and quantitation of proteins recovered from purified mitochondria of CR and non-CR yeast [32]. Our comparative analysis of mitochondrial proteomes of these yeast revealed that CR altered the levels of numerous proteins that function in essential processes confined to mitochondria. This chapter of my thesis describes the spectrum of mitochondria-confined processes affected by CR. We found that CR modulates oxidation-reduction processes and ROS production in yeast mitochondria, reduces the frequency of mtDNA mutations, and alters the abundance and mtDNA-binding activity of mitochondrial nucleoid-associated proteins. Findings described here provide evidence that these mitochondrial processes play essential roles in regulating longevity of chronologically active yeast by defining their viability following cell entry into a quiescent state. Based on these findings, we propose a hypothesis that ROS, which are mostly generated as by-products of mitochondrial respiration, play a dual role in regulating longevity of chronologically aging yeast. On the one hand, if yeast mitochondria are unable (due to a dietary regimen) to maintain ROS concentration below a toxic threshold, ROS promote

aging by oxidatively damaging certain mitochondrial proteins and mtDNA. On the other hand, if yeast mitochondria can (due to a dietary regimen) maintain ROS concentration at a certain “optimal” level, ROS delay chronological aging. We propose that this “optimal” level of ROS is insufficient to damage cellular macromolecules but can activate certain signaling networks that extend lifespan by increasing the abundance or activity of stress-protecting and other anti-aging proteins. In addition, studies presented in this chapter of my thesis imply that mtDNA mutations do not contribute to longevity regulation in yeast grown under non-CR conditions but make important contribution to longevity regulation in yeast placed on a CR diet.

2.2 Introduction

Because longevity signaling pathways and mechanisms underlying their modulation by genetic, dietary and pharmacological interventions are evolutionarily conserved, the budding yeast *S. cerevisiae* is a valuable model system in aging research [13 - 20]. Our laboratory uses *S. cerevisiae* as a model organism for unveiling the molecular and cellular mechanisms underlying longevity regulation and extension by genetic, dietary and pharmacological interventions. To address the inherent complexity of aging from a systems perspective and to build an integrative model of aging process, we recently investigated the effect of caloric restriction (CR), a low-calorie dietary regimen, on longevity and metabolic history of chronologically aging yeast [32, 40, 110, 114]. The full growth cycle of yeast cultured in complete YP medium (1% yeast extract, 2% peptone) initially containing 0.2%, 0.5%, 1% or 2% glucose began with logarithmic (L) phase and progressed through diauxic (D) and post-diauxic (PD) phases to stationary

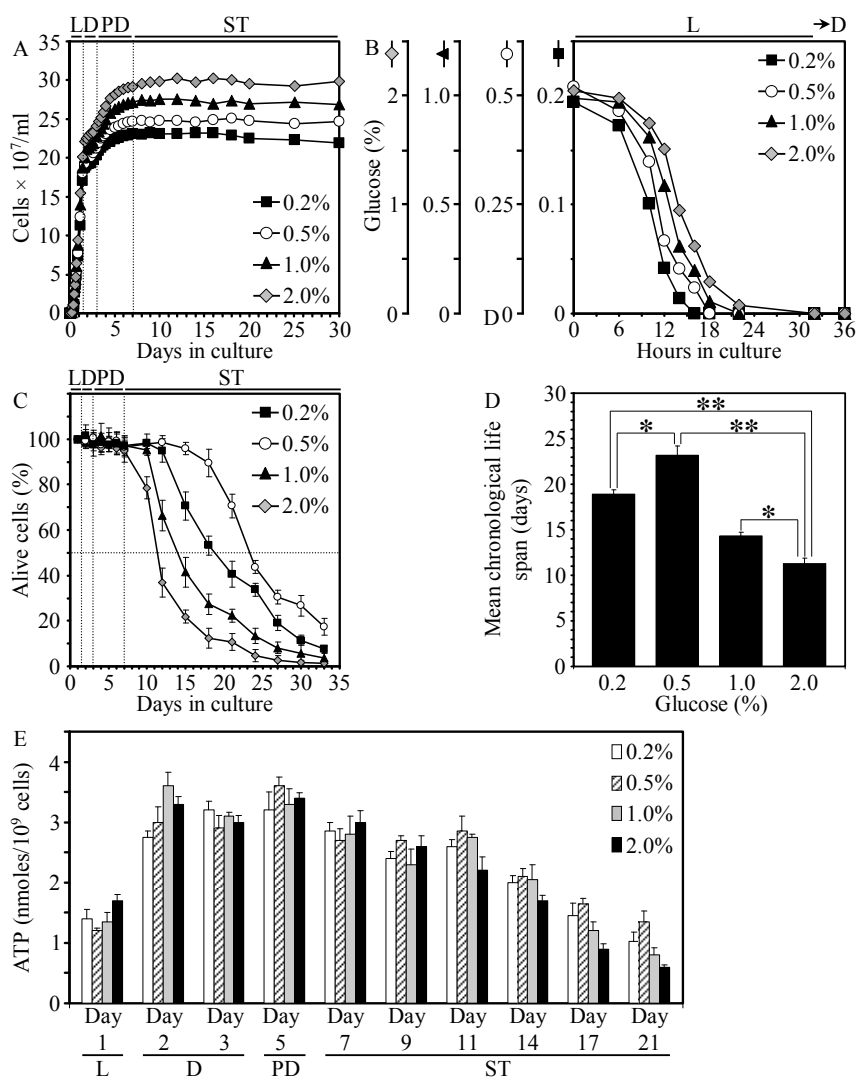


Figure 2.1. CR extends the chronological lifespan of yeast. (A and B) Kinetics of growth (A) and glucose consumption (B) for the WT strain BY4742. Each plot shows a representative experiment repeated 4-6 times in triplicate with similar results. (C) Survival of chronologically aging WT cells. Data are presented as mean \pm SEM (n = 16-28). $p < 0.001$ at days 10 to 33 for cells grown on 0.2% or 0.5% glucose vs. cells grown on 2% glucose. (D) The mean chronological lifespans of WT cells. Data are presented as mean \pm SEM (n = 16-28); * $p < 0.01$, ** $p < 0.001$. (E) ATP levels in chronologically aging WT cells. Data are presented as mean \pm SEM (n = 3-5). (A-E) Cells were cultured in YP medium containing 0.2%, 0.5%, 1% or 2% glucose. Abbreviations: Diauxic (D), logarithmic (L), post-diauxic (PD) or stationary (ST) phase. From [32], with permission.

(ST) phase (Figure 2.1A). The rates of growth (Figure 2.1A) and glucose consumption (Figure 2.1B) in L phase were similar for cells cultured in any of the four media, whereas the maximum cell density in ST-phase cultures varied within a 28-% range and correlated with the initial glucose concentration (Figure 2.1A). CR cells grown on 0.2% or 0.5% glucose lived significantly longer than cells grown under non-CR conditions on 1% or 2% glucose (Figure 2.1C). In fact, the mean chronological lifespan of cells grown on 0.2% glucose was extended by more than 60% and that of cells grown on 0.5% glucose was extended by almost 2-fold, as compared to the mean chronological lifespan of cells grown on 2% glucose (Figure 2.1D). Importantly, ATP levels and the dynamics of their change during chronological aging were very similar for CR and non-CR yeast (Figure 2.1E). Thus, CR yeast are not starving. Based on this important conclusion, our laboratory put forward a hypothesis that: 1) CR yeast remodel their metabolism in order to match the level of ATP produced in non-CR yeast; and 2) such specific remodeling of metabolism in CR yeast prolongs their lifespan [32, 114].

It has been recently predicted that the application of the concepts and methodologies of so-called metabolic control analysis (MCA) to the analysis of empirical data on the cell metabolic histories of model organisms will enable to 1) infer the relative contributions of various cellular processes to aging; and 2) define how interventions such as dietary restriction delay aging by modulating these processes [31, 151]. To make a first step towards the use of MCA for defining the molecular causes of cellular aging by elucidating the effect of CR on the metabolic history of chronologically aging yeast, our laboratory recently carried out the mass spectrometry-based identification and quantitation of proteins recovered from purified mitochondria of chronologically aging

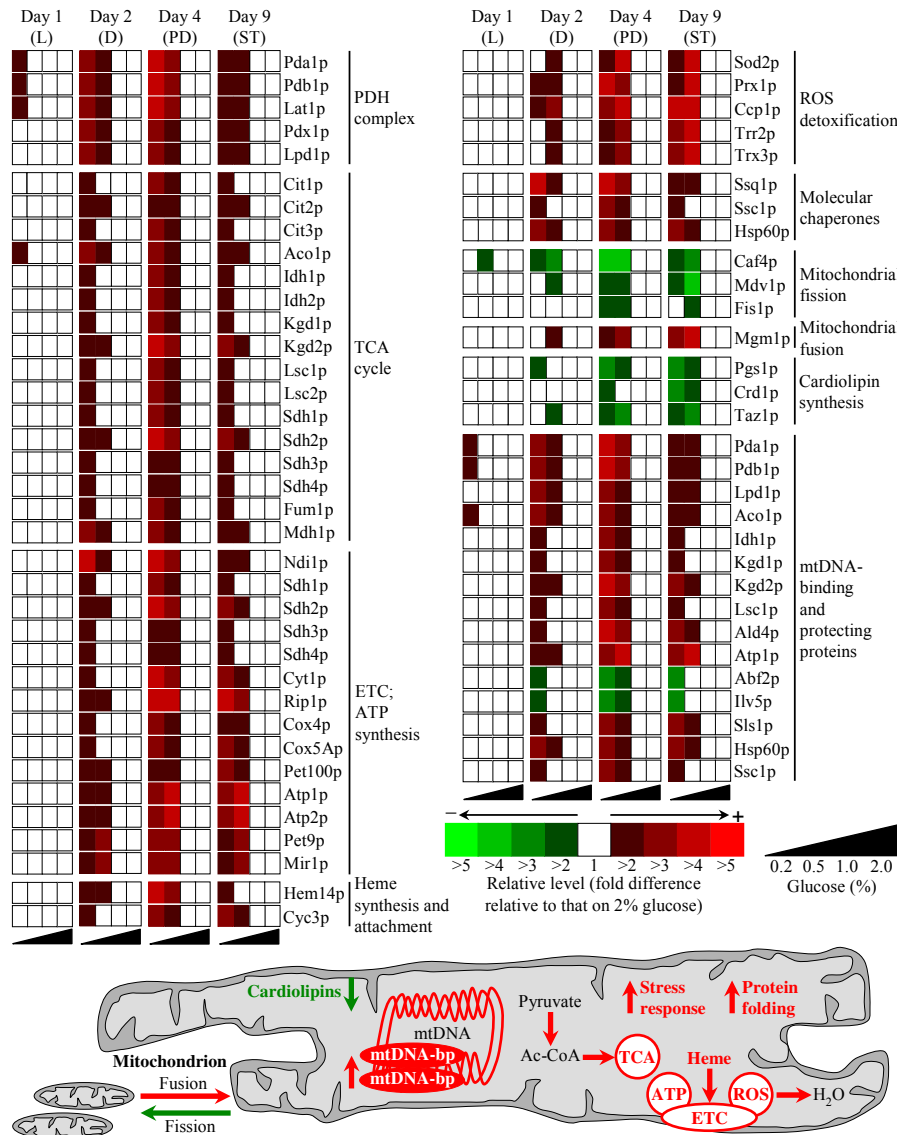


Figure 2.2. CR alters the abundance of a distinct set of proteins in mitochondria of chronologically aging yeast. Relative levels (fold difference relative to that on 2% glucose) of proteins recovered in purified yeast mitochondria. Proteins were identified and quantitated using mass spectrometry. The complete list of proteins and their relative levels are provided in Tables 2.1 and 2.2, respectively. From the data of proteomic analysis, I inferred an outline of mitochondria-confined processes that were activated (red arrows) or inhibited (green arrows) by CR prior to entry of yeast into the non-proliferative ST phase. Abbreviations: Ac-CoA, acetyl-CoA; ETC, the mitochondrial electron transport chain; mtDNA, mitochondrial DNA; mtDNA-bp, mitochondrial DNA-binding proteins; PDH, the mutienzyme pyruvate dehydrogenase complex; ROS, reactive oxygen species; TCA, the tricarboxylic acid cycle in mitochondria.

CR and non-CR cells [32]. Our comparative analysis of mitochondrial proteomes of CR and non-CR yeast revealed that CR altered the levels of numerous proteins that function in essential processes confined to mitochondria (Figure 2.2).

In studies described in this chapter of the thesis, we investigated the spectrum of mitochondrial processes affected by CR. These studies revealed that CR modulates oxidation-reduction processes and ROS production in yeast mitochondria, reduces the frequency of mtDNA mutations, and alters the abundance and mtDNA-binding activity of mitochondrial nucleoid-associated proteins. Our findings provide evidence that these mitochondria-confined processes play essential roles in regulating longevity of chronologically active yeast by defining their viability during ST growth phase, following cell entry into a quiescent state.

2.3 Materials and Methods

Strains and media

The wild-type strain BY4742 (*MAT α his3 Δ 1 leu2 Δ 0 lys2 Δ 0 ura3 Δ 0*) was grown in YP medium (1% yeast extract, 2% peptone) containing 0.2%, 0.5%, 1% or 2% glucose as carbon source. Cells were cultured at 30°C with rotational shaking at 200 rpm in Erlenmeyer flasks at a “flask volume/medium volume” ratio of 5:1.

Oxygen consumption assay

The rate of oxygen consumption by yeast cells recovered at various time points was measured continuously in a 2-ml stirred chamber using a custom-designed biological oxygen monitor (Science Technical Center of Concordia University) equipped with a

Clark-type oxygen electrode. 1 ml of YP medium supplemented with 0.2% glucose was added to the electrode for approximately 5 minutes to obtain a baseline. Cultured cells of a known titre were spun down at $3,000 \times g$ for 5 minutes. The resulting pellet was resuspended in YP medium supplemented with 0.2% glucose and then added to the electrode with the medium that was used to obtain a baseline. The resulting slope was used to calculate the rate of oxygen consumption in $O_2\% \times \text{min}^{-1} \times 10^9$ cells.

Monitoring the formation of ROS

Cells grown in YP medium containing 0.2%, 0.5%, 1% or 2% glucose as carbon source were tested microscopically for the production of ROS by incubation with dihydrorhodamine 123 (DHR). In the cell, this nonfluorescent compound can be oxidized to the fluorescent chromophore rhodamine 123 by ROS. Cells were also probed with a fluorescent counterstain Calcofluor White M2R (CW), which stains the yeast cell walls fluorescent blue. CW was added to each sample in order to label all cells for their proper visualization. DHR was stored in the dark at -20°C as 50 μl aliquots of a 1 mg/ml solution in ethanol. CW was stored in the dark at -20°C as the 5 mM stock solution in anhydrous DMSO (dimethylsulfoxide).

The concurrent staining of cells with DHR and CW was carried out as follows. The required amounts of the 50 μl DHR aliquots (1 mg/ml) and of the 5 mM stock solution of CW were taken out of the freezer and warmed to room temperature. The solutions of DHR and CW were then centrifuged at $21,000 \times g$ for 5 min in order to clear them of any aggregates of fluorophores. For cell cultures with a titre of $\sim 10^7$ cells/ml, 100 μl was taken out of the culture to be treated. If the cell titre was lower, proportionally larger

volumes were used. 6 μl of the 1 mg/ml DHR and 1 μl of the 5 mM CW solutions were added to each 100 μl aliquot of culture. After a 2-h incubation in the dark at room temperature, the samples were centrifuged at $21,000 \times g$ for 5 min. Pellets were resuspended in 10 μl of PBS buffer (20 mM $\text{KH}_2\text{PO}_4/\text{KOH}$, pH 7.5, and 150 mM NaCl). Each sample was then supplemented with 5 μl of mounting medium, added to a microscope slide, covered with a coverslip, and sealed using nail polish. Once the slides were prepared, they were visualized under the Zeiss Axioplan fluorescence microscope mounted with a SPOT Insight 2 megapixel color mosaic digital camera. Several pictures of the cells on each slide were taken, with two pictures taken of each frame. One of the two pictures was of the cells seen through a rhodamine filter in order to detect cells dyed with DHR. The second picture was of the cells seen through a DAPI filter in order to visualize CW, and therefore all the cells present in the frame.

For evaluating the percentage of DHR-positive cells, the UTHSCSA Image Tool (Version 3.0) software was used to calculate both the total number of cells and the number of stained cells. Fluorescence of individual DHR-positive cells in arbitrary units was determined by using the UTHSCSA Image Tool software (Version 3.0). In each of 3-5 independent experiments, the value of median fluorescence was calculated by analyzing at least 800-1000 cells that were collected at each time point. The median fluorescence values were plotted as a function of the number of days cells were cultured.

Monitoring the mitochondrial membrane potential

The mitochondrial membrane potential ($\Delta\Psi$) was measured in live yeast by fluorescence microscopy of Rhodamine 123 (R123) staining. For R123 staining, 5×10^6 cells were

harvested by centrifugation for 1 min at $21,000 \times g$ at room temperature and then resuspended in 100 μ l of 50 mM sodium citrate buffer (pH 5.0) containing 2% glucose. R123 (Invitrogen) was added to a final concentration of 10 μ M. Following incubation in the dark for 30 min at room temperature, the cells were washed twice in 50 mM sodium citrate buffer (pH 5.0) containing 2% glucose and then analyzed by fluorescence microscopy. Images were collected with a Zeiss Axioplan fluorescence microscope (Zeiss) mounted with a SPOT Insight 2 megapixel color mosaic digital camera (Spot Diagnostic Instruments). For evaluating the percentage of R123-positive cells or cells with fragmented nucleus the UTHSCSA Image Tool (Version 3.0) software was used to calculate both the total number of cells and the number of stained cells or cells with fragmented nucleus. Fluorescence of individual R123-positive cells in arbitrary units was determined by using the UTHSCSA Image Tool software (Version 3.0). In each of 3-6 independent experiments, the value of median fluorescence was calculated by analyzing at least 800-1000 cells that were collected at each time-point. The median fluorescence values were plotted as a function of the number of days cells were cultured.

Measurement of mitochondrial mutations and nuclear mutations affecting mitochondrial components

The frequency of spontaneous single-gene (*mit⁻* and *syn⁻*) and deletion (*rho⁻* and *rho^o*) mutations in mtDNA and spontaneous single-gene nuclear mutations (*pet⁻*) affecting essential mitochondrial components was evaluated by measuring the fraction of respiratory-competent (*rho⁺*) yeast cells remaining in their aging population. *rho⁺* cells maintained intact their mtDNA and their nuclear genes encoding essential mitochondrial

components. Therefore, *rho*⁺ cells were able to grow on glycerol, a non-fermentable carbon source. In contrast, mutant cells deficient in mitochondrial respiration were unable to grow on glycerol. Most of these mutant cells carried mutations in mtDNA (including single-gene *mit*⁻ and *syn*⁻ mutations or large deletions *rho*⁻) or completely lacked this DNA (*rho*^o mutants), whereas some of them carried so-called *pet*⁻ mutations in nuclear genes that code for essential mitochondrial components [140]. Serial dilutions of cell samples removed from different phases of growth were plated in duplicate onto YP plates containing either 2% glucose or 3% glycerol as carbon source. Plates were incubated at 30°C. The number of CFU on YP plates containing 2% glucose was counted after 2 d of incubation, whereas the number of CFU on YP plates containing 3% glycerol was counted after 6 d of incubation. For each culture, the percentage of respiratory-deficient (*mit*⁻, *syn*⁻, *rho*⁻, *rho*^o and *pet*⁻) cells was calculated as follows: $100 - \left[\frac{\text{number of CFU per ml on YP plates containing 3\% glycerol}}{\text{number of CFU per ml on YP plates containing 2\% glucose}} \times 100 \right]$. The frequency of spontaneous point mutations in the *rib2* and *rib3* loci of mtDNA was evaluated by measuring the frequency of mtDNA mutations that caused resistance to the antibiotic erythromycin [141]. These mutations impair only mtDNA [142, 143]. In each of the seven independent experiments performed, ten individual yeast cultures were grown in YP medium containing 0.2%, 0.5%, 1% or 2% glucose as carbon source. A sample of cells was removed from each culture at various time-points. Cells were plated in duplicate onto YP plates containing 3% glycerol and erythromycin (1 mg/ml). In addition, serial dilutions of each sample were plated in duplicate onto YP plates containing 3% glycerol as carbon source for measuring the number of respiratory-competent (*rho*⁺) cells. The number of CFU was counted after 6 d

of incubation at 30°C. For each culture, the frequency of mutations that caused resistance to erythromycin was calculated as follows: number of CFU per ml on YP plates containing 3% glycerol and erythromycin/number of CFU per ml on YP plates containing 3% glycerol.

Isolation of the crude mitochondrial fraction

The crude mitochondrial fraction was isolated as we described previously [144]. Yeast cells were pelleted at $3,000 \times g$ for 5 min at room temperature, washed twice with distilled water, resuspended in DTT buffer (100 mM Tris- H_2SO_4 , pH 9.4, 10 mM dithiothreitol [DTT]), and incubated for 20 min at 30°C to weaken the cell wall. The cells were then washed with Zymolyase buffer (1.2 M sorbitol, 20 mM potassium phosphate, pH 7.4), centrifuged at $3,000 \times g$ for 5 min at room temperature, and incubated with 3 mg/g (wet wt) of Zymolyase-100T in 7 ml/g (wet wt) Zymolyase buffer for 45 min at 30°C. Following an 8-min centrifugation at $2,200 \times g$ at 4°C, the isolated spheroplasts were washed in ice-cold homogenization buffer (5 ml/g) (0.6 M sorbitol, 10 mM Tris-HCl, pH 7.4, 1 mM EDTA, 0.2% (w/v) BSA) and then centrifuged at $2,200 \times g$ for 8 min at 4°C. Washed spheroplasts were homogenized in ice-cold homogenization buffer using 15 strokes. The cell debris was removed by centrifuging the resulting homogenates at $1,500 \times g$ for 5 min at 4°C. The supernatant was further centrifuged at $3,000 \times g$ for 5 min at 4°C to remove residual cell debris. The resulting supernatant was then centrifuged at $12,000 \times g$ for 15 min at 4°C to pellet mitochondria. The remnant cell debris was removed by centrifuging the mitochondrial fraction at $3,000 \times g$ for 5 min at 4°C. The resulting supernatant was then centrifuged at $12,000 \times g$ for 15 min at 4°C to obtain the

crude mitochondrial pellet, which was then resuspended in 3 ml of SEM Buffer (250 mM sucrose, 1 mM EDTA, 10 mM MOPS, pH 7.2) and used for the purification of mitochondria as described below.

Purification of mitochondria devoid of microsomal and cytosolic contaminations

Mitochondria devoid of microsomal and cytosolic contaminations were purified as we described previously [144]. A sucrose gradient was made by carefully overlaying 1.5 ml of 60% sucrose with 4 ml of 32% sucrose, 1.5 ml of 23% sucrose, and then 1.5 ml of 15% sucrose (all in EM buffer; 1 mM EDTA, 10 mM MOPS, pH 7.2). Finally, a 3-ml aliquot of the crude mitochondrial fraction in SEM buffer was applied to the gradient and centrifuged at $134,000 \times g$ (33,000 rpm) overnight at 4°C in vacuum (Rotor SW50Ti, Beckman). The purified mitochondria found at the 60%/32% sucrose interface were carefully removed and stored at - 80°C.

Purification of proteins that bind to mitochondrial DNA (mtDNA)

Purification of *in organello* formaldehyde-fixed proteins that bind to mtDNA was performed as previously described [145, 146]. Purified mitochondria were diluted in FB15 buffer (10 mM Tricine/KOH, pH 7.5, 0.1 mM EDTA, 50 mM NaCl, 15% sucrose) and pelleted by centrifugation at $40,000 \times g$ at 4°C for 1.5 h. The sedimented mitochondria were resuspended (10 mg/ml) in FB15, adjusted to 40 mM Tris/HCl, pH 8.0, 2.5 mM MgCl₂ and treated with DNase I (1 unit/50 µg) for 1 h on ice. The reaction was terminated with 5 mM EDTA, pH 8.0; the mitochondria were pelleted, washed with RB buffer (20 mM HEPES, pH 7.6, 2 mM EDTA, 1 mM EGTA, 0.5 M sucrose), and

diluted to 2 mg/ml in CB buffer (RB buffer plus 50 mM Hepes, 50 mM NaCl, 7 mM β -mercaptoethanol, 1 mM PMSF, 1 mM spermidine, 1 \times Protease Inhibitor mixture from Roche Molecular Biochemicals). Formaldehyde was added to the final concentration of 1%, and the mitochondria were incubated at 4°C for 16 h with slow mixing. The reaction was quenched with 125 mM glycine, pH 7.0, and the mitochondria were pelleted, resuspended in CB buffer plus 50 mM glycine, and lysed with 0.5% NP-40. The lysate was diluted 3-fold, and the mtDNA-enriched pellet was collected by centrifugation (110,000 \times g, 4°C, 1 h) through 20% sucrose (in 50 mM HEPES, pH 7.6, 50 mM NaCl, 0.5% NP-40). The pellet was resuspended in CB buffer using a dounce homogenizer and treated with 1% sarkosyl and RNase A (50 μ g/ml) for 1 h at room temperature. The mixture was adjusted to RI = 1.365 with CsCl (in TE, 1% sarkosyl), and 5 mg of the purified mitochondria was loaded into 11-ml tubes. Gradients were centrifuged (260,000 \times g, 25°C, 16 h) in a fixed angle rotor and fractionated into 0.5-ml fractions.

Miscellaneous procedures

SDS-PAGE and immunoblotting using a Trans-Blot SD semi-dry electrophoretic transfer system (Bio-Rad) were performed as previously described [147]. Blots were decorated with polyclonal antisera raised against Aco1p (kind gift of the late Dr. Ronald A. Butow, University of Texas Southwestern Medical Center). Antigen-antibody complexes were detected by enhanced chemiluminescence using an Amersham ECL Western blotting detection reagents (GE Healthcare). Enzymatic activities of cytochrome c oxidase [148], succinate dehydrogenase [149] and aconitase [150] were determined by established methods.

2.4 Results

2.4.1 In chronologically aging yeast, CR modulates oxidation-reduction processes in mitochondria and alters the age-related dynamics of mitochondrially produced ROS

Because our comparative analysis of mitochondrial proteomes of CR and non-CR yeast revealed that CR altered the levels of numerous proteins that function in essential processes confined to mitochondria (Figure 2.2) [32], we sought to define the spectrum of mitochondrial processes affected by CR. We found that, through D, PD and ST phases, mitochondria of CR yeast maintained the amplified rate of oxygen consumption, elevated the mitochondrial membrane potential ($\Delta\Psi$), and increased enzymatic activities of cytochrome c oxidase (CCO), succinate dehydrogenase (SDH) and aconitase (ACO), as compared to mitochondria of non-CR yeast (Figure 2.3). The observed amplification of these essential mitochondrial processes in CR yeast can be adequately explained by the CR-promoted rise in the levels of mitochondrial proteins that serve the formation of acetyl-CoA from pyruvate and its subsequent oxidation via the tricarboxylic acid (TCA) cycle, electron transport, and ATP-producing oxidative phosphorylation (Figure 2.2).

Despite the elevated levels of cytosolic and mitochondrial ROS scavenging proteins in CR yeast (Figure 2.2), CR elevated the level of intracellular ROS (Figure 2.3E). ROS are mostly generated as by-products of mitochondrial respiration [152 - 154]. Thus, it is conceivable that, by promoting electron flow through the mitochondrial electron transport chain (ETC), CR enhanced the ROS-generating transfer of a single electron to oxygen in mitochondria.

We also found that the degree of CR influenced essential mitochondrial processes and activities such as oxygen consumption and ROS production, the establishment and maintenance of $\Delta\Psi$, and enzymatic activities of CCO, SDH and ACO. In fact, in CR yeast grown on 0.2% glucose, a glucose concentration providing only a moderate CR-dependent lifespan extension, the efficiencies of all these processes and enzymatic activities were 1) greatly amplified when yeast entered D phase; and 2) sharply declined through the following PD and ST phases (Figure 2.3). Of note, the sharply declined activity of ACO recovered from CR yeast grown on 0.2% glucose could be substantially increased *in vitro* by incubation of cell lysate with Fe^{3+} and S^{2-} (Figure 2.3F), which are able to restore the oxidation-dependent loss of one iron from the [4Fe-4S] cluster of ACO [155]. As we found, in CR yeast grown on 0.5% glucose, a glucose concentration that provides the maximal benefit of CR for longevity, the efficiencies of all these mitochondrial processes and enzymatic activities were 1) amplified to a much lesser extent during D phase than they were amplified in yeast grown on 0.2% glucose; and 2) reached a plateau in PD phase and remained mainly unchanged during the following ST phase (Figure 2.3). During the non-proliferative ST phase, the efficiencies and activities of all monitored mitochondrial processes and enzymes in CR yeast grown on 0.5% glucose exceeded those seen in CR yeast grown on 0.2% glucose.

Altogether, these findings suggest that the observed early spike in oxygen consumption by mitochondria of yeast grown on 0.2% glucose, which exceeded the modest increase seen in yeast grown on 0.5% glucose, resulted in a greatly elevated level of mitochondrial ROS. This, in turn, led to the oxidative damage and inactivation of CCO, SDH, ACO and, perhaps, some other components of the mitochondrial ETC and

TCA cycle. Late in ST phase, the resulting decline in the rate of electron flow through the mitochondrial ETC of yeast grown on 0.2% glucose substantially decreased mitochondrial ROS below the level observed in mitochondria of yeast grown on 0.5% glucose (Figure 2.3).

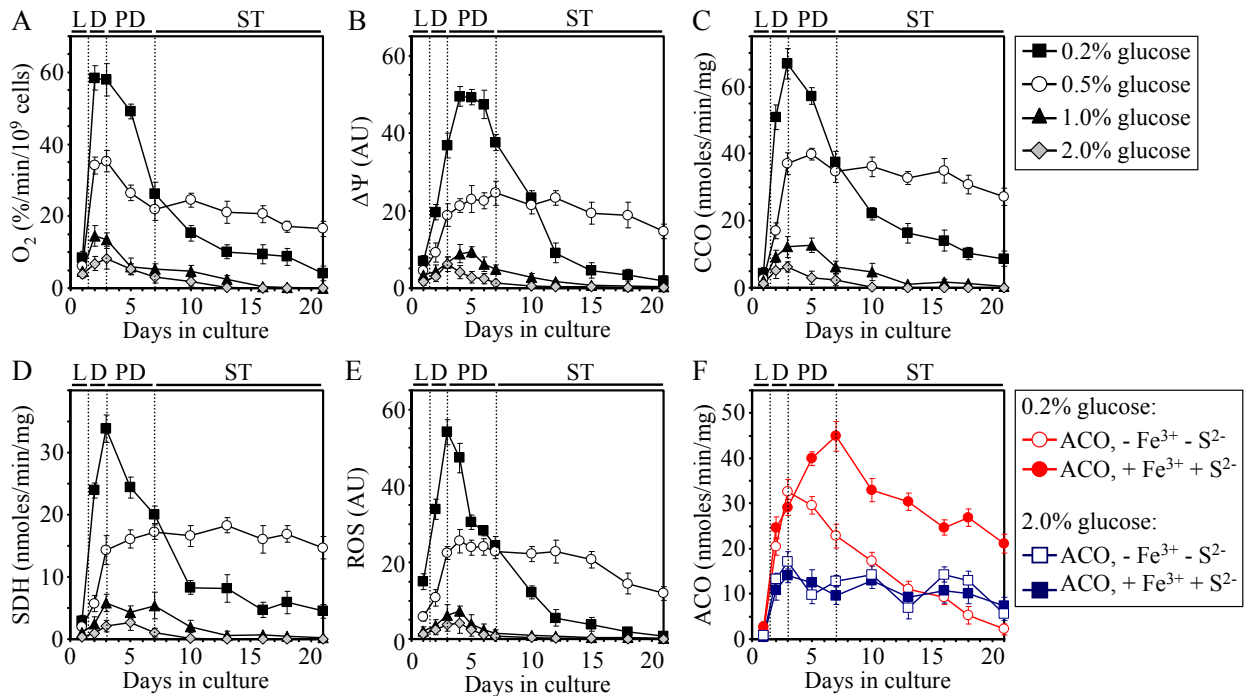


Figure 2.3. CR influences oxidation-reduction processes in mitochondria and modulates the level of mitochondrially produced ROS. (A) The dynamics of age-dependent changes in the rate of oxygen consumption by cells. Data are presented as mean \pm SEM (n = 15-19). (B) The dynamics of age-dependent changes in the mitochondrial membrane potential ($\Delta\Psi$) during chronological aging of yeast. $\Delta\Psi$ was visualized using R123. At least 800 cells were used for quantitation of R123 staining for each of 3 independent experiments. Data are presented as mean \pm SEM (n = 15-19). (C and D) Enzymatic activities of CCO (C) and SDH (D) in purified mitochondria. Data are presented as mean \pm SEM (n = 6-10). (E) The dynamics of age-dependent changes in the intracellular levels of ROS during chronological aging of yeast. ROS were visualized using DHR. At least 800 cells were used for quantitation of DHR staining for each of 5 independent experiments. Data are presented as mean \pm SEM (n = 8-13). (F) Enzymatic activities of ACO in total cell lysates. The ACO activity was measured with or without the reactivation agents Fe³⁺ and Na₂S.

Data are presented as mean \pm SEM (n = 5). (A-E) Cells were cultured in YP media initially containing four different concentrations of glucose. (F) Cells were cultured in YP medium initially containing 0.2% or 2% glucose.

2.4.2 CR influences the frequency of mitochondrial DNA (mtDNA) mutations and modulates the abundance and mtDNA-binding activity of mitochondrial nucleoid-associated proteins

Our data imply that the observed during D and PD phases spike in ROS production by mitochondria of CR yeast grown on 0.2% glucose can oxidatively damage their mtDNA, eventually (*i.e.*, during ST phase) introducing deletions and point mutations into it. In fact, during ST phase, the population of these CR cells accumulated an increasing fraction of respiratory-deficient mutants (Figure 2.4A). Most of these mutants are known to carry mutations in mtDNA (including single-gene *mit⁻* and *syn⁻* mutations or large deletions *rho⁻*) or completely lack mtDNA (*rho^o* mutants), whereas some of them carry so-called *pef* mutations in nuclear genes that code for essential mitochondrial components [156, 157]. We also found that only cells under CR at 0.2% glucose exhibited an increased frequency of mtDNA mutations that caused resistance to erythromycin (Figure 2.4B). Resistance to this antibiotic can be acquired only through a distinct set of point mutations in the mitochondrial *rib2* and *rib3* genes that encode two different rRNAs confined to mitochondria [158 - 160]. Noteworthy, the highest amplitude of the early spike in ROS production by yeast under CR at 0.2% glucose (Figure 2.4E) correlated with their elevated frequencies of mtDNA mutations (Figures 2.4A and 2.4B) and shortened lifespan (Figures 2.1C and 2.1D), as compared to yeast under CR at 0.5% glucose. Thus, it is conceivable that the frequency of ROS-induced

deletions and point mutations in mtDNA influence yeast longevity under CR conditions. This hypothesis could satisfactorily explain my observation that yeast under CR at 0.5% glucose live longer than yeast under CR at 0.2% glucose. Conversely, it seems that the frequency of mtDNA deletions and point mutations does not affect the longevity of chronologically aging yeast grown on 1% or 2% glucose, *i.e.* under non-CR conditions. In fact, we found that, despite these yeast had much lower frequencies of mtDNA mutations than CR yeast grown on 0.2% glucose (Figures 2.4A and 2.4B), they lived a shorter life (Figures 2.1C and 2.1D).

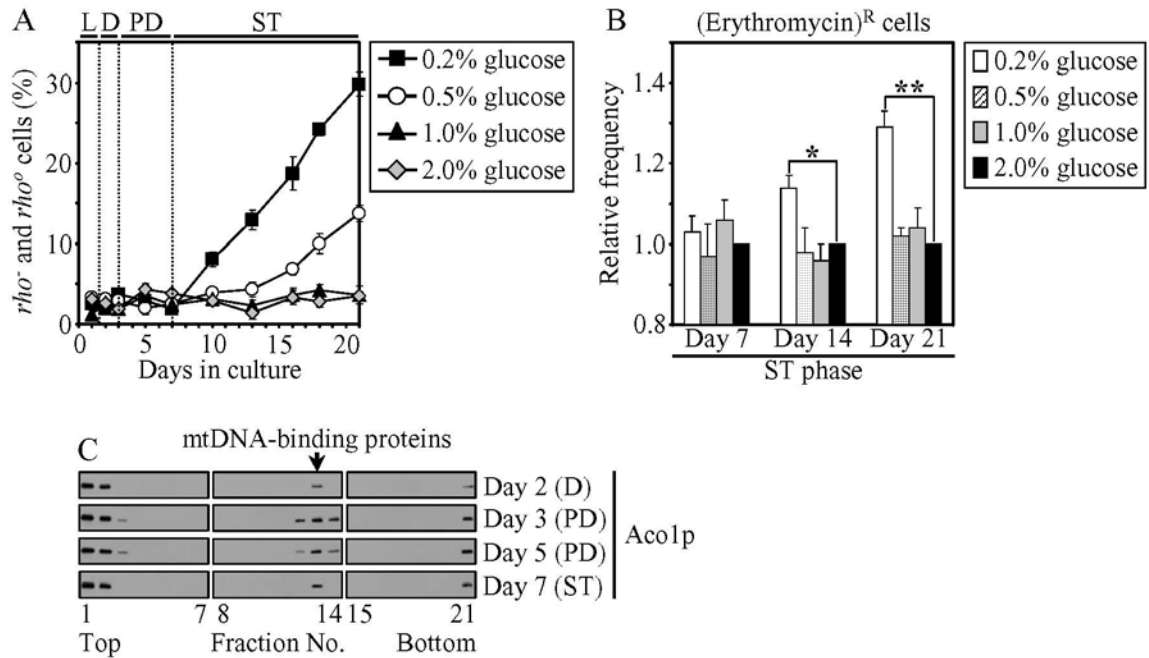


Figure 2.4. CR modulates the frequency of mtDNA mutations and influences the efficiency of aconitase binding to mtDNA. (A) The percentage of respiratory-deficient cells that were unable to grow in medium containing 3% glycerol because they carried large mtDNA deletions (ρ^{-}) or lacked mtDNA (ρ^{0}). Data are presented as mean \pm SEM (n = 7). (B) Relative frequencies (fold difference relative to that on 2% glucose) of mtDNA point mutations that caused resistance to erythromycin. Data are presented as mean \pm SEM (n = 70); *p < 0.01, **p < 0.001. (C) Western blot analysis of aconitase (Aco1p) recovery in fractions of a CsCl gradient that was used for the purification of mitochondrial nucleoids. The peak fraction for the

mitochondrial Aco1p-DNA complex (arrow) is indicated. (A and B) Cells were cultured in YP media initially containing four different concentrations of glucose. (C) Cells were cultured in YP medium initially containing 0.2% glucose.

It should be emphasized that the observed elevated frequencies of mtDNA deletions and point mutations in CR yeast grown on 0.2% glucose occurred despite an effort that these yeast have made to protect the stability of mtDNA by remodeling mitochondrial nucleoids early in their life. In fact, during D and PD phases, these CR yeast induced the synthesis of a distinct set of mtDNA-binding proteins (Figure 2.2) known for their essential role in maintaining mtDNA and protecting it from oxidative damage [157]. One of these proteins, the TCA-cycle enzyme aconitase (Aco1p) known for its ability to interact with mtDNA and to maintain its integrity when cells are shifted to respiratory conditions [161], associated with mtDNA of aging CR yeast grown on 0.2% glucose (Figure 2.4C). As we found, the efficiency of such Aco1p binding to mtDNA at different stages of the aging process (Figure 2.4C) correlated with the concentration of ROS generated by mitochondria of these CR yeast (Figure 2.3E). Of note, CR decreased the levels of mitochondrial Abf2p and Ilv5p (Figure 2.2), the two mtDNA-binding proteins that associate with mitochondrial nucleoids under conditions of low respiration or amino-acid starvation, respectively [157]. Therefore, we suggest the following scenario for metabolic remodeling of mitochondrial nucleoids in chronologically aging CR yeast. In response to the early spike in oxygen consumption and ROS generation by their mitochondria, CR yeast induce the synthesis of Aco1p and other bifunctional mitochondrial proteins that, in addition to their essential role in respiratory metabolism, are able to interact specifically with mtDNA. Concomitantly, CR

yeast repress the synthesis of both Abf2p and Ilv5p. Because of their increased concentrations and due to their partial oxidation by mitochondrial ROS, Aco1p and other mtDNA-binding proteins bind to mtDNA in order to protect it from oxidative damage. Such binding of Aco1p and other respiratory-metabolism sensing proteins to mtDNA may substitute for Abf2p and Ilv5p, thereby remodeling mitochondrial nucleoids by converting them into the conformation that is more resistant to oxidative damage. Noteworthy, the level of Aco1p in yeast cells is known to be modulated by the mitochondrial retrograde (RTG) signaling pathway. This pathway activates transcription of the *ACO1* gene in response to a decline in mitochondrial respiratory function caused by mtDNA damage [162, 163]. It is conceivable therefore that chronologically aging CR yeast respond to the partial oxidative damage of their mtDNA by turning on the RTG pathway. By activating transcription of *ACO1* and, perhaps, other genes encoding bifunctional mtDNA-binding proteins known to maintain the integrity of mtDNA in yeast shifted to respiratory conditions [161, 162], this signaling pathway may govern the resulting conversion of mitochondrial nucleoids into the conformation that is more resistant to oxidative damage.

2.5 Discussion

Findings described in this chapter of my thesis suggest a hypothesis that ROS, which are mostly generated as by-products of mitochondrial respiration [152 - 154], play a dual role in regulating longevity of chronologically aging yeast. First, if yeast mitochondria are unable (due to a dietary regimen) to maintain ROS concentration below a toxic threshold, ROS promote aging by oxidatively damaging certain mitochondrial

proteins (such as CCO, SDH and ACO) and mtDNA. In fact, we found that the highest amplitude of the early spike in ROS production in CR yeast entering D phase on 0.2% glucose (Figure 2.3E) correlated with their 1) shortened (as compared to CR yeast grown on 0.5% glucose) lifespan (Figures 2.1C and 2.1D); 2) sharply declined activities of CCO, SDH and ACO through the following PD and ST phases (Figures 2.3C, 2.3D and 2.3F); and 3) elevated frequencies of mtDNA deletions and point mutations, as compared to yeast under CR at 0.5% glucose (Figures 2.4A and 2.4B). Second, if yeast mitochondria can (due to a dietary regimen) maintain ROS concentration at a certain “optimal” level, ROS delay chronological aging. We propose that this “optimal” level of ROS is insufficient to damage cellular macromolecules but can activate certain signaling networks [152 - 154, 164] that extend lifespan by increasing the abundance or activity of stress-protecting and other anti-aging proteins; the term “mitohormesis” has been coined for such anti-aging role of mitochondrially produced ROS [165]. Indeed, we found that elevated (as compared to non-CR yeast) ROS concentrations in CR yeast (Figure 2.3E) correlated with their extended chronological longevity (Figures 2.1C and 2.1D), increased abundance of numerous mitochondrial and cytosolic anti-stress chaperones and mtDNA-binding proteins (Figure 2.2), and augmented resistance to chronic thermal and oxidative stresses [32]. Moreover, although the low concentration of ROS seen in non-CR yeast could play a key role in protecting their mtDNA from “spontaneous” mutagenesis (Figures 2.4A and 2.4B), the inability of these yeast to generate ROS in sufficiently high, “optimal” quantities could contribute to their lowered (as compared to CR yeast) levels of cytosolic and mitochondrial stress-protecting proteins (Figure 2.2) and reduced resistance to chronic thermal and oxidative stresses [32]. Noteworthy, the

view that mitochondrially produced ROS in “optimal” concentrations contribute to extension of yeast lifespan by promoting “mitohormesis” is controversial [166, 167].

Studies presented in this chapter of my thesis also imply that mtDNA mutations do not contribute to longevity regulation in non-CR yeast grown on 1% or 2% glucose. In fact, despite these yeast lived a shorter life than CR yeast grown on 0.2% glucose (Figures 2.1C and 2.1D), they had much lower frequencies of mtDNA deletions and point mutations, as compared to yeast under CR at 0.2% glucose (Figures 2.4A and 2.4B). In contrast, it seems that the frequency of mtDNA mutations is an important contributing factor to yeast longevity under CR conditions. Indeed, the elevated frequencies of mtDNA mutations in yeast under CR at 0.2% glucose (Figures 2.4A and 2.4B) correlated with their shortened lifespan, as compared to yeast under CR at 0.5% glucose (Figures 2.1C and 2.1D).

2.6 Conclusions

As the reported here investigation of the spectrum of mitochondrial processes affected by CR revealed, the low-calorie diet modulates oxidation-reduction processes and ROS production in yeast mitochondria, reduces the frequency of mtDNA mutations, and alters the abundance and mtDNA-binding activity of mitochondrial nucleoid-associated proteins. These findings provide evidence that these mitochondria-confined processes play essential roles in regulating longevity of chronologically active yeast by defining cell viability following entry into a quiescent state. A challenge for the future will be to examine whether the pattern established in yeast cells grown under CR conditions can be reversed upon their transfer to calorie-rich medium. Another challenge

for the future will be to test the validity of the proposed here hypothesis that chronologically aging CR yeast protect their mitochondrial nucleoids from oxidative damage by turning on the RTG signaling pathway, which then activates transcription of *ACO1* and other genes encoding bifunctional mtDNA-binding proteins known to maintain the integrity of mtDNA under respiratory conditions. It is conceivable that this knowledge will be instrumental for designing high-throughput screens aimed at discovering novel anti-aging drugs and natural compounds that can increase lifespan by modulating the longevity-defining processes confined to mitochondria.

3 Caloric restriction (CR) extends yeast chronological lifespan by altering a pattern of age-related changes in trehalose concentration

3.1 Abstract

The nonreducing disaccharide trehalose has been long considered only as a reserve carbohydrate. However, recent studies in yeast suggested that this osmolyte can protect cells and cellular proteins from oxidative damage elicited by exogenously added reactive oxygen species (ROS). Trehalose has been also shown to affect stability, folding and aggregation of bacterial and firefly proteins heterologously expressed in heat-shocked yeast cells. Our recent investigation of how a lifespan-extending caloric restriction (CR) diet alters the metabolic history of chronologically aging yeast suggested that their longevity is programmed by the level of metabolic capacity - including trehalose biosynthesis and degradation - that yeast cells developed prior to entry into quiescence [32]. To investigate whether trehalose homeostasis in chronologically aging yeast may play a role in longevity extension by CR, in studies described in this chapter of my thesis we examined how single-gene-deletion mutations affecting trehalose biosynthesis and degradation impact 1) the age-related dynamics of changes in trehalose concentration; 2) yeast chronological lifespan under CR conditions; 3) the chronology of oxidative protein damage, intracellular ROS level and protein aggregation; and 4) the timeline of thermal inactivation of a protein in heat-shocked yeast cells and its subsequent reactivation in yeast returned to low temperature. Our data imply that CR extends yeast chronological lifespan in part by altering a pattern of age-related changes in trehalose concentration. We outline a model for molecular mechanisms underlying the

essential role of trehalose in defining yeast longevity by modulating protein folding, misfolding, unfolding, refolding, oxidative damage, solubility and aggregation throughout lifespan.

3.2 Introduction

CR, a dietary regimen in which only calorie intake is reduced but the supply of amino acids, vitamins and other nutrients is not compromised, is known to have the most profound longevity-extending effect across phyla and to improve overall health by delaying the onset of age-related diseases [3, 9, 47 - 49, 168]. The longevity benefit associated with CR is mediated by a signaling network that integrates the insulin/insulin-like growth factor 1 (IGF-1), AMP-activated protein kinase/target of rapamycin (AMPK/TOR) and cAMP/protein kinase A (cAMP/PKA) longevity regulation pathways and governs a distinct group of cellular processes [3, 9, 30, 33, 36, 40]. Our recent investigation of how CR alters the metabolic history of chronologically aging yeast suggested that trehalose metabolism is one of these longevity-defining processes [32]. Trehalose is a nonreducing disaccharide that until recently has been considered only as a reserve carbohydrate [169]. However, the demonstrated abilities of this osmolyte to protect yeast cells and cellular proteins from oxidative damage caused by exogenously added ROS [170] and to impact stability, folding and aggregation of bacterial and firefly proteins heterologously expressed in heat-shocked yeast [171, 172] suggested that trehalose may exhibit similar effects on endogenous proteins in cells of yeast and other organisms [171 - 174]. It is conceivable therefore that trehalose may be involved in modulating cellular protein homeostasis (proteostasis). By maintaining proper synthesis,

post-translational modifications, folding, trafficking, degradation and turnover of proteins within a cell, an evolutionarily conserved proteostasis network governs various cellular activities, influences diverse age-related pathologies, and defines organismal healthspan and longevity [175, 176].

To evaluate a potential role of trehalose in lifespan extension by CR, in studies described in this chapter of the thesis we monitored how single-gene-deletion mutations that alter trehalose concentrations in pre-quiescent and quiescent yeast cells affect longevity of chronologically aging yeast under CR conditions. We also elucidated how these mutations influence the chronology of oxidative protein carbonylation, intracellular ROS, protein aggregation, thermal inactivation of a protein in heat-shocked yeast cells and a subsequent reactivation of this protein in yeast shifted to low temperature. Our findings provide evidence that the longevity-extending effect of a CR diet in chronologically aging yeast is due in part to a specific pattern of age-related changes in trehalose concentration elicited by CR. Based on these findings, we propose a model for molecular mechanisms by which trehalose modulates cellular proteostasis throughout lifespan, thereby defining yeast longevity.

3.3 Materials and Methods

Yeast strains and growth conditions

The wild-type (WT) strain BY4742 (*MAT α his3 Δ 1 leu2 Δ 0 lys2 Δ 0 ura3 Δ 0*) and single-gene-deletion mutant strains in the BY4742 genetic background (all from Open Biosystems) were grown in YP medium (1% yeast extract, 2% peptone) containing 0.2%

glucose as carbon source. Cells were cultured at 30°C with rotational shaking at 200 rpm in Erlenmeyer flasks at a “flask volume/medium volume” ratio of 5:1.

Chronological lifespan assay

A sample of cells was taken from a culture at a certain time-point. A fraction of the sample was diluted in order to determine the total number of cells using a hemacytometer. Another fraction of the cell sample was diluted and serial dilutions of cells were plated in duplicate onto YP plates containing 2% glucose as carbon source. After 2 d of incubation at 30°C, the number of colony forming units (CFU) per plate was counted. The number of CFU was defined as the number of viable cells in a sample. For each culture, the percentage of viable cells was calculated as follows: (number of viable cells per ml/total number of cells per ml) × 100. The percentage of viable cells in mid-logarithmic phase was set at 100%. The lifespan curves were validated using a LIVE/DEAD yeast viability kit (Invitrogen) following the manufacturer's instructions.

Trehalose concentration measurement

Preparation of alkali cellular extract and a microanalytic biochemical assay for measuring trehalose concentration were performed as previously described [177]. To prepare an alkali cellular extract, 2×10^9 cells were harvested by centrifugation for 1 min at 21,000 × g at 4°C. The cells were washed three times in ice-cold PBS (20 mM KH₂PO₄/KOH, pH 7.5, and 150 mM NaCl). The cell pellet was quickly resuspended in 200 µl of ice-cold SHE solution (50 mM NaOH, and 1 mM EDTA), and 800 µl of ice-cold SHE solution were added to the cell suspension. The resulting alkali extract was incubated at 60°C for

30 min to destroy endogenous enzyme activities and pyridine nucleotides. The extract was neutralized by adding 500 μ l of THA solution (100 mM Tris/HCl, pH 8.1, and 50 mM HCl), divided into 150- μ l aliquots, quickly frozen in liquid nitrogen, and stored at -80°C prior to use. To measure trehalose concentration, 50 μ l of alkali extract (recovered from the total of 6.5×10^7 cells) were added to 150 μ l of trehalose reagent (25 mM $\text{KH}_2\text{PO}_4/\text{KOH}$, pH 7.5, and 0.02% BSA; with or without 15 mU trehalase (Sigma)). The mixture was incubated for 60 min at 37°C. 800 μ l of glucose reagent (100 mM Tris/HCl, pH 8.1, 2 mM MgCl_2 , 1 mM DTT, 1 mM ATP, 0.2 mM NADP^+ , and mixture of hexokinase (7 U) and glucose-6-phosphate dehydrogenase (8 U) (Sigma)) was added and the mixture incubated for 30 min at 25°C. The NADPH generated from NADP^+ was measured fluorimetrically (excitation at 365 nm, emission monitored at 460 nm).

Hexokinase activity measurement

Preparation of cellular lysate and a microanalytic biochemical assay for measuring hexokinase enzymatic activity were performed as previously described [177]. To prepare a cellular lysate, 2×10^7 cells were harvested by centrifugation for 1 min at $21,000 \times g$ at 4°C. The cells were washed three times in ice-cold PBS (20 mM $\text{KH}_2\text{PO}_4/\text{KOH}$, pH 7.5, and 150 mM NaCl). The cell pellet was quickly resuspended in 800 μ l of EB buffer (20 mM $\text{KH}_2\text{PO}_4/\text{KOH}$, pH 7.5, 0.02% BSA, 0.5 mM EDTA, 5 mM β -mercaptoethanol, 25% glycerol, and 0.5% Triton X-100) and incubated for 5 min at 25°C. The resulting lysate was divided into 40- μ l aliquots and stored at -80°C prior to use. To measure hexokinase activity, 4 μ l of cellular lysate (recovered from the total of 1×10^5 cells) were added to 996 μ l of hexokinase reagent (100 mM Tris/HCl, pH 8.1, 0.05% BSA, 7 mM MgCl_2 , 5

mM ATP, 5 mM glucose, 0.5 mM DTT, 100 μ M NADP⁺, 0.5% Triton X-100, and 2 U glucose-6-phosphate dehydrogenase (Sigma)). The mixture was incubated for 1 h at 25°C. The NADPH generated from NADP⁺ was measured fluorimetrically (excitation at 365 nm, emission monitored at 460 nm). To monitor the extent of thermal inactivation of hexokinase in heat-shocked yeast cells and the efficacy of its reactivation during subsequent incubation of these cells at low temperature, yeast were grown at 29°C and recovered upon entry into a quiescent state at day 7 or following such an entry at day 13. These cells were treated with cycloheximide for 5 min at 29°C, heat shocked for 60 min at 43°C, then shifted to 29°C and incubated for 60 min. Hexokinase enzymatic activity was measured every 15 min of heat shock treatment and every 15 min of the following incubation at 29°C.

Immunodetection of carbonyl groups in oxidatively damaged cellular proteins

Total cell lysates were made by vortexing the cells in ice-cold TCL buffer (25 mM MOPS/KOH, pH 7.2, 150 mM NaCl, 50 mM DTT, and 1% CHAPS) with glass beads three times for 1 min. Lysates were then centrifuged for 5 min at 21,000 \times g at 4°C, and the supernatants of total cell lysates were collected. The carbonyl groups of proteins recovered in total cell lysates were derivatized to 2,4-dinitrophenylhydrazones using the OxyBlotTM Protein Oxidation Detection Kit (Chemicon), according to the manufacturer's instructions. Briefly, total cellular proteins were denatured by adding 12% SDS to an equal volume of the total cell lysate containing 10 μ g of protein. Denatured proteins were incubated with 2,4-dinitrophenylhydrazine for 15 min at room temperature. Proteins were separated by 12.5% SDS-PAGE. Immunoblotting using a Trans-Blot SD semi-dry

electrophoretic transfer system (Bio-Rad) was performed as described [178]. The derivatized carbonyl groups were detected with a 2,4-dinitrophenyl-specific antibody (Chemicon) and the Amersham ECL Western Blotting System (GE Healthcare).

ROS measurement

ROS were measured in live yeast by fluorescence microscopy of Dihydrorhodamine 123 (DHR) staining according to established procedures [32, 179]. Briefly, 5×10^6 cells were harvested by centrifugation for 1 min at $21,000 \times g$ at room temperature and then resuspended in 100 μ l of PBS. DHR (Sigma) was added to a final concentration of 10 μ M. Following incubation in the dark for 60 min at room temperature, the cells were washed in PBS and then analyzed by fluorescence microscopy. Images were collected with a Zeiss Axioplan fluorescence microscope (Zeiss) mounted with a SPOT Insight 2 megapixel color mosaic digital camera (Spot Diagnostic Instruments). Fluorescence of individual DHR-positive cells in arbitrary units was determined by using the UTHSCSA Image Tool software (Version 3.0). In each of 3-6 independent experiments, the value of median fluorescence was calculated by analyzing at least 800-1000 cells that were collected at each time-point. The median fluorescence values were plotted as a function of the number of days cells were cultured.

Recovery of insoluble aggregates of denatured proteins

Insoluble aggregates of denatured proteins were recovered according to established procedures [180, 181], with the following modifications. Total cell lysates were made by vortexing the cells in ice-cold MBS buffer (25 mM MOPS/KOH, pH 7.2, and 150 mM

NaCl) with glass beads four times for 1 min. Unbroken cells and cell debris were removed by centrifugation for 3 min at $1,000 \times g$ at 4°C . The supernatants of total cell lysates were collected and normalized by dilution to a final concentration of 1 mg/ml. Equal aliquots of the total cell lysates were supplemented with 3-[(3-Cholamidopropyl)dimethylammonio]-1-propanesulfonate (CHAPS; Sigma) to a final concentration of 10 mM. CHAPS is a zwitterionic, non-denaturing and electrically neutral detergent; although it protects a native state of soluble proteins and efficiently solubilizes intrinsic membrane proteins (including proteins associated with lipid raft membrane domains), it is unable to solubilize aggregates of denatured proteins [181 - 184]. After incubation on ice for 30 min, samples were subjected to centrifugation at $100,000 \times g$ for 30 min at 4°C . The pellet fractions of insoluble aggregates of denatured proteins were analyzed by 12.5% SDS-PAGE, followed by silver staining.

3.4 Results

3.4.1 Lifespan extension by CR requires a specific pattern of age-related changes in trehalose concentration

To evaluate the effect of trehalose on lifespan extension by CR, we incubated WT strain and several mutant strains, each carrying a single-gene-deletion mutation affecting trehalose biosynthesis or degradation [169], 2001), in YP medium initially containing 0.2% glucose. We monitored the chronological lifespans of all these strains and assessed the dynamics of changes in trehalose concentration during their aging.

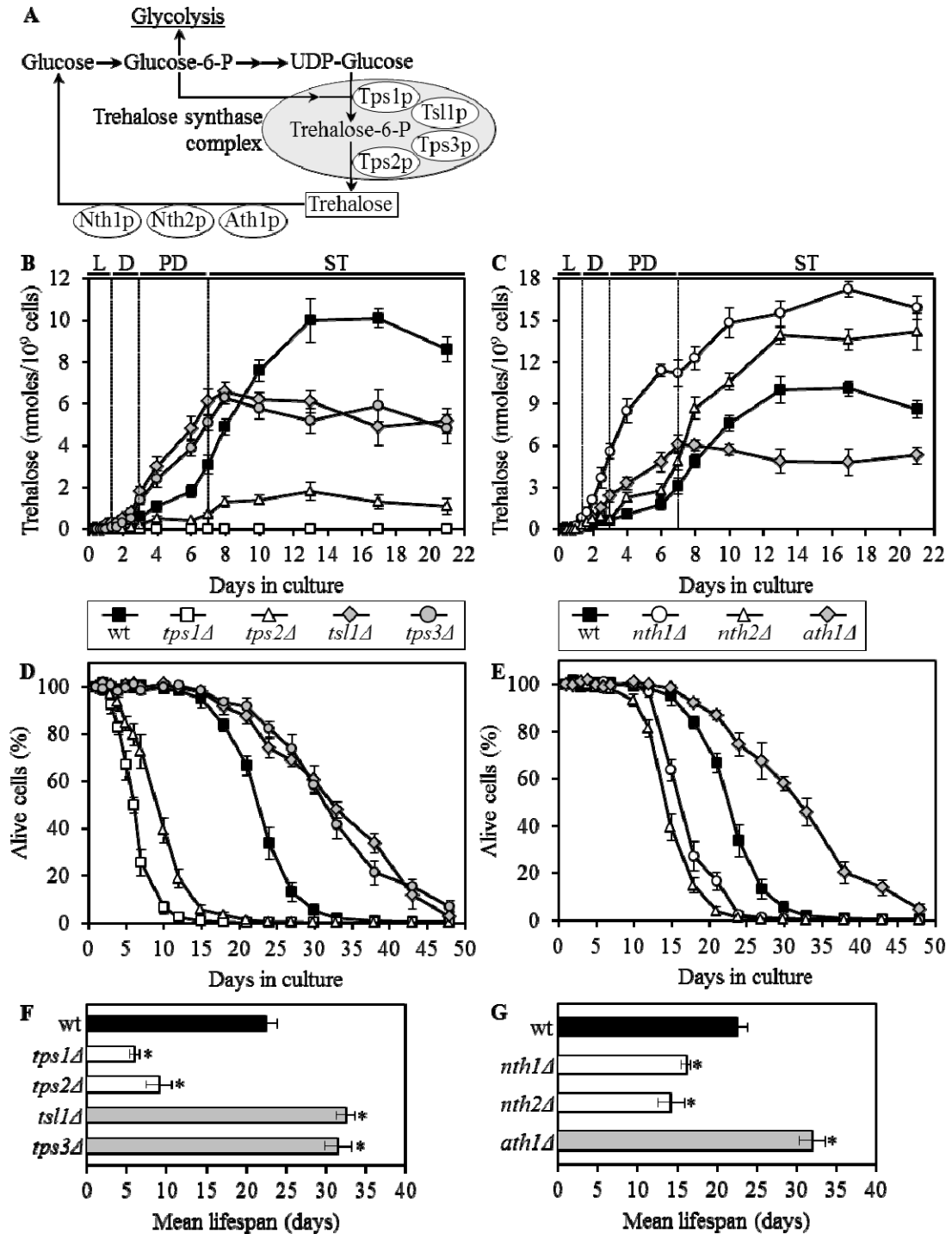


Figure 3.1. The chronological lifespan of yeast grown under CR conditions can be extended by mutations that simultaneously increase trehalose concentration prior to quiescence and reduce trehalose concentration following entry into a quiescent state. (A) Outline of metabolic pathways of trehalose biosynthesis and degradation. (B, C) The dynamics of age-dependent changes in the intracellular levels of trehalose during

chronological aging of wild-type (wt) and mutant strains. (D-G) Survival (D, E) and the mean lifespans (F, G) of chronologically aging wt and mutant strains. Each mutant carried a single-gene-deletion mutation that affects trehalose biosynthesis or degradation. Cells were cultured in YP medium initially containing 0.2% glucose. Data are presented as mean \pm SEM (n = 5-6); *p < 0.01 (relative to the mean lifespan of wt strain). Abbreviations: D, diauxic growth phase; L, logarithmic growth phase; PD, post-diauxic growth phase; ST, stationary growth phase.

The *tps1* Δ and *tps2* Δ mutations, which eliminate two different catalytic subunits of the trehalose synthase complex (Figure 3.1A), substantially decreased trehalose concentration in yeast cells grown under CR conditions and shortened their lifespans (Figures 3.1B and 3.1D). CR yeast whose trehalose level was significantly increased before they have entered the non-proliferative stationary (ST) growth phase and remained significantly elevated during ST phase - as it was observed in mutant cells lacking the Nth1p isozyme of neutral trehalase - were short-lived (Figures 3.1C and 3.1E). Moreover, even if trehalose concentration exceeded the level seen in WT only after CR yeast have entered ST phase - as it occurred in mutant cells lacking the Nth2p isozyme of neutral trehalase - cells had shortened lifespan (Figure 3.1C and 3.1E).

Importantly, some genetic manipulations altering trehalose concentration extended the lifespan of CR yeast. Specifically, in long-lived mutants lacking the Tsl1p or Tps3p regulatory subunit of the trehalose synthase complex, trehalose concentration exceeded that in WT until the end of post-diauxic (PD) growth phase, but then in ST phase reached a plateau at the level that was 50-70% of that seen in WT (Figures 3.1B and 3.1D). Similar dynamics of age-related changes in trehalose concentration was observed in the long-lived mutant *ath1* Δ lacking acid trehalase (Figures 3.1C and 3.1E).

Altogether, these findings imply that the extended chronological lifespan of CR yeast (as compared to that of non-CR yeast) can be further prolonged by genetic manipulations that simultaneously 1) increase trehalose concentration by 70-160% during PD phase, prior to entry into a quiescent state; and 2) reduce trehalose concentration by 60-80% during ST phase, following entry into quiescence. Thus, lifespan extension by a low calorie diet requires a specific pattern of age-related changes in the intracellular level of trehalose.

3.4.2 Mutations that increase trehalose concentration prior to entry into quiescence reduce oxidative damage to cellular proteins throughout lifespan, irrespective of their effects on longevity

Trehalose accumulation in exponentially grown yeast cells exposed to elevated temperature or to a proteasome inhibitor has been shown to increase their ability to survive a subsequent treatment with exogenous ROS and to protect cellular proteins from oxidative carbonylation caused by such a treatment [170]. According to the mitochondrial free radical theory of aging, the gradual accumulation of macromolecular damage caused by mitochondrially produced ROS throughout lifespan accelerates cellular dysfunction and later in life leads to a functional decline and increased mortality [185, 186]. Although a body of evidence does not validate the core statement of this theory on a casual role of ROS generation in aging, the importance of ROS in mediating a stress response to age-related cellular damage is supported by numerous findings [187 - 192]. To evaluate a potential role of trehalose in linking a ROS-dependent oxidative macromolecular damage to lifespan extension by CR, we assessed how the *ts11Δ* and *nth1Δ* mutations influence

the dynamics of age-related changes in protein carbonylation and ROS in yeast grown under CR conditions.

Both the *ts11Δ* and *nth1Δ* mutations elevated trehalose concentration (Figures 3.1B and 3.1C) and reduced oxidative carbonylation of cellular proteins (Figure 3.2A) during PD phase, prior to entry into a quiescent state under CR conditions. None of these mutations altered ROS levels in pre-quiescent cells limited in calories (Figure 3.2B). Thus, it is unlikely that the observed reduction of oxidative damage to cellular proteins in pre-quiescent *ts11Δ* and *nth1Δ* cells was due to the previously proposed by Benaroudj et al. [170] ability of trehalose, a nonreducing disaccharide, to quench ROS. It is conceivable therefore that prior to quiescence trehalose protects cellular proteins from oxidative carbonylation (Figure 3.2A) by interacting with their carbonylation-prone misfolded and unfolded species. These aberrantly folded protein species are known to be much more sensitive to oxidative carbonylation than their properly folded counterparts [193, 194]. Several mechanisms responsible for protein stabilization by trehalose molecules have been recently proposed [173, 174].

The extent of protein carbonylation reached prior to entry into a quiescent state was not significantly altered in *ts11Δ* and *nth1Δ* cells following entry into quiescence (Figure 3.2A), likely due to greatly diminished ROS levels observed in quiescent *ts11Δ* and *nth1Δ* cells under CR conditions (Figure 3.2B). Trehalose concentration in quiescent *ts11Δ* cells was substantially lower than that seen in quiescent WT cells (Figure 3.1B). In contrast, the concentration of trehalose in quiescent *nth1Δ* cells exceeded the level detected in quiescent WT cells (Figure 3.1C). We therefore concluded that genetic manipulations that increase trehalose concentration prior to entry into a quiescent state

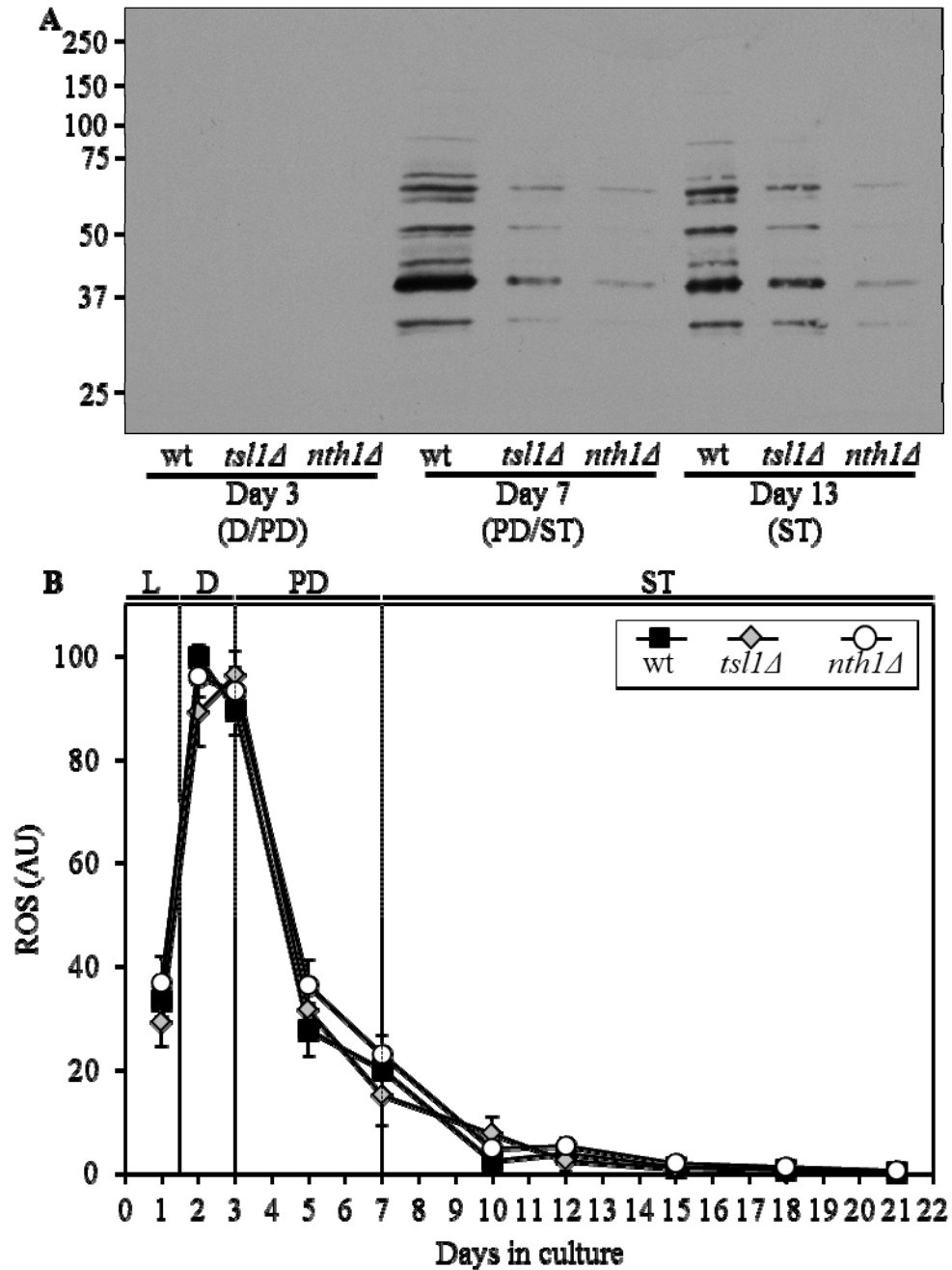


Figure 3.2. Although mutations that in yeast grown under CR conditions increase trehalose concentration prior to entry into quiescence do not alter ROS levels, they reduce oxidative damage to cellular proteins throughout lifespan. (A) Immunodetection of carbonyl groups in oxidatively damaged cellular proteins in chronologically aging wt and mutant strains. (B) The dynamics of age-related changes in intracellular ROS levels during chronological aging of wt and mutant strains. wt, *tsl1Δ* and *nth1Δ* cells were cultured in YP

medium initially containing 0.2% glucose. Data are presented as mean \pm SEM (n = 3-4). Abbreviations: D, diauxic growth phase; PD, post-diauxic growth phase; ST, stationary growth phase.

reduce oxidative damage to cellular proteins throughout lifespan, regardless of their effects on the intracellular concentration of this nonreducing disaccharide following entry into quiescence.

Although both the *ts11Δ* and *nth1Δ* mutations reduced oxidative carbonylation of cellular proteins throughout lifespan (Figure 3.2A), their effects on longevity differed. The *ts11Δ* mutation extended the chronological lifespan of CR yeast, whereas the *nth1Δ* mutations shortened it (Figures 3.1D – 3.1G). Hence, it is unlikely that the observed ability of these genetic manipulations to protect cellular proteins from oxidative damage plays a role in defining longevity of chronologically aging yeast under CR conditions.

3.4.3 A pattern of age-related changes in trehalose concentration defines the dynamics of protein aggregation throughout lifespan

Trehalose has been shown to 1) stabilize bacterial and firefly luciferases in their native (folded) states in heat-shocked yeast cells; 2) prevent aggregation and maintain non-native (misfolded or partially folded) states of these two luciferases, as well as of firefly rhodanese, following their guanidinium-induced denaturation in vitro and in yeast cells briefly exposed to elevated temperature; and 3) inhibit the refolding and reactivation of these pre-denatured bacterial and firefly proteins in vitro and in yeast cells by interfering with chaperone-assisted folding of their non-native (misfolded or partially folded) species [171]. It has been predicted that trehalose may exhibit similar effects on

the stability, folding and aggregation of endogenous proteins in cells of yeast and other organisms [171 – 174].

Furthermore, our investigation of how a CR diet affects the metabolic history of chronologically aging yeast suggested that the elevated level of trehalose observed prior to entry into quiescence in slowly aging CR yeast (as compared to that seen in rapidly aging non-CR yeast) protects from aggregation proteins that have been completely or partially unfolded and/or oxidatively carbonylated due to their exposure to intracellular ROS [32]. We hypothesized that such protective effect of high trehalose concentrations could contribute to the enhanced survival of CR yeast (as compared to survival of non-CR yeast) following their entry into quiescence [32].

Moreover, we also hypothesized that a dietary or genetic intervention providing yeast with the ability to maintain trehalose concentration at a certain “optimal” level prior and following entry into a quiescent state would extend their longevity [32]. We predicted that at such an “optimal” level trehalose concentration is 1) sufficiently high prior to entry into quiescence to allow this osmolyte to prevent aggregation of proteins that have been completely or partially unfolded and/or oxidatively carbonylated; and 2) sufficiently low following entry into quiescence to reduce the efficiency with which trehalose inhibits the refolding and reactivation of partially unfolded and/or oxidatively carbonylated proteins [32].

To test the validity of our hypothesis, we assessed how the *ts11Δ* and *nth1Δ* mutations influence the dynamics of age-related changes in the extent of protein aggregation in yeast limited in calories. We found that both these mutations, which we demonstrated to elevate trehalose concentration (Figures 3.1B and 3.1C) and to decrease

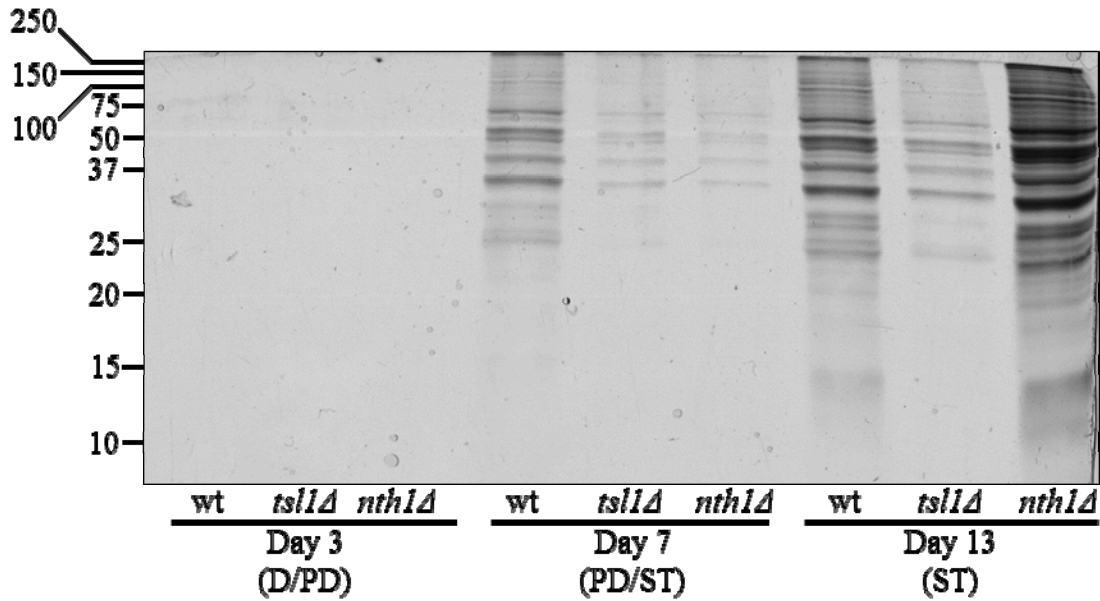


Figure 3.3. In yeast grown under CR conditions, a pattern of age-related changes in trehalose concentration defines the dynamics of protein aggregation throughout lifespan. Total cell lysates were made by vortexing the cells in ice-cold buffer with glass beads. Unbroken cells and cell debris were removed by centrifugation for 3 min at $1,000 \times g$ at 4°C . The supernatants of total cell lysates were collected and normalized by dilution to a final concentration of 1 mg/ml. Equal aliquots of the total cell lysates were supplemented with CHAPS, a zwitterionic, non-denaturing and electrically neutral detergent that protects a native state of soluble proteins and efficiently solubilizes membrane proteins, but is unable to solubilize aggregates of denatured proteins. After incubation on ice for 30 min, samples were subjected to centrifugation at $100,000 \times g$ for 30 min at 4°C . The pellet fractions of insoluble aggregates of denatured proteins were analyzed by 12.5% SDS-PAGE, followed by silver staining. wt, *ts11Δ* and *nth1Δ* cells were cultured in YP medium initially containing 0.2% glucose. Abbreviations: D, diauxic growth phase; PD, post-diauxic growth phase; ST, stationary growth phase.

oxidative protein carbonylation (Figure 3.2A) during PD phase under CR conditions, significantly reduce the extent of aggregation of cellular proteins during this growth phase preceding entry into a quiescent state (Figure 3.3). Following entry into

quiescence, the extent of protein aggregation in *ts11Δ* cells was substantially lower than that seen in quiescent WT cells and especially in quiescent *nth1Δ* cells (Figure 3.3). As we mentioned above, trehalose concentration in quiescent *ts11Δ* cells was significantly reduced as compared to that in WT (Figure 3.1B) and especially in *nth1Δ* (Figure 3.1C) cells reached reproductive maturation. Furthermore, both the concentration of trehalose (Figures 3.1B and 3.1C) and the extent of protein aggregation (Figure 3.3) in quiescent *nth1Δ* cells were significantly higher than that observed in WT cells and especially in *ts11Δ* cells entered a quiescent state.

In sum, these findings validate our hypothesis in which a genetic intervention will extend longevity of calorically restricted yeast if it 1) elevates trehalose concentration prior to entry into quiescence to allow this osmolytic disaccharide to prevent aggregation of completely or partially unfolded and/or oxidatively carbonylated cellular proteins; and 2) reduces the concentration of trehalose following entry into quiescence to limit its inhibitory effect on the refolding and reactivation of partially unfolded and/or oxidatively carbonylated proteins.

3.4.4 Trehalose concentration in yeast cells defines the sensitivity of an endogenous enzyme to thermal inactivation and the extent of its subsequent reactivation at low temperature

To use a complementary experimental approach for validating our hypothesis on a longevity-defining role of trehalose concentration in maintaining biological activities of proteins in chronologically aging yeast under CR conditions, we assessed how the *ts11Δ* and *nth1Δ* mutations influence 1) the extent of thermal inactivation of hexokinase, an

endogenous enzyme protein, in heat-shocked yeast cells; and 2) the efficacy of its reactivation during subsequent incubation of these cells at low temperature. In these experiments, yeast grown at 29°C and recovered upon entry into a quiescent state or following such an entry were treated with cycloheximide for 5 min at 29°C, heat shocked for 60 min at 43°C, then shifted to 29°C and incubated for 60 min (Figure 3.4).

In *ts11Δ* and *nth1Δ* cells recovered at day 7, upon entry into a quiescent state, the activity of hexokinase synthesized prior to a cycloheximide-induced inhibition of protein synthesis at 29°C was significantly less susceptible to thermal inactivation at 43°C than in identically treated and chronologically aged WT cells (Figure 3.4C). Under these conditions, trehalose concentrations in both *ts11Δ* and *nth1Δ* cells significantly exceeded that in WT cells of the same chronological age (Figure 3.4A). If cells were recovered at day 13, following entry into a quiescent state, hexokinase activity in *ts11Δ* cells having a lower trehalose concentration than WT cells (Figure 3.4B) was more susceptible to the thermal inactivation at 43°C than in WT cells (Figure 3.4D). In contrast, in *nth1Δ* cells recovered at day 13 and having a higher trehalose concentration than WT cells of the same chronological age (Figure 3.4B) hexokinase activity was less susceptible to such thermal inactivation than in WT cells (Figure 3.4D). These findings imply that in calorically restricted pre-quiescent yeast trehalose preserves biological activities of partially inactivated cellular proteins, perhaps by stabilizing their native (folded) state, preventing their unfolding and/or inhibiting their subsequent aggregation.

In *ts11Δ* and *nth1Δ* cells recovered at day 7, upon entry into quiescence, the reactivation of thermally inactivated hexokinase during the subsequent incubation at low temperature occurred significantly less efficient than in WT cells of the same

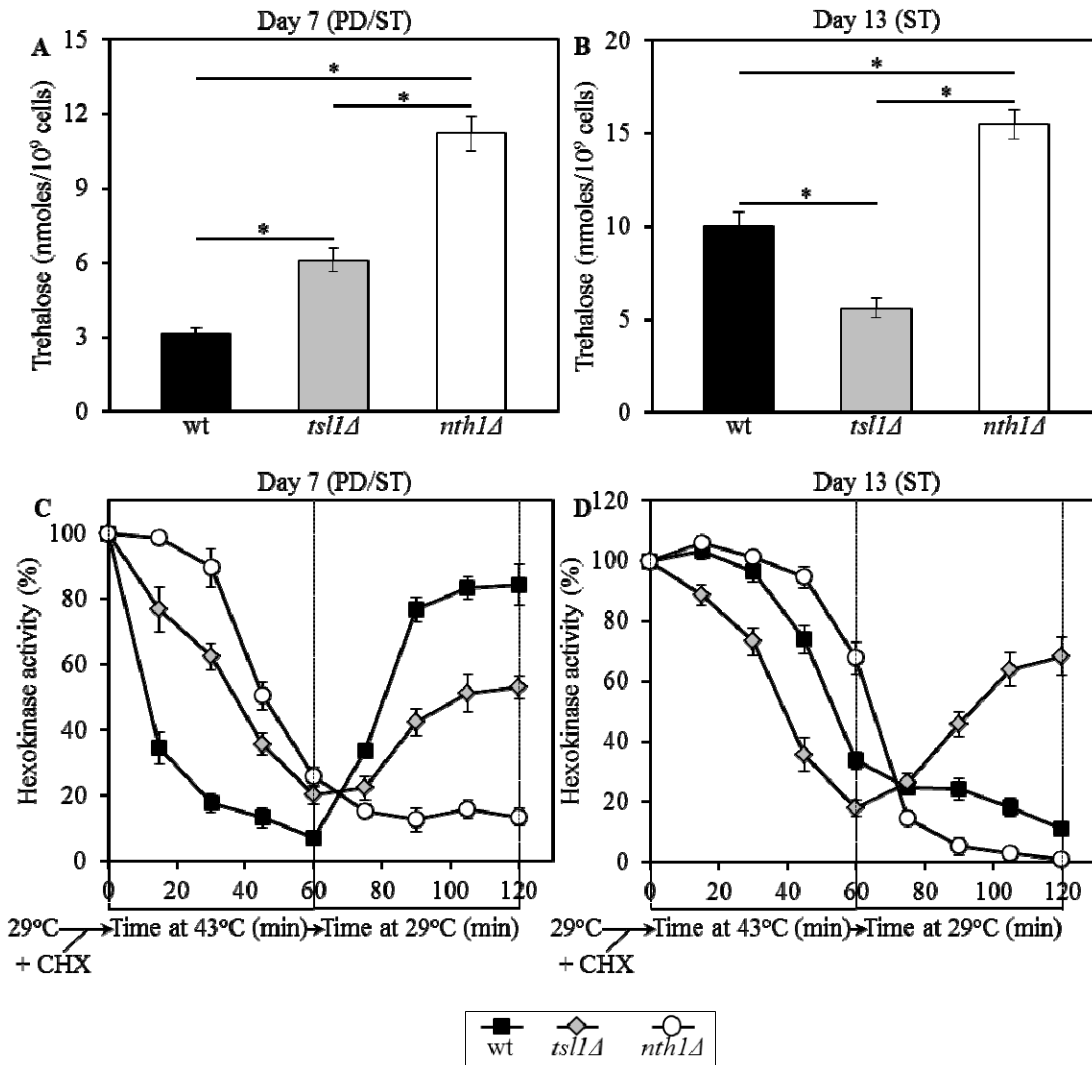


Figure 3.4. In yeast grown under CR conditions, trehalose concentration defines the sensitivity of hexokinase, an endogenous enzyme, to thermal inactivation and the extent of its subsequent reactivation at low temperature. Yeast cells grown at 29°C were recovered upon entry into a quiescent state at day 7 or following such an entry at day 13. The cells were treated with cycloheximide for 5 min at 29°C to inhibit protein synthesis, heat shocked for 60 min at 43°C, then shifted to 29°C and incubated for 60 min. (A, B) The intracellular levels of trehalose prior to cell treatment with cycloheximide. (C, D) Changes in hexokinase enzymatic activity following cell exposure to cycloheximide, during heat shock treatment for 60 min at 43°C and subsequent incubation for 60 min at 29°C. *wt*, *tsl1Δ* and *nth1Δ* cells were cultured in YP medium initially containing 0.2% glucose. Data are presented as mean ± SEM (n = 3-5). Abbreviations: CHX, cycloheximide; PD, post-diauxic growth phase; ST, stationary growth phase.

chronological age (Figure 3.4C). Noteworthy, the efficacy of such hexokinase reactivation was inversely proportional to trehalose concentration in yeast cells that reached a transition to a quiescent state (Figures 3.4A and 3.4C). If cells were recovered at day 13, following entry into a quiescent state, the reactivation of thermally inactivated hexokinase during the subsequent incubation at low temperature occurred only in *ts11Δ* cells having significantly lower trehalose concentration as compared to WT and especially to *nth11Δ* cells of the same chronological age (Figures 3.4B and 3.4D). In *nth11Δ* cells recovered at day 13 and having a higher trehalose concentration than WT cells of the same chronological age (Figure 3.4B), thermally inactivated hexokinase was further inactivated during the subsequent incubation at low temperature with the efficiency exceeding that in WT cells (Figure 3.4D). These findings imply that in calorically restricted quiescent yeast trehalose inhibits the reactivation of inactivated cellular proteins, perhaps by interfering with chaperone-assisted folding of their non-native (misfolded or partially folded) species.

3.5 Discussion

To investigate whether trehalose homeostasis in yeast cells may play a role in longevity extension by CR, we assessed how single-gene-deletion mutations that in chronologically aging yeast alter trehalose concentrations prior to quiescence and following entry into a quiescent state impact lifespan. We also examined the effects of these mutations on the chronology of oxidative protein carbonylation, intracellular ROS, protein aggregation, thermal inactivation of a protein in heat-shocked yeast cells and a subsequent reactivation of this protein in yeast shifted to low temperature. Our findings

provide evidence that CR extends yeast chronological lifespan in part by altering a pattern of age-related changes in trehalose concentration. Based on our data, we propose a model for molecular mechanisms underlying the essential role of trehalose in defining yeast longevity by modulating cellular proteostasis throughout lifespan (Figure 3.5). This outlined below model adequately explains how genetic interventions altering a pattern of age-related changes in trehalose concentration influence a longevity-defining balance between protein folding, misfolding, unfolding, refolding, oxidative damage, solubility and aggregation.

Pre-quiescent WT cells proliferating under CR conditions cope with a flow of misfolded, partially folded and unfolded protein species in the non-native folding state (Figure 3.5A, process 1). The continuous formation of these protein species within a proliferating cell is due to a number of factors, including 1) macromolecular crowding, which is caused by the very high intracellular protein concentration and leads to inappropriate intermolecular contacts; 2) stochastic fluctuations in protein structure; 3) transcriptional errors; 4) inherited genetic polymorphisms, including gene copy number variations; 5) intrinsic errors in gene expression that may create an excess of unassembled subunits of oligomeric protein complexes; 6) errors in protein translation – such as missense incorporation of amino acids, frame-shifting, stop-codon readthrough and premature termination; 7) defects in posttranslational protein modifications and turnover; and 8) inefficient translocation of secretory and mitochondrial precursor proteins across membranes of their target organelles [195 - 197]. In pre-quiescent WT cells, trehalose stabilizes the native state of proteins and thereby reduces the formation of their aberrantly folded species (Figure 3.5A, process 2). The promoted by trehalose shift

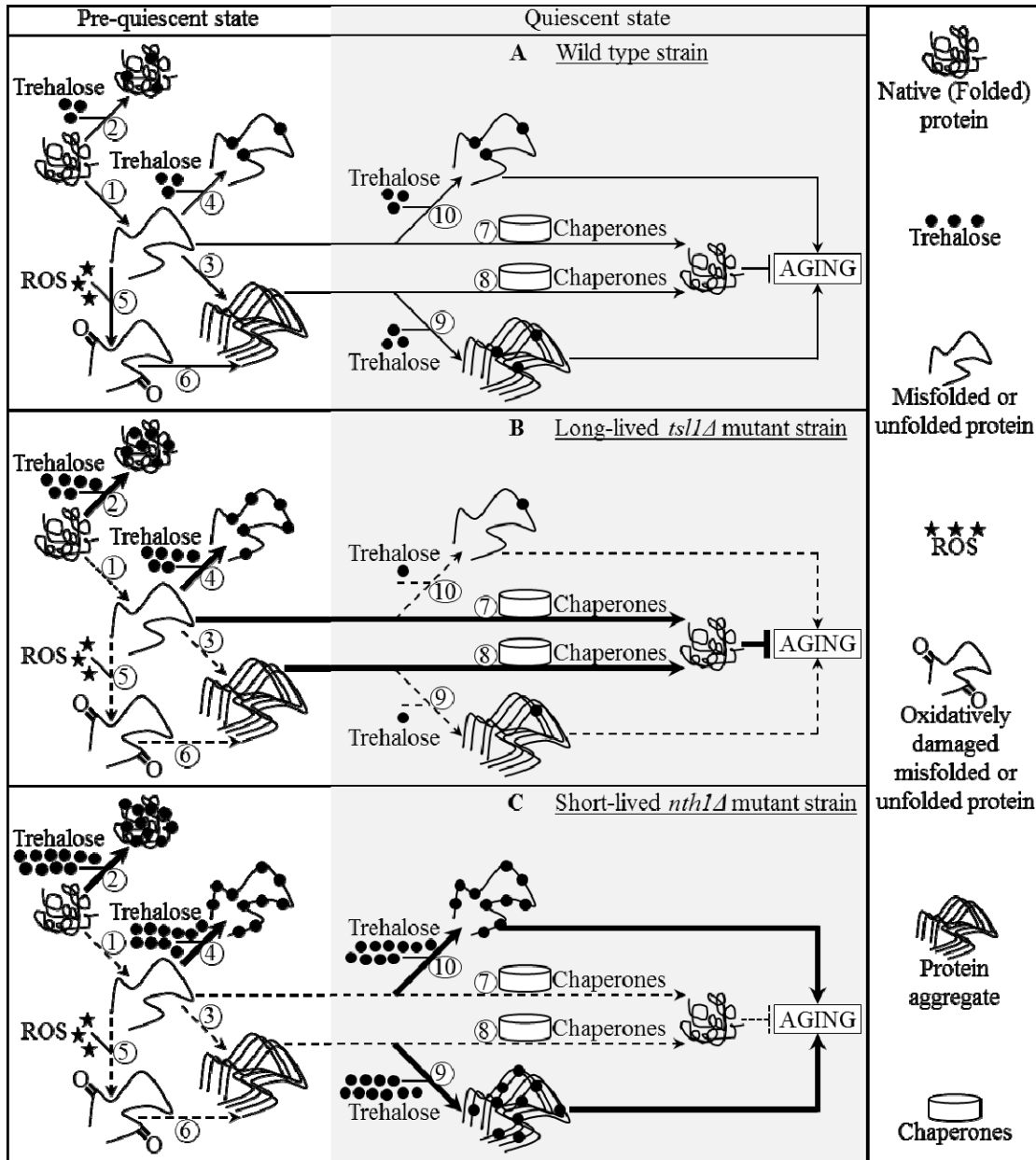


Figure 3.5. A model for molecular mechanisms underlying the essential role of trehalose in defining yeast longevity by modulating cellular proteostasis throughout lifespan. The outlined model adequately explains how the *ts1Δ* and *nth1Δ* mutations altering a pattern of age-related changes in trehalose concentration influence a longevity-defining balance between protein folding, misfolding, unfolding, refolding, oxidative damage, solubility and aggregation. See text for details. The thickness of arrows and T bars correlates with the rates of the processes taking place in chronologically aging yeast prior to entry into a quiescent state

and following such an entry under CR conditions. T bars denote inhibition of the process. Abbreviation: ROS, reactive oxygen species.

of a balance between native and non-native protein folding states towards properly folded protein species is amplified by the *ts11Δ* and *nth1Δ* mutations, both of which significantly elevate trehalose concentration prior to entry into a quiescent state (Figures 3.5B and 3.5C, process 2). Our finding that the enzymatic activity of an endogenous hexokinase synthesized prior to a cycloheximide-induced inhibition of protein synthesis at 29°C in pre-quiescent *ts11Δ* and *nth1Δ* cells is significantly less susceptible to thermal inactivation at 43°C than in identically treated and chronologically aged WT cells (Figure 3.4C) supports the role of trehalose in stabilizing the native state of cellular proteins. Moreover, a previously demonstrated ability of trehalose to stabilize bacterial and firefly luciferases in their native states in heat-shocked yeast cells [171] provides additional support for the validity of our conclusion on the essential role of this osmolyte in shifting a balance between native and non-native protein folding states towards native folding structures. It is conceivable that trehalose may stabilize the native state of proteins in pre-quiescent yeast cells via any of the three recently proposed mechanisms [173, 174].

In pre-quiescent WT cells, the aberrantly folded protein species that have not been refolded into functional three-dimensional native conformations or degraded within an elaborate network of molecular chaperones and protein degradation factors [195 - 197] form insoluble aggregates (Figure 3.5A, process 3). In these cells, trehalose reduces the formation of such protein aggregates, perhaps by shielding the contiguous exposed hydrophobic side chains of amino acids that are abundant in misfolded, partially folded and unfolded protein species and promote their aggregation (Figure 3.5A, process 4). Our

finding that the *tsl1Δ* and *nth1Δ* mutations, both of which elevate trehalose concentration prior to entry into quiescence (Figures 3.1B and 3.1C), significantly reduce the extent of protein aggregation in pre-quiescent cells (Figure 3.3) supports the essential role of trehalose in preventing the formation of insoluble protein aggregates in these proliferation-competent cells (Figures 3.5B and 3.5C, process 4). Moreover, a previously demonstrated ability of trehalose to prevent aggregation and maintain non-native states of bacterial and firefly luciferases, as well as of firefly rhodanese, following their guanidinium-induced denaturation in vitro and in heat-shocked yeast cells [171] further validates our conclusion that trehalose inhibits aggregation of the aberrantly folded protein species accumulating in pre-quiescent yeast.

The misfolded, partially folded and unfolded protein species present in pre-quiescent WT cells are known to be more sensitive to ROS-driven oxidative carbonylation than their properly folded counterparts [193, 194]. These cells accumulate substantial levels of ROS (Figure 3.2B), which oxidatively damage a pool of the aberrantly folded and unfolded proteins (Figure 3.2A) prior to entry into a quiescent state (Figure 3.5A, process 5). Prior to quiescence, trehalose protects cellular proteins from oxidative carbonylation by interacting with their carbonylation-prone misfolded and unfolded species (Figure 3.5A, process 4) but not by quenching ROS (as it has been previously proposed by Benaroudj et al. [170]). In support of this mechanism for the protection of proteins from ROS-elicited oxidative damage by trehalose, we found that in pre-quiescent cells the *tsl1Δ* and *nth1Δ* mutations reduce oxidative carbonylation of cellular proteins (Figure 3.2A) but do not alter ROS levels (Figure 3.2B; Figures 3.5B and 3.5C, process 5).

The oxidatively carbonylated protein species present in pre-quiescent WT cells are known to have a tendency to form insoluble aggregates that escape degradation and can compromise the cellular proteostasis network by inhibiting the proteasomal protein degradation machinery [193, 194, 198]. By protecting cellular proteins from oxidative carbonylation (Figure 3.5A, process 5; see above), trehalose reduces the formation of insoluble protein aggregates prior to entry into senescence (Figure 3.5A, process 6). This indirect inhibitory effect of trehalose on protein aggregation supplements its direct inhibition by trehalose (Figure 3.5A, process 3; see above), which could shield the patches of exposed hydrophobic side chains of amino acids tending to promote aggregation of aberrantly folded and unfolded protein species (Figure 3.5A, process 4; see above).

Following entry into a quiescent state, a network of molecular chaperones in WT cells promotes a refolding of misfolded, partially folded and unfolded protein species, either soluble or extracted from protein aggregates accumulated in pre-quiescent cells (Figure 3.5A, processes 7 and 8). This chaperone-assisted refolding of aberrantly folded protein species is the essential anti-aging process [195, 197 - 199]. By shielding the contiguous exposed hydrophobic side chains of amino acids that are abundant in misfolded, partially folded and unfolded protein species, trehalose in quiescent WT cells competes with molecular chaperones for binding with these patches of hydrophobic amino acid residues (Figure 3.5A, processes 9 and 10) known to be mandatory for enabling the chaperone-assisted refolding of aberrantly folded protein species [195, 197 - 199]. By interfering with this essential anti-aging process in quiescent WT cells, trehalose operates as a pro-aging compound (Figure 3.5A). In support of our hypothesis that this

mechanism underlies the essential role of trehalose homeostasis in defining longevity of chronologically aging yeast under CR conditions (Figures 3.5B and 3.5C, processes 9 and 10) we found that 1) the *ts11Δ* mutation reduces trehalose concentration following entry into quiescence (Figure 3.1B), decreases the extent of protein aggregation in quiescent cells (Figure 3.3) and extends yeast chronological lifespan (Figure 3.1D); and 2) the *nth1Δ* mutation elevates trehalose concentration following entry into quiescence (Figure 3.1C), increases the extent of protein aggregation in quiescent cells (Figure 3.3) and shortens yeast chronological lifespan (Figure 3.1E).

The major challenge now is to get a greater insight into the proposed mechanism underlying the essential role of trehalose homeostasis in defining longevity of chronologically aging yeast under lifespan-extending CR conditions. To address this challenge, many important questions need to be answered. What are the identities of oxidatively damaged proteins whose accumulation in pre-quiescent WT cells proliferating under CR conditions is reduced by genetic manipulations that elevate trehalose concentration prior to entry into quiescence (Figure 3.2A)? Are these proteins known for their essential role in defining longevity? Will genetic manipulations eliminating any of these proteins or altering their levels affect the chronological lifespan of yeast? What kind of proteins form insoluble aggregates that accumulate, in a trehalose-dependent fashion, in WT cells prior to and/or following entry into a quiescent state (Figure 3.3)? Are they known to be modifiers of lifespan in yeast? How will genetic manipulations eliminating any of these proteins or altering their levels influence longevity of chronologically aging yeast? Do oxidatively damaged and/or aggregated protein species concentrate in certain protein quality control compartments, such as the

juxtannuclear quality control compartment, the insoluble protein deposit compartment and/or aggresome [195, 200, 201], or are they randomly distributed throughout a cell prior to and/or following entry into quiescence? Does trehalose reside, permanently or temporarily, in any of these protein quality control compartments or is this osmolyte dispersed within a cell before and/or after it enters a quiescent state? What molecular chaperones constitute the proteostasis machinery whose ability to refold aberrantly folded proteins is compromised by trehalose in quiescent cells? We shall have to answer these important questions if we want to understand the complexity of the proteostasis network that defines longevity by sensing the dynamics of age-related changes in trehalose concentration.

3.6 Conclusions

Findings presented in this chapter of my thesis provide evidence that CR extends yeast chronological lifespan in part by altering a pattern of age-related changes in trehalose concentration. Based on these findings, we propose a model for molecular mechanisms underlying the essential role of trehalose in defining yeast longevity by modulating cellular proteostasis throughout lifespan. A challenge now is to get a greater insight into these mechanisms. To name just some of the many important questions needed to be answered to address this challenge, we need to 1) identify the oxidatively damaged proteins whose accumulation in pre-quiescent yeast cells proliferating under CR conditions is reduced by genetic manipulations that elevate trehalose concentration prior to entry into quiescence; 2) establish the identities of proteins forming insoluble aggregates that accumulate in yeast cells prior to and/or following entry into a quiescent

state; and 3) define molecular chaperones constituting the proteostasis machinery whose ability to refold aberrantly folded proteins is compromised by trehalose in quiescent cells.

4 A proper balance between the biosynthesis and degradation of glycogen is obligatory for lifespan extension by caloric restriction (CR)

4.1 Abstract

Our recent comparative analysis of cellular proteomes of CR and non-CR yeast revealed that the administration of a low-calorie diet increased the levels of key enzymes involved in the biosynthesis of glycogen [32], known to be the major glucose store in yeast [169]. Moreover, CR reduced the levels of key enzymes catalyzing the degradation of glycogen in chronologically aging yeast [32]. To evaluate a potential role of glycogen metabolism in lifespan extension by CR, in studies described in this chapter of the thesis we monitored the dynamics of age-related changes in its intracellular level. We also assessed how various single-gene-deletion mutations that differently alter glycogen concentrations in pre-quiescent and quiescent yeast cells affect longevity of chronologically aging yeast under CR conditions. Our findings provide evidence that a proper balance between the biosynthesis and degradation of glycogen is obligatory for lifespan extension by CR.

4.2 Introduction

To make another step towards the use of metabolic control analysis (MCA) for defining the molecular causes of cellular aging by elucidating the effect of CR on the metabolic history of chronologically aging yeast, our laboratory recently carried out the mass spectrometry-based identification and quantitation of proteins recovered in total cell lysates of aging CR and non-CR cells [32]. Our comparative analysis of cellular

proteomes of CR and non-CR yeast revealed that CR altered the levels of numerous proteins that function in various processes (Figure 4.1). Noteworthy, CR increased the levels of key enzymes involved in the biosynthesis of glycogen (Figure 4.1), known to be the major glucose store in yeast [169]. Moreover, the administration of this low-calorie dietary regimen resulted in a reduction of the levels of key enzymes catalyzing the degradation of glycogen (Figure 4.1).

To evaluate a potential role of glycogen metabolism in lifespan extension by CR, in studies described in this chapter of the thesis we monitored the dynamics of age-related changes in its intracellular level. We also assessed how various single-gene-deletion mutations that differently alter glycogen concentrations in pre-quiescent and quiescent yeast cells affect longevity of chronologically aging yeast under CR conditions. Our findings provide evidence that a proper balance between the biosynthesis and degradation of glycogen is obligatory for lifespan extension by CR.

4.3 Materials and Methods

Strains and media

The wild-type strain *Saccharomyces cerevisiae* BY4742 (*MAT α his3 Δ 1 leu2 Δ 0 lys2 Δ 0 ura3 Δ 0*) and mutant strains *glg2 Δ* (*MAT α his3 Δ 1 leu2 Δ 0 lys2 Δ 0 ura3 Δ 0* *glg2 Δ ::kanMX4*), *glc3 Δ* (*MAT α his3 Δ 1 leu2 Δ 0 lys2 Δ 0 ura3 Δ 0* *glc3 Δ ::kanMX4*), *gsy2 Δ* (*MAT α his3 Δ 1 leu2 Δ 0 lys2 Δ 0 ura3 Δ 0* *gsy2 Δ ::kanMX4*), *pig1 Δ* (*MAT α his3 Δ 1 leu2 Δ 0 lys2 Δ 0 ura3 Δ 0* *pig1 Δ ::kanMX4*), *pcl8 Δ* (*MAT α his3 Δ 1 leu2 Δ 0 lys2 Δ 0 ura3 Δ 0* *pcl8 Δ ::kanMX4*), *gph1 Δ* (*MAT α his3 Δ 1 leu2 Δ 0 lys2 Δ 0 ura3 Δ 0* *gph1 Δ ::kanMX4*), *gdb1 Δ* (*MAT α his3 Δ 1 leu2 Δ 0 lys2 Δ 0 ura3 Δ 0* *gdb1 Δ ::kanMX4*), *snf1 Δ* (*MAT α his3 Δ 1 leu2 Δ 0*

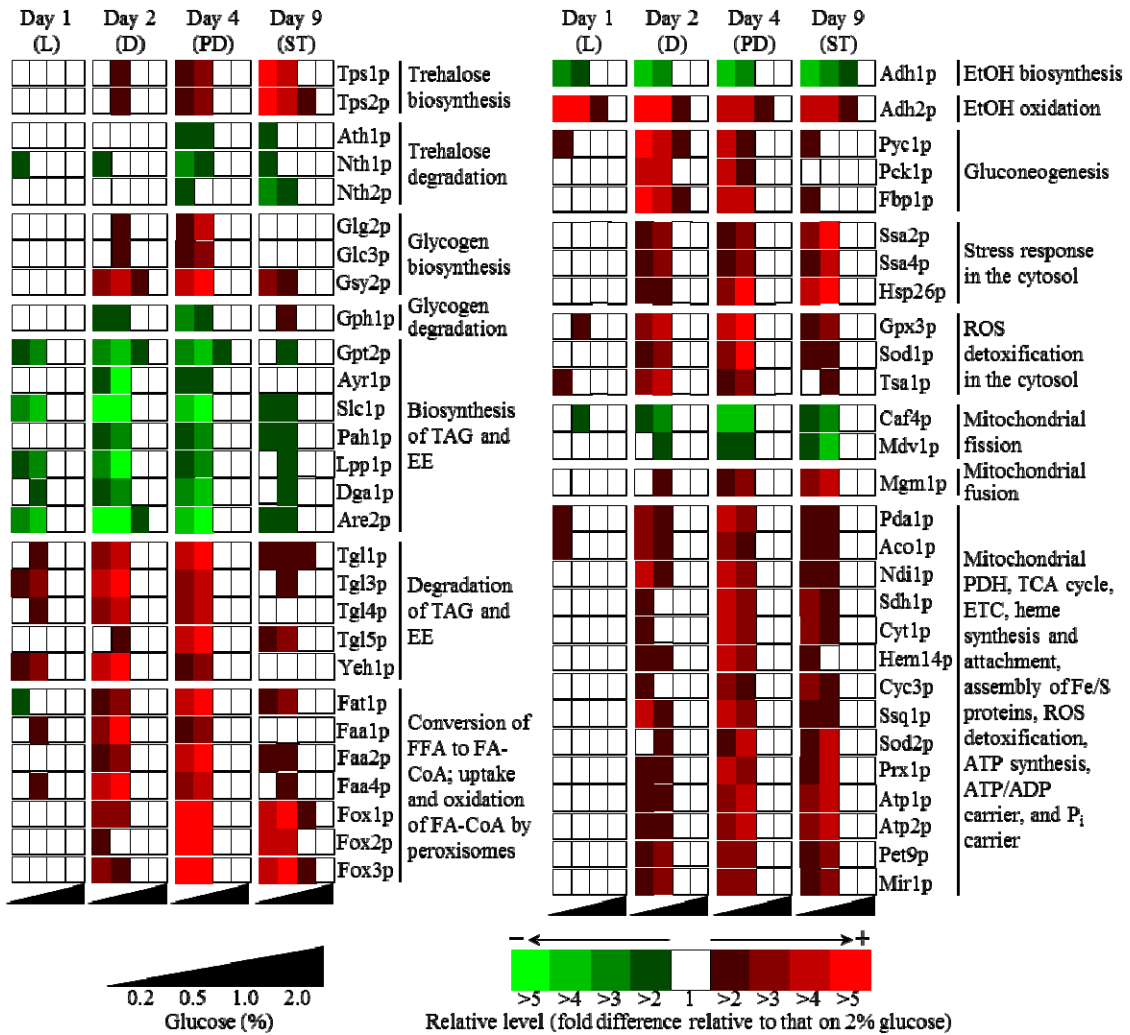


Figure 4.1. In chronologically aging yeast cells, CR alters the abundance of proteins that function in carbohydrate and lipid metabolism, stress protection, ROS detoxification, and essential processes confined to mitochondria. Relative levels (fold difference relative to that on 2% glucose) of proteins recovered in total lysates of yeast cells are shown. Proteins were identified and quantitated using mass spectrometry. The

complete list of proteins and their relative levels are provided in [32] (Tables S1 and S2, respectively). From the data of proteomic analysis, we inferred an outline of metabolic pathways and interorganellar communications that were activated (red arrows) or inhibited (green arrows) by CR prior to entry of yeast into the non-proliferative ST phase. Abbreviations: Ac-CoA, acetyl-CoA; AcOH, acetic acid; DAG, diacylglycerols; EE, ethyl esters; ER, endoplasmic reticulum; ERG, ergosterol; EtOH, ethanol; FA-CoA, CoA esters of fatty acids; FFA, free fatty acids; LB, lipid bodies; PL, phospholipids; ROS, reactive oxygen species; TAG, triacylglycerols; TCA, the tricarboxylic acid cycle in mitochondria.

lys2Δ0 ura3Δ0 snf1Δ::kanMX4) and *tpk1Δ (MATα his3Δ1 leu2Δ0 lys2Δ0 ura3Δ0 tpk1Δ::kanMX4)* (all from Open Biosystems) were grown in YP medium (1% yeast extract, 2% peptone) containing 0.2%, 0.5%, 1% or 2% glucose as carbon source. Cells were cultured at 30°C with rotational shaking at 200 rpm in Erlenmeyer flasks at a “flask volume/medium volume” ratio of 5:1.

Chronological lifespan assay

A sample of cells was taken from a culture at a certain time-point. A fraction of the sample was diluted in order to determine the total number of cells using a hemacytometer. Another fraction of the cell sample was diluted and serial dilutions of cells were plated in duplicate onto YP plates containing 2% glucose as carbon source. After 2 d of incubation at 30°C, the number of colony forming units (CFU) per plate was counted. The number of CFU was defined as the number of viable cells in a sample. For each culture, the percentage of viable cells was calculated as follows: (number of viable cells per ml/total number of cells per ml) × 100. The percentage of viable cells in mid-logarithmic phase was set at 100%. The lifespan curves were validated using a LIVE/DEAD yeast viability kit (Invitrogen) following the manufacturer's instructions.

Glycogen concentration measurement

Preparation of alkali cellular extract and a microanalytic biochemical assay for measuring glycogen concentration were performed as previously described [177]. To prepare an alkali cellular extract, 2×10^9 cells were harvested by centrifugation for 1 min at $21,000 \times g$ at 4°C . The cells were washed three times in ice-cold PBS (20 mM $\text{KH}_2\text{PO}_4/\text{KOH}$, pH 7.5, and 150 mM NaCl). The cell pellet was quickly resuspended in 200 μl of ice-cold SHE solution (50 mM NaOH, and 1 mM EDTA), and 800 μl of ice-cold SHE solution were added to the cell suspension. The resulting alkali extract was incubated at 60°C for 30 min to destroy endogenous enzyme activities and pyridine nucleotides. The extract was neutralized by adding 500 μl of THA solution (100 mM Tris/HCl, pH 8.1, and 50 mM HCl), divided into 150- μl aliquots, quickly frozen in liquid nitrogen, and stored at -80°C prior to use. To measure glycogen concentration, 50 μl of alkali extract (recovered from the total of 6.5×10^7 cells) were added to 500 μl of glycogen reagent [50 mM sodium acetate, pH 4.6, 0.02% BSA; with or without 5 $\mu\text{g}/\text{ml}$ amyloglucosidase (14 U/mg; Roche)]. The mixture was incubated for 30 min at 25°C . 500 μl of glucose reagent [100 mM Tris/HCl, pH 8.1, 2 mM MgCl_2 , 1 mM DTT, 1 mM ATP, 0.2 mM NADP^+ , 5 $\mu\text{g}/\text{ml}$ glucose-6-phosphate dehydrogenase (Sigma), 20 $\mu\text{g}/\text{ml}$ hexokinase (450 U/mg; Roche) was added and the mixture incubated for 30 min at 25°C . The NADPH generated from NADP^+ was measured fluorimetrically (excitation at 365 nm, emission monitored at 460 nm).

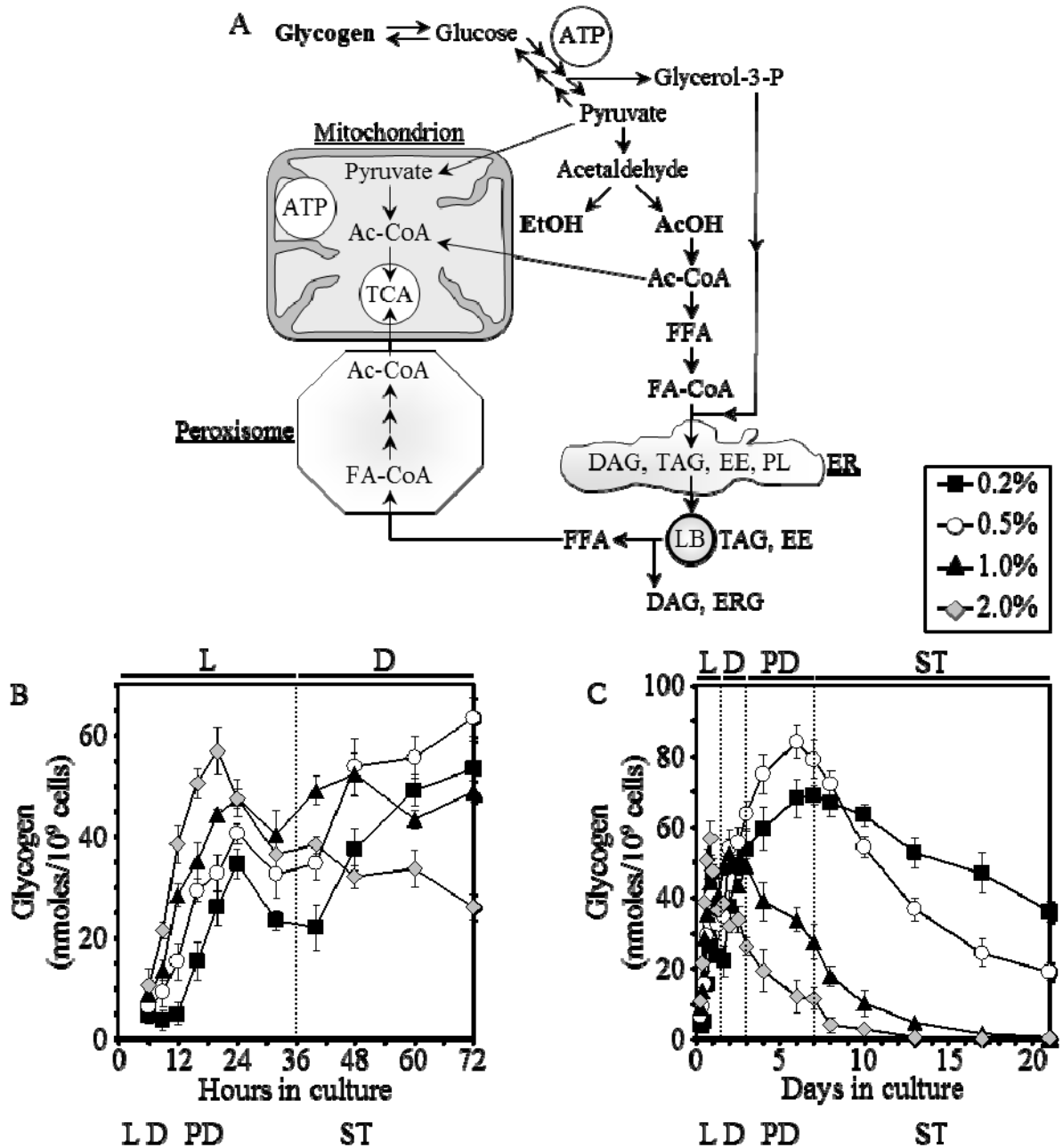


Figure 4.2. CR remodels glycogen metabolism. (A) Outline of metabolic pathways and interorganellar communications operating in chronologically aging yeast. (B, C) The dynamics of age-dependent changes in the intracellular levels of glycogen during chronological aging of yeast. Cells were cultured in YP medium initially containing 0.2%, 0.5%, 1% or 2% glucose. Data are presented as mean \pm SEM (n = 4-6). For glycogen levels, $p < 0.001$ at days 3 to 21 for cells grown on 0.2% or 0.5% glucose versus cells grown on 2% glucose. Abbreviations: Ac-CoA, acetyl-CoA; AcOH, acetic acid; DAG, diacylglycerols; EE, ethyl esters; ER, endoplasmic reticulum; ERG, ergosterol; EtOH, ethanol; FA-CoA, CoA esters of fatty acids; FFA, free fatty acids; LB, lipid bodies; PL, phospholipids; TAG, triacylglycerols; TCA, the tricarboxylic acid cycle in mitochondria.

4.4 Results

4.4.1 CR remodels glycogen metabolism

Our monitoring of the dynamics of age-related changes in glycogen concentration revealed that the intracellular levels of this major reserve carbohydrate in yeast [169] increased sharply in L phase, regardless of initial glucose concentration in the medium (Figure 4.2B). During the subsequent D and PD phases, CR yeast continued to accumulate glycogen, whereas non-CR yeast rapidly consumed it (Figure 4.2C). In contrast to non-CR yeast, yeast under CR began to degrade their reserved glycogen only when they entered ST phase (Figure 4.2C). Of note, the degree of CR influenced both glycogen storage and its consumption. In fact, CR yeast grown on 0.5% glucose reserved more glycogen by the end of PD phase and then consumed it in ST phase somewhat faster, as compared to CR yeast grown on 0.2% glucose (Figure 4.2C).

4.4.2 The maintenance of a proper balance between the biosynthesis and degradation of glycogen is mandatory for lifespan extension by CR

We next used a collection of mutants, each lacking a single protein that functions in glycogen biosynthesis or degradation (Figure 4.3A) [169], for functional analysis of the role for age-dependent glycogen dynamics in lifespan extension by CR. We found that any genetic manipulation that substantially reduced glycogen concentration in CR cells entering ST phase of growth on 0.2% glucose shortened their chronological lifespan. This pattern was seen in mutants that lacked 1) the Glg2p isoform of self-glucosylating glycogenin glucosyltransferase; 2) the Gsy2p isoform of glycogen synthase; 3) Gac1p,

Pig1p or Snf1p, all of which promote the dephosphorylation and activation of Gsy2p; or 4) the glycogen branching enzyme Glc3p (Figures 4.3B – 4.3D). Our findings also revealed that the chronological lifespan of CR yeast could be prolonged only by a genetic manipulation that simultaneously accelerates 1) glycogen biosynthesis during growth phases preceding ST phase; and 2) glycogen degradation during ST phase. In fact, lack of some proteins, although accelerated glycogen biosynthesis during growth phases preceding ST phase, impaired glycogen degradation during ST phase and resulted in a shortened lifespan. We observed this pattern in mutants that lacked 1) the Pcl8p or Pho85p, each promoting the phosphorylation and inactivation of Gsy2p; or 2) the Gph1p isoform of glycogen phosphorylase (Figures 4.3B – 4.3D). Only in the *tpk1Δ* mutant,

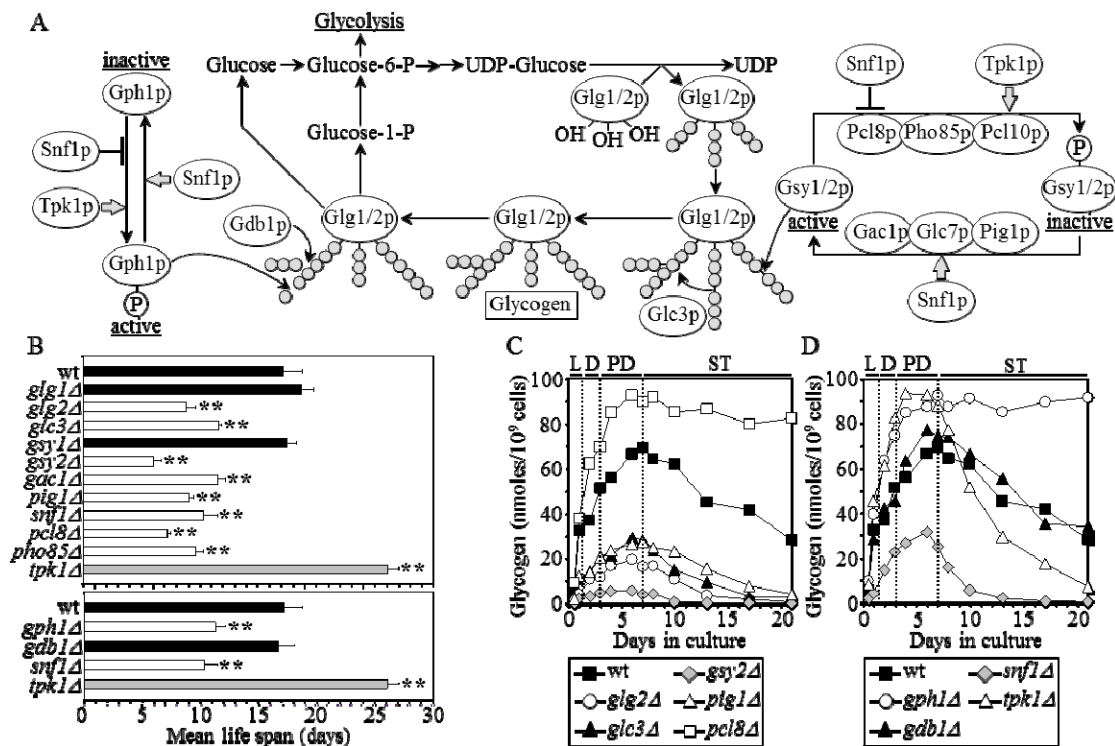


Figure 4.3. CR extends lifespan in part by maintaining a proper balance between the biosynthesis and degradation of glycogen. (A) Outline of metabolic pathways of glycogen biosynthesis and degradation. (B) The mean lifespans of WT and mutant strains. Each mutant lacked a single enzyme that functions in

glycogen biosynthesis or degradation. Each plot represents the average of 2-3 experiments; error bars show SEM. (C, D) Glycogen concentrations in cells of a WT strain and mutant strains. Each mutant carried a single-gene-deletion mutation that affects glycogen biosynthesis or degradation. Each plot shows a representative experiment repeated 2-3 times with similar results. (B-D) Cells were cultured in YP medium initially containing 0.2% glucose.

which lacked the catalytic subunit Tpk1p of cAMP-dependent protein kinase, the acceleration of both glycogen biosynthesis prior to ST phase and glycogen degradation during ST phase led to a substantially extended lifespan (Figures 4.3B and 4.3D). Of note, we found that lifespan was not affected by any of the single-gene-deletion mutations that, by eliminating a low-abundance redundant component functioning in glycogen biosynthesis or degradation, did not have an effect on concentration of this major reserve carbohydrate. This pattern was seen in mutants that lacked 1) the Glg1p isoform of self-glucosylating glycogenin glucosyltransferase; 2) the Gsy1p isoform of glycogen synthase; or 3) the Gdb1p glycogen debranching enzyme (Figures 4.3B and 4.3D).

4.5 Discussion

Along with other data from our laboratory on the molecular mechanism underlying the ability of CR to extend longevity of chronologically aging yeast [32, 40, 110, 114], findings presented in this chapter of my thesis imply that, by activating the synthesis of enzymes catalyzing the biosynthesis of glycogen and by suppressing the synthesis of enzymes required for its degradation, CR promotes the accumulation of this major reserve carbohydrate. Our functional analysis of the role for age-dependent

glycogen dynamics in lifespan extension by CR with the help of a collection of mutants, each lacking a single protein that functions in glycogen biosynthesis or degradation, provides evidence that lifespan extension by CR relies in part on the establishment of a proper balance between the biosynthesis and degradation of glycogen. Current studies in our laboratory are aimed at establishing molecular mechanisms underlying the longevity-defining role of such balance in chronologically aging yeast.

4.6 Conclusions

Findings presented in this chapter of my thesis provide conclusive evidence that lifespan extension by CR in chronologically aging yeast relies in part on the establishment of a proper balance between the biosynthesis and degradation of glycogen, the major reserve carbohydrate.

5 Caloric restriction (CR) extends yeast chronological lifespan by reducing ethanol concentration

5.1 Abstract

In studies described in this chapter of the thesis, we monitored the dynamics of age-related changes in ethanol concentration in chronologically aging yeast cultured under CR and non-CR conditions. We also assessed how single-gene-deletion mutations eliminating Adh1p (an enzyme that is required for ethanol synthesis) or Adh2p (an enzyme that catalyzes ethanol degradation) affect longevity of chronologically aging yeast under CR and non-CR conditions. Furthermore, we examined the effects of the *adh1Δ* and *adh2Δ* mutations on the intracellular levels of trehalose, glycogen, neutral lipids, free fatty acids (FFA) and diacylglycerols (DAG) in chronologically aging yeast under non-CR conditions. Moreover, we monitored how single-gene-deletion mutations eliminating Adh1p or Adh2p influence the abundance of Fox1p, Fox2p and Fox3p, all of which are the core enzymes of fatty acid β -oxidation in peroxisomes. Our findings provide evidence that ethanol accumulated in yeast placed on a calorie-rich diet represses the synthesis of Fox1p, Fox2p and Fox3p, thereby suppressing peroxisomal oxidation of FFA that originate from triacylglycerols synthesized in the endoplasmic reticulum (ER) and deposited within LBs. The resulting build-up of arrays of FFA (so-called gnarls) within LBs of non-CR yeast initiates several negative feedback loops regulating the metabolism of triacylglycerols. Due to the action of these negative feedback loops, chronologically aging non-CR yeast not only amass triacylglycerols in LBs but also accumulate DAG and FFA in the ER. The resulting remodeling of lipid dynamics in

chronologically aging non-CR yeast shortens their lifespan by causing their premature death due to 1) necrosis triggered by the inability of their peroxisomes to oxidize FFA; 2) lipoapoptosis initiated in response to the accumulation of DAG and FFA; and 3) the DAG-induced reorganization of the protein kinase C-dependent signal transduction network affecting multiple longevity-related cellular targets.

5.2 Introduction

Our recent mass spectrometry-based identification and quantitation of proteins recovered in total cell lysates of chronologically aging CR and non-CR yeast revealed that CR alters the levels of numerous proteins that function in various processes (Figure 4.1) [32]. Of note, the administration of this low-calorie dietary regimen reduced the level of Adh1p (an enzyme that is required for ethanol synthesis) and elevated the level of Adh2p (an enzyme that catalyzes ethanol degradation) (Figure 4.1) [32].

To evaluate a potential role of ethanol metabolism in lifespan extension by CR, in studies described in this chapter of the thesis we monitored the dynamics of age-related changes in its intracellular level. We also assessed how single-gene-deletion mutations eliminating Adh1p or Adh2p affect longevity of chronologically aging yeast under CR and non-CR conditions. In addition, we examined the effects of the *adh1Δ* and *adh2Δ* mutations on the intracellular levels of trehalose, glycogen, neutral lipids, free fatty acids and diacylglycerols in chronologically aging yeast under non-CR conditions. Moreover, we monitored how single-gene-deletion mutations eliminating Adh1p or Adh2p influence the abundance of Fox1p, Fox2p and Fox3p, all of which are the core enzymes of fatty acid β -oxidation in peroxisomes. Our findings provide evidence that CR extends yeast

chronological lifespan by reducing ethanol concentration, thereby causing a remodeling of carbohydrate and lipid metabolism.

5.3 Materials and Methods

Strains and media

The wild-type strain *Saccharomyces cerevisiae* BY4742 (*MAT α his3 Δ 1 leu2 Δ 0 lys2 Δ 0 ura3 Δ 0*) and mutant strains *adh1 Δ* (*MAT α his3 Δ 1 leu2 Δ 0 lys2 Δ 0 ura3 Δ 0 *adh1 Δ ::kanMX4*) and *adh2 Δ* (*MAT α his3 Δ 1 leu2 Δ 0 lys2 Δ 0 ura3 Δ 0 *adh2 Δ ::kanMX4*) were grown in YP medium (1% yeast extract, 2% peptone) containing 0.2%, 0.5%, 1% or 2% glucose as carbon source. Cells were cultured at 30°C with rotational shaking at 200 rpm in Erlenmeyer flasks at a “flask volume/medium volume” ratio of 5:1.**

Chronological lifespan assay

A sample of cells was taken from a culture at a certain time-point. A fraction of the sample was diluted in order to determine the total number of cells using a hemacytometer. Another fraction of the cell sample was diluted and serial dilutions of cells were plated in duplicate onto YP plates containing 2% glucose as carbon source. After 2 d of incubation at 30°C, the number of colony forming units (CFU) per plate was counted. The number of CFU was defined as the number of viable cells in a sample. For each culture, the percentage of viable cells was calculated as follows: (number of viable cells per ml/total number of cells per ml) \times 100. The percentage of viable cells in mid-logarithmic phase was set at 100%. The lifespan curves were validated using a LIVE/DEAD yeast viability kit (Invitrogen) following the manufacturer's instructions.

Visualization of intracellular lipid bodies (LBs)

Wild-type and mutant cells grown in YP supplemented with 0.2% glucose were tested microscopically for the presence of intracellular LBs by incubation with BODIPY 493/503. Cells were also probed with a fluorescent counterstain Calcofluor White M2R (CW) in order to visualize all cells in the population. BODIPY 493/503 was stored in the dark at -20°C as 100 μl aliquots of a 1 mM solution in ethanol. CW was stored in the dark at -20°C as the 5 mM stock solution in anhydrous DMSO.

The concurrent staining of cells with BODIPY 493/503 and CW was carried out as follows. The required amounts of the 100 μl BODIPY 493/503 aliquots (1 mM) and of the 5 mM stock solution of CW were taken out of the freezer and warmed to room temperature. The solutions of DHR and CW were then centrifuged at $21,000 \times g$ for 5 min in order to clear them of any aggregates of fluorophores. For cell cultures with a titre of $\sim 10^7$ cells/ml, 100 μl was taken out of the culture to be treated. If the cell titre was lower, proportionally larger volumes were used. The samples were then centrifuged at $21,000 \times g$ for 1 min, and pelleted cells were resuspended in 100 μl of TNT buffer (25 mM Tris/HCl (pH 7.5), 150 mM NaCl and 0.2 % Triton X-100). After a 10-min incubation at room temperature, the samples were centrifuged at $21,000 \times g$ for 1 min. Pellets were then resuspended in 100 μl of TN buffer (25 mM Tris/HCl (pH 7.5), 150 mM NaCl), and the samples were subjected to centrifugation at $21,000 \times g$ for 1 min. Pelleted cells were finally resuspended in 100 μl of TN buffer. Each 100 μl aliquot of cells was then supplemented with 1 μl of the 1 mM BODIPY 493/503 and 1 μl of the 5 mM CW solutions. After a 15-min incubation in the dark at room temperature, the samples were centrifuged at $21,000 \times g$ for 5 min. Pellets were resuspended in 100 μl of

TN buffer. The samples were centrifuged again at $21,000 \times g$ for 5 min, and pellets were resuspended in 100 μ l of TN buffer. 10 μ l of the BODIPY 493/503- and CW-treated cell suspension was then added to a microscope slide and covered with a coverslip. The slides were then sealed using nail polish. Once the slides were prepared, they were visualized under the Zeiss Axioplan fluorescence microscope mounted with a SPOT Insight 2 megapixel color mosaic digital camera. Several pictures of the cells on each slide were taken, with two pictures taken of each frame. One of the two pictures was of the cells seen through a fluorescein filter in order to detect cells dyed with BODIPY 493/503. The second picture was of the cells seen through a DAPI filter in order to visualize CW, and therefore all the cells present in the frame. For evaluating the percentage of BODIPY 493/503-positive cells, the UTHSCSA Image Tool (Version 3.0) software was used to calculate both the total number of cells and the number of stained cells.

Trehalose concentration measurement

Preparation of alkali cellular extract and a microanalytic biochemical assay for measuring trehalose concentration were performed as previously described [177]. To prepare an alkali cellular extract, 2×10^9 cells were harvested by centrifugation for 1 min at $21,000 \times g$ at 4°C . The cells were washed three times in ice-cold PBS (20 mM $\text{KH}_2\text{PO}_4/\text{KOH}$, pH 7.5, and 150 mM NaCl). The cell pellet was quickly resuspended in 200 μ l of ice-cold SHE solution (50 mM NaOH, and 1 mM EDTA), and 800 μ l of ice-cold SHE solution were added to the cell suspension. The resulting alkali extract was incubated at 60°C for 30 min to destroy endogenous enzyme activities and pyridine nucleotides. The extract was neutralized by adding 500 μ l of THA solution (100 mM Tris/HCl, pH 8.1, and 50

mM HCl), divided into 150- μ l aliquots, quickly frozen in liquid nitrogen, and stored at -80°C prior to use. To measure trehalose concentration, 50 μ l of alkali extract (recovered from the total of 6.5×10^7 cells) were added to 150 μ l of trehalose reagent (25 mM $\text{KH}_2\text{PO}_4/\text{KOH}$, pH 7.5, and 0.02% BSA; with or without 15 mU trehalase (Sigma)). The mixture was incubated for 60 min at 37°C. 800 μ l of glucose reagent (100 mM Tris/HCl, pH 8.1, 2 mM MgCl_2 , 1 mM DTT, 1 mM ATP, 0.2 mM NADP^+ , and mixture of hexokinase (7 U) and glucose-6-phosphate dehydrogenase (8 U) (Sigma)) was added and the mixture incubated for 30 min at 25°C. The NADPH generated from NADP^+ was measured fluorimetrically (excitation at 365 nm, emission monitored at 460 nm).

Glycogen concentration measurement

Preparation of alkali cellular extract and a microanalytic biochemical assay for measuring glycogen concentration were performed as previously described [177]. To prepare an alkali cellular extract, 2×10^9 cells were harvested by centrifugation for 1 min at 21,000 \times g at 4°C. The cells were washed three times in ice-cold PBS (20 mM $\text{KH}_2\text{PO}_4/\text{KOH}$, pH 7.5, and 150 mM NaCl). The cell pellet was quickly resuspended in 200 μ l of ice-cold SHE solution (50 mM NaOH, and 1 mM EDTA), and 800 μ l of ice-cold SHE solution were added to the cell suspension. The resulting alkali extract was incubated at 60°C for 30 min to destroy endogenous enzyme activities and pyridine nucleotides. The extract was neutralized by adding 500 μ l of THA solution (100 mM Tris/HCl, pH 8.1, and 50 mM HCl), divided into 150- μ l aliquots, quickly frozen in liquid nitrogen, and stored at -80°C prior to use. To measure glycogen concentration, 50 μ l of alkali extract (recovered from the total of 6.5×10^7 cells) were added to 500 μ l of glycogen reagent [50 mM

sodium acetate, pH 4.6, 0.02% BSA; with or without 5 µg/ml amyloglucosidase (14 U/mg; Roche)]. The mixture was incubated for 30 min at 25°C. 500 µl of glucose reagent [100 mM Tris/HCl, pH 8.1, 2 mM MgCl₂, 1 mM DTT, 1 mM ATP, 0.2 mM NADP⁺, 5 µg/ml glucose-6-phosphate dehydrogenase (Sigma), 20 µg/ml hexokinase (450 U/mg; Roche) was added and the mixture incubated for 30 min at 25°C. The NADPH generated from NADP⁺ was measured fluorimetrically (excitation at 365 nm, emission monitored at 460 nm).

Preparation of total cell lysates

An aliquot containing 1×10^9 cells was centrifuged for 7 min at 3,000 rpm at room temperature. Pelleted cells were washed twice with distilled water and further centrifuged for 3 min at $16,000 \times g$ at room temperature. The recovered cell pellet was then resuspended in 500 µl of 4% CHAPS in 25 mM Tris/HCl buffer (pH 8.5) and centrifuged for 15 sec at $16,000 \times g$ at room temperature. The cells were then washed again, first by resuspending them in 500 µl of 4% CHAPS in 25 mM Tris/HCl buffer (pH 8.5) and then by centrifuging for 15 sec at $16,000 \times g$ at room temperature. The pellet of washed cells was then resuspended in 1 ml of ice-cold 4% CHAPS in 25 mM Tris/HCl buffer (pH 8.5), divided into 5 equal aliquots of 200 µl each and placed in Eppendorf tubes kept on ice. Each 200 µl aliquot was supplemented with ~100 µl of glass beads and vortexed three times for 1 minute. Apart from the vortexing steps, the samples were kept on ice at all times. Glass beads and cell debris were then pelleted by 5 min centrifugation at $16,000 \times g$ at 4°C. The resulting supernatant of the glass bead lysate was immediately transferred into a pre-chilled Eppendorf tube and stored at -20°C for further analysis.

Protein precipitation, SDS-PAGE and immunoblotting

Protein concentration was determined using the RC DC protein assay kit (Bio-Rad) according to the manufacturer's instructions. Proteins were precipitated by adding trichloroacetic acid (TCA) to the final concentration of 10%, incubated on ice for 30 min, pelleted by centrifugation, and then washed with ice-cold 80% acetone. Dried protein pellets were then resuspended in the SDS-PAGE sample buffer and the pH was adjusted to neutral using 2 M Tris/HCl (pH 8.8). The samples were boiled for 5 min at 63°C, centrifuged for 30 sec at 16,000 x g, loaded onto a 12.5% gel and resolved by SDS-PAGE. Immunoblotting using a Trans-Blot SD semi-dry electrophoretic transfer system (Bio-Rad) were performed as previously described [202]. Blots were decorated with monoclonal antibodies raised against actin (Abcam), Fox1p, Fox2p or Fox3p (kind gift of Dr. Richard A. Rachubinski, University of Alberta). Antigen-antibody complexes were detected by enhanced chemiluminescence using an Amersham ECL Western blotting detection reagents (GE Healthcare).

Ethanol and acetic acid concentrations measurement

1-ml aliquots of yeast cultures were centrifuged for 1 min at 16,000 × g at 4°C and supernatants frozen at -80°C. The supernatants were subjected to gas chromatography using an Agilent 6890 Networked GC system equipped with a Supelco Equity-1 (0.32 mm × 30 cm) column and FID detector. Ethanol and acetic acid concentrations were calculated using the Chemstation 3 software (Agilent).

Miscellaneous procedures

Protocols for lipid extraction, separation by TLC, visualization by 5% phosphomolybdic acid in ethanol, and quantitation by densitometric analysis of TLC plates have been described elsewhere [203].

5.4 Results

5.4.1 Concentration of ethanol is one of the key factors influencing chronological aging

As one can expect judging from the reduced level of Adh1p (an enzyme that is required for ethanol synthesis) and elevated level of Adh2p (an enzyme that catalyzes ethanol degradation) in yeast grown under CR conditions (Figure 4.1), the administration of this low-calorie dietary regimen by cell culturing on 0.2% or 0.5% glucose accelerated the depletion of ethanol from yeast cells (Figure 5.1B). Thus, the steady-state level of ethanol depends on a balance of enzymatic activities of the Adh1p and Adh2p isozymes of alcohol dehydrogenase (Figure 5.2A).

To evaluate the effect of endogenously produced ethanol on longevity, we incubated WT, *adh1Δ* and *adh2Δ* strains in media containing different glucose concentrations. We monitored the chronological lifespans of these strains and assessed the dynamics of changes in ethanol concentration during their aging. When yeast were placed on the CR diet by incubating them on 0.2% or 0.5% glucose, lack of Adh1p or Adh2p did not affect ethanol concentration (Figures 5.2B and 5.2C) or chronological lifespan (Figures 5.2F and 5.2G). Conversely, lack of Adh1p substantially decreased

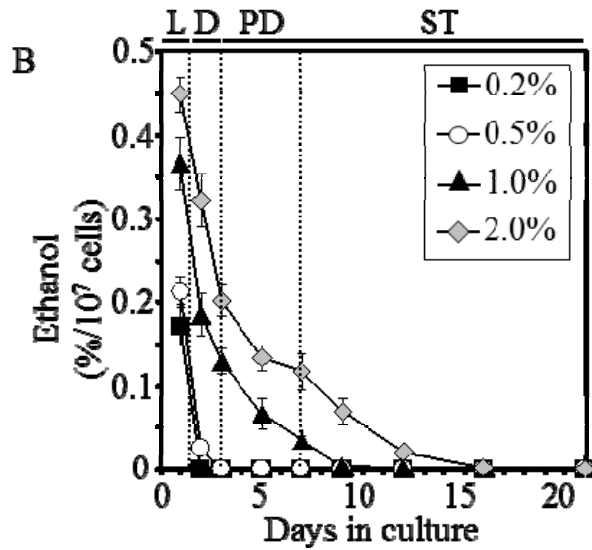
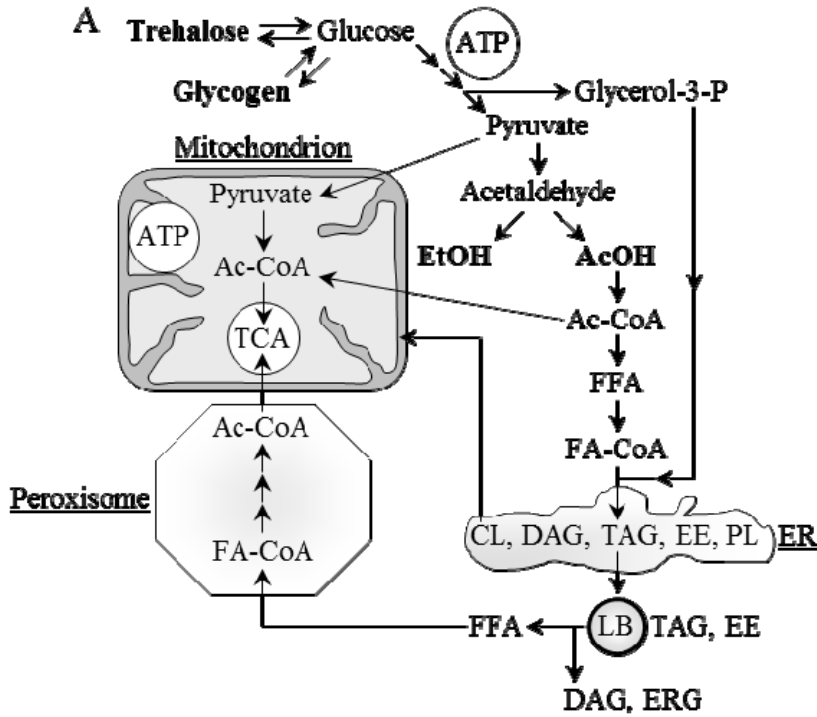


Figure 5.1. CR accelerates ethanol catabolism. (A) Outline of metabolic pathways and interorganellar communications operating in chronologically aging yeast. (B) The dynamics of age-dependent changes in the extracellular concentrations of ethanol during chronological aging of wild-type yeast strain. Cells were cultured in rich YP medium initially containing 0.2%, 0.5%, 1% or 2% glucose. Data are presented as mean \pm SEM (n = 3-5). For ethanol levels, $p < 0.001$ at days 1 to 9 for cells grown on 0.2% or 0.5% glucose versus cells grown on 2% glucose. Abbreviations: Ac-CoA, acetyl-CoA; AcOH, acetic acid; CL,

cardiolipins; DAG, diacylglycerols; EE, ethyl esters; ER, endoplasmic reticulum; EtOH, ethanol; FA-CoA, CoA esters of fatty acids; FFA, free fatty acids; LB, lipid bodies; PL, phospholipids; TAG, triacylglycerols.

ethanol concentration when yeast were grown on 1% or 2% glucose (Figures 5.2D and 5.2E), prolonging their lifespan (Figures 5.2F and 5.2G). Furthermore, lack of Adh2p led to a considerable rise of ethanol concentration in non-CR yeast grown on 1% or 2% glucose (Figures 5.2D and 5.2E), shortening their lifespan (Figures 5.2F and 5.2G). By extending lifespan of non-CR yeast, *adh1Δ* to a great extent abolished the positive effect of CR on longevity (Figures 5.2H and 5.2I). Alternatively, by shortening lifespan of non-CR yeast, *adh2Δ* enhanced the benefit of CR for longevity (Figures 5.2H and 5.2I). We therefore concluded that a genetic or dietary intervention that lowers ethanol concentration will extend yeast longevity.

5.4.2 Ethanol remodels metabolism of trehalose, glycogen and several lipid species in chronologically aging yeast

We found that in chronologically aging yeast ethanol modulates the age-related dynamics of changes in concentrations of trehalose, glycogen and several lipid species. In fact, by decreasing ethanol concentration in non-CR yeast, *adh1Δ* remodelled the metabolism of these key for longevity compounds (see Chapters 3 and 4 of this thesis, as well as [32, 40, 110, 114]) in non-CR yeast by making it similar to the metabolic design of CR yeast. Specifically, the *adh1Δ* mutation 1) increased the level of trehalose (Figure 5.3B); 2) redesigned glycogen metabolism by promoting glycogen accumulation in PD phase and delaying its consumption until ST phase (Figure 5.3C); 3) accelerated the lipolytic consumption of triacylglycerols (TAG) and ergosteryl esters (EE) (Figures

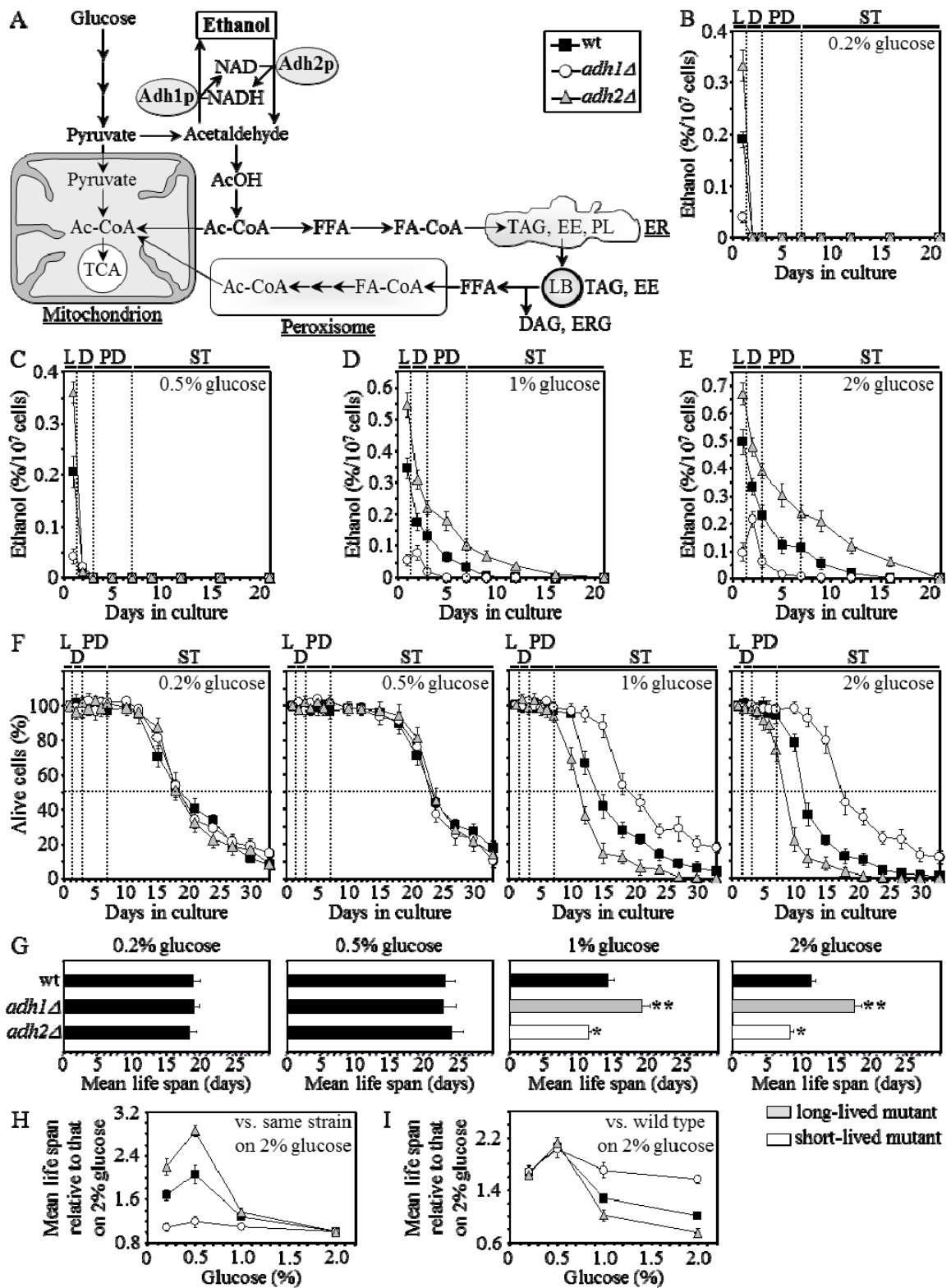


Figure 5.2. Ethanol is one of the key factors regulating longevity. (A) Outline of metabolic pathways and interorganellar communications operating in chronologically aging yeast cells. (B-E) The dynamics of age-dependent changes in the extracellular concentration of ethanol for WT, *adh1Δ* and *adh2Δ*. Data are presented as mean ± SEM (n = 3-5). (F and G) Survival (F) and the mean chronological lifespans (G) of WT, *adh1Δ* and *adh2Δ*. Data are presented as mean ± SEM (n = 3-5); *p < 0.05, **p < 0.005. (H and I) A dose-response relationship between the mean chronological lifespan and the degree of CR for WT, *adh1Δ* and *adh2Δ*. Data are presented as mean ± SEM (n = 3-5). (B-I) Cells were cultured in YP medium initially containing 0.2%, 0.5%, 1% or 2% glucose.

5.3D - 5.3F), the two major neutral lipids that in yeast are synthesized in the endoplasmic reticulum (ER) and then deposited in lipid bodies (LBs) (204); and 4) accelerated the consumption of free fatty acids (FFA) and diacylglycerols (DAG) during late PD and early ST phases (Figures 5.3G and 5.3H). In contrast, by elevating ethanol level in non-CR yeast, *adh2Δ* enhanced the negative effect of a calorie-rich diet on longevity by further decreasing trehalose concentration, accelerating glycogen consumption, slowing down neutral lipids lipolysis, and decelerating FFA and DAG consumption (Figure 5.3). In sum, based on the findings presented in Chapters 5.4.1 and 5.4.2, we concluded that ethanol is one of the key factors regulating longevity by specifically modulating the metabolism of trehalose, glycogen, neutral lipids, FFA and DAG in chronologically aging yeast.

5.4.3 Ethanol decelerates fatty acid oxidation in peroxisomes of chronologically aging yeast

We sought to define a mechanism by which ethanol modulates the dynamics of

(B), glycogen (C), TAG (E), EE (F), FFA (G) and DAG (H) during chronological aging of WT, *adh1Δ* and *adh2Δ*. Data are presented as mean ± SEM (n = 3-4). (D) Percent of WT, *adh1Δ* and *adh2Δ* cells that contain lipid bodies. Data are presented as mean ± SEM (n = 4). (B-H) Cells were cultured in rich YP medium initially containing 2% glucose. Abbreviations: Ac-CoA, acetyl-CoA; AcOH, acetic acid; DAG, diacylglycerols; EE, ethyl esters; ER, endoplasmic reticulum; FA-CoA, CoA esters of fatty acids; FFA, free fatty acids; LB, lipid bodies; PL, phospholipids; TAG, triacylglycerols.

neutral lipids, FFA and DAG in chronologically aging yeast. Importantly, we found that the observed rapid depletion of ethanol seen in CR yeast (Figure 5.1B) coincides with 1) elevated levels of Fox1p, Fox2p and Fox3p (Figure 4.1), all of which are the core enzymes of peroxisomal fatty acid β -oxidation [205]; and 2) rapid consumption of FFA during PD phase [32]. Noteworthy, it has been previously shown that in the yeast species that need peroxisomes to utilize methanol as a sole carbon source for growth, ethanol suppresses the synthesis of peroxisomal enzymes catalyzing methanol oxidation [206]. Based on these findings, we hypothesized that the accumulation of ethanol in non-CR yeast cultures (Figure 5.1B) suppresses peroxisomal oxidation of FFA by repressing the synthesis of Fox1p, Fox2p and Fox3p, thereby causing the accumulation of FFA during PD phase (Figure 5.3G). This hypothesis was confirmed by our finding that a premature depletion of ethanol from non-CR cells of *adh1Δ* (Figures 5.2D and 5.2E) led to an early synthesis of Fox1p, Fox2p and Fox3p in PD phase (Figure 5.4B) and promoted FFA consumption (Figure 5.3G). In addition, we found that a postponed depletion of ethanol from non-CR cells of *adh2Δ* (Figures 5.2D and 5.2E) delays the synthesis of Fox1p, Fox2p and Fox3p (Figure 5.4B) and slows down FFA consumption (Figure 5.3G).

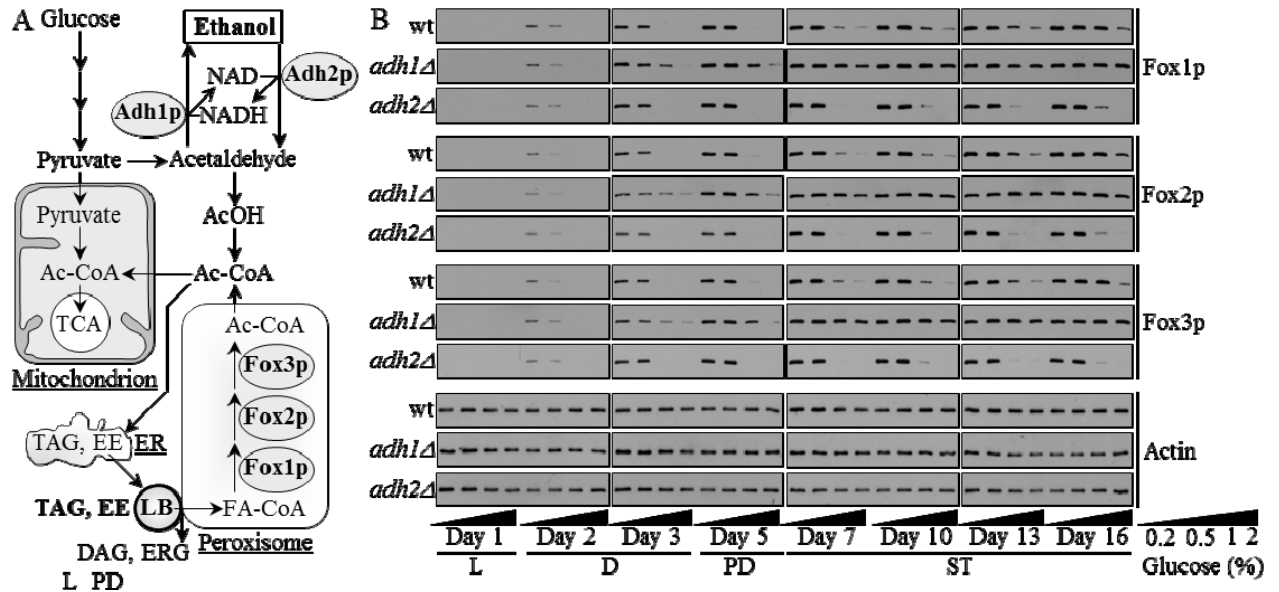


Figure 5.4. Ethanol suppresses the synthesis of Fox1p, Fox2p and Fox3p, all of which are the core enzymes of peroxisomal fatty acid β -oxidation. (A) Outline of metabolic pathways and interorganelle communications operating in chronologically aging yeast cells. (B) Western blot analysis of Fox1p, Fox2p, Fox3p and actin in aging WT, *adh1Δ* and *adh2Δ* cultured in YP medium initially containing 0.2%, 0.5%, 1% or 2% glucose. Protein recovered in total cell lysates were resolved by SDS-PAGE and detected by immunoblotting. A representative of 3 independent experiments is shown.

How exactly ethanol modulates the dynamics of neutral lipids in chronologically aging yeast? By substantially decreasing ethanol concentration in non-CR yeast, *adh1Δ* accelerated not only the consumption of FFA but also the lipolysis of neutral lipids deposited in LBs (Figures 5.3D-5.3G). Moreover, by elevating ethanol level in non-CR yeast, *adh2Δ* decelerated both these processes (Figures 5.3D-5.3G). These findings strongly suggest that a diet or genetic manipulation that decelerates peroxisomal oxidation of FFA by Fox1p, Fox2p and/or Fox3p could also slow down the lipolysis of

neutral lipids in LBs, perhaps due to a feedback inhibition of the lipolysis by the concentrations of FFA or FA-CoA exceeding a critical level.

5.5 Discussion

Findings described in this chapter of my thesis imply that the accumulation of ethanol in non-CR yeast suppresses peroxisomal oxidation of FFA by repressing the synthesis of Fox1p, Fox2p and Fox3p, thereby causing the build-up of FFA. Of note, it has been shown that the β -oxidation of FFA in yeast peroxisomes is facilitated by their physical association with LBs. The extensive physical contact existing between peroxisomes and LBs stimulates the lipolysis of neutral lipids within LBs, thereby initiating the conversion of newly formed free fatty acids to their CoA esters that then get imported and oxidized by peroxisomes [207]. The LBs-peroxisome association can lead to peroxisome invasion into the lipid core of LBs, thereby generating the so-called pexopodia that exist as individual peroxisomes or as their extensions penetrating the core of LBs [207]. Importantly, pexopodia of yeast mutants that were unable to oxidize FFA due to the absence of Fox1p, Fox2p or Fox3p caused the accumulation of the so-called gnarls within the core of LBs [207]. Gnarls represent electron-dense arrays of free fatty acids accumulated in excessive amounts within LBs of *fox1 Δ* , *fox2 Δ* and *fox3 Δ* mutants [207]. In addition, lack of Fox1p, Fox2p or Fox3p resulted in the build-up of triacylglycerols within the core of LBs [207]. By extending these observations to lipid dynamics in LBs and peroxisomes of chronologically aging non-CR yeast, one could expect that the accumulation of ethanol in non-CR yeast and the resulting repression of the synthesis of Fox1p, Fox2p and Fox3p cause the build-up of arrays of FFA (gnarls)

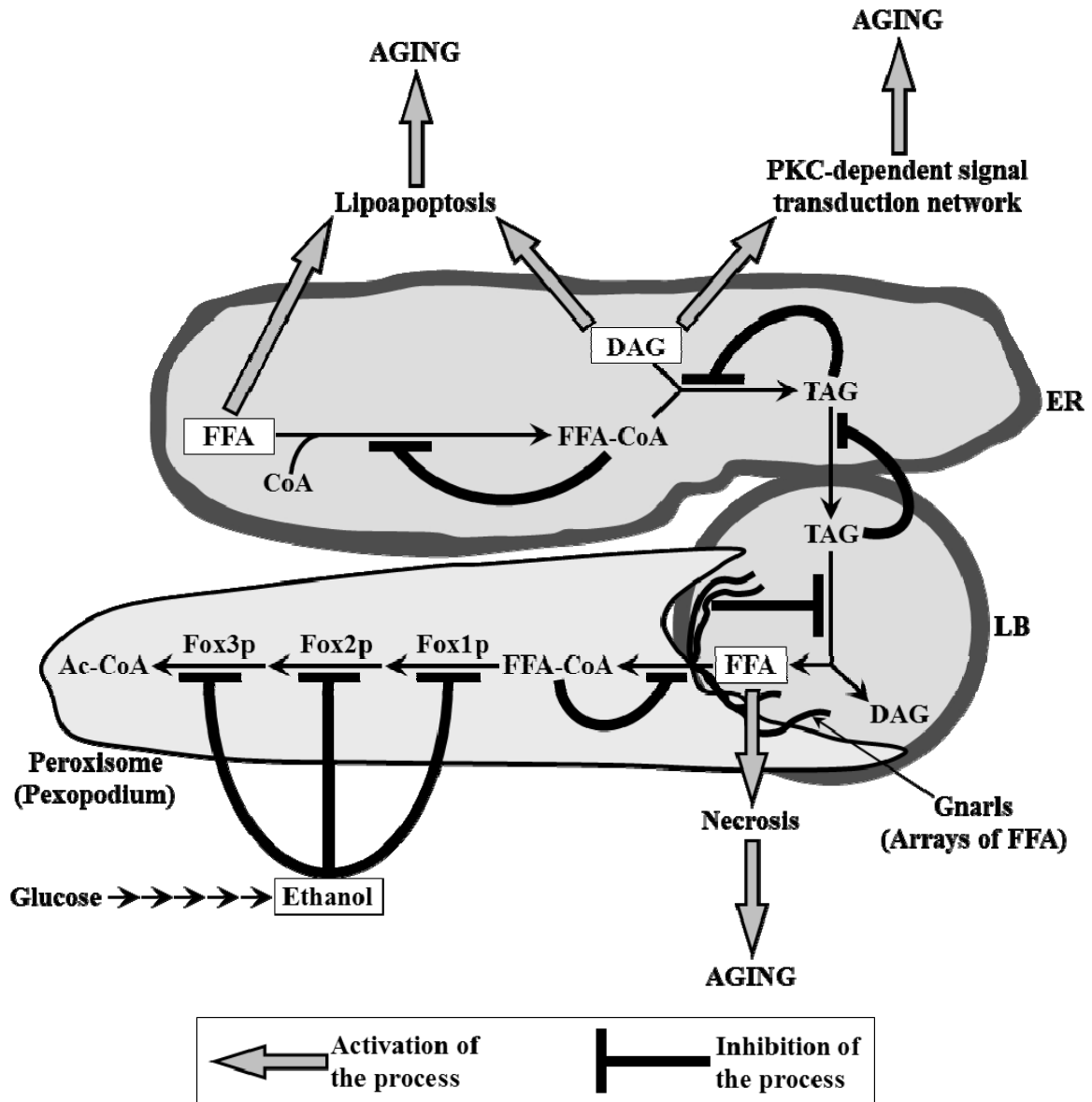


Figure 5.5. A possible mechanism linking longevity and lipid dynamics in the endoplasmic reticulum (ER), lipid bodies (LBs) and peroxisomes of yeast placed on a calorie-rich diet. LBs in yeast cells function as a hub in a regulatory network that modulates neutral lipids synthesis in the ER and fatty acid oxidation in peroxisomes. The LBs-peroxisome association leads to peroxisome invasion into the lipid core of LBs, thereby generating the so-called pexopodium. Ethanol accumulated in yeast placed on a calorie-rich diet represses the synthesis of Fox1p, Fox2p and Fox3p, thereby suppressing peroxisomal oxidation of free fatty acids (FFA) that originate from triacylglycerols (TAG) synthesized in the ER and deposited within LBs. The resulting build-up of arrays of FFA (gnarls) within LBs of these yeast initiates several negative feedback loops regulating the metabolism of TAG. Due to the action of these negative feedback loops, chronologically aging yeast placed on a calorie-rich diet not only amass TAG in LBs but also accumulate

diacylglycerol (DAG) and FFA in the ER. The resulting remodeling of lipid dynamics in these yeast shortens their lifespan by causing their premature death due to 1) necrosis triggered by the inability of their peroxisomes to oxidize FFA; 2) lipoapoptosis initiated in response to the accumulation of DAG and FFA; and 3) a DAG-induced reorganization of the protein kinase C (PKC)-dependent signal transduction network affecting multiple stress response- and longevity-related processes. Other abbreviations: FFA-CoA, CoA esters of fatty acids.

and triacylglycerols within the core of their LBs.

Taken together, these findings suggest a mechanism linking yeast longevity and lipid dynamics in the ER, LBs and peroxisomes (Figure 5.5). In this mechanism, LBs in yeast cells function as a hub in a regulatory network that modulates neutral lipids synthesis in the ER and FFA oxidation in peroxisomes. As we found, ethanol accumulated in yeast placed on a calorie-rich diet represses the synthesis of Fox1p, Fox2p and Fox3p, thereby suppressing peroxisomal oxidation of FFA that originate from triacylglycerols synthesized in the ER and deposited within LBs (Figures 5.3G, 5.3H and 5.4B). In our hypothesis, the resulting build-up of arrays of FFA (gnarls) within LBs of non-CR yeast initiates several negative feedback loops regulating the metabolism of triacylglycerols (Figure 5.5). Due to the action of these negative feedback loops, chronologically aging non-CR yeast not only amass triacylglycerols in LBs but also accumulate DAG and FFA in the ER (Figures 5.3G and 5.3H) [32]. Of note, it has been recently revealed that 1) loss of peroxisome function triggers necrosis [208, 209]; 2) both FFA and DAG induce lipoapoptosis (a caspase- and mitochondria-independent form of programmed cell death) [210]; and 3) the accumulation of DAG triggers a protein kinase C-dependent signal transduction network affecting multiple stress response- and longevity-related processes [211, 212]. We therefore hypothesize that the proposed remodeling of lipid dynamics in chronologically aging non-CR yeast shortens their

lifespan by causing their premature death due to 1) necrosis triggered by the inability of their peroxisomes to oxidize FFA; 2) lipoapoptosis initiated in response to the accumulation of DAG and FFA; and 3) the DAG-induced reorganization of the protein kinase C-dependent signal transduction network affecting multiple longevity-related cellular targets (Figure 5.5).

Recently, we assessed the effect of CR on the dynamics of age-related changes in the proteomes and lipidomes of ER, LBs and peroxisomes in chronologically aging yeast (Kyryakov, P. et al., manuscript in preparation). We also examined how mutations that extend yeast longevity by impairing lipid metabolism in these organelles influence their morphologies, abundance, association with each other, and protein and lipid compositions during chronological aging (Kyryakov, P. et al., manuscript in preparation). Our findings support the proposed here model (Figure 5.5) for a mechanism in which LBs function as a hub in a regulatory network that defines the chronological lifespan of yeast by modulating both neutral lipids synthesis in the ER and FFA oxidation in peroxisomes. By orchestrating several negative feedback loops that coordinate lipid dynamics in a diet- and genotype-dependent fashion, this network controls age-related necrotic cell death and multiple stress response-related processes (Kyryakov, P. et al., manuscript in preparation). Implementing our understanding of the mechanism linking longevity and age-related dynamics of LBs, we developed a lifespan assay that was used for a high-throughput screening of extensive libraries of small molecules [40]. We identified five groups of novel anti-aging natural compounds that significantly delay yeast aging by remodeling lipid metabolism in the ER, LBs and peroxisomes and by

activating a distinct set of stress response-related processes in mitochondria (see next chapter of this thesis).

5.6 Conclusions

Findings presented in this chapter of my thesis provide conclusive evidence that CR extends yeast chronological lifespan by reducing ethanol concentration, thereby causing a remodeling of carbohydrate and lipid metabolism. Our data suggest that the remodeling of lipid dynamics in chronologically aging non-CR yeast shortens their lifespan by causing their premature death due to 1) necrosis triggered by the inability of their peroxisomes to oxidize FFA; 2) lipoapoptosis initiated in response to the accumulation of DAG and FFA; and 3) the DAG-induced reorganization of the protein kinase C-dependent signal transduction network affecting multiple longevity-related cellular targets.

6 Lithocholic acid (LCA), a novel anti-aging compound, alters mitochondrial structure and function, reduces cell susceptibility to mitochondria-controlled apoptosis, and increases cell resistance to oxidative and thermal stresses

6.1 Abstract

We sought to identify small molecules that increase the chronological lifespan of yeast under caloric restriction (CR) conditions by targeting lipid metabolism and modulating “housekeeping” longevity assurance pathways. We predicted that such housekeeping pathways 1) modulate longevity irrespective of the organismal and intracellular nutrient and energy status; and 2) do not overlap (or only partially overlap) with the “adaptable” longevity pathways that are under the stringent control of calorie and/or nutrient availability. In studies presented in this chapter of my thesis, we found that in yeast grown under CR conditions the *pex5Δ* mutation not only remodels lipid metabolism but also causes the profound changes in longevity-defining processes in mitochondria, resistance to chronic (long-term) stresses, susceptibility to mitochondria-controlled apoptosis, and frequencies of mutations in mitochondrial and nuclear DNA. We therefore chose the single-gene-deletion mutant strain *pex5Δ* as a short-lived strain for carrying out a chemical genetic screen aimed at the identification of novel anti-aging compounds targeting housekeeping longevity assurance pathways. By screening the total of approximately 19,000 representative compounds from seven commercial libraries, our laboratory recently identified 24 small molecules that greatly extend the chronological lifespan of *pex5Δ* under CR conditions and belong to 5 chemical groups. One of these groups consisted of 6 bile acids, including LCA. Findings presented in this chapter of my

thesis imply that LCA modulates housekeeping longevity assurance pathways by 1) attenuating the pro-aging process of mitochondrial fragmentation, a hallmark event of age-related cell death; 2) altering oxidation-reduction processes in mitochondria - such as oxygen consumption, the maintenance of membrane potential and ROS production - known to be essential for longevity regulation; 3) enhancing cell resistance to oxidative and thermal stresses, thereby activating the anti-aging process of stress response; 4) suppressing the pro-aging process of mitochondria-controlled apoptosis; and 5) enhancing stability of nuclear and mitochondrial DNA, thus activating the anti-aging process of genome maintenance. The observed pleiotropic effect of LCA on a compendium of housekeeping longevity assurance processes implies that this bile acid is a multi-target life-extending compound that increases chronological lifespan in yeast by modulating a network of the highly integrated cellular events that are not controlled by the adaptable AMP-activated protein kinase/target of rapamycin (AMPK/TOR) and cAMP/protein kinase A (cAMP/PKA) pathways.

6.2 Introduction

Longevity in evolutionarily distant organisms, from yeast to primates, can be extended by administering the following dietary and pharmacological interventions: 1) caloric restriction (CR), a diet in which only calorie intake is reduced but the supply of amino acids, vitamins and other nutrients is not compromised [3, 7, 9, 16, 24 - 26, 213 - 216]; 2) dietary restriction (DR), in which the intake of nutrients (but not necessarily of calories) is reduced by limiting food supply without causing malnutrition [3, 7, 9, 213 - 221]; and 3) a limited set of anti-aging compounds, including resveratrol, rapamycin,

spermidine, caffeine and metformin [3, 16, 24, 28, 40, 49, 222 - 224]. All these longevity-extending interventions target a limited number of nutrient- and energy-sensing longevity signaling pathways that are conserved across phyla and include the insulin/insulin-like growth factor 1 (IGF-1), AMP-activated protein kinase/target of rapamycin (AMPK/TOR) and cAMP/protein kinase A (cAMP/PKA) pathways [3, 9, 16, 27, 30, 36, 40, 43, 44]. The commonly accepted paradigm of longevity regulation posits that most, if not all, longevity signaling pathways are “adaptable” by nature - *i.e.*, that all these pathways modulate longevity only in response to certain changes in the extracellular and intracellular nutrient and energy status of an organism [3, 9, 16, 27, 30, 33, 40, 226 - 231]. However, Li⁺ in worms and rapamycin in fruits flies extend lifespan even under DR conditions, in which all adaptable pro-aging pathways are fully suppressed and all adaptable anti-aging pathways are fully activated [232, 233]. Therefore, our laboratory suggested that some longevity pathways could be “constitutive” or “housekeeping” by nature, *i.e.*, that they: 1) modulate longevity irrespective of the organismal and intracellular nutrient and energy status; and 2) do not overlap (or only partially overlap) with the adaptable longevity pathways that are under the stringent control of calorie and/or nutrient availability [40]. A challenge of identifying such housekeeping longevity pathways could be met by conducting a chemical screen for compounds that can extend longevity even under CR or DR conditions. Because under such conditions the adaptable pro-aging pathways are fully suppressed and the adaptable anti-aging pathways are fully activated, a compound that can increase lifespan is expected to target the housekeeping longevity pathways [40].

Of note, lipid metabolism has been shown to be involved in longevity regulation in

yeast [32, 110, 114], worms [20, 234 - 236], fruit flies [20, 237] and mice [20, 238 - 242]. Recently, we proposed a mechanism linking yeast longevity and lipid dynamics in the endoplasmic reticulum, lipid bodies and peroxisomes (see Chapter 5 of this thesis). In this mechanism, a CR diet extends yeast chronological lifespan by activating fatty acid oxidation in peroxisomes (see Figure 5.5 of this thesis). It is conceivable that the identification of small molecules targeting this mechanism could yield novel anti-aging compounds. Such compounds can be used as research tools for defining the roles for different longevity pathways in modulating lipid metabolism and in integrating lipid dynamics with other longevity-related processes. Furthermore, the availability of such compounds would enable a quest for housekeeping longevity assurance pathways that do not overlap (or only partially overlap) with the adaptable pathways. Moreover, such compounds would have a potential to be used as pharmaceutical agents for increasing lifespan and promoting healthy aging by delaying the onset of age-related diseases, regardless of an organism's dietary regimen.

To identify small molecules that increase the chronological lifespan of yeast under CR conditions by targeting lipid metabolism and modulating housekeeping longevity assurance pathways, in studies described in this chapter of the thesis we first chose the single-gene-deletion mutant strain *pex5Δ* as a short-lived strain for carrying out a chemical genetic screen aimed at the identification of such anti-aging molecules. We found that the *pex5Δ* mutation causes the profound changes not only in lipid metabolism but also in mitochondrial structure and function, cell susceptibility to mitochondria-controlled apoptosis, and resistance to oxidative, thermal and osmotic stresses. By screening the total of approximately 19,000 representative compounds from seven

commercial libraries, we identified 24 small molecules that greatly extend the chronological lifespan of *pex5Δ* under CR and belong to 5 chemical groups [40]. One of these groups consisted of 6 bile acids, including lithocholic acid (LCA) [40]. To define a compendium of cellular processes affected by LCA in wild-type yeast, in studies described in this chapter of the thesis we examined the effect of this bile acid on longevity-defining processes confined to mitochondria. Here, we demonstrate that LCA extends longevity of chronologically aging yeast by altering mitochondrial structure and function, reducing cell susceptibility to mitochondria-controlled apoptosis, and increasing cell resistance to oxidative and thermal stresses.

6.3 Materials and Methods

Strains and media

The wild-type strain *Saccharomyces cerevisiae* BY4742 (*MATα his3ΔI leu2Δ0 lys2Δ0 ura3Δ0*) and mutant strain *pex5Δ* (*MATα his3ΔI leu2Δ0 lys2Δ0 ura3Δ0 pex5Δ::kanMX4*) were grown in YP medium (1% yeast extract, 2% peptone) containing 0.2%, 0.5%, 1% or 2% glucose as carbon source. Cells were cultured at 30°C with rotational shaking at 200 rpm in Erlenmeyer flasks at a “flask volume/medium volume” ratio of 5:1.

Chronological lifespan (CLS) assay

A sample of cells was taken from a culture at a certain time-point. A fraction of the sample was diluted in order to determine the total number of cells using a hemacytometer. Another fraction of the cell sample was diluted and serial dilutions of cells were plated in duplicate onto YP plates containing 2% glucose as carbon source.

After 2 d of incubation at 30°C, the number of colony forming units (CFU) per plate was counted. The number of CFU was defined as the number of viable cells in a sample. For each culture, the percentage of viable cells was calculated as follows: (number of viable cells per ml/total number of cells per ml) × 100. The percentage of viable cells in mid-logarithmic phase was set at 100%. The lifespan curves were validated using a LIVE/DEAD yeast viability kit (Invitrogen) following the manufacturer's instructions.

Plating assays for the analysis of resistance to various stresses

For the analysis of hydrogen peroxide resistance, serial dilutions (1:10⁰ to 1:10⁵) of wild-type and mutant cells removed from mid-logarithmic phase (day 1) and from diauxic phase (days 2 and 3) in YP medium containing 0.2% glucose were spotted onto two sets of plates. One set of plates contained YP medium with 2% glucose alone, whereas the other set contained YP medium with 2% glucose supplemented with 5 mM hydrogen peroxide. Pictures were taken after a 3-day incubation at 30°C.

For the analysis of oxidative stress resistance, serial dilutions (1:10⁰ to 1:10⁵) of wild-type and mutant cells removed from mid-logarithmic phase (day 1) and from diauxic phase (days 2 and 3) in YP medium with 0.2% glucose were spotted onto two sets of plates. One set of plates contained YP medium with 2% glucose alone, whereas the other set contained YP medium with 2% glucose supplemented with 2.5 mM of the superoxide/hydrogen peroxide-generating agent paraquat. Pictures were taken after a 3-day incubation at 30°C.

For the analysis of heat-shock resistance, serial dilutions (1:10⁰ to 1:10⁵) of wild-type and mutant cells removed from mid-logarithmic phase (day 1) and from diauxic

phase (days 2 and 3) in YP medium with 0.2% glucose were spotted onto two sets of YP medium with 2% glucose plates. One set of plates was incubated at 30°C. The other set of plates was initially incubated at 55°C for 30 min, and was then transferred to 30°C.

Pictures were taken after a 3-day incubation at 30°C.

For the analysis of salt stress resistance, serial dilutions (1:10⁰ to 1:10⁵) of wild-type and mutant cells removed from mid-logarithmic phase (day 1) and from diauxic phase (days 2 and 3) in YP medium with 0.2% glucose were spotted onto two sets of plates. One set of plates contained YP medium with 2% glucose alone, whereas the other set contained YP medium with 2% glucose supplemented with 0.5 M NaCl. Pictures were taken after a 3-day incubation at 30°C.

For the analysis of osmotic stress resistance, serial dilutions (1:10⁰ to 1:10⁵) of wild-type and mutant cells removed from mid-logarithmic phase (day 1) and from diauxic phase (days 2 and 3) in YP medium contained 0.2% glucose were spotted onto two sets of plates. One set of plates contained YP medium with 2% glucose alone, whereas the other set contained YP medium with 2% glucose supplemented with 1 M sorbitol. Pictures were taken after a 3-day incubation at 30°C.

Pharmacological manipulation of CLS

CLS analysis was performed as described above in this section. The lithocholic (LCA; L6250) bile acid was from Sigma. Their stock solution of LCA in DMSO was made on the day of adding this compound to cell cultures. LCA was added to growth medium at the indicated concentration immediately following cell inoculation. The final

concentration of DMSO in yeast cultures supplemented with LCA (and in the corresponding control cultures supplemented with drug vehicle) was 1% (v/v).

Monitoring the formation of reactive oxygen species (ROS)

Cells grown in YP medium containing 0.2%, 0.5%, 1% or 2% glucose as carbon source were tested microscopically for the production of ROS by incubation with dihydrorhodamine 123 (DHR). In the cell, this nonfluorescent compound can be oxidized to the fluorescent chromophore rhodamine 123 by ROS. Cells were also probed with a fluorescent counterstain Calcofluor White M2R (CW), which stains the yeast cell walls fluorescent blue. CW was added to each sample in order to label all cells for their proper visualization. DHR was stored in the dark at -20°C as 50 μl aliquots of a 1 mg/ml solution in ethanol. CW was stored in the dark at -20°C as the 5 mM stock solution in anhydrous DMSO (dimethylsulfoxide).

The concurrent staining of cells with DHR and CW was carried out as follows. The required amounts of the 50 μl DHR aliquots (1 mg/ml) and of the 5 mM stock solution of CW were taken out of the freezer and warmed to room temperature. The solutions of DHR and CW were then centrifuged at $21,000 \times g$ for 5 min in order to clear them of any aggregates of fluorophores. For cell cultures with a titre of $\sim 10^7$ cells/ml, 100 μl was taken out of the culture to be treated. If the cell titre was lower, proportionally larger volumes were used. 6 μl of the 1 mg/ml DHR and 1 μl of the 5 mM CW solutions were added to each 100 μl aliquot of culture. After a 2-h incubation in the dark at room temperature, the samples were centrifuged at $21,000 \times g$ for 5 min. Pellets were resuspended in 10 μl of PBS buffer (20 mM $\text{KH}_2\text{PO}_4/\text{KOH}$, pH 7.5, and 150 mM NaCl).

Each sample was then supplemented with 5 μ l of mounting medium, added to a microscope slide, covered with a coverslip, and sealed using nail polish. Once the slides were prepared, they were visualized under the Zeiss Axioplan fluorescence microscope mounted with a SPOT Insight 2 megapixel color mosaic digital camera. Several pictures of the cells on each slide were taken, with two pictures taken of each frame. One of the two pictures was of the cells seen through a rhodamine filter in order to detect cells dyed with DHR. The second picture was of the cells seen through a DAPI filter in order to visualize CW, and therefore all the cells present in the frame.

For evaluating the percentage of DHR-positive cells, the UTHSCSA Image Tool (Version 3.0) software was used to calculate both the total number of cells and the number of stained cells. Fluorescence of individual DHR-positive cells in arbitrary units was determined by using the UTHSCSA Image Tool software (Version 3.0). In each of 3-5 independent experiments, the value of median fluorescence was calculated by analyzing at least 800-1000 cells that were collected at each time point. The median fluorescence values were plotted as a function of the number of days cells were cultured.

Immunofluorescence microscopy

Cell cultures were fixed in 3.7% formaldehyde for 45 min at room temperature. The cells were washed in solution B (100 mM $\text{KH}_2\text{PO}_4/\text{KOH}$ pH 7.5, 1.2 M sorbitol), treated with Zymolyase 100T (MP Biomedicals, 1 μ g Zymolyase 100T/1 mg cells) for 30 min at 30°C and then processed as previously described [249]. Monoclonal antibody raised against porin (Invitrogen, 0.25 μ g/ μ l in TBSB buffer [20 mM Tris/HCl pH 7.5, 150 mM NaCl, 1 mg/ml BSA]) was used as a primary antibody. Alexa Fluor 568 goat anti-mouse IgG

(Invitrogen, 2 $\mu\text{g}/\mu\text{l}$ in TBSB buffer) was used as a secondary antibody. The labeled samples were mounted in mounting solution (16.7 mM Tris/HCl pH 9.0, 1.7 mg/ml *p*-phenylenediamine, 83% glycerol). Images were collected with a Zeiss Axioplan fluorescence microscope (Zeiss) mounted with a SPOT Insight 2 megapixel color mosaic digital camera (Spot Diagnostic Instruments).

Oxygen consumption assay

The rate of oxygen consumption by yeast cells recovered at various time points was measured continuously in a 2-ml stirred chamber using a custom-designed biological oxygen monitor (Science Technical Center of Concordia University) equipped with a Clark-type oxygen electrode. 1 ml of YP medium supplemented with 0.2% glucose was added to the electrode for approximately 5 minutes to obtain a baseline. Cultured cells of a known titre were spun down at $3,000 \times g$ for 5 minutes. The resulting pellet was resuspended in YP medium supplemented with 0.2% glucose and then added to the electrode with the medium that was used to obtain a baseline. The resulting slope was used to calculate the rate of oxygen consumption in $\text{O}_2\% \times \text{min}^{-1} \times 10^9$ cells.

Monitoring the mitochondrial membrane potential

The mitochondrial membrane potential ($\Delta\Psi$) was measured in live yeast by fluorescence microscopy of Rhodamine 123 (R123) staining. For R123 staining, 5×10^6 cells were harvested by centrifugation for 1 min at $21,000 \times g$ at room temperature and then resuspended in 100 μl of 50 mM sodium citrate buffer (pH 5.0) containing 2% glucose. R123 (Invitrogen) was added to a final concentration of 10 μM . Following incubation in

the dark for 30 min at room temperature, the cells were washed twice in 50 mM sodium citrate buffer (pH 5.0) containing 2% glucose and then analyzed by fluorescence microscopy. Images were collected with a Zeiss Axioplan fluorescence microscope (Zeiss) mounted with a SPOT Insight 2 megapixel color mosaic digital camera (Spot Diagnostic Instruments). For evaluating the percentage of R123-positive cells or cells with fragmented nucleus the UTHSCSA Image Tool (Version 3.0) software was used to calculate both the total number of cells and the number of stained cells or cells with fragmented nucleus. Fluorescence of individual R123-positive cells in arbitrary units was determined by using the UTHSCSA Image Tool software (Version 3.0). In each of 3-6 independent experiments, the value of median fluorescence was calculated by analyzing at least 800-1000 cells that were collected at each time-point. The median fluorescence values were plotted as a function of the number of days cells were cultured.

Measurement of mitochondrial mutations and nuclear mutations affecting mitochondrial components

The frequency of spontaneous single-gene (*mit⁻* and *syn⁻*) and deletion (*rho⁻* and *rho^o*) mutations in mtDNA and spontaneous single-gene nuclear mutations (*pet⁻*) affecting essential mitochondrial components was evaluated by measuring the fraction of respiratory-competent (*rho⁺*) yeast cells remaining in their aging population. *rho⁺* cells maintained intact their mtDNA and their nuclear genes encoding essential mitochondrial components. Therefore, *rho⁺* cells were able to grow on glycerol, a non-fermentable carbon source. In contrast, mutant cells deficient in mitochondrial respiration were unable to grow on glycerol. Most of these mutant cells carried mutations in mtDNA (including

single-gene *mit*⁻ and *syn*⁻ mutations or large deletions *rho*⁻) or completely lacked this DNA (*rho*^o mutants), whereas some of them carried so-called *pet*⁻ mutations in nuclear genes that code for essential mitochondrial components [140]. Serial dilutions of cell samples removed from different phases of growth were plated in duplicate onto YP plates containing either 2% glucose or 3% glycerol as carbon source. Plates were incubated at 30°C. The number of CFU on YP plates containing 2% glucose was counted after 2 d of incubation, whereas the number of CFU on YP plates containing 3% glycerol was counted after 6 d of incubation. For each culture, the percentage of respiratory-deficient (*mit*⁻, *syn*⁻, *rho*⁻, *rho*^o and *pet*⁻) cells was calculated as follows: $100 - [(\text{number of CFU per ml on YP plates containing 3\% glycerol} / \text{number of CFU per ml on YP plates containing 2\% glucose}) \times 100]$. The frequency of spontaneous point mutations in the *rib2* and *rib3* loci of mtDNA was evaluated by measuring the frequency of mtDNA mutations that caused resistance to the antibiotic erythromycin [141]. These mutations impair only mtDNA [142, 143]. In each of the seven independent experiments performed, ten individual yeast cultures were grown in YP medium containing 0.2%, 0.5%, 1% or 2% glucose as carbon source. A sample of cells was removed from each culture at various time-points. Cells were plated in duplicate onto YP plates containing 3% glycerol and erythromycin (1 mg/ml). In addition, serial dilutions of each sample were plated in duplicate onto YP plates containing 3% glycerol as carbon source for measuring the number of respiratory-competent (*rho*⁺) cells. The number of CFU was counted after 6 d of incubation at 30°C. For each culture, the frequency of mutations that caused resistance to erythromycin was calculated as follows: number of CFU per ml on YP plates

containing 3% glycerol and erythromycin/number of CFU per ml on YP plates containing 3% glycerol.

6.4 Results

6.4.1 The *pex5Δ* mutation causes the profound changes in mitochondrial structure and function, cell susceptibility to mitochondria-controlled apoptosis, and resistance to oxidative, thermal and osmotic stresses

To perform a chemical genetic screen for small molecules that increase the chronological lifespan of yeast by targeting lipid metabolism, our laboratory chose the single-gene-deletion mutant strain *pex5Δ*. Because *pex5Δ* lacks a cytosolic shuttling receptor for peroxisomal import of Fox1p and Fox2p, these two enzymes of the β -oxidation of free fatty acids (FFA) reside in the cytosol of *pex5Δ* cells [40, 243]. In contrast, the Pex5p-independent peroxisomal import of Fox3p, the third enzyme of the FFA β -oxidation pathway, sorts it to the peroxisome in *pex5Δ* cells [40, 243]. By spatially separating Fox1p and Fox2p from Fox3p within a cell, the *pex5Δ* mutation impairs FFA oxidation. In chronologically aging yeast grown under CR conditions on 0.2% or 0.5% glucose, peroxisomal FFA oxidation regulates longevity by 1) efficiently generating acetyl-CoA to synthesize the bulk of ATP in mitochondria; and 2) acting as a rheostat that modulates the age-related dynamics of FFA and diacylglycerol (DAG), two regulatory lipids known to promote longevity-defining cell death [32, 40, 44, 110, 114, 244]. Unlike CR yeast, chronologically aging non-CR yeast grown on 1% or 2% glucose are unable to generate significant quantities of ATP by oxidizing peroxisome-derived

acetyl-CoA in mitochondria and, instead, produce the bulk of ATP via glycolytic oxidation of glycogen- and trehalose-derived glucose [32, 40, 44, 110, 114]. Consistent with the essential role of peroxisomal FFA oxidation as a longevity assurance process only under CR, we found that the *pex5Δ* mutation substantially shortened the chronological lifespan of CR yeast but caused a significantly lower reduction of longevity in non-CR yeast, especially in yeast grown on 2% glucose [40]. Our studies revealed that by impairing the ability of peroxisomal FFA oxidation to act as a rheostat that regulates cellular aging by modulating the age-related dynamics of FFA, diacylglycerols (DAG) and triacylglycerols (TAG) in the ER and lipid bodies (see Chapter 5 of this thesis), the *pex5Δ* mutation: 1) causes the accumulation of the closely apposed ER membranes and ER-originated lipid bodies in CR yeast; 2) increases the concentrations of FFA, DAG and TAG in CR yeast, promoting their build-up in the ER and lipid bodies; 3) leads to the buildup of the ER-derived and lipid bodies-deposited ergosteryl esters (EE), neutral lipid species; and 4) enhances the susceptibility of CR yeast to necrotic death caused by a short-term exposure to exogenous FFA or DAG, perhaps due to the increased concentrations of endogenous FFA and DAG seen in *pex5Δ* cells under CR [40].

In studies described in this chapter of my thesis, we examined the effects of the *pex5Δ* mutation on longevity-defining cellular processes that are confined to mitochondria. As we found, this mutation altered mitochondrial morphology and oxidation-reduction processes in mitochondria of CR yeast. In fact, the *pex5Δ* mutation caused the fragmentation of a tubular mitochondrial network into individual mitochondria under CR conditions (Figures 6.1A and 6.1B). Furthermore, in CR yeast the *pex5Δ* mutation 1) greatly reduced the rate of oxygen consumption by mitochondria (Figure

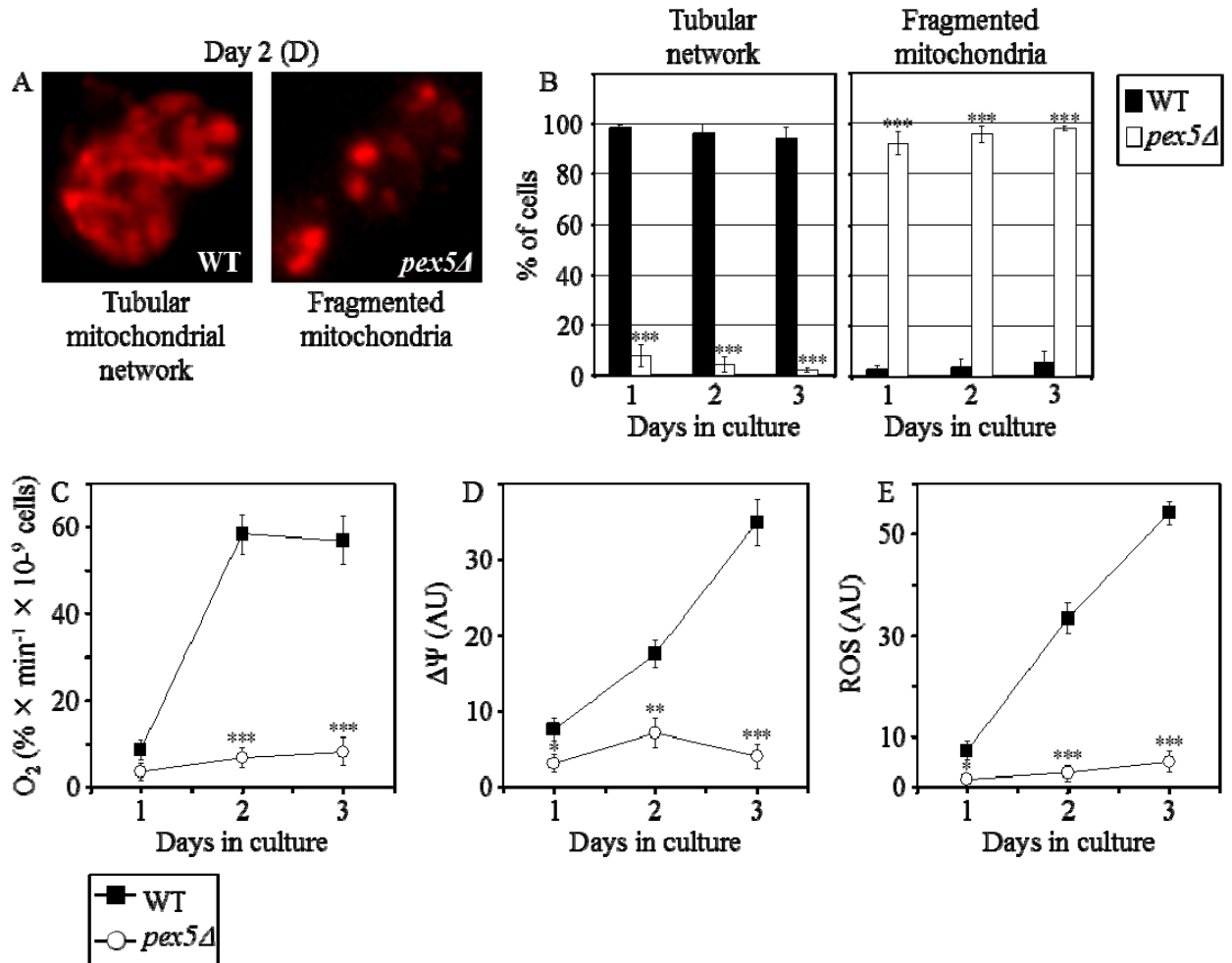


Figure 6.1. The *pex5Δ* mutation alters mitochondrial morphology and functions in CR yeast. (A) Morphology of mitochondria in WT and *pex5Δ* cells. Mitochondria were visualized by indirect immunofluorescence microscopy using monoclonal anti-porin primary antibodies and Alexa Fluor 568-conjugated goat anti-mouse IgG secondary antibodies. (B) Percent of WT and *pex5Δ* cells exhibiting a tubular mitochondrial network or fragmented mitochondria. (C - E) Oxygen consumption (C) by WT and *pex5Δ* cells, their mitochondrial membrane potential $\Delta\Psi$ (D) and their ROS levels (E). $\Delta\Psi$ and ROS were visualized in living cells by fluorescence microscopy using fluorescent dyes Rhodamine 123 or Dihydrorhodamine 123, respectively. CR yeast grown on 0.2% glucose were taken for analyses at the indicated time-points. Data in B - E are presented as means \pm SEM (n = 4-15; ***p < 0.001; **p < 0.01; *p < 0.05). Abbreviation: D, diauxic growth phase.

6.1C); 2) substantially decreased the mitochondrial membrane potential (Figure 6.1D); and 3) diminished the level of intracellular ROS (Figure 6.1E), known to be generated mostly as by-products of mitochondrial respiration [245, 246]. Interestingly, all these mitochondrial abnormalities in *pex5Δ* yeast under CR were reminiscent of changes in mitochondrial morphology and functions seen in mice with hepatocyte-specific elimination of the *PEX5* gene, a model for the peroxisome biogenesis disorder Zellweger syndrome [247].

Besides its profound effect on mitochondrial morphology and functions, the *pex5Δ* mutation also 1) reduced the resistance of chronologically aging CR yeast to chronic (long-term) oxidative, thermal and osmotic stresses (Figure 6.2A); 2) sensitized CR yeast to death that was initiated in response to a short-term exposure to exogenous hydrogen peroxide or acetic acid (Figure 6.2B) and that is known to be caused by mitochondria-controlled apoptosis [248, 249]; and 3) elevated the frequencies of deletion and point mutations in mitochondrial and nuclear DNA of CR yeast (Figures 6.2C to 6.2E).

Because of the profound changes in longevity-defining processes in mitochondria, resistance to chronic (long-term) stresses, susceptibility to mitochondria-controlled apoptosis, and frequencies of mutations in mitochondrial and nuclear DNA that we observed in *pex5Δ* yeast under CR conditions, our laboratory chose the single-gene-deletion mutant strain *pex5Δ* as a short-lived strain for carrying out a chemical genetic screen for novel anti-aging compounds. This screen was aimed at the identification of small molecules that increase the chronological lifespan of yeast under CR conditions by targeting lipid metabolism and modulating housekeeping longevity assurance pathways.

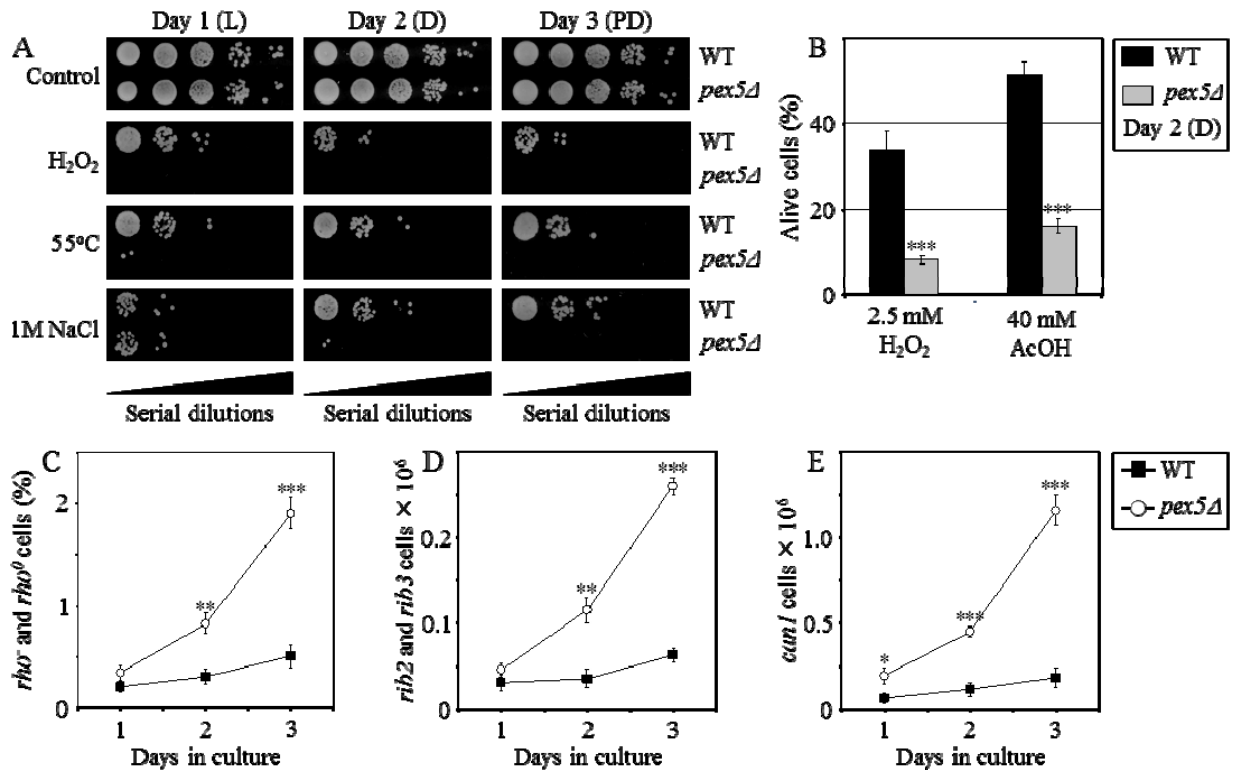


Figure 6.2. The *pex5Δ* mutation reduces the resistance of CR yeast to stresses, sensitizes them to exogenously induced apoptosis and elevates the frequencies of mutations in their mitochondrial and nuclear DNA. (A) The resistance of WT and *pex5Δ* to chronic oxidative, thermal and osmotic stresses. (B) Viability of WT and *pex5Δ* cells treated for 1 h with hydrogen peroxide or acetic acid (AcOH) to induce mitochondria-controlled apoptosis. (C - E) The frequencies of *rho*⁻ and *rho*⁰ deletion mutations in mitochondrial DNA (C), *rib2* and *rib3* point mutations in mitochondrial DNA (D), and of *can1* point mutations in nuclear DNA (E) of WT and *pex5Δ* cells. CR yeast grown on 0.2% glucose were taken for analyses at the indicated time-points. Data in B to E are presented as means ± SEM (n = 6-9; ***p < 0.001; **p < 0.01; *p < 0.05). Abbreviations: AcOH, acetic acid; D, diauxic growth phase; L, logarithmic growth phase; PD, post-diauxic growth phase.

6.4.2 LCA, a novel anti-aging compound, extends longevity of chronologically aging yeast by altering mitochondrial structure and function, reducing cell

susceptibility to mitochondria-controlled apoptosis, and increasing cell resistance to oxidative and thermal stresses

By screening the total of approximately 19,000 representative compounds from seven commercial libraries, we identified 24 small molecules that greatly extend the chronological lifespan of *pex5Δ* under CR and belong to 5 chemical groups [40]. One of these groups consisted of 6 bile acids, including LCA [40]. To define a compendium of cellular processes affected by LCA in wild-type (WT) yeast, in studies described in this chapter of the thesis we examined the effect of this bile acid on longevity-defining processes confined to mitochondria.

We found that in reproductively mature WT cells that entered the non-proliferative ST phase under CR conditions on 0.2% glucose, LCA 1) attenuated the fragmentation of a tubular mitochondrial network into individual mitochondria (Figure 6.3A); 2) elevated the rate of oxygen consumption by mitochondria (Figure 6.3B); 3) reduced the mitochondrial membrane potential (Figure 6.3C); and 4) decreased the level of intracellular ROS (Figure 6.3D) known to be generated mainly in mitochondria [245, 246]. Moreover, we also found that in WT yeast reached reproductive maturation by entering into ST phase under CR conditions on 0.2% glucose, LCA 1) enhanced cell resistance to chronic oxidative and thermal (but not to osmotic) stresses (Figure 6.3E); 2) reduced cell susceptibility to death triggered by a short-term exposure to exogenous hydrogen peroxide or acetic acid (Figure 6.3F) known to be caused by mitochondria-controlled apoptosis [248, 250]; and 3) decreased the frequencies of deletions and point mutations in mitochondrial and nuclear DNA (Figures 6.3G to 6.3I).

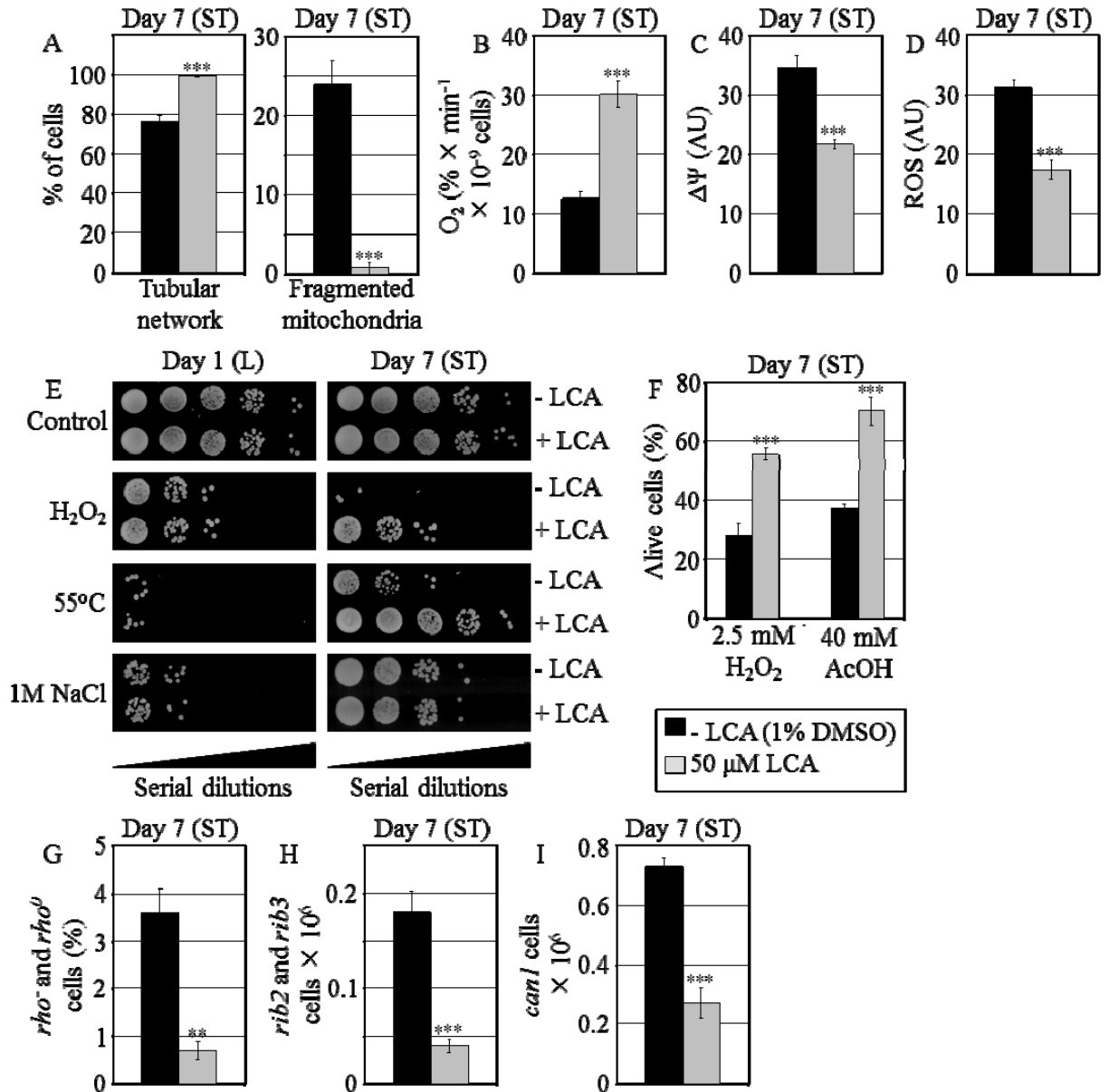


Figure 6.3. In reproductively mature WT yeast that entered the non-proliferative stationary (ST) phase under CR, LCA modulates mitochondrial morphology and functions, enhances stress resistance, attenuates mitochondria-controlled apoptosis, and increases stability of nuclear and mitochondrial DNA. (A) Percent of WT cells grown in medium with or without LCA and exhibiting a tubular mitochondrial network or fragmented mitochondria. Mitochondria were visualized by indirect immunofluorescence microscopy using monoclonal anti-porin primary antibodies and Alexa Fluor 568-conjugated goat anti-mouse IgG secondary antibodies. (B - D) Oxygen consumption by WT cells grown in medium with or without LCA (B), their

mitochondrial membrane potential $\Delta\Psi$ (C) and their ROS levels (D). $\Delta\Psi$ and ROS were visualized in living cells by fluorescence microscopy using fluorescent dyes Rhodamine 123 or Dihydrorhodamine 123, respectively. (E) The resistance of WT cells pre-grown in medium with or without LCA to chronic oxidative, thermal and osmotic stresses. (F) Viability of WT cells pre-grown in medium with or without LCA and then treated for 1 h with hydrogen peroxide or acetic acid (AcOH) to induce mitochondria-controlled apoptosis. (G - I) The frequencies of *rho*⁻ and *rho*⁰ mutations in mitochondrial DNA (G), *rib2* and *rib3* mutations in mitochondrial DNA (H), and of *can1* (*Can*^r) mutations in nuclear DNA (I) of WT cells grown in medium with or without LCA. Data in A - D and F - I are presented as means \pm SEM (n = 4-17; ***p < 0.001; **p < 0.01). WT cells grown on 0.2% glucose in the presence or absence of LCA were taken for analyses at day 7, when they reached reproductive maturation by entering into ST phase.

6.5 Discussion

Our findings described in this chapter of my thesis, together with some recently published data from Dr. Titorenko laboratory [40, 114], identify a compendium of processes that compose LCA-targeted housekeeping longevity assurance pathways. These findings imply that LCA modulates such pathways by 1) suppressing the pro-aging process [32, 110, 114, 244] of lipid-induced necrotic cell death, perhaps due to its observed ability to reduce the intracellular levels of FFA and DAG that trigger such death; 2) attenuating the pro-aging process [32, 251, 252] of mitochondrial fragmentation, a hallmark event of age-related cell death; 3) altering oxidation-reduction processes in mitochondria - such as oxygen consumption, the maintenance of membrane potential and ROS production - known to be essential for longevity regulation [32, 245, 253 - 255]; 4) enhancing cell resistance to oxidative and thermal stresses, thereby activating the anti-aging process [32, 110, 255 - 257] of stress response; 5) suppressing the pro-aging process [32, 251, 252] of mitochondria-controlled apoptosis; and 6)

enhancing stability of nuclear and mitochondrial DNA, thus activating the anti-aging process [32, 258, 259] of genome maintenance. The observed pleiotropic effect of LCA on a compendium of housekeeping longevity assurance processes implies that this bile acid is a multi-target life-extending compound that increases chronological lifespan in yeast by modulating a network of the highly integrated cellular events not controlled by the adaptable TOR and cAMP/PKA pathways. The major challenge now is to define the molecular mechanisms by which LCA modulates each of these pro- and anti-aging housekeeping processes and integrates them in chronologically aging yeast.

6.6 Conclusions

Because of the profound changes in longevity-defining processes in mitochondria, resistance to chronic (long-term) stresses, susceptibility to mitochondria-controlled apoptosis, and frequencies of mutations in mitochondrial and nuclear DNA that we observed in the single-gene-deletion mutant strain *pex5Δ* under CR conditions, our laboratory chose this short-lived strain for carrying out a chemical genetic screen for novel anti-aging compounds. This screen was designed to identify small molecules that increase the chronological lifespan of yeast under CR conditions by targeting lipid metabolism and modulating housekeeping longevity assurance pathways. The screen identified LCA, a bile acid, as one of these novel anti-aging compounds. The described here pleiotropic effect of LCA on a compendium of housekeeping longevity assurance processes implies that this bile acid is a multi-target life-extending compound that increases chronological lifespan in yeast by modulating a network of the highly

integrated cellular events not controlled by the currently known adaptable TOR and cAMP/PKA pathways.

7 Lithocholic acid (LCA), a novel anti-aging compound, extends longevity of chronologically aging yeast only if added at certain critical periods of their lifespan

7.1 Abstract

We provide evidence that in yeast grown under CR conditions on 0.2% glucose, there are two critical periods when the addition of LCA to growth medium can increase both their mean and maximum chronological lifespans. One of these two critical periods includes logarithmic and diauxic growth phases, whereas the other period exists in the early stationary (ST) phase of growth. In contrast, LCA does not cause a significant extension of the mean or maximum chronological lifespan of CR yeast if it is added in post-diauxic or late ST growth phases.

Because aging of multicellular and unicellular eukaryotic organisms affects numerous anti- and pro-aging processes within cells [2, 3, 7, 9, 14, 17 - 21, 27 - 36], we hypothesized that the observed ability of LCA to delay chronological aging of yeast grown under CR conditions only if added at certain critical periods (checkpoints) of their lifespan could be due to its differential effects on certain anti- and pro-aging processes at different checkpoints. To test the validity of our hypothesis, in studies described in this chapter of my thesis we examined how the addition of LCA at different periods of chronological lifespan in yeast grown under CR conditions influences anti- and pro-aging processes taking place during each of these periods. Our empirical validation of this hypothesis suggests a mechanism linking the ability of LCA to delay chronological aging of yeast only if added at certain periods (checkpoints) of their lifespan to the differential

effects of this natural anti-aging compound on certain anti- and pro-aging processes at each of these checkpoints.

7.2 Introduction

One way to look at the complexity of the aging process, in which a limited number of master regulators orchestrate numerous cellular processes in space and time [3, 4, 6, 17, 31, 33, 36], is to consider each of these processes as a functional module integrated with other modules into a longevity network [1, 6, 8, 31, 32]. The synergistic action of individual modules could establish the rate of aging. Furthermore, the relative impact of each module on the rate of aging in a particular organism or cell type could differ at various stages of its lifetime and could also vary in different organisms and cell types [1, 6, 8, 31, 32]. In this conceptual framework, the longevity network could progress through a series of checkpoints. At each of these checkpoints, a distinct set of master regulators senses the functional states of critical modules comprising the network. Based on this information and considering the input of some environmental cues (such as caloric and dietary intake, environmental stresses, endocrine factors, etc.), master regulators modulate certain processes within monitored modules in order to limit the age-related accumulation of molecular and cellular damage [31, 32]. The resulting changes in the dynamics of individual modules comprising the network and in its general configuration are critically important for specifying the rate of aging during late adulthood.

A confirmation of this concept for a stepwise development of a longevity network configuration at a series of checkpoints, each being monitored by a limited set of checkpoint-specific master regulators, comes from studies that revealed distinctive timing

requirements for modulating the pace of chronological aging in the nematode *Caenorhabditis elegans*. It seems that this organism employs at least three independent regulatory systems that, by monitoring a particular cellular process or processes during a specific stage of life, use this information to establish the rate of chronological aging later in life (Figure 7.1A). The first of these three regulatory systems influences lifespan by operating only during larval development [261 - 263]. By monitoring mitochondrial respiration, electrochemical potential and ATP production early in life, during the L3/L4 larval stage, it establishes the rate of chronological aging that persists during adulthood [261 - 263] (Figure 7.1A). Mechanisms underlying the essential role of this first regulatory system in defining longevity of *C. elegans* may involve 1) a remodeling of mitochondria-confined ATP production pathways during larval development, which may establish a specific configuration of the longevity-defining metabolic network in a cell-autonomous manner [265, 266]; and 2) a retrograde signalling pathway that in response to mild mitochondrial impairment and stress during the L3/L4 larval stage activates UBL-5/DVE-1-driven expression of the mitochondria-specific unfolded protein response (UPR^{mt}) genes in the nucleus, thereby stimulating synthesis of a subset of UPR^{mt} proteins that can extend longevity not only cell-autonomously but also in a cell-non-autonomous fashion [267, 268]. The second regulatory system operates exclusively during adulthood, mainly during early adulthood, to influence the lifespan of *C. elegans* via the insulin/IGF-1 longevity signaling pathway and the transcription factor DAF-16 (Figure 7.1A) [269 - 271]. Of note, the magnitude of the effect of this second regulatory system on lifespan declines with age, becoming insignificant after several days of adulthood [269]. The third regulatory system influences the lifespan of *C. elegans* in a diet-restriction-specific

fashion by operating exclusively during adulthood (Figure 7.1A) [272]. This system regulates longevity via the transcription factor PHA-4 only in response to reduced food intake. Importantly, the PHA-4-mediated regulatory system operates independently of the other two regulatory systems modulating the rate of chronological aging in *C. elegans* (Figure 7.1A) [272]. In the concept for a stepwise development of a longevity network configuration at a series of checkpoints, a genetic, dietary or pharmacological anti-aging intervention may modulate the key cellular process or processes that are monitored at a particular checkpoint by a master regulator of the longevity control system. In *C. elegans*, UBL-5/DVE-1, DAF-16 and PHA-4 may function as the checkpoint-specific master regulators of chronological lifespan by governing progression through the three consecutive checkpoints operating during larval development and early adulthood (Figure 7.1A) [267, 269 - 272].

Importantly, some general aspects of the proposed concept of the longevity control system progressing through a series of checkpoints could be applicable to laboratory mice and rats. In fact, although a caloric restriction (CR) diet considerably extends lifespan in these organisms even if it is implemented at the age at which skeletal development is complete, the maximal benefit of this low-calorie diet for longevity can be achieved only if CR is initiated during the rapid growth period [273 - 275]. It is tempting to speculate that rodents 1) employ a CR-dependent longevity control system that, by monitoring some key, longevity-defining cellular processes, can establish a particular rate of chronological aging; and 2) have at least two checkpoints, one in early adulthood and another in late adulthood, at which the proposed CR-dependent longevity control system senses the rate and/or efficiency of the critical cellular processes that define longevity

(Figure 7.1B). It is conceivable therefore that the proposed CR-dependent longevity control system in rodents can extend longevity even if the rate and efficiency of the critical, CR-modulated cellular processes are appropriate only at the late-adulthood checkpoint, but not as markedly as if they are suitable already at the checkpoint in early adulthood.

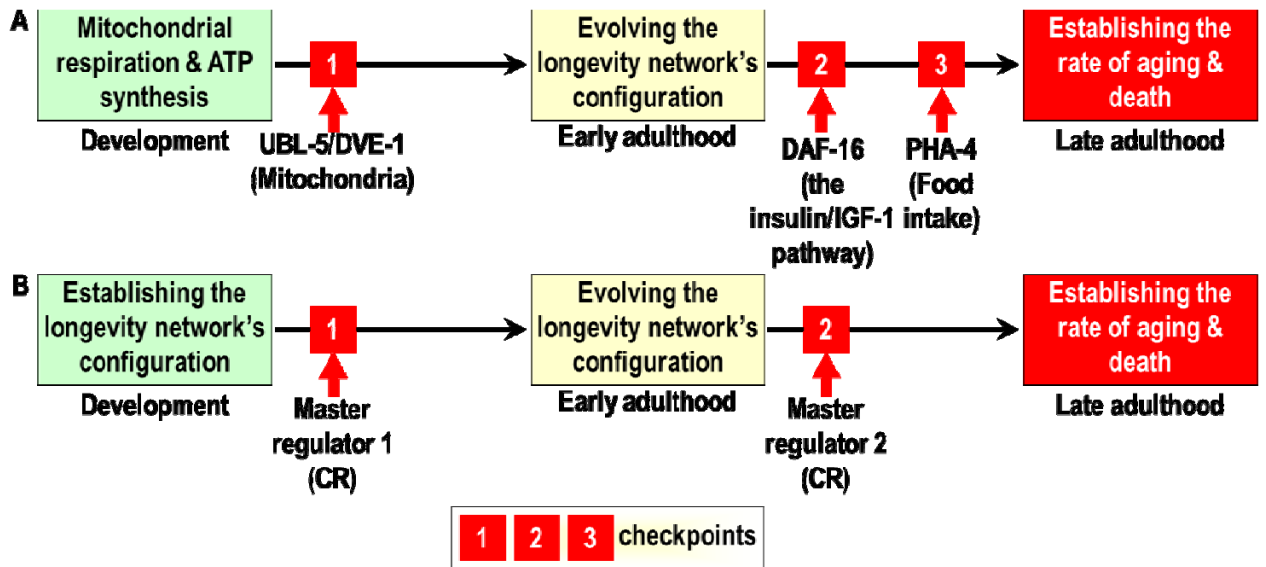


Figure 7.1. A concept for a stepwise development of a longevity network configuration at a series of checkpoints. In this concept, a genetic, dietary or pharmacological anti-aging intervention may modulate the key cellular process or processes that are monitored at a particular checkpoint by a master regulator of the longevity control system. (A) In *C. elegans*, UBL-5/DVE-1, DAF-16 and PHA-4 may function as the checkpoint-specific master regulators of chronological lifespan by governing progression through the three consecutive checkpoints operating during larval development and early adulthood. (B) In laboratory mice and rats, a CR-dependent longevity control system can establish a particular rate of chronological aging by monitoring some key, longevity-defining cellular processes at the two consecutive checkpoints operating during early and late adulthood, respectively.

According to the concept for a stepwise development of a longevity network configuration at a series of checkpoints, a pharmacological anti-aging intervention may

modulate the key longevity-defining cellular processes that are monitored at a particular checkpoint by a master regulator of the longevity control system. Several pharmacological anti-aging interventions are currently known for their ability to extend longevity across phyla and improve health by beneficially influencing age-related pathologies (Table 7.1). Only one of these anti-aging compounds, a macrocyclic lactone rapamycin synthesized by soil bacteria to inhibit growth of fungal competitors [276 - 278], has been examined for its effects on lifespan and healthspan if implemented at different ages of an organism. If fed to genetically heterogeneous mice beginning at 270 days or 600 days of age (*i.e.*, at the ages approximately equivalent to 27 or 60 years, respectively, in humans), this specific inhibitor of the nutrient-sensory protein kinase mTORC1 has been shown to be equally efficient in extending lifespan and beneficially influencing age-related pathologies [279 - 284]. Our recent studies provided evidence that 1) lithocholic acid (LCA), a bile acid, extends longevity of chronologically aging yeast if added to growth medium at the time of cell inoculation [40, 114]; and 2) longevity in chronologically aging yeast is programmed by the level of metabolic capacity and organelle organization they developed, in a diet-specific fashion, prior to entry into a non-proliferative state - and, thus, that chronological aging in yeast is the final step of a developmental program progressing through at least one checkpoint prior to entry into quiescence [32, 110, 114]. We therefore decided to investigate how LCA influences longevity and a compendium of longevity-defining cellular processes in chronologically aging yeast if added to growth medium at different periods of their lifespan.

Table 7.1. Known anti-aging compounds, their abilities to increase life span in different organisms (under caloric or dietary restriction [CR or DR, respectively], on a standard diet or fed a high-calorie diet), and the mechanisms of their anti-aging action.

Compound	Increases life span*		Mechanism
	CR/DR	Standard or high-calorie diet	
Caffeine	Not tested (NT)	+ (yeast, CLS) [285]	By inhibiting TORC1, modulates unspecified longevity-related processes [285] governed by the TOR pathway [286, 287]
Li ⁺	+ (nematodes ^{**}) [288]	+ (nematodes) [288]	By altering transcription of genes involved in histone methylation, nucleosome composition and chromatin structure, modulates unspecified longevity-related processes [288] known to be influenced by age-related chromatin reorganization [289]
Lipoic acid, propyl gallate, trolox and taxifolin	NT	+ (nematodes [290] (all); fruit flies [291] (lipoic acid))	Antioxidants that may increase life span by detoxifying free radicals and/or enhancing resistance to age-related oxidative stress [290, 291]
Metformin, buformin and phenformin	- (nematodes ^{**}) [292]	+ (nematodes [292]; mice [293])	Type 2 diabetes therapeutics that - by activating LKB1/AMPK signaling and thereby inhibiting TORC1 [294, 295] - modulate unspecified longevity-related processes [292, 293] known to be governed by the TOR

			pathway [286, 287, 295]
Methionine sulfoximine	NT	+ (yeast, CLS) [296]	By inhibiting glutamine synthetase and reducing both intracellular glutamine level and TORC1-signaling [297], increases life span - perhaps by activating gluconeogenesis and enhancing stress resistance [296]
Mianserin	- (nematodes) [298]	+ (nematodes) [298]	A serotonin receptor antagonist used as an antidepressant in humans; may increase life span by inhibiting neurotransmission related to food sensing, thereby mimicking a DR-like physiological state [298]***
Rapamycin	+ (fruit flies) [299]	+ (yeast, CLS [285, 296, 300] and RLS [301]; fruit flies [299]; mice [302]; rodent fibroblasts, human epithelium and fibrosarcoma cells - all RLS [296])	By inhibiting TORC1 (yeast and fruit flies) [285, 287, 299, 300] and mTORC1 (mammals) [295, 287, 302], increases life span by activating macroautophagy (yeast and fruit flies) [299, 303] and inhibiting cap-dependent protein translation (fruit flies and mice) [299, 302] as well as - perhaps - by promoting gluconeogenesis (yeast) [296], enhancing stress resistance (yeast) [296, 301], and increasing neutral lipid

			levels (fruit flies) [299]
Resveratrol	- (yeast, RLS [304]; fruit flies [305]; mice [306])	+ (yeast, RLS [304] but not CLS [304]; nematodes [305]; fruit flies [305]; fishes [307]; mice [306, 309]; human fibroblasts, RLS [308]) ^{****}	Increases life span by modulating a number of longevity-related processes (<i>e.g.</i> , by altering transcription of numerous genes involved in key longevity pathways, stimulating p53 deacetylation, increasing insulin sensitivity and mitochondrial number, reducing IGF-1 levels, activating AMPK and PGC-1 α , promoting ER stress response, repressing transcription of PPAR- γ , inhibiting adipocyte differentiation, accelerating storage fat mobilization, inhibiting mTORC1, and activating autophagy [304, 306, 308 - 316]; its life-extending ability in yeast, nematodes and fruit flies depends on Sir2p - a member of the conserved sirtuin family of NAD ⁺ -dependent protein deacetylases/mono-ADP-ribosyltransferases [304, 305, 310]) ^{****}
SkQ1	NT	+ (fungi, daphnias, fruit flies, mice) [317]	By being specifically targeted to mitochondria, acts as an antioxidant that may increase life span by preventing

			oxidative damage to proteins and lipids (<i>i.e.</i> , cardiolipin), altering mitochondrial morphology, reducing hydrogen peroxide-induced apoptosis and necrosis, and/or slowing down the age-related phosphorylation of histone H2AX [317]
Sodium nitroprusside	NT	+ (human PBMC, RLS) [318]	By activating expression of the human sirtuin SIRT1 and thereby increasing the extent of SIRT1-dependent histone H4 lysine 16 deacetylation, may cause the development of an anti-aging pattern of transcription of numerous genes involved in longevity regulation [318]
Spermidine	NT	+ (yeast, CLS; nematodes; fruit flies; human PBMC, RLS) [319]	By inhibiting histone acetyltransferases and promoting histone H3 deacetylation, increases life span by activating transcription of numerous autophagy-related genes; the resulting induction of autophagy suppresses age-related necrotic cell death [319]
Valproic acid	NT	+ (nematodes) [320]	Is used as a mood stabilizer and an anticonvulsant in humans; may increase life span by promoting nuclear localization of the DAF-16 forkhead

			transcription factor, thereby reducing the pro-aging effect of the insulin/IGF-1 signaling pathway [320]
LY294002	NT	+ (human fibrosarcoma cells, RLS) [321]	An inhibitor of phosphatidylinositol-3-kinase that – by reducing mTORC1 signaling [286, 287] – modulates unspecified longevity-related processes [321] known to be governed by the TOR pathway [286, 287, 295]
U0126	NT	+ (human fibrosarcoma cells, RLS) [321]	An inhibitor of the protein kinase MEK that – by reducing mTORC1 signaling [286, 287] – modulates unspecified longevity-related processes [321] known to be governed by the TOR pathway [286, 287, 295]
Aspirin	NT	+ male, but not female, mice [330]	An anti-inflammatory, anti-thrombotic and anti-oxidant compound that inhibits the cyclooxygenases COX-1 and COX-2 and activates the NF-kappaB signaling pathway [331 - 336]
Nordihydroguaiaretic acid	NT	+ fruit flies [337]; mosquitoes [338]; rats [339]; male, but not female, mice [330]	An anti-inflammatory and anti-oxidant compound that enhances glucose clearance and insulin sensitivity, reduces serum triglycerides, inhibits lipoprotein lipase and 5-

			lipoxygenase, reduces activities of the insulin-like growth factor IGF-1R and the receptor tyrosine kinase c-erbB2/HER2/neu, and inhibits leukotriene synthesis [340 - 347]
--	--	--	---

* Mean, median and/or maximum life spans.

** Nematodes carrying mutations that mimic DR under non-DR conditions [288, 290].

*** The ability of mianserin to increase nematode life span can only be seen in liquid media [298], whereas in solid media the compound reduces life span [322].

**** Increases the replicative life span of yeast grown under non-CR conditions [304] only in one out of four different yeast strain backgrounds [323]; one group has been unable to reproduce the life span extension by resveratrol in nematodes and fruit flies [324]; increases the life of mice only if fed a high-calorie diet, but not a standard diet [306, 309].

***** Although the life-extending ability of resveratrol in yeast, nematodes and fruit flies depends on Sir2p [304, 305, 310], it is currently debated whether this anti-aging compound binds to Sir2p (or SIRT1, a mammalian sirtuin) in vivo and/or activates Sir2p or SIRT1 in living cells [311, 323 - 327]; importantly, resveratrol has been shown to inhibit or activate many proteins other than sirtuins by interacting with them [328, 329].

Abbreviations: AMPK, the AMP-activated serine/threonine protein kinase; CLS, chronological life span; IGF-1, insulin-like growth factor 1; LKB1, a serine/threonine protein kinase that phosphorylates and activates AMPK; mTORC1, the mammalian target of rapamycin complex 1; NT, not tested; PBMC, peripheral blood mononuclear cells; PGC-1 α , peroxisome proliferator-activated receptor- γ co-activator 1 α ; RLS, replicative life span; TORC1, the yeast target of rapamycin complex 1.

Studies described in this chapter of the thesis provide evidence that LCA extends longevity of chronologically aging yeast only if added at certain critical periods of their

lifespan. Our findings imply that 1) during the lifespan of yeast grown under CR conditions on 0.2% glucose, there are two critical periods (checkpoints) when the addition of LCA can extend longevity; 2) one of these two critical periods, which we call period 1, includes logarithmic (L) and diauxic (D) growth phases; 3) the other critical period, which is called period 3, exists in the early stationary (ST) phase of growth; 4) LCA does not extend longevity of chronologically aging yeast if added at periods 2 or 4 (which exist in post-diauxic (PD) or late ST growth phases, respectively); and 5) the observed ability of LCA to extend longevity of CR yeast only if it added at periods 1 or 3 of their lifespan is due to differential effects of this bile acid on various anti- and pro-aging processes at different checkpoints.

7.3 Materials and Methods

Strains and media

The wild-type strain *Saccharomyces cerevisiae* BY4742 (*MAT α his3 Δ 1 leu2 Δ 0 lys2 Δ 0 ura3 Δ 0*) was grown in YP medium (1% yeast extract, 2% peptone) containing 0.2% or 2% glucose as carbon source. Cells were cultured at 30°C with rotational shaking at 200 rpm in Erlenmeyer flasks at a “flask volume/medium volume” ratio of 5:1.

Chronological lifespan assay

A sample of cells was taken from a culture at a certain time-point. A fraction of the sample was diluted in order to determine the total number of cells using a hemacytometer. Another fraction of the cell sample was diluted and serial dilutions of cells were plated in duplicate onto YP plates containing 2% glucose as carbon source.

After 2 d of incubation at 30°C, the number of colony forming units (CFU) per plate was counted. The number of CFU was defined as the number of viable cells in a sample. For each culture, the percentage of viable cells was calculated as follows: (number of viable cells per ml/total number of cells per ml) × 100. The percentage of viable cells in mid-logarithmic phase was set at 100%. The lifespan curves were validated using a LIVE/DEAD yeast viability kit (Invitrogen) following the manufacturer's instructions.

Pharmacological manipulation of chronological lifespan

Chronological lifespan analysis was performed as described above in this section. The lithocholic (LCA; L6250) bile acid was from Sigma. The stock solution of LCA in DMSO was made on the day of adding this compound to cell cultures. LCA was added to growth medium at the final concentration of 50 µM immediately following cell inoculation into the medium or on days 1, 2, 3, 5, 7, 9, 11 or 14 of cell culturing in the medium, as indicated. The final concentration of DMSO in yeast cultures supplemented with LCA (and in the corresponding control cultures supplemented with drug vehicle) was 1% (v/v).

Cell viability assay for monitoring the susceptibility of yeast to an apoptotic mode of cell death induced by hydrogen peroxide

A sample of cells was taken from a culture at a certain time-point. A fraction of the sample was diluted in order to determine the total number of cells using a hemacytometer. 2×10^7 cells were harvested by centrifugation for 1 min at $21,000 \times g$ at room temperature and resuspended in 2 ml of YP medium containing 0.2% glucose as

carbon source. Each cell suspension was divided into 2 equal aliquots. One aliquot was supplemented with hydrogen peroxide to the final concentration of 2.5 mM, whereas other aliquot remained untreated. Both aliquots were then incubated for 2 h at 30°C on a Labquake rotator set for 360° rotation. Serial dilutions of cells were plated in duplicate onto plates containing YP medium with 2% glucose as carbon source. After 2 d of incubation at 30°C, the number of colony forming units (CFU) per plate was counted. The number of CFU was defined as the number of viable cells in a sample. For each aliquot of cells exposed to hydrogen peroxide, the % of viable cells was calculated as follows: (number of viable cells per ml in the aliquot exposed to hydrogen peroxide/number of viable cells per ml in the control aliquot that was not exposed to hydrogen peroxide) × 100.

Cell viability assay for monitoring the susceptibility of yeast to a necrotic mode of cell death induced by palmitoleic acid

A sample of cells was taken from a culture at a certain time-point. A fraction of the sample was diluted in order to determine the total number of cells using a hemacytometer. 2×10^7 cells were harvested by centrifugation for 1 min at $21,000 \times g$ at room temperature and resuspended in 2 ml of YP medium containing 0.2% glucose as carbon source. Each cell suspension was divided into 2 equal aliquots. One aliquot was supplemented with palmitoleic acid from a 50 mM stock solution (in 10% chloroform, 45% hexane and 45% ethanol); the final concentration of palmitoleic acid was 0.15 mM (in 0.03% chloroform, 0.135% hexane and 0.135% ethanol). Other aliquot was supplemented with chloroform, hexane and ethanol added to the final concentrations of

0.03%, 0.135% and 0.135%, respectively. Both aliquots were then incubated for 2 h at 30°C on a Labquake rotator set for 360° rotation. Serial dilutions of cells were plated in duplicate onto plates containing YP medium with 2% glucose as carbon source. After 2 d of incubation at 30°C, the number of colony forming units (CFU) per plate was counted. The number of CFU was defined as the number of viable cells in a sample. For each aliquot of cells exposed to palmitoleic acid, the % of viable cells was calculated as follows: (number of viable cells per ml in the aliquot exposed to palmitoleic acid/number of viable cells per ml in the control aliquot that was not exposed to palmitoleic acid) × 100.

Measurement of the frequency of nuclear mutations

The frequency of spontaneous point mutations in the *CAN1* gene of nuclear DNA was evaluated by measuring the frequency of mutations that caused resistance to the antibiotic canavanine [260]. A sample of cells was removed from each culture at various time-points. Cells were plated in triplicate onto YNB (0.67% Yeast Nitrogen Base without amino acids) plates containing 2% glucose, L-canavanine (50 mg/L), histidine, leucine, lysine and uracil. In addition, serial dilutions of each sample were plated in triplicate onto YP plates containing 2% glucose for measuring the number of viable cells. The number of CFU was counted after 4 d of incubation at 30°C. For each culture, the frequency of mutations that caused resistance to canavanine was calculated as follows: number of CFU per ml on YNB plates containing 2% glucose, L-canavanine (50 mg/L), histidine, leucine, lysine and uracil/number of CFU per ml on YP plates containing 2% glucose.

Measurement of the frequency of mitochondrial mutations affecting mitochondrial components

The frequency of spontaneous single-gene (*mit⁻* and *syn⁻*) and deletion (*rho⁻* and *rho^o*) mutations in mtDNA affecting essential mitochondrial components was evaluated by measuring the fraction of respiratory-competent (*rho⁺*) yeast cells remaining in their aging population. *rho⁺* cells maintained intact their mtDNA and their nuclear genes encoding essential mitochondrial components. Therefore, *rho⁺* cells were able to grow on glycerol, a non-fermentable carbon source. In contrast, mutant cells deficient in mitochondrial respiration were unable to grow on glycerol. These mutant cells carried mutations in mtDNA (including single-gene *mit⁻* and *syn⁻* mutations or large deletions *rho⁻*) or completely lacked this DNA (*rho^o* mutants) [140]. Serial dilutions of cell samples removed from different phases of growth were plated in triplicate onto YP plates containing either 2% glucose or 3% glycerol as carbon source. Plates were incubated at 30°C. The number of CFU on YP plates containing 2% glucose was counted after 2 d of incubation, whereas the number of CFU on YP plates containing 3% glycerol was counted after 6 d of incubation. For each culture, the percentage of respiratory-deficient (*mit⁻*, *syn⁻*, *rho⁻*, *rho^o* and *pet⁻*) cells was calculated as follows: $100 - [(\text{number of CFU per ml on YP plates containing 3\% glycerol} / \text{number of CFU per ml on YP plates containing 2\% glucose}) \times 100]$.

The frequency of spontaneous point mutations in the *rib2* and *rib3* loci of mtDNA was evaluated by measuring the frequency of mtDNA mutations that caused resistance to the antibiotic erythromycin [141]. These mutations impair only mtDNA [142, 143]. A sample of cells was removed from each culture at various time-points. Cells were plated

in triplicate onto YP plates containing 3% glycerol and erythromycin (1 mg/ml). In addition, serial dilutions of each sample were plated in triplicate onto YP plates containing 3% glycerol as carbon source for measuring the number of respiratory-competent (*rho*⁺) cells. The number of CFU was counted after 6 d of incubation at 30°C. For each culture, the frequency of mutations that caused resistance to erythromycin was calculated as follows: number of CFU per ml on YP plates containing 3% glycerol and erythromycin/number of CFU per ml on YP plates containing 3% glycerol.

Plating assays for the analysis of resistance to various stresses

For the analysis of hydrogen peroxide (oxidative stress) resistance, serial dilutions (1:10⁰ to 1:10⁵) of cells removed from each culture at various time-points were spotted onto two sets of plates. One set of plates contained YP medium with 2% glucose alone, whereas the other set contained YP medium with 2% glucose supplemented with 5 mM hydrogen peroxide. Pictures were taken after a 3-day incubation at 30°C.

For the analysis of thermal stress resistance, serial dilutions (1:10⁰ to 1:10⁵) of wild-type and mutant cells removed from each culture at various time-points were spotted onto two sets of plates containing YP medium with 2% glucose. One set of plates was incubated at 30°C. The other set of plates was initially incubated at 55°C for 30 min, and was then transferred to 30°C. Pictures were taken after a 3-day incubation at 30°C.

For the analysis of osmotic stress resistance, serial dilutions (1:10⁰ to 1:10⁵) of wild-type and mutant cells removed from each culture at various time-points were spotted onto two sets of plates. One set of plates contained YP medium with 2% glucose alone,

whereas the other set contained YP medium with 2% glucose supplemented with 1 M sorbitol. Pictures were taken after a 3-day incubation at 30°C.

Statistical analysis

Statistical analysis was performed using Microsoft Excel's (2010) Analysis ToolPack-VBA. All data are presented as mean \pm SEM. The *p* values were calculated using an unpaired two-tailed *t* test.

7.4 Results

7.4.1 LCA delays chronological aging of yeast grown under CR or non-CR conditions only if added at certain critical periods of their lifespan

We sought to examine if the addition of LCA to chronologically aging yeast at different periods of their lifespan has an effect on the longevity-extending efficacy of this bile acid. Yeast were grown in YP medium under CR conditions on 0.2% glucose or under non-CR conditions on 2% glucose, and LCA was added to a cell culture immediately following cell inoculation into the medium (on day 0) or on days 1, 2, 3, 5, 7, 9, 11 or 14 of cell culturing in this growth medium. LCA was used at the final concentration of 50 μ M, at which this natural anti-aging compound has been shown to exhibit the greatest beneficial effect on longevity of chronologically aging yeast under both CR and non-CR conditions [40].

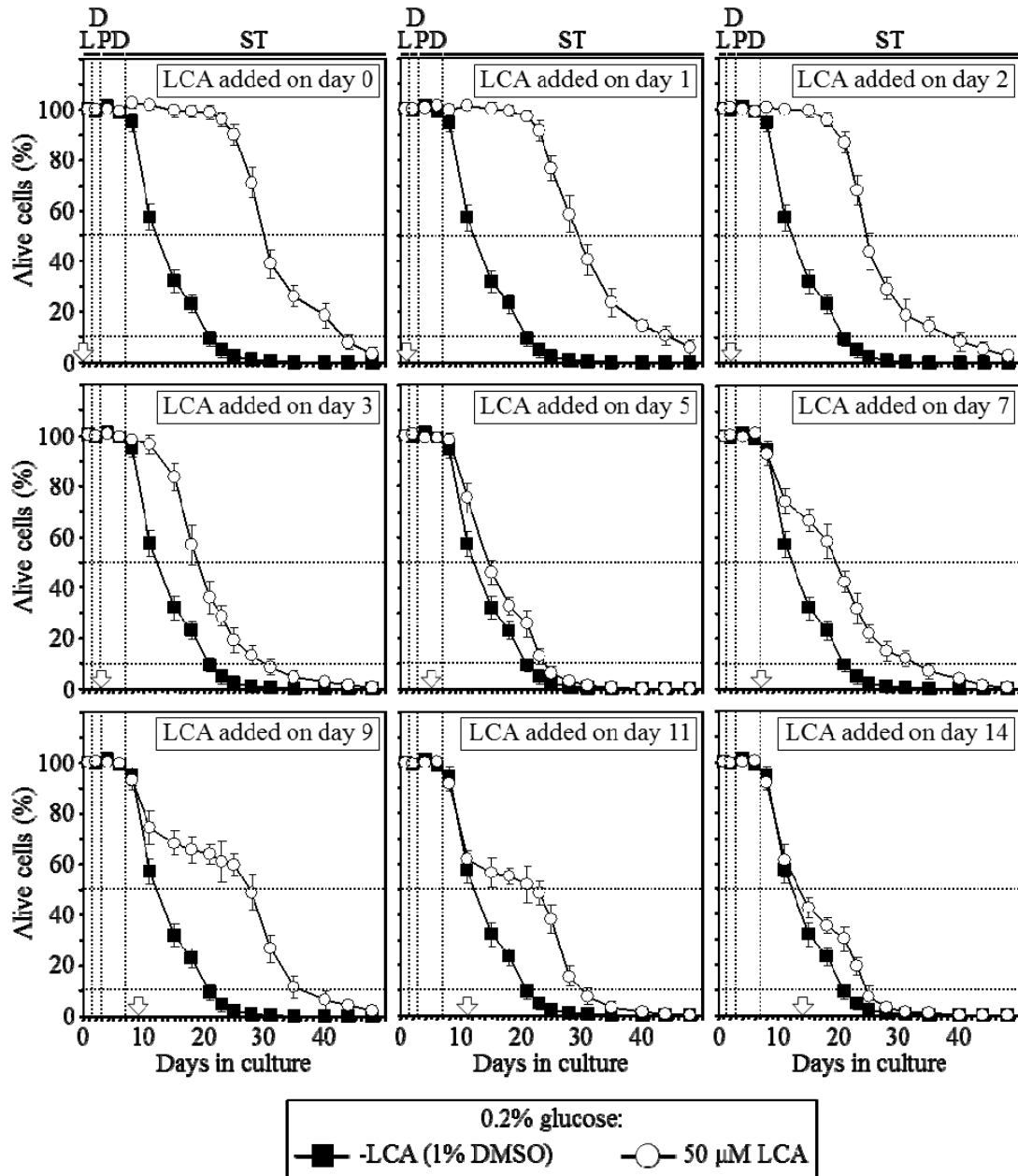


Figure 7.2. In yeast grown under CR conditions on 0.2% glucose, there are two critical periods when the addition of LCA to growth medium can extend longevity. Yeast were cultured in YP medium initially containing 0.2% glucose, and LCA was added at the final concentration of 50 μM to a cell culture immediately following cell inoculation into the medium (on day 0) or on days 1, 2, 3, 5, 7, 9, 11 or 14 of cell culturing in this growth medium. Chronological lifespan analysis was performed as described in “Materials and Methods”. Data are presented as mean \pm SEM ($n = 8$). *Abbreviations:* diauxic (D), logarithmic (L), post-diauxic (PD) or stationary (ST) phase.

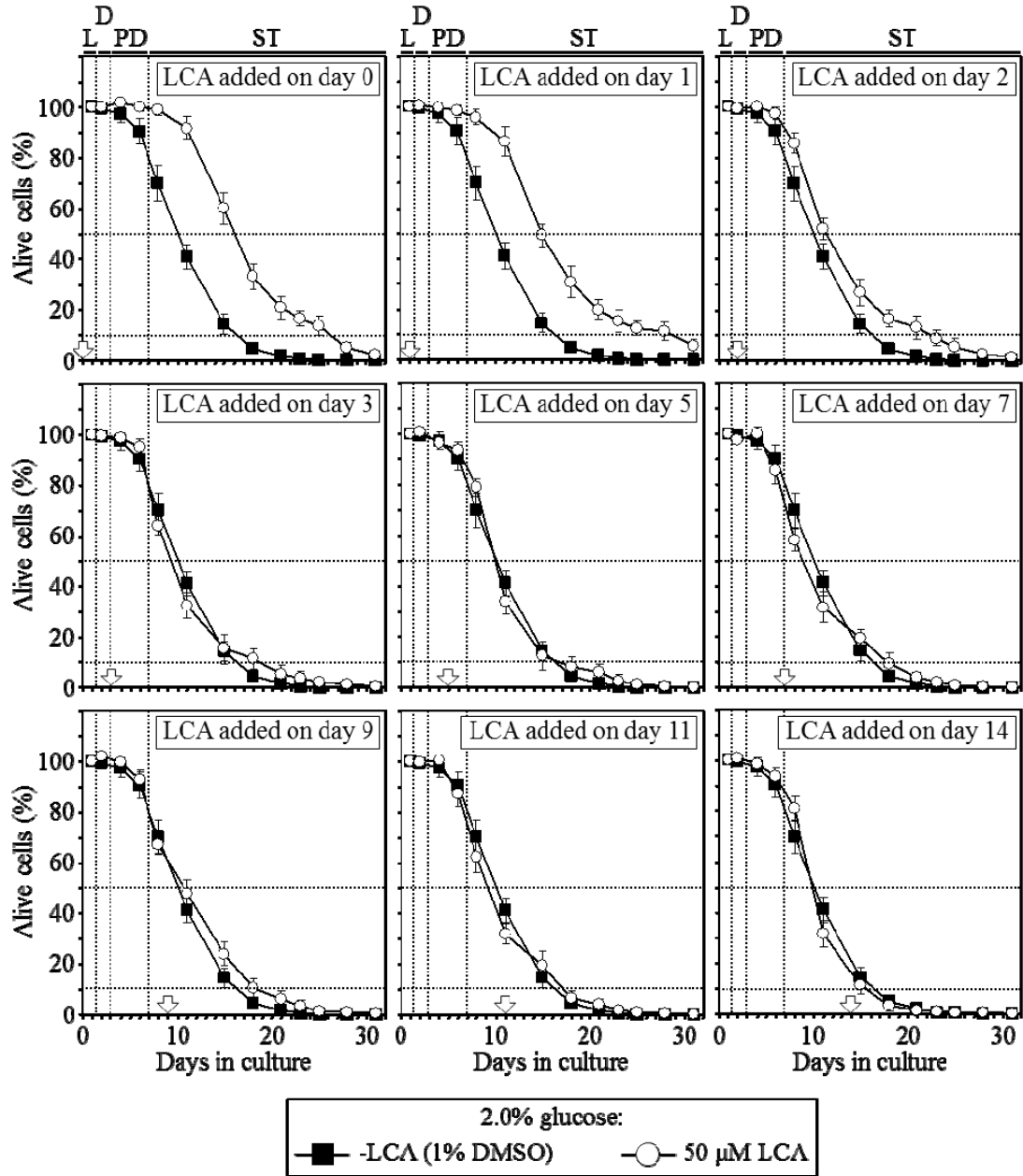


Figure 7.3. In yeast grown under non-CR conditions on 2% glucose, there is only one critical period when the addition of LCA to growth medium can extend longevity. Yeast were cultured in YP medium initially containing 2% glucose, and LCA was added at the final concentration of 50 μ M to a cell culture immediately following cell inoculation into the medium (on day 0) or on days 1, 2, 3, 5, 7, 9, 11 or 14 of cell culturing in this growth medium. Chronological lifespan analysis was performed as described in

“Materials and Methods”. Data are presented as mean \pm SEM (n = 5-6). *Abbreviations:* diauxic (D), logarithmic (L), post-diauxic (PD) or stationary (ST) phase.

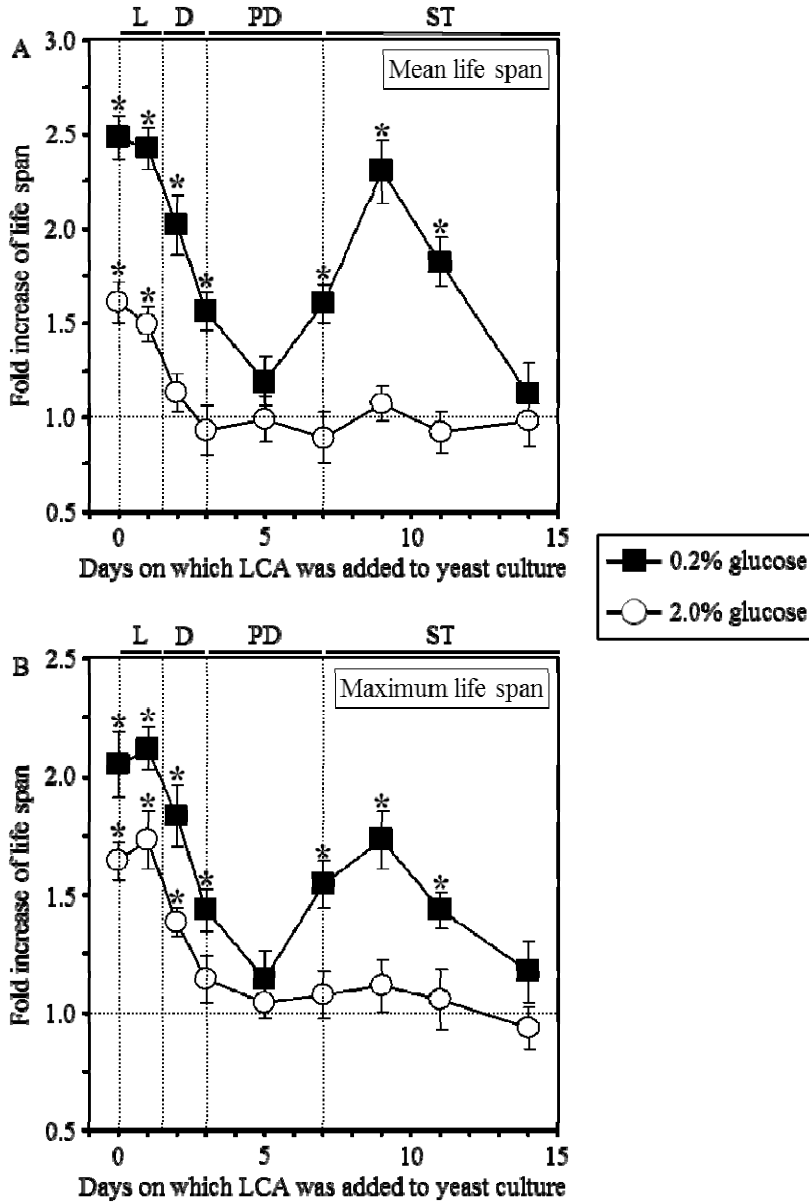


Figure 7.4. In yeast grown under CR conditions on 0.2% glucose, there are two critical periods when the addition of LCA to growth medium can extend longevity. In yeast grown under non-CR conditions on 2% glucose, there is only one such a period. The mean (A) and maximum (B) chronological lifespans of different yeast cultures are shown. Yeast were cultured under CR or non-CR conditions and LCA was added as described in the legends for Figures 7.2 and 7.3, respectively. Chronological lifespan analysis was

performed as described in “Materials and Methods”. Data are presented as mean \pm SEM (n = 5-8); *p < 0.01 (relative to the mean or maximum chronological lifespan of yeast not exposed to LCA).

Abbreviations: diauxic (D), logarithmic (L), post-diauxic (PD) or stationary (ST) phase.

We found that in yeast grown under CR conditions on 0.2% glucose, there are two critical periods when the addition of LCA to growth medium can increase both their mean and maximum chronological lifespans (Figures 7.2 and 7.4). One of these two critical periods, which we call period 1, includes logarithmic (L) and diauxic (D) growth phases. The other critical period, which is called period 3, exists in the early stationary (ST) phase of growth. In contrast, LCA did not cause a significant extension of the mean or maximum chronological lifespan of CR yeast if it was added at periods 2 or 4; these two periods exist in post-diauxic (PD) or late ST growth phases, respectively (Figures 7.2 and 7.4).

We also found that in yeast grown under non-CR conditions on 2% glucose, there is only one critical period, during L and D phases, when the addition of LCA to growth medium can increase both their mean and maximum chronological lifespans (Figures 7.3 and 7.4). However, if LCA was added to non-CR yeast at any time-point after this critical period ended, it did not cause a significant extension of their mean or maximum chronological lifespan (Figures 7.3 and 7.4). Thus, unlike a substantial beneficial effect of LCA on yeast longevity seen if it was added in early ST phase under CR conditions, this bile acid was unable to delay yeast chronological aging under non-CR conditions if added in the same phase of growth.

7.4.2 The ways through which LCA could differentially influence longevity if added to CR yeast at different periods of their lifespan

Aging of multicellular and unicellular eukaryotic organisms affects numerous anti- and pro-aging processes within cells [2, 3, 7, 9, 14, 17 - 21, 27 - 36]. It is conceivable therefore that the observed ability of LCA to delay chronological aging of yeast grown under CR conditions only if added at certain critical periods (checkpoints) of their lifespan could be due to its differential effects on certain anti- and pro-aging processes at different checkpoints. There are several ways through which LCA could differentially influence some anti- and pro-aging processes if it is added at different checkpoints of the chronological lifespan of yeast (Figure 7.5). For example, LCA could activate an anti-aging process (or several processes) during the checkpoints 1 and 2 in L/D and early ST growth phases (respectively), without influencing pro-aging processes during these checkpoints or having an effect on anti- and pro-aging processes during PD and late ST phases (Figure 7.5; the 1st way). Alternatively, LCA could inhibit a pro-aging process (or several processes) during the checkpoints 1 and 2 in L/D and early ST phases (respectively), without influencing anti-aging processes during these checkpoints or having an effect on anti- and pro-aging processes during PD and late ST phases (Figure 7.5; the 2nd way). Moreover, the observed ability of LCA to delay chronological aging of yeast grown under CR conditions only if added at certain checkpoints of their lifespan could be also due to various combinations of the 1st and the 2nd ways outlined above (Figure 7.5; other ways). We therefore sought to examine how the addition of LCA at different periods of chronological lifespan in yeast grown under CR conditions influences anti- and pro-aging processes taking place during each of these periods.

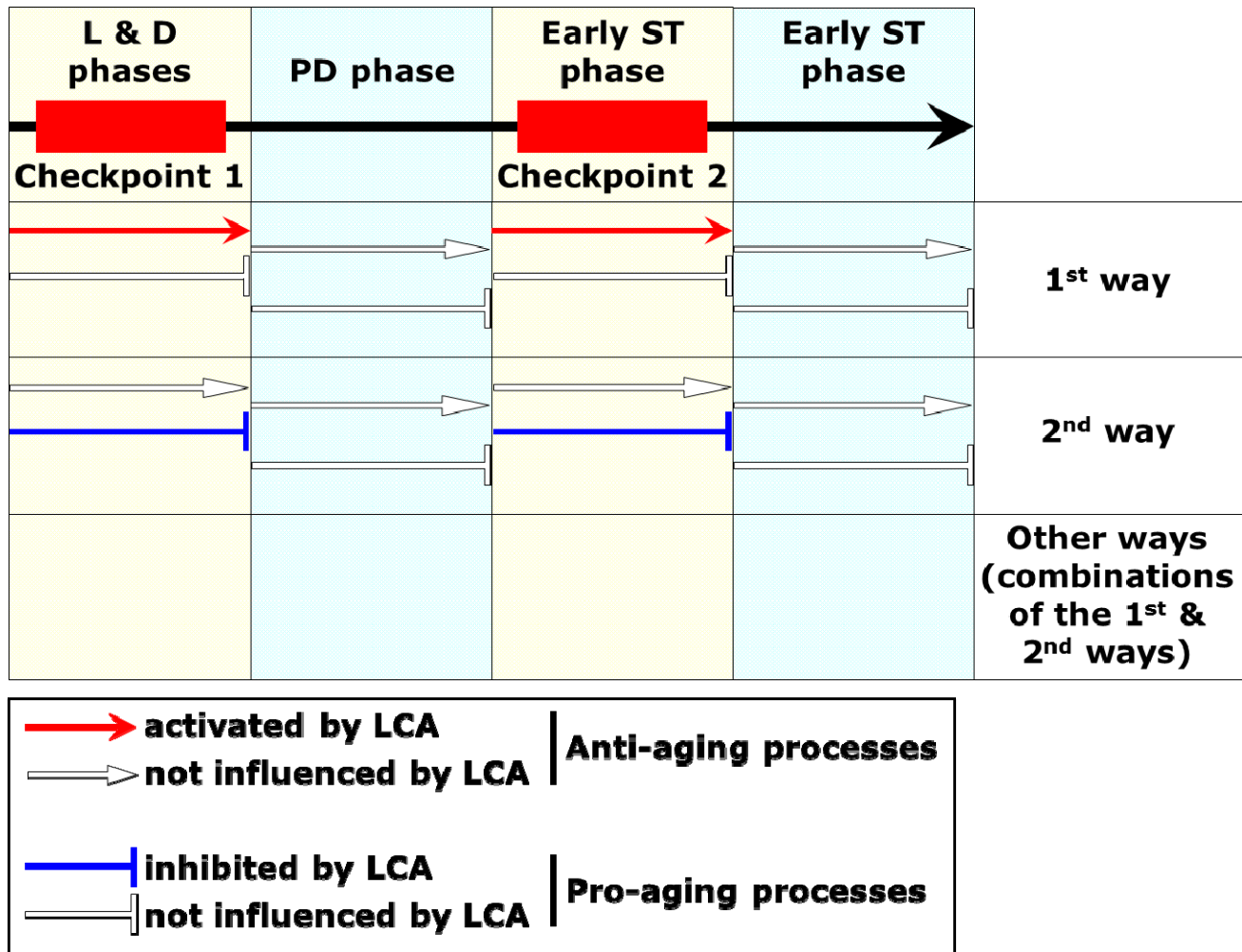


Figure 7.5. There are several ways through which LCA could differentially influence some anti- and pro-aging processes if it is added at different checkpoints of the chronological lifespan of yeast. In the 1st way, LCA could activate an anti-aging process (or several processes) during the checkpoints 1 and 2 in L/D and early ST growth phases (respectively), without influencing pro-aging processes during these checkpoints or having an effect on anti- and pro-aging processes during PD and late ST phases. In the 2nd way, LCA could inhibit a pro-aging process (or several processes) during the checkpoints 1 and 2 in L/D and early ST phases (respectively), without influencing anti-aging processes during these checkpoints or having an effect on anti- and pro-aging processes during PD and late ST phases. The observed ability of LCA to delay chronological aging of yeast grown under CR conditions only if added at certain checkpoints of their

lifespan could be also due to various combinations of the 1st and the 2nd ways, here referred to as “other ways”.

7.4.3 LCA makes yeast cells resistant to mitochondria-controlled apoptotic death, a pro-aging process, only if added at periods 1, 2 or 3 of their chronological lifespan

A short-term exposure of yeast to hydrogen peroxide, acetic acid, hyperosmotic stress or α pheromone causes apoptotic cell death [348 - 351] that has been linked to mitochondrial fragmentation, mitochondrial outer membrane permeabilization and the release of several intermembrane space proteins from mitochondria [352 - 359]. The exit of the apoptosis inducing factor Aif1p and endonuclease G (Nuc1p) from yeast mitochondria and their subsequent import into the nucleus trigger such exogenously induced apoptosis by promoting DNA cleavage [354, 357]. Another intermembrane space protein that is released from yeast mitochondria during exogenously induced apoptosis is cytochrome c [352, 355, 359]. Although some data suggest that - akin to its essential role in triggering the apoptotic caspase cascade in mammalian cells [360, 361] - cytochrome c in the cytosol of yeast cells activates the metacaspase Yca1p [355, 362 - 365], the involvement of cytosolic cytochrome c in Yca1p activation remains a controversial issue [359, 366]. Importantly, chronologically aging yeast die, in an Aif1p-, Nuc1p- and Yca1p-dependent fashion, exhibiting characteristic markers of apoptosis such as chromatin condensation, nuclear fragmentation, DNA cleavage, phosphatidylserine externalization, ROS production and caspase activation [354, 357, 367 - 370]. Thus, the chronological aging of yeast is linked to an apoptosis-like, mitochondria-controlled programmed cell death [371 - 375]. It should be emphasized that mutations eliminating

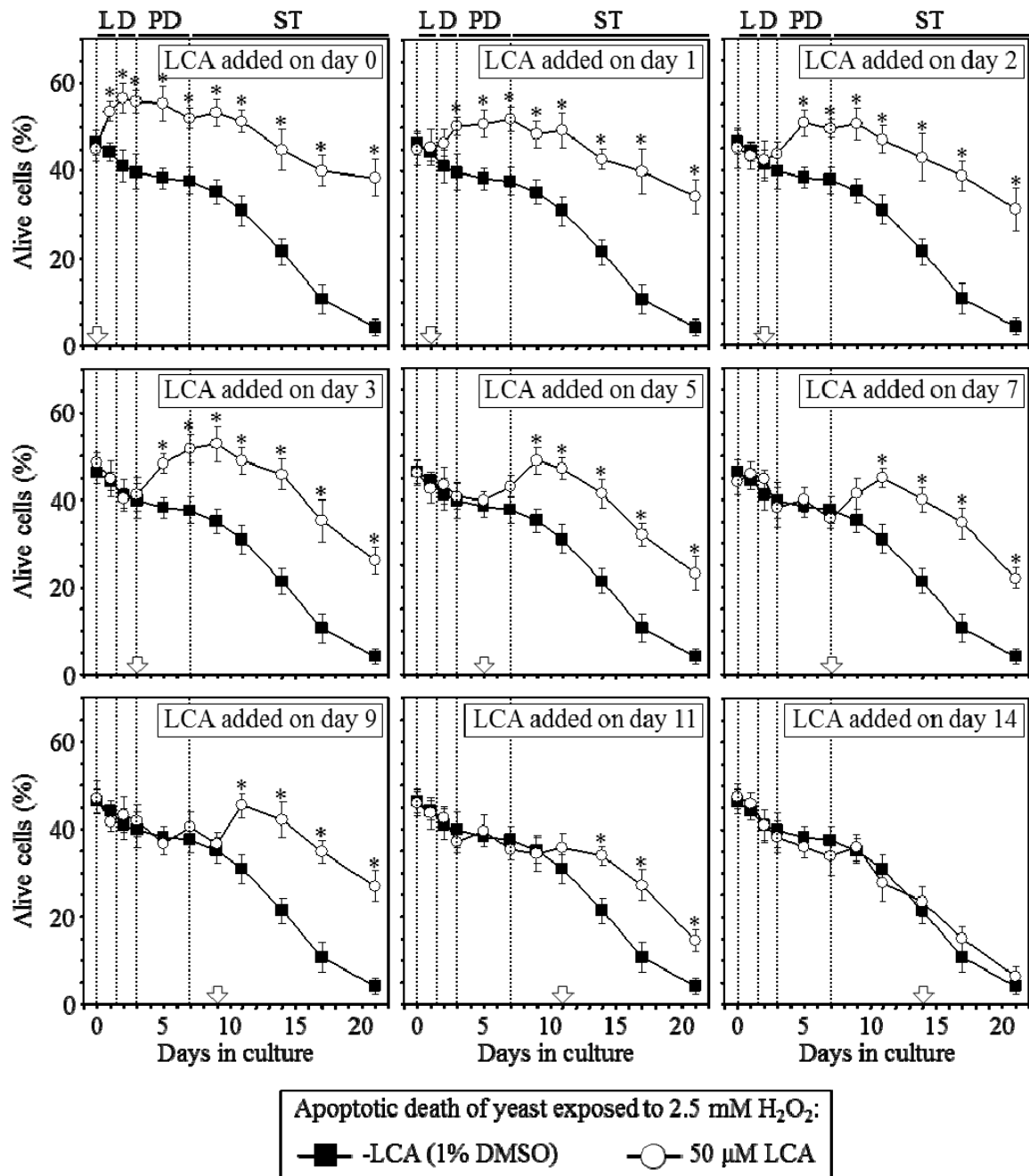


Figure 7.6. LCA makes yeast cells resistant to mitochondria-controlled apoptotic death, a pro-aging process, only if added at periods 1, 2 or 3 of their chronological lifespan. Yeast were cultured in YP medium initially containing 0.2% glucose, and LCA was added at the final concentration of 50 μM to a cell culture immediately following cell inoculation into the medium (on day 0) or on days 1, 2, 3, 5, 7, 9, 11 or 14 of cell culturing in this growth medium. Cell viability assay for monitoring the susceptibility of yeast to

an apoptotic mode of cell death induced by a 1-h exposure to exogenous hydrogen peroxide was performed as described in “Materials and Methods”. Data are presented as mean \pm SEM (n = 3 - 5); *p < 0.01 (relative to the % of alive cells in yeast cultures not exposed to LCA). *Abbreviations:* diauxic (D), logarithmic (L), post-diauxic (PD) or stationary (ST) phase.

pro-apoptotic proteins as well as such potent anti-aging interventions as a CR diet and LCA 1) extend longevity of chronologically aging yeast; 2) delay age-related apoptotic death controlled by mitochondria; and 3) reduce the susceptibility of yeast to cell death triggered by a short-term exposure to exogenous hydrogen peroxide and known to be caused by mitochondria-controlled apoptosis [32, 40, 114, 348, 349, 351, 353, 354, 357, 367 - 375].

Taken together, these findings strongly support the notion that mitochondria-controlled apoptotic death plays an essential role in regulating longevity of chronologically aging yeast. This form of longevity-defining cell death can be triggered by a brief exposure of yeast to exogenous hydrogen peroxide [32, 40, 348, 349, 351, 353]. We therefore examined how the addition of LCA at different periods of chronological lifespan influences a pro-aging process of mitochondria-controlled apoptotic cell death in yeast grown under CR on 0.2% glucose. To attain this objective, we monitored the susceptibility of yeast to cell death triggered by a short-term (for 1 h) exposure to exogenous hydrogen peroxide known to cause mitochondria-controlled apoptosis. We found that if added to growth medium on days 0, 1, 2, 3, 5, 7, 9 or 11, LCA reduces the susceptibility of CR yeast to apoptosis induced by a brief exposure to exogenous hydrogen peroxide following LCA addition (Figure 7.6). In contrast, if added to growth medium on day 14, LCA does not have effect on the susceptibility of CR yeast

to this form of apoptotic cell death (Figure 7.6). Thus, LCA makes yeast cells resistant to mitochondria-controlled apoptotic death, a pro-aging process, only if added at periods 1, 2 or 3 of their chronological lifespan. Period 1 includes L and D growth phases, period 2 exists in PD phase, whereas periods 3 and 4 include early and late ST phases (respectively) (Figures 7.4 and 7.5).

7.4.4 LCA differentially influences the susceptibility of chronologically aging yeast to palmitoleic acid-induced necrotic cell death, a pro-aging process, if added at different periods of their lifespan

In our model for a mechanism linking yeast longevity and lipid dynamics in the endoplasmic reticulum, lipid bodies and peroxisomes (Figure 5.5), a remodeling of lipid metabolism in chronologically aging non-CR yeast shortens their lifespan by causing premature death in part due to necrotic cell death triggered by the accumulation of free fatty acids [32, 40, 44, 110, 114]. Importantly, both CR and LCA not only extend longevity of chronologically aging yeast but also reduce their susceptibility to a form of necrotic cell death triggered by a short-term exposure to exogenous palmitoleic fatty acid [32, 40, 44, 110, 114]. These imply that palmitoleic acid-induced necrotic cell death plays an essential role in regulating longevity of chronologically aging yeast. We therefore examined how the addition of LCA at different periods of chronological lifespan influences a pro-aging process of necrotic cell death in yeast grown under CR on 0.2% glucose. To attain this objective, we monitored the susceptibility of yeast to cell death triggered by a short-term (for 2 h) exposure to exogenous palmitoleic acid. We found that if added to growth medium on days 0, 1 or 2, LCA reduces the susceptibility of CR yeast

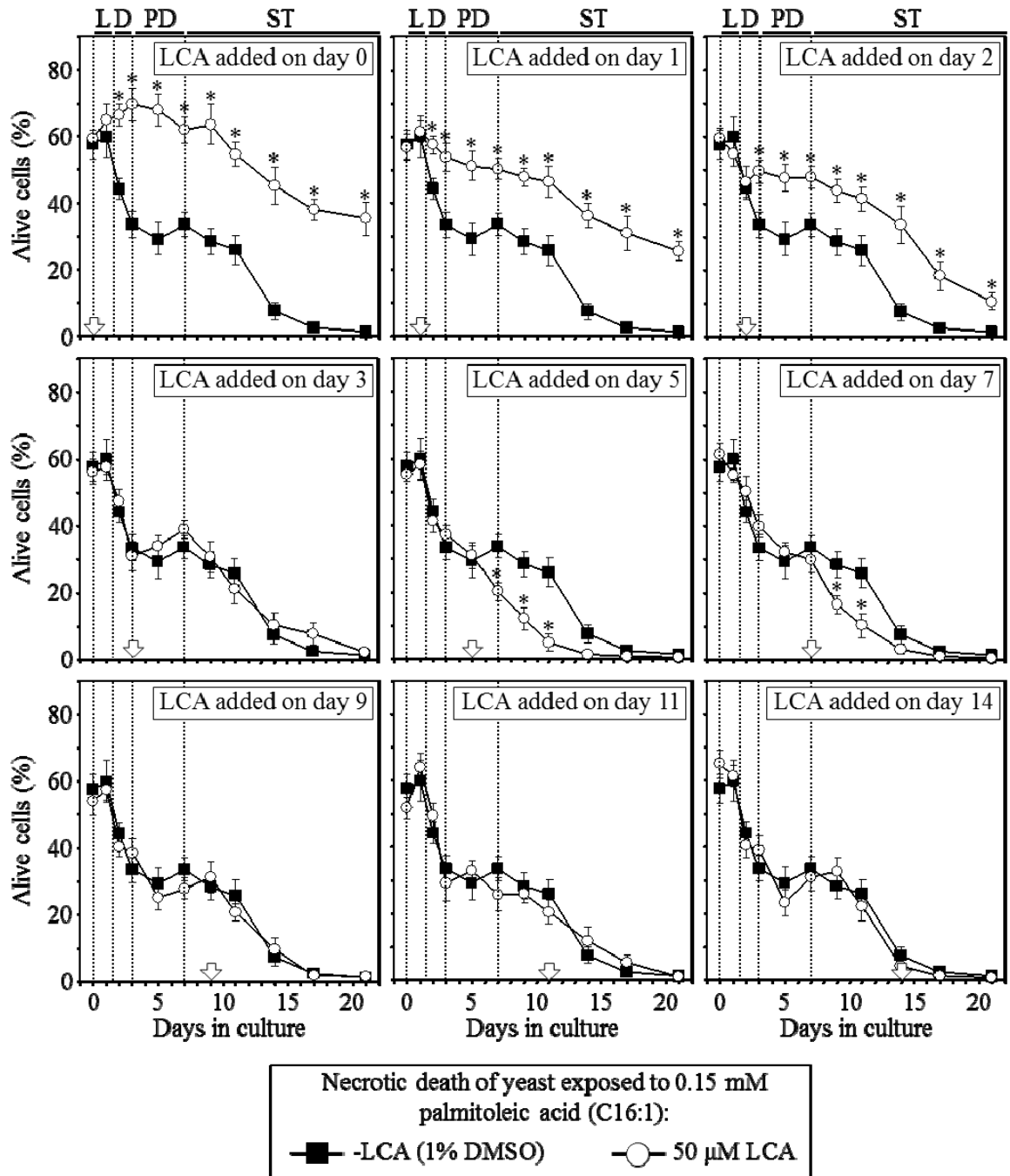


Figure 7.7. LCA differentially influences the susceptibility of chronologically aging yeast to palmitoleic acid-induced necrotic cell death, a pro-aging process, if added at different periods of their lifespan. Yeast were cultured in YP medium initially containing 0.2% glucose, and LCA was added at the final concentration of 50 μ M to a cell culture immediately following cell inoculation into the medium (on day 0) or on days 1, 2, 3, 5, 7, 9, 11 or 14 of cell culturing in this growth medium. Cell viability assay for

monitoring the susceptibility of yeast to a necrotic mode of cell death induced by a 2-h exposure to exogenous palmitoleic acid was performed as described in “Materials and Methods”. Data are presented as mean \pm SEM (n = 4); *p < 0.01 (relative to the % of alive cells in yeast cultures not exposed to LCA).

Abbreviations: diauxic (D), logarithmic (L), post-diauxic (PD) or stationary (ST) phase.

to necrosis induced by a brief exposure to palmitoleic acid following LCA addition (Figure 7.7). In contrast, LCA either does not influence (if added on days 3, 9, 11 or 14) or increases (if added on days 5 or 7) the susceptibility of CR yeast to this form of necrotic cell death (Figure 7.7).

Thus, LCA makes yeast cells resistant to palmitoleic acid-induced necrotic death, a pro-aging process, only if added at period 1 of their chronological lifespan; this period includes L and D growth phases when LCA addition can extend longevity (Figures 7.2, 7.4 and 7.5). It is conceivable that the observed inability of LCA to delay aging of yeast if added at period 2 of their chronological lifespan (Figures 7.2 and 7.4) could be due to its stimulating effect on the pro-aging process of necrotic cell death (Figure 7.7); this period exists in PD phase (Figures 7.4 and 7.5). Furthermore, despite LCA extends longevity of chronologically aging yeast if added at period 3 (which includes early ST phase; see Figures 7.2, 7.4 and 7.5), it does not affect their susceptibility to necrotic cell death if added at this period (Figure 7.7). Moreover, the observed lack of an effect of LCA on yeast longevity if added at period 4 of chronological lifespan (Figures 7.2, 7.4 and 7.5) coincides with its inability to alter cell susceptibility to necrotic cell death if added at this period in late ST phase (Figure 7.7).

7.4.5 In chronologically aging yeast, LCA differentially influences the anti-aging processes of nuclear and mitochondrial genomes maintenance if added at different periods of their lifespan

A body of evidence supports the view that the maintenance of nuclear DNA (nDNA) and mitochondrial DNA (mtDNA) integrity is an essential anti-aging process in evolutionarily distant organisms, including yeast [2, 7, 15, 21, 32, 40, 258, 259]. We therefore examined how the addition of LCA to yeast grown under CR on 0.2% glucose at different periods of chronological lifespan influences 1) the frequency of spontaneous point mutations in the *CAN1* gene of nDNA; 2) the frequencies of spontaneous single-gene (*mit⁻* and *syn⁻*) and deletion (*rho⁻* and *rho^o*) mutations in mtDNA, all causing a deficiency in mitochondrial respiration and impairing growth on glycerol; and 3) the frequencies of spontaneous point mutations in the *rib2* and *rib3* loci of mtDNA.

We found that if added to growth medium on days 0, 1 or 2, LCA reduces the frequency of spontaneous point mutations in the *CAN1* gene of nDNA following LCA addition (Figure 7.8). In contrast, LCA either does not influence (if added on days 3, 9, 11 or 14) or increases (if added on days 5 or 7) the frequency of these spontaneous point mutations in nDNA (Figure 7.8). Thus, LCA stimulates the maintenance of nDNA integrity, an essential anti-aging process, only if added at period 1 of their chronological lifespan; this period includes L and D growth phases when LCA addition can extend longevity (Figures 7.2, 7.4 and 7.5). Our findings also suggest that the observed inhibitory effect of LCA on the maintenance of nDNA integrity if it is added at period 2 of yeast chronological lifespan (Figure 7.8) could in part be responsible for the inability of LCA to delay aging of yeast if added at this period during PD phase (Figures 7.2, 7.4

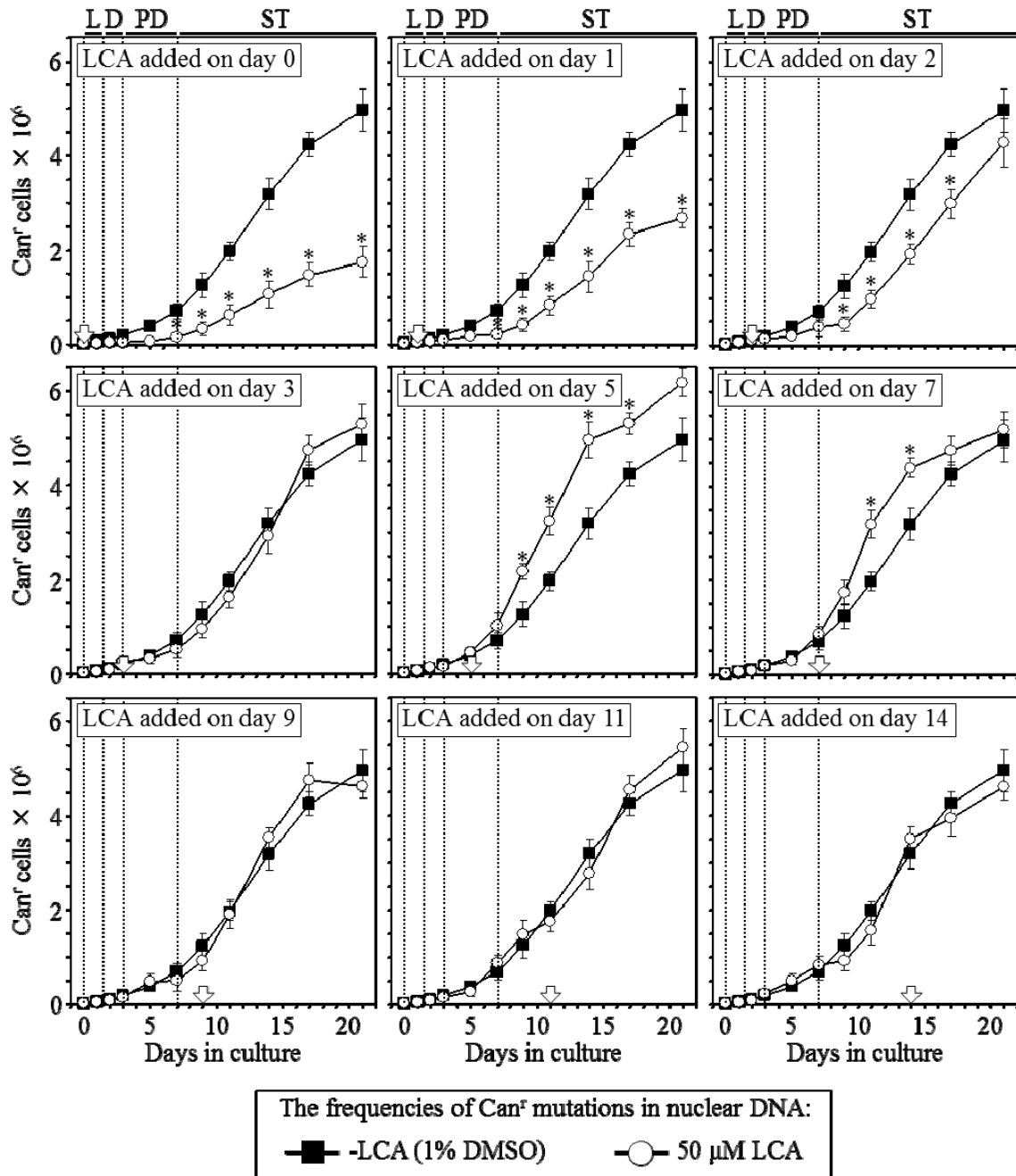


Figure 7.8. LCA differentially influences the maintenance of nDNA integrity, an essential anti-aging process, if added at different periods of yeast lifespan. Yeast were cultured in YP medium initially containing 0.2% glucose, and LCA was added at the final concentration of 50 μ M to a cell culture immediately following cell inoculation into the medium (on day 0) or on days 1, 2, 3, 5, 7, 9, 11 or 14 of cell culturing in this growth medium. The frequency of spontaneous point mutations in the *CAN1* gene of nDNA was measured as described in “Materials and Methods”. Data are presented as mean \pm SEM (n = 3);

* $p < 0.01$ (relative to the frequency of spontaneous point mutations in the *CAN1* gene of nDNA in yeast cultures not exposed to LCA). *Abbreviations*: diauxic (D), logarithmic (L), post-diauxic (PD) or stationary (ST) phase.

and 7.5). Furthermore, despite LCA extends longevity of chronologically aging yeast if added at period 3 (which includes early ST phase; see Figures 7.2, 7.4 and 7.5), it does not influence the maintenance of nDNA integrity if added at this period (Figure 7.8). Moreover, the observed lack of an effect of LCA on yeast longevity if added at period 4 of chronological lifespan (Figures 7.2, 7.4 and 7.5) coincides with its inability to alter the efficacy of the maintenance of nDNA integrity if added at this period in late ST phase (Figure 7.8).

We also found that if added to growth medium on days 0, 1, 2, 3, 5, 7, 9 or 11, LCA reduces 1) the frequencies of spontaneous single-gene (*mit⁻* and *syn⁻*) and deletion (*rho⁻* and *rho^o*) mutations in mtDNA, all causing a deficiency in mitochondrial respiration and impairing growth on glycerol (Figure 7.9); and 2) the frequencies of spontaneous point mutations in the *rib2* and *rib3* loci of mtDNA (Figure 7.10). In contrast, if added to growth medium on day 14, LCA does not have effect on the frequencies of these spontaneous mutations in mtDNA (Figures 7.9 and 7.10). Thus, LCA stimulates the maintenance of mtDNA integrity, an essential anti-aging process, only if added at periods 1, 2 or 3 of yeast chronological lifespan. Period 1 includes L and D growth phases, period 2 exists in PD phase, whereas periods 3 and 4 include early and late ST phases (respectively) (Figures 7.4 and 7.5). Moreover, the observed lack of an effect of LCA on yeast longevity if added at period 4 of chronological lifespan (Figures 7.2, 7.4

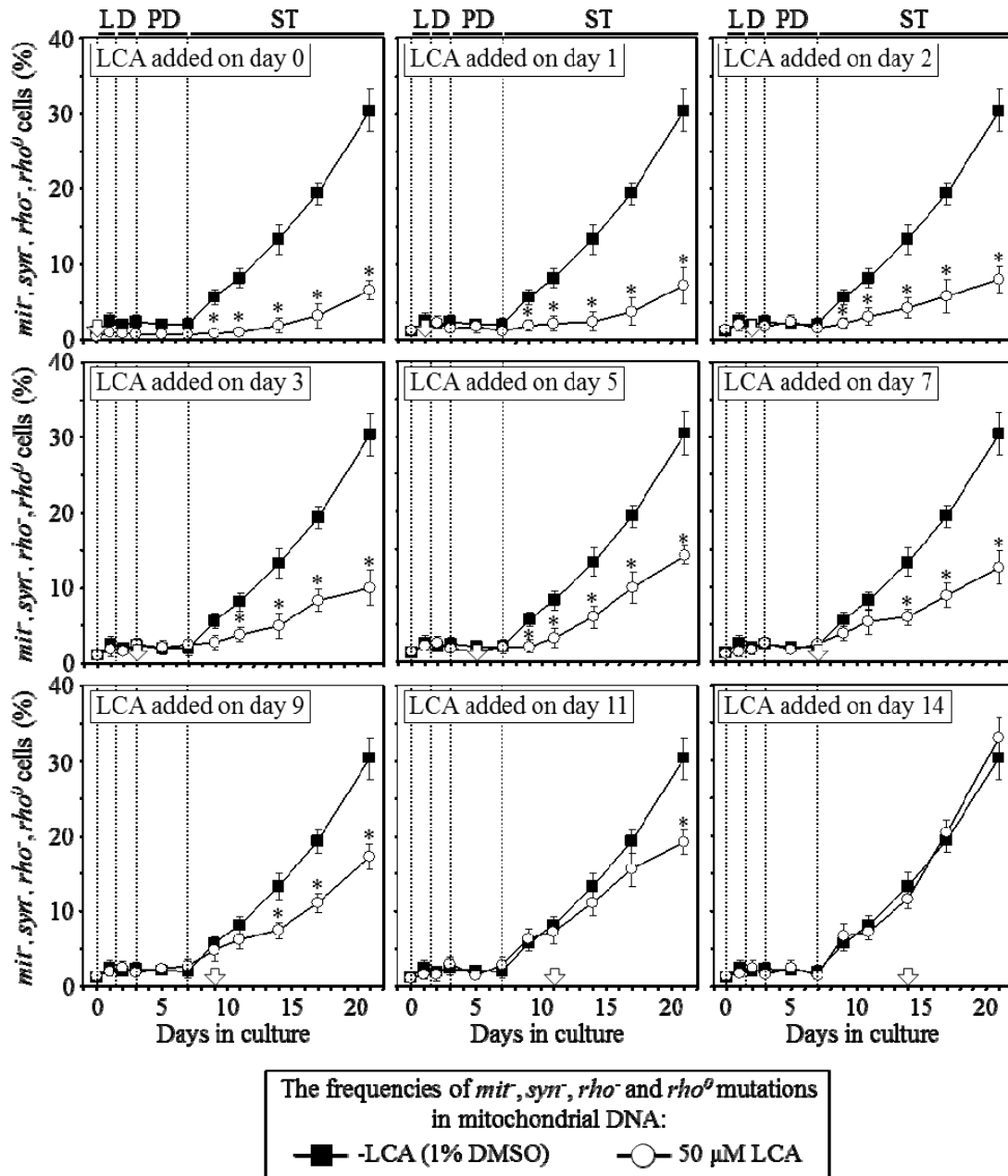


Figure 7.9. LCA differentially influences the maintenance of mtDNA integrity, an essential anti-aging process, if added at different periods of yeast lifespan. Yeast were cultured in YP medium initially containing 0.2% glucose, and LCA was added at the final concentration of 50 μM to a cell culture immediately following cell inoculation into the medium (on day 0) or on days 1, 2, 3, 5, 7, 9, 11 or 14 of cell culturing in this growth medium. The frequencies of spontaneous single-gene (*mit*⁻ and *syn*⁻) and deletion (*rho*⁻ and *rho*^o) mutations in mtDNA, all causing a deficiency in mitochondrial respiration and impairing growth on glycerol, were measured as described in “Materials and Methods”. Data are presented

as mean \pm SEM (n = 5-6); *p < 0.01 (relative to the frequencies of spontaneous *mit*⁻, *syn*⁻, *rho*⁻ and *rho*^o mutations in mtDNA in yeast cultures not exposed to LCA). *Abbreviations*: diauxic (D), logarithmic (L), post-diauxic (PD) or stationary (ST) phase.

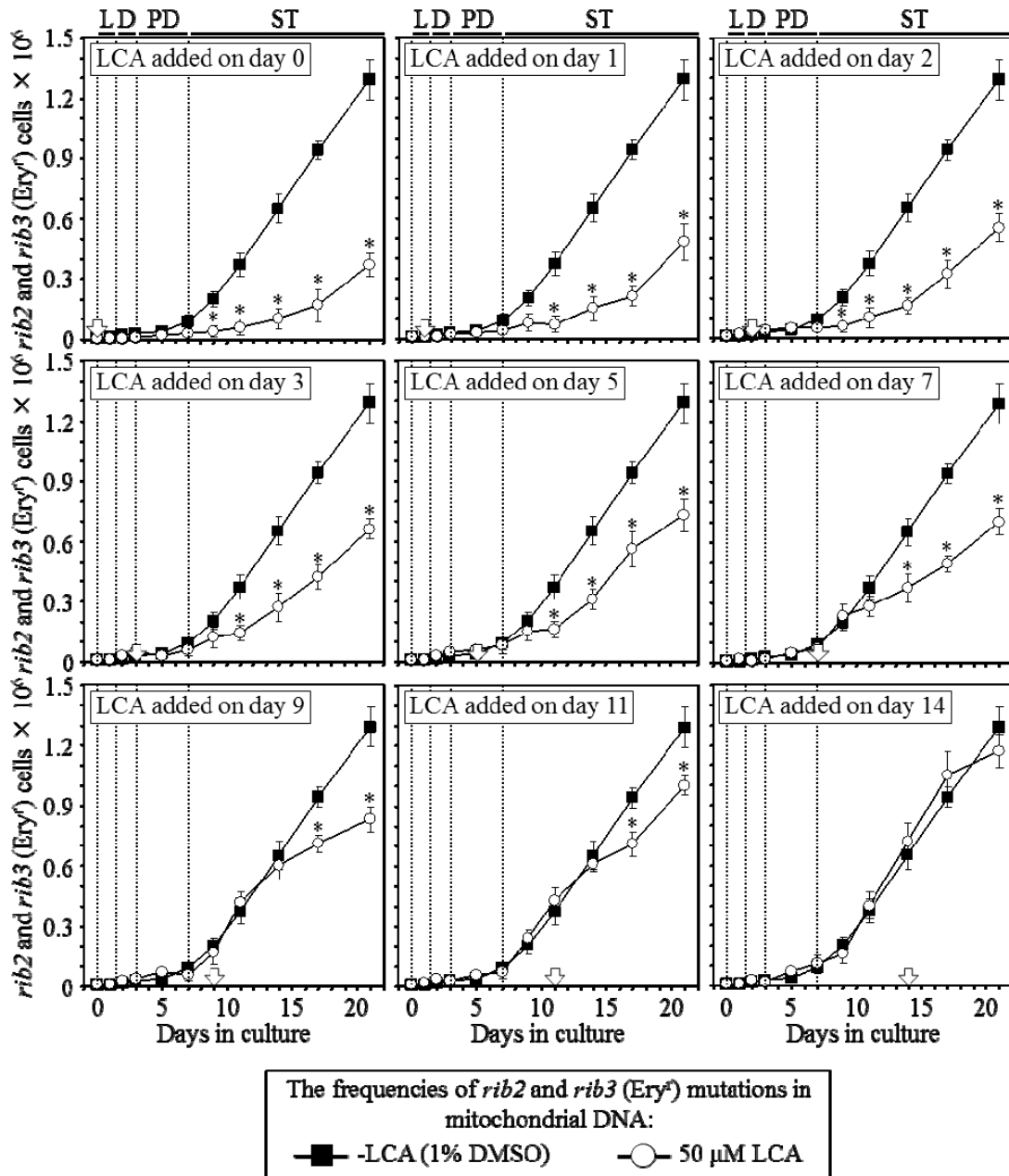


Figure 7.10. LCA differentially influences the maintenance of mtDNA integrity, an essential anti-aging process, if added at different periods of yeast lifespan. Yeast were cultured in YP medium initially

containing 0.2% glucose, and LCA was added at the final concentration of 50 μ M to a cell culture immediately following cell inoculation into the medium (on day 0) or on days 1, 2, 3, 5, 7, 9, 11 or 14 of cell culturing in this growth medium. The frequencies of spontaneous point mutations in the *rib2* and *rib3* loci of mtDNA were measured as described in “Materials and Methods”. Data are presented as mean \pm SEM (n = 3-4); *p < 0.01 (relative to the frequencies of spontaneous *rib2* and *rib3* mutations in mtDNA in yeast cultures not exposed to LCA). *Abbreviations*: diauxic (D), logarithmic (L), post-diauxic (PD) or stationary (ST) phase.

and 7.5) coincides with its inability to alter the efficacy of the maintenance of mtDNA integrity if added at this period in late ST phase (Figures 7.9 and 7.10).

7.4.6 In chronologically aging yeast, LCA differentially influences the anti-aging processes of development of resistance to chronic (long-term) oxidative, thermal and osmotic stresses if added at different periods of their lifespan

It is well established that the development of resistance to chronic (long-term) oxidative, thermal and osmotic stresses is an essential anti-aging process in evolutionarily distant organisms, including yeast [2, 3, 7, 16 - 19, 22, 27, 32, 35, 40, 84 - 86, 91 - 93]. We therefore examined how the addition of LCA to yeast grown under CR on 0.2% glucose at different periods of chronological lifespan influences their resistance to each of these chronic stresses.

We found that if added to growth medium on days 0, 1, 2 or 3, LCA increases the resistance of yeast to chronic oxidative and thermal stresses, but does not alter cell susceptibility to chronic osmotic stress (Figures 7.11, 7.12, 7.13, 7.14, 7.15, 7.16 and

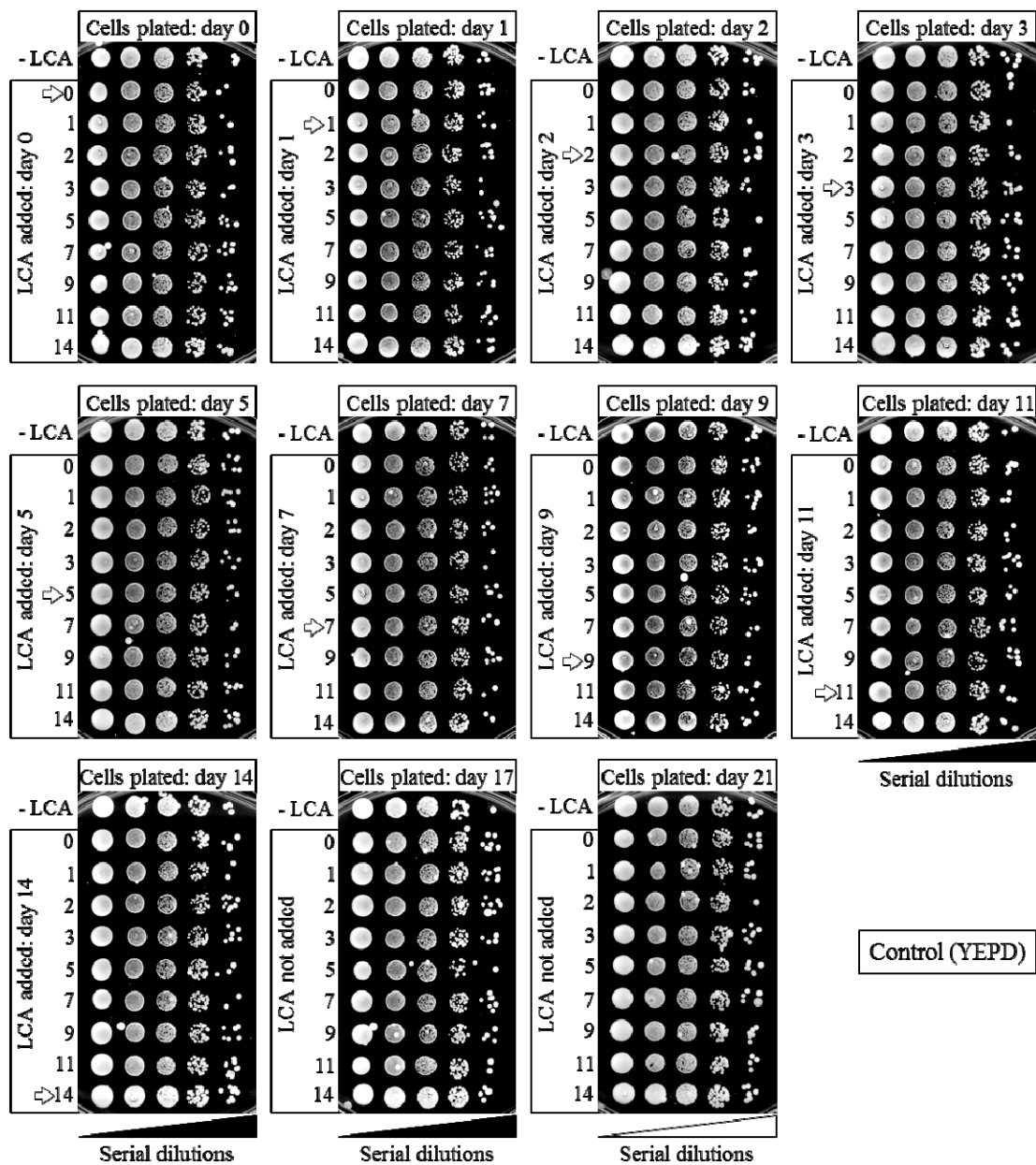


Figure 7.11. Effect of LCA added at different periods of yeast chronological lifespan on cell growth under non-stressful conditions. Yeast were cultured in YP medium initially containing 0.2% glucose, and LCA was added at the final concentration of 50 μ M to a cell culture immediately following cell inoculation into the medium (on day 0) or on days 1, 2, 3, 5, 7, 9, 11 or 14 of cell culturing in this growth medium. Spot assays were performed as described in “Materials and Methods”. Serial ten-fold dilutions of cells were spotted on plates with solid YP medium containing 2% glucose as carbon source. All pictures were taken after a 3-day incubation at 30°C.

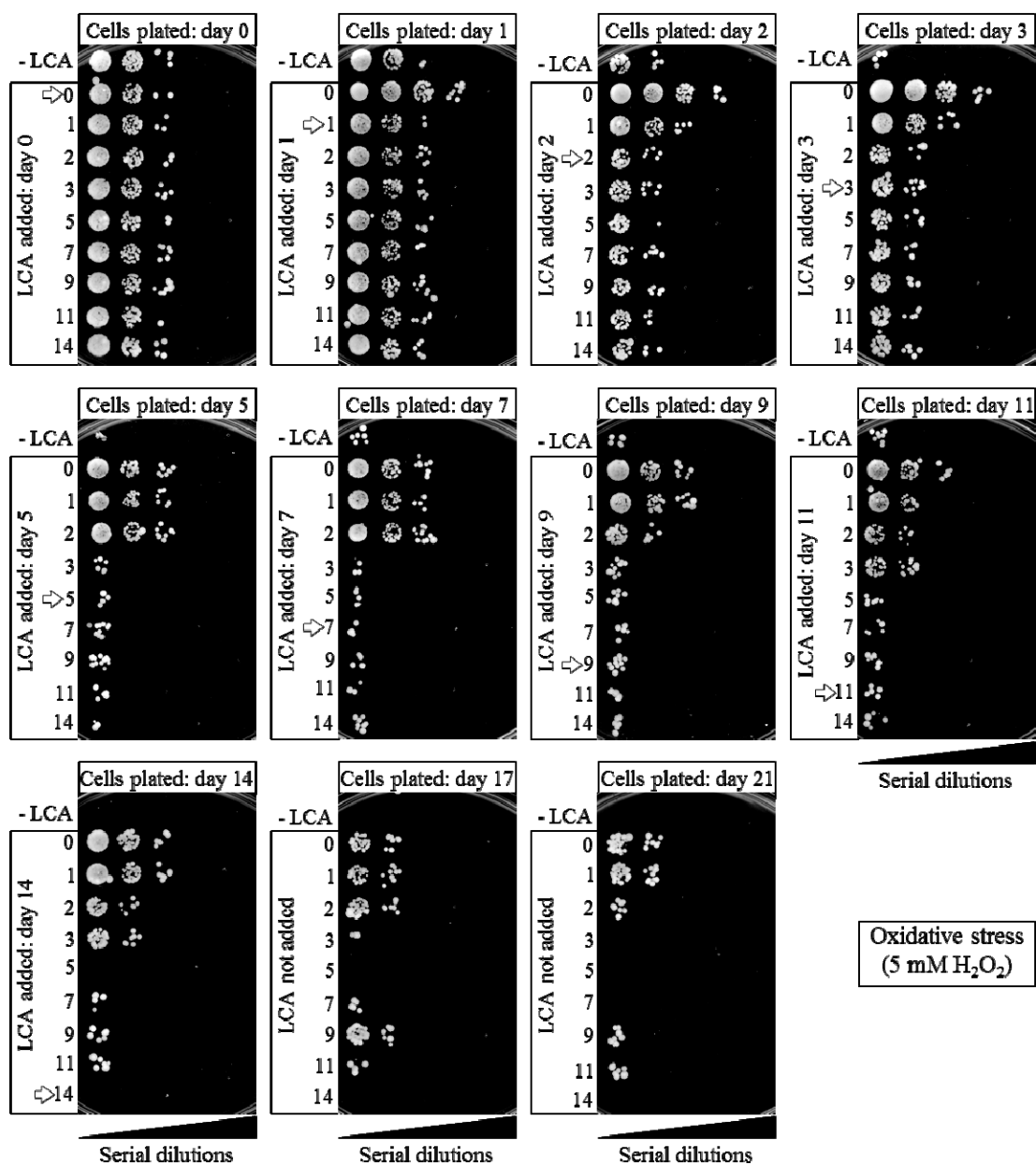


Figure 7.12. Effect of LCA added at different periods of chronological lifespan on the ability of yeast to resist chronic oxidative stress. Yeast were cultured in YP medium initially containing 0.2% glucose, and LCA was added at the final concentration of 50 μM to a cell culture immediately following cell inoculation into the medium (on day 0) or on days 1, 2, 3, 5, 7, 9, 11 or 14 of cell culturing in this growth medium. Spot assays for monitoring oxidative stress resistance were performed as described in “Materials and Methods”. Serial ten-fold dilutions of cells were spotted on plates with solid YP medium containing 2%

glucose as carbon source and 5 mM hydrogen peroxide. All pictures were taken after a 3-day incubation at 30°C.

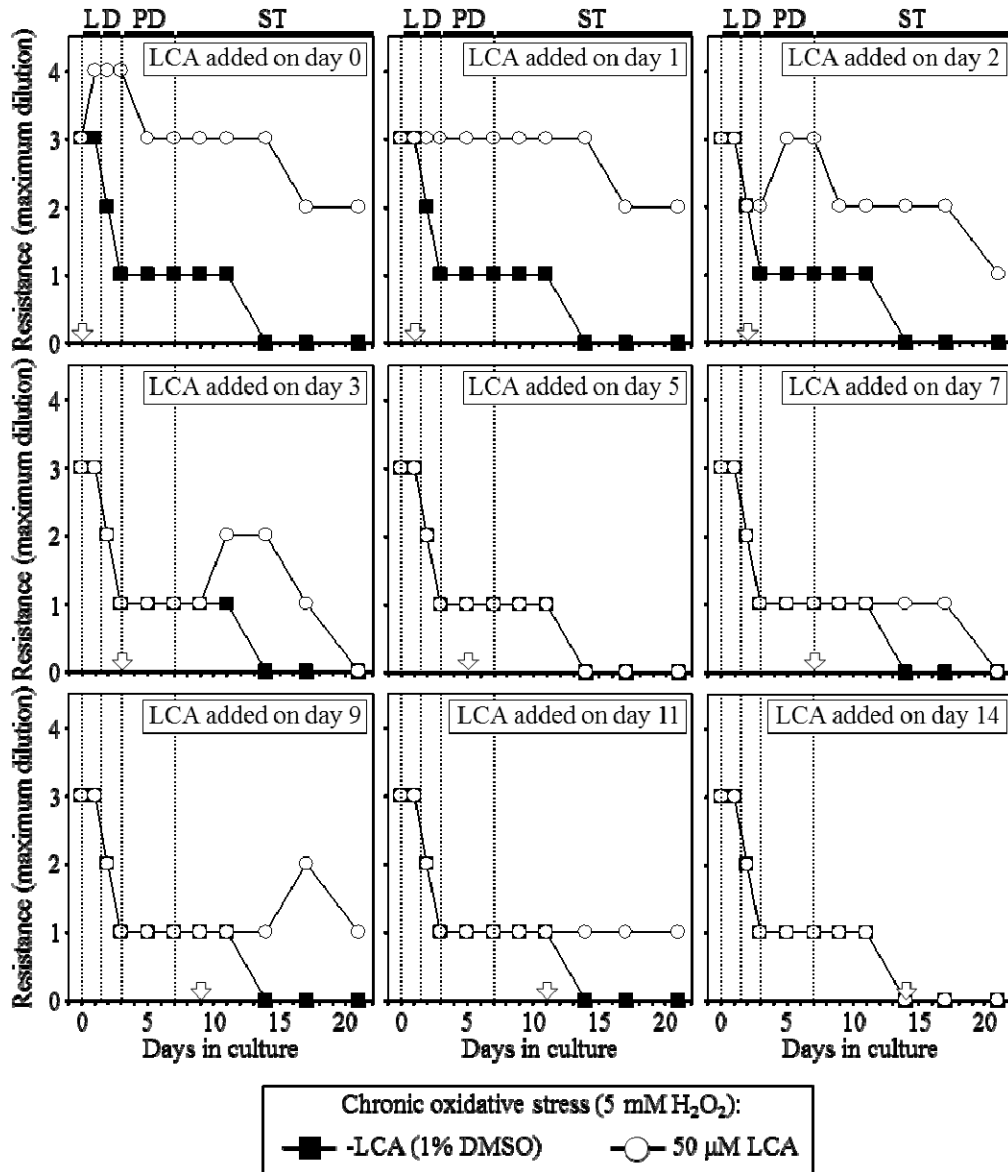


Figure 7.13. LCA differentially influences the anti-aging process of development of resistance to chronic oxidative stress if added at different periods of yeast chronological lifespan. A graphic presentation of the results of spot assays for monitoring oxidative stress resistance, which is shown in Figure 7.12.

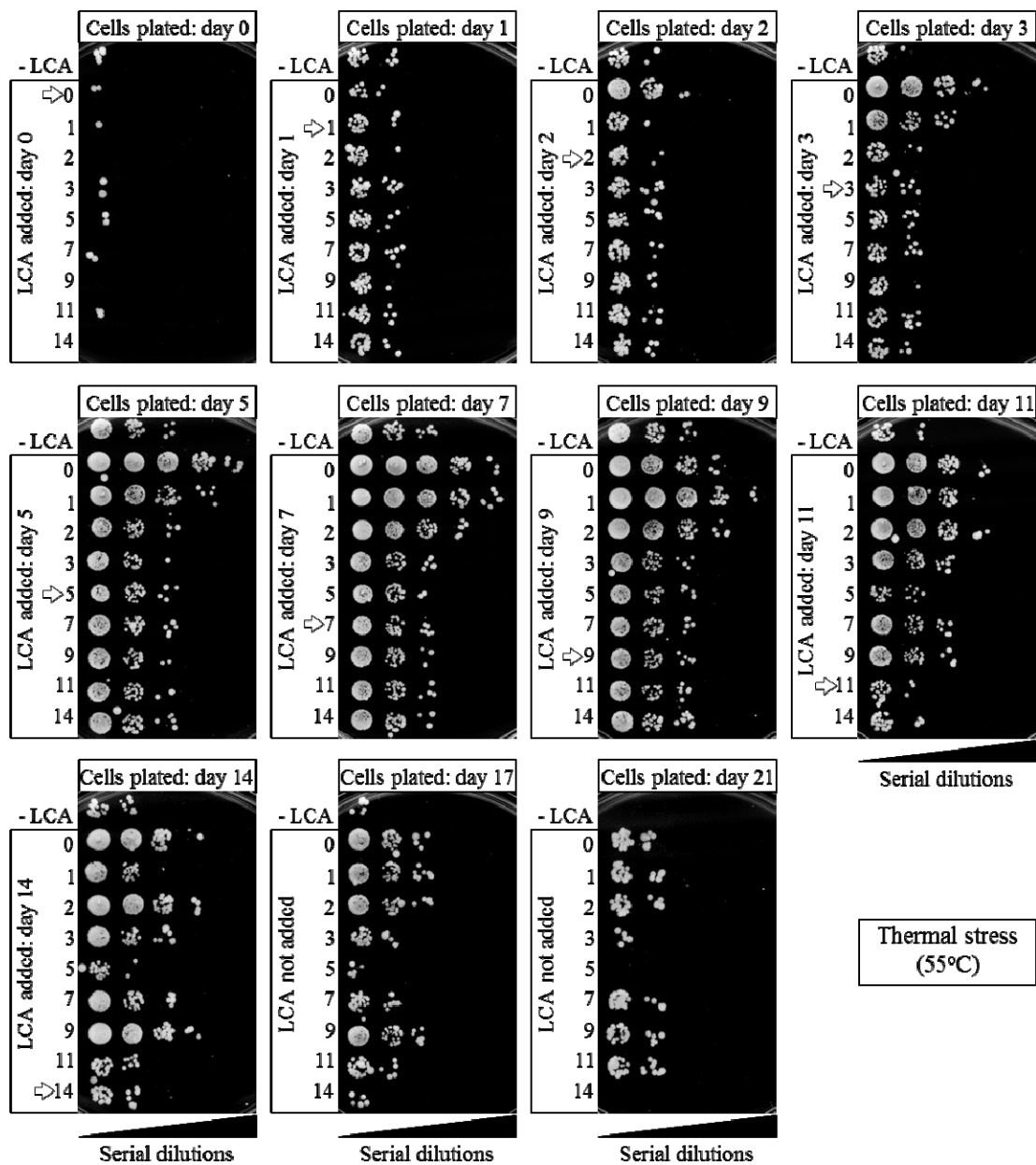


Figure 7.14. Effect of LCA added at different periods of chronological lifespan on the ability of yeast to resist chronic thermal stress. Yeast were cultured in YP medium initially containing 0.2% glucose, and LCA was added at the final concentration of 50 μM to a cell culture immediately following cell inoculation into the medium (on day 0) or on days 1, 2, 3, 5, 7, 9, 11 or 14 of cell culturing in this growth medium. Spot assays for monitoring thermal stress resistance were performed as described in “Materials and Methods”. Serial ten-fold dilutions of cells were spotted on plates with solid YP medium containing 2%

glucose as carbon source. Plates were initially incubated at 55°C for 30 min, and were then transferred to 30°C. All pictures were taken after a 3-day incubation at 30°C.

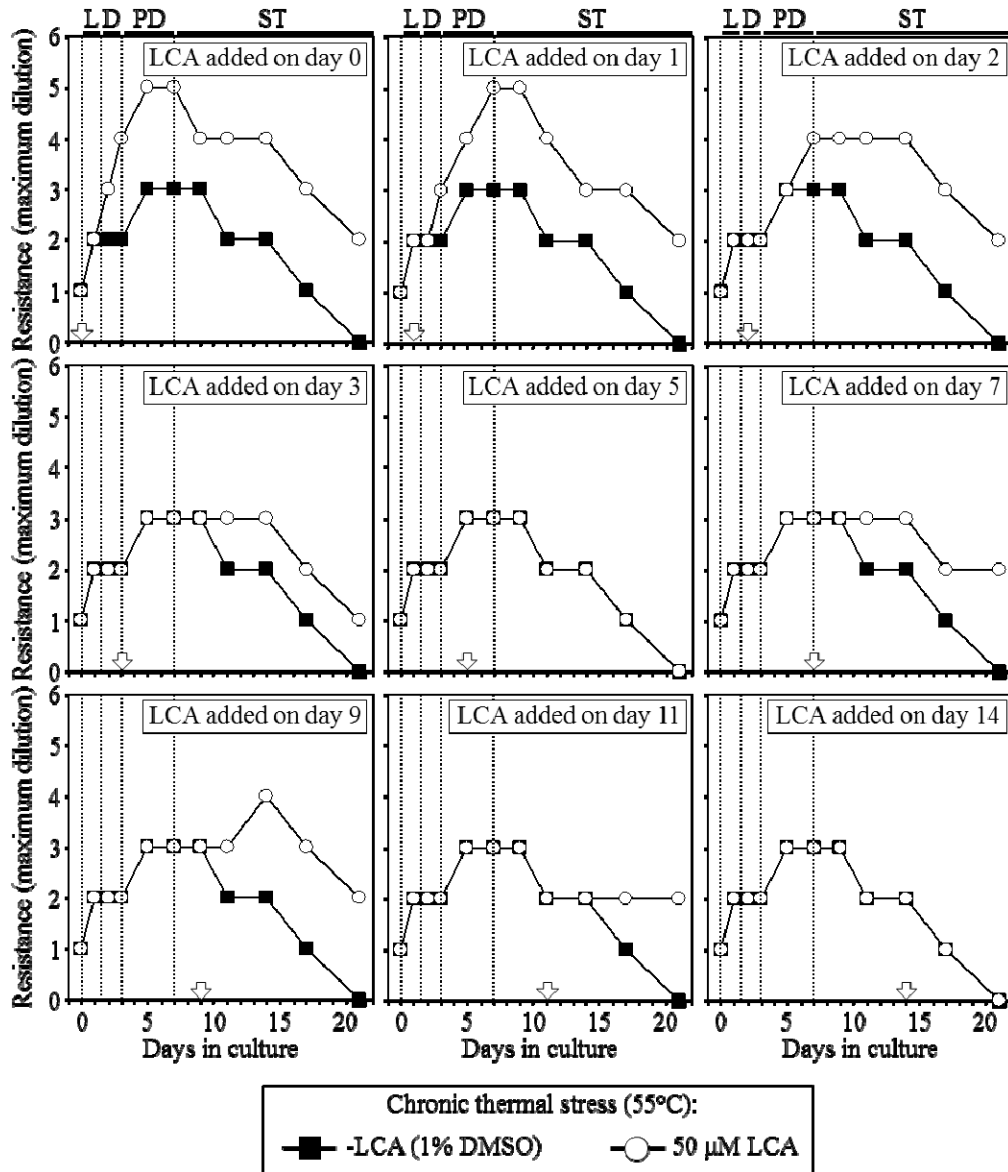


Figure 7.15. LCA differentially influences the anti-aging process of development of resistance to chronic thermal stress if added at different periods of yeast chronological lifespan. A graphic presentation of the results of spot assays for monitoring thermal stress resistance, which is shown in Figure 7.14.

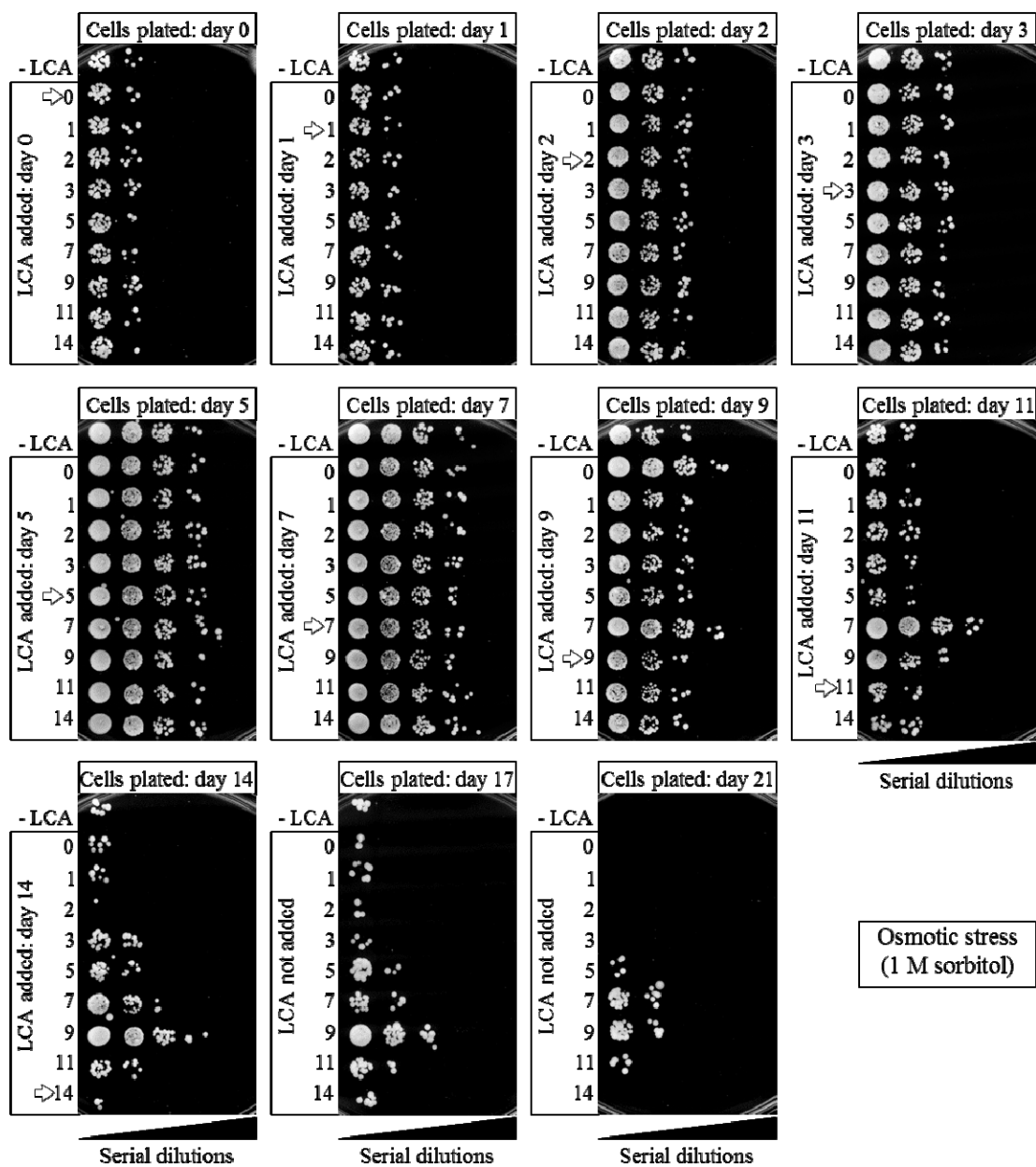


Figure 7.16. Effect of LCA added at different periods of chronological lifespan on the ability of yeast to resist chronic osmotic stress. Yeast were cultured in YP medium initially containing 0.2% glucose, and LCA was added at the final concentration of 50 μ M to a cell culture immediately following cell inoculation into the medium (on day 0) or on days 1, 2, 3, 5, 7, 9, 11 or 14 of cell culturing in this growth medium. Spot assays for monitoring osmotic stress resistance were performed as described in “Materials and Methods”. Serial ten-fold dilutions of cells were spotted on plates with solid YP medium containing 2% glucose as carbon source and 1 M sorbitol. All pictures were taken after a 3-day incubation at 30°C.

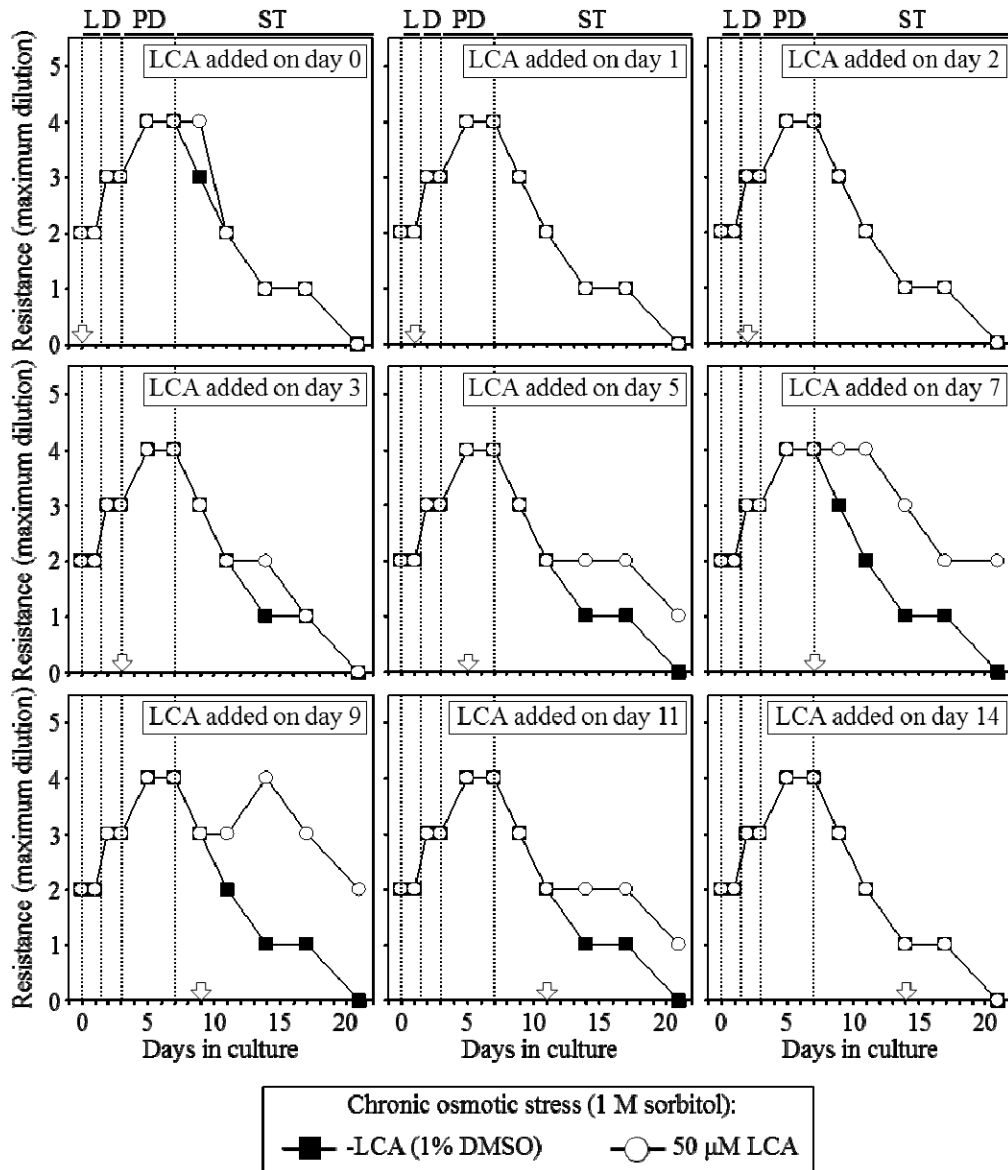


Figure 7.17. LCA differentially influences the anti-aging process of development of resistance to chronic osmotic stress if added at different periods of yeast chronological lifespan. A graphic presentation of the results of spot assays for monitoring osmotic stress resistance, which is shown in Figure 7.16.

7.17). Moreover, LCA increases the resistance of yeast to all three chronic stresses if added to growth medium on days 7, 9 or 11 (Figures 7.11, 7.12, 7.13, 7.14, 7.15, 7.16 and

7.17). In contrast, LCA does not alter cell susceptibility to any of these chronic stresses if added on days 5 or 14 (Figures 7.11, 7.12, 7.13, 7.14, 7.15, 7.16 and 7.17).

Thus in chronologically aging yeast LCA stimulates the anti-aging processes of development of resistance to chronic oxidative and thermal stresses if added at period 1 (which includes L and D growth phases). If added at period 3 (which includes early ST phase), LCA not only stimulates the development of resistance to chronic oxidative and thermal stresses but also enhances the anti-aging process of developing resistance to chronic osmotic stress. If added at any of these two periods, LCA addition can extend longevity (Figures 7.2, 7.4 and 7.5). Noteworthy, the observed lack of an effect of LCA on yeast longevity if added at period 2 or period 4 of chronological lifespan (Figures 7.2, 7.4 and 7.5) coincides with its inability to alter cell susceptibility to any of these stresses at these two periods in PD and late ST phases, respectively.

7.5 Discussion

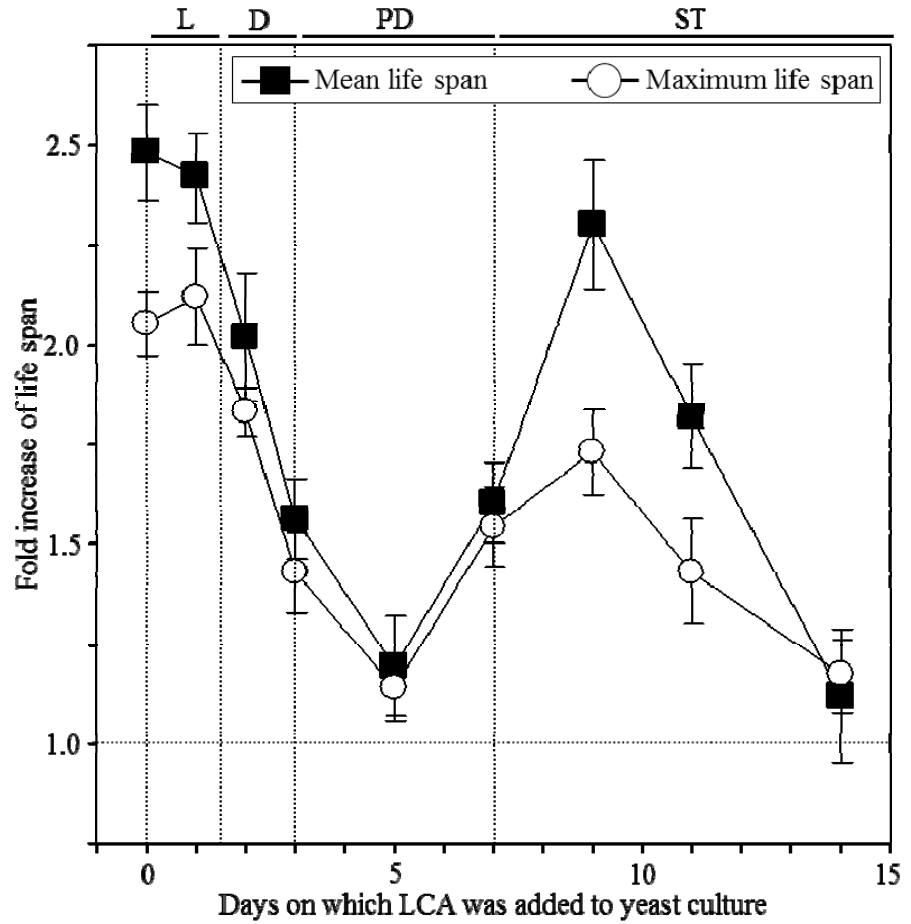
Findings described in this chapter of my thesis imply that in yeast grown under CR conditions on 0.2% glucose, there are two critical periods when the addition of LCA to growth medium can increase both their mean and maximum chronological lifespans. One of these two critical periods, which we call period 1, includes L and D growth phases. The other critical period, which is called period 3, exists in the early ST phase of growth. In contrast, LCA does not cause a significant extension of the mean or maximum chronological lifespan of CR yeast if it was added at periods 2 or 4; these two periods exist in PD or late ST growth phases, respectively (Figures 7.2 and 7.4). In contrast, in yeast grown under non-CR conditions on 2% glucose, there is only one critical period,

during L and D phases, when the addition of LCA to growth medium can increase both their mean and maximum chronological lifespans (Figures 7.3 and 7.4). However, if LCA was added to non-CR yeast at any time-point after this critical period ended, it did not cause a significant extension of their mean or maximum chronological lifespan (Figures 7.3 and 7.4). Thus, unlike a substantial beneficial effect of LCA on yeast longevity seen if it was added in early ST phase under CR conditions, this bile acid was unable to delay yeast chronological aging under non-CR conditions if added in the same phase of growth.

Because aging of multicellular and unicellular eukaryotic organisms affects numerous anti- and pro-aging processes within cells [2, 3, 7, 9, 14, 17 - 21, 27 - 36], we hypothesized that the observed ability of LCA to delay chronological aging of yeast grown under CR conditions only if added at certain critical periods (checkpoints) of their lifespan could be due to its differential effects on certain anti- and pro-aging processes at different checkpoints (Figure 7.5). To test the validity of our hypothesis, we examined how the addition of LCA at different periods of chronological lifespan in yeast grown under CR conditions influences anti- and pro-aging processes taking place during each of these periods.

Findings described in this chapter of my thesis suggest the following mechanism linking the ability of LCA to delay chronological aging of CR yeast only if added at certain critical periods (checkpoints) of their lifespan to the differential effects of this natural anti-aging compound on certain anti- and pro-aging processes at different checkpoints (Figure 7.18).

The ability of LCA to delay aging in yeast if added at period 1 of their chronological lifespan could be due to its following effects on different longevity-



Life span period		1	2	3	4
Effect of LCA added at a particular life span period on:	Pro-aging effect	Decreases	Decreases	Decreases	No effect
	Anti-aging effect	Decreases	Increases	No effect	No effect
	Susceptibility to apoptosis	Decreases	Decreases	Decreases	No effect
	Susceptibility to necrosis	Decreases	Increases	No effect	No effect
	Nuclear DNA stability	Increases	Decreases	No effect	No effect
	Mitochondrial DNA stability	Increases	Increases	Increases	No effect
	Oxidative stress resistance	Increases	No effect	Increases	No effect
Thermal stress resistance	Increases	No effect	Increases	No effect	
Osmotic stress resistance	No effect	No effect	Increases	No effect	

Figure 7.18. A mechanism linking the ability of LCA to delay chronological aging of CR yeast only if added at certain critical periods (checkpoints) of their lifespan to the differential effects of this natural anti-aging compound on certain anti- and pro-aging processes at different checkpoints. See text for details.

defining processes during this critical period: 1) LCA makes yeast cells resistant to mitochondria-controlled apoptotic death, a pro-aging process; 2) LCA increases cell resistance to the pro-aging process of palmitoleic acid-induced necrotic death; 3) LCA stimulates the anti-aging processes of nuclear and mitochondrial genome maintenance; and 4) LCA stimulates the anti-aging processes of development of resistance to chronic oxidative and thermal stresses (Figure 7.18). The ability of LCA to delay aging in yeast if added at period 1 of chronological lifespan by imposing all these beneficial effects on longevity-defining cellular processes could be enhanced by the lack of any pro-aging effect of LCA added at period 1 on the various lifespan-defining processes monitored in this study (Figure 7.18).

Although the addition of LCA at period 2 imposes some beneficial effects on longevity-defining cellular process (*i.e.*, it enhances cell resistance to mitochondria-controlled apoptotic death and stimulates mitochondrial genome maintenance), the observed inability of the compound to delay aging in yeast if added at this period of chronological lifespan could be due to the two pro-aging effects that LCA exhibits when added at period 2. These pro-aging effects of LCA added during period 2 include a reduction of cell resistance to the pro-aging process of palmitoleic acid-induced necrotic death and a decrease of the efficacy with which the integrity of nuclear genome is maintained (Figure 7.18).

The ability of LCA to delay aging in yeast if added at period 3 of their chronological lifespan could be due to its following effects on different longevity-defining processes during this critical period: 1) LCA makes yeast cells resistant to mitochondria-controlled apoptotic death, a pro-aging process; 2) LCA stimulates the anti-

aging process of mitochondrial genome maintenance; and 3) LCA stimulates the anti-aging processes of development of resistance to chronic oxidative, thermal and osmotic stresses (Figure 7.18). It is conceivable that the ability of LCA to delay aging in yeast if added at period 3 of chronological lifespan by imposing these beneficial effects on longevity-defining cellular processes could be enhanced by the lack of any pro-aging effect of LCA added at period 3 on the various lifespan-defining processes monitored in this study (Figure 7.18).

Because the addition of LCA at period 4 does not influence any of the various longevity-defining processes monitored in this study, it is not surprising that it is unable to delay aging in yeast if added at this period of their chronological lifespan (Figure 7.18).

7.6 Conclusions

Findings presented in this chapter of my thesis provide conclusive evidence that the natural anti-aging compound LCA extends longevity of chronologically aging yeast only if added at certain critical periods of their lifespan. Our data imply that during the chronological lifespan of yeast grown under CR conditions on 0.2% glucose, there are two critical periods (checkpoints) when the addition of LCA can extend longevity. One of these two critical periods (which we call period 1) includes L and D growth phases, whereas the other period (which is called period 3) exists in the early ST phase of growth. In contrast, LCA does not extend longevity of chronologically aging yeast if added at periods 2 or 4. These two periods exist in PD and late ST growth phases, respectively. Based on our findings, we propose a mechanism that links the ability of LCA to delay

chronological aging of CR yeast only if added at certain critical periods (checkpoints) of their lifespan to the differential effects of this bile acid on certain anti- and pro-aging processes at different checkpoints.

8 Mitophagy is a longevity assurance process that in yeast sustains functional mitochondria and protects cells from apoptotic and necrosis-like “lipoptotic” modes of cell death

8.1 Abstract

Recent findings in mammals suggest that mitophagy, a selective macroautophagic removal of dysfunctional mitochondria, is an essential cellular process aimed at maintaining mitochondrial functionality and suppressing cellular and organismal pathologies that arise due to dysfunction of mitochondria. However, the physiological roles of mitophagy in yeast and underlying mechanisms remained to be discovered. This chapter of my thesis describes studies aimed at exploring possible roles of mitophagy in regulating yeast longevity, maintaining functional mitochondria, and protecting yeast from apoptotic and a recently discovered by our laboratory necrosis-like “lipoptotic” modes of age-related cell death. In studies described in this chapter of my thesis, we used a combination of functional genetic, chemical biological, cell biological and electron microscopical analyses to carry out comparative analyses of the single-gene-deletion mutant strain *atg32Δ*, which is impaired only in the mitophagic pathway of selective macroautophagy, and wild-type (WT) strain. *atg32Δ* is known to lack a mitochondrial outer membrane protein Atg32p whose binding to an adaptor protein Atg11p drives the recruitment of mitochondria to the phagophore assembly site, thereby initiating the mitophagy process. Our findings imply that mitophagy defines yeast longevity, facilitates yeast chronological lifespan extension by a recently discovered anti-aging natural compound, sustains functional mitochondria, and protects yeast from apoptotic and

necrosis-like “lipoptotic” forms of cell death.

8.2 Introduction

Autophagy is an evolutionarily conserved process for degradation of damaged and dysfunctional organelles or portions of cytoplasm following their sequestration and delivery to lysosomes in mammalian cells or vacuoles in yeast cells (see Chapter 1 of this thesis for a comprehensive discussion of this topic) [126 - 129]. As an essential cytoprotective mechanism initiated in response to various cellular stresses, autophagic degradation plays an essential role in longevity regulation and has been implicated in the incidence of diverse age-related pathologies, including neurodegeneration and cancer [126 - 130]. In addition to non-selective degradation of cellular components sequestered into double-membrane vesicles called autophagosomes and then targeted to lysosomes/vacuoles via a so-called non-selective macroautophagy pathway (see Chapter 1 of this thesis), autophagy can selectively degrade specific organelles and supramolecular cellular assemblies [126 - 128]. The selective degradation of mitochondria via autophagy is called mitophagy [126, 128 - 130]. Although recent findings in evolutionarily distant organisms from yeast to mammals suggest that mitophagy may operate as an essential mechanism in ensuring quality control of mitochondria, the physiological roles of mitophagy and underlying mechanisms remain to be determined. The objective of studies described in this chapter of my thesis was to explore the involvement of mitophagy in regulating yeast longevity, maintaining functional mitochondria, and protecting yeast from apoptotic and a recently discovered by our laboratory necrosis-like “lipoptotic” modes of age-related cell death.

8.3 Materials and Methods

Yeast strains and growth conditions

The wild-type (WT) strain BY4742 (*MAT α his3 Δ 1 leu2 Δ 0 lys2 Δ 0 ura3 Δ 0*) and the single-gene-deletion mutant strain *atg32 Δ* (*MAT α his3 Δ 1 leu2 Δ 0 lys2 Δ 0 ura3 Δ 0 atg32 Δ ::kanMX4*) in the BY4742 genetic background (both from Open Biosystems) were grown in YP medium (1% yeast extract, 2% peptone) containing 0.2% or 2% glucose as carbon source. Cells were cultured at 30°C with rotational shaking at 200 rpm in Erlenmeyer flasks at a “flask volume/medium volume” ratio of 5:1.

Chronological lifespan assay

A sample of cells was taken from a culture at a certain time-point. A fraction of the sample was diluted in order to determine the total number of cells using a hemacytometer. Another fraction of the cell sample was diluted and serial dilutions of cells were plated in duplicate onto YP plates containing 2% glucose as carbon source. After 2 d of incubation at 30°C, the number of colony forming units (CFU) per plate was counted. The number of CFU was defined as the number of viable cells in a sample. For each culture, the percentage of viable cells was calculated as follows: (number of viable cells per ml/total number of cells per ml) \times 100. The percentage of viable cells in mid-logarithmic phase was set at 100%. The lifespan curves were validated using a LIVE/DEAD yeast viability kit (Invitrogen) following the manufacturer's instructions.

Pharmacological manipulation of chronological lifespan

Chronological lifespan analysis was performed as described above in this section. The lithocholic (LCA; L6250) bile acid was from Sigma. The stock solution of LCA in DMSO was made on the day of adding this compound to cell cultures. LCA was added to growth medium immediately following cell inoculation. It was used at a final concentration of 50 μ M, at which it displays the greatest beneficial effect on both the mean and maximum chronological lifespans of WT strain [40]. The final concentration of DMSO in yeast cultures supplemented with LCA (and in the corresponding control cultures supplemented with drug vehicle) was 1% (v/v).

Oxygen consumption assay

A sample of cells was taken from a culture at a certain time-point. Cells were pelleted by centrifugation and resuspended in 1 ml of fresh YP medium containing 0.05% glucose. Oxygen uptake by cells was measured continuously in a 2-ml stirred chamber using a custom-designed biological oxygen monitor (Science Technical Center of Concordia University) equipped with a Clark-type oxygen electrode.

Electron microscopy

Whole cells were fixed in 1.5% (w/v) KMnO_4 at room temperature for 20 min, incubated with 0.5% (w/v) sodium periodate for 15 min and exposed to 1% (w/v) ammonium chloride for 15 min. Cells were then post-stained in 1% (w/v) uranyl acetate overnight, dehydrated by successive incubations in increasing concentrations of ethanol (60%, 80%, 95%, 98% and 100%), followed by wash in propylene oxide (100%) and gradually infiltrated with Epon resin. Ultrathin sections were cut with a diamond knife, stained

with 4% aqueous uranyl acetate and 0.2% lead citrate, and then examined in a T12 transmission electron microscope at 120 KV at different magnification.

Cell viability assay for monitoring the susceptibility of yeast to an apoptotic mode of cell death induced by hydrogen peroxide

Cells were cultured in YP medium initially containing 0.2% or 2% glucose. A 5-ml sample of cells was taken from a culture at days 1, 2 and 4. A 10- μ l aliquot of the sample was diluted in order to determine the total number of cells using a hemacytometer. An aliquot of the culture containing the total of 4×10^7 cells was subjected to centrifugation for 3 min at $16,000 \times g$ at room temperature. The pellet of cells was then resuspended in 4 ml of YP medium supplemented with 0.2% or 2% glucose. Cell suspension was divided into four 1-ml aliquots, and 10- μ l aliquots of a serially diluted stock solution of 30% hydrogen peroxide in MilliQ water were added to the indicated final concentrations ranging from 0.1 to 20 mM. A control aliquot of cells was supplemented with 10 μ l of MilliQ water. Cells were incubated for 2 h at 30°C on a Labquake tube shaker/rotator. A 100 μ l-aliquot of each sample was serially diluted in 10-fold steps. To determine cell viability by plate assay, a 100 μ l-aliquot of each dilution was plated in duplicate onto YP plates containing 2% glucose as carbon source. After 2 d of incubation at 30°C, the number of colony forming units (CFU) per plate was counted. The number of CFU was defined as the number of viable cells in a sample. For each culture, the percentage of viable cells was calculated as follows: (number of viable cells per ml/ 10^7 [*i.e.*, the total number of cells per ml]) \times 100. The percentage of viable cells in a control cell aliquot, which was supplemented with 10 μ l of MilliQ water, was set at 100%.

Cell viability assay for monitoring the susceptibility of yeast to a necrotic mode of cell death induced by palmitoleic acid

Cells were cultured in YP medium initially containing 0.2% or 2% glucose. A 5-ml sample of cells was taken from a culture at days 1, 2 and 4. A 10- μ l aliquot of the sample was diluted in order to determine the total number of cells using a hemacytometer. An aliquot of the culture containing the total of 4×10^7 cells was subjected to centrifugation for 3 min at $16,000 \times g$ at room temperature. The pellet of cells was then resuspended in 4 ml of YP medium supplemented with 0.2% or 2% glucose. Cell suspension was divided into four 1-ml aliquots, and 10- μ l aliquots of a serially diluted stock solution of 50 mM palmitoleic acid in a Chloroform/Hexane/Ethanol (1:4.5:4.5) mix were added to the indicated final concentrations ranging from 0.05 to 0.8 mM. A control aliquot of cells was supplemented with 10 μ l of the Chloroform/Hexane/Ethanol (1:4.5:4.5) mix. Cells were incubated for 2 h at 30°C on a Labquake tube shaker/rotator. A 100 μ l-aliquot of each sample was serially diluted in 10-fold steps. To determine cell viability by plate assay, a 100 μ l-aliquot of each dilution was plated in duplicate onto YP plates containing 2% glucose as carbon source. After 2 d of incubation at 30°C, the number of colony forming units (CFU) per plate was counted. The number of CFU was defined as the number of viable cells in a sample. For each culture, the percentage of viable cells was calculated as follows: (number of viable cells per ml/ 10^7 [*i.e.*, the total number of cells per ml]) \times 100. The percentage of viable cells in a control cell aliquot, which was supplemented with 10 μ l of the Chloroform/Hexane/Ethanol (1:4.5:4.5) mix, was set at 100%.

DAPI staining for visualizing nuclei

An aliquot containing the total of 10^7 cells was subjected to centrifugation for 1 min at $16,000 \times g$ at room temperature. Cells were washed twice in a PBS buffer (20 mM $\text{KH}_2\text{PO}_4/\text{KOH}$, pH 7.5; 150 mM NaCl), each time by re-suspending the cell pellet in the buffer and harvesting cells by centrifugation for 1 min at $16,000 \times g$ at room temperature. The pellet of cells was resuspended in 250 μl of the PBS buffer. Cell suspension was supplemented with 12.5 μl of a stock solution of 0.1 mg/ml DAPI in PBS to the final concentration of 5 $\mu\text{g}/\text{ml}$ DAPI. Samples were incubated in the dark for 10 min at room temperature. Cells were washed 5 times in PBS, each time by re-suspending the cell pellet in the buffer and harvesting cells by centrifugation for 1 min at $16,000 \times g$ at room temperature. The pellet of washed cells was resuspended in 20 μl of the PBS buffer. Cells were analyzed by fluorescence microscopy. Images were collected with a Zeiss Axioplan fluorescence microscope (Zeiss) mounted with a SPOT Insight 2 megapixel color mosaic digital camera (Spot Diagnostic Instruments). For evaluating the percentage of cells with fragmented nucleus the UTHSCSA Image Tool (Version 3.0) software was used to calculate both the total number of cells and the number of stained cells or cells with fragmented nucleus. In each of 2-5 independent experiments, the percentage of cells with fragmented nuclei was calculated by analyzing at least 500 cells.

Statistical analysis

Statistical analysis was performed using Microsoft Excel's (2010) Analysis ToolPack-VBA. All data are presented as mean \pm SEM. The p values were calculated using an unpaired two-tailed t test.

8.4 Results

8.4.1 Mitophagy is a longevity assurance process

As the first step towards addressing a possible role of selective macroautophagic mitochondrial removal in sustaining essential biological processes, we evaluated the importance of mitophagy in longevity assurance in the yeast *Saccharomyces cerevisiae*. We compared the chronological lifespan of the single-gene-deletion mutant strain *atg32Δ*, which is impaired only in the mitophagic pathway of selective macroautophagy [376, 377], to that of wild-type (WT) strain. *atg32Δ* lacks a mitochondrial outer membrane protein Atg32p whose binding to an adaptor protein Atg11p drives the recruitment of mitochondria to the phagophore assembly site, thereby initiating the mitophagy process [376, 377]. We assessed the importance of mitophagy in longevity assurance in chronologically aging yeast grown in the nutrient-rich YP medium either under lifespan-extending caloric restriction (CR) conditions on 0.2% glucose or under lifespan-shortening non-CR conditions on 2% glucose [32, 40]. We found that the *atg32Δ* mutation substantially shortens both the mean and maximum chronological lifespans of yeast not only under CR at 0.2% glucose (Figure 8.1) but also under non-CR conditions administered by culturing cells in medium initially containing 2% glucose (unpublished data; a personal communication from Alejandra Gomez-Perez in our laboratory). We therefore concluded that under both CR and non-CR conditions mitophagy is an essential longevity assurance process.

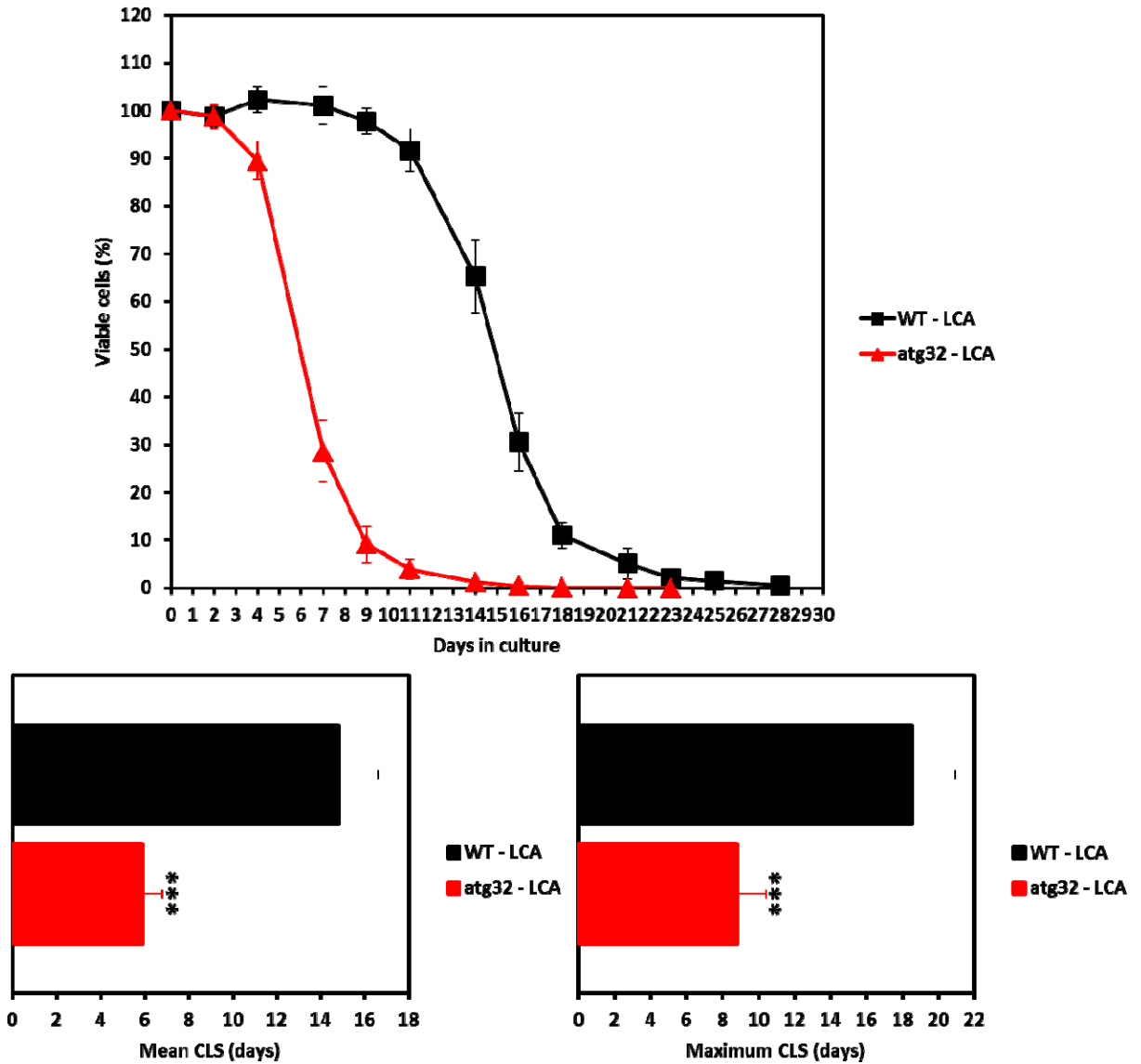


Figure 8.1. Under CR conditions, the *atg32Δ*-dependent mutational block of mitophagy substantially shortens both the mean and maximum chronological life spans (CLS) of yeast. Wild-type (WT) and *atg32Δ* strains were cultured in YP medium initially containing 0.2% glucose. Data are presented as means \pm SEM (n = 4; ***p < 0.001).

8.4.2 Mitophagy is required for longevity extension by an anti-aging compound

In a recent study, we found that lithocholic acid (LCA), a bile acid, greatly increases the chronological lifespan of yeast grown under CR and non-CR conditions

[40]. To assess a role of selective macroautophagic mitochondrial removal in longevity extension by LCA, we tested if this bile acid added to growth medium at the time of cell inoculation is able to extend longevity of the mitophagy-deficient *atg32Δ* mutant. As we found, the *atg32Δ* mutation abolishes the ability of LCA to increase both the mean and maximum chronological lifespans of yeast not only under CR at 0.2% glucose (Figure 8.2) but also under non-CR conditions on 2% glucose (unpublished data; a personal communication from Alejandra Gomez-Perez in our laboratory). Thus, mitophagy is essential for the ability of LCA to extend longevity of chronologically aging yeast.

8.4.3 Mitophagy is essential for maintaining functional mitochondria

A decline in mitochondrial function is a common feature of aging cells and one of the driving forces in cellular and organismal aging [378]. The age-related mitochondrial dysfunction is manifested in reduced respiration, which not only causes a decline in the mitochondrial membrane potential ($\Delta\Psi$) and ATP synthesis but also leads to the excessive production of reactive oxygen species (ROS) known to be generated mainly in mitochondria [379]. The gradual, age-related increase in mitochondrial ROS production elicits the progressive oxidative damage to mitochondrial DNA, proteins and lipids – thereby driving a “vicious cycle” accelerating a self-perpetuating decline in mitochondrial function and eventually leading to mitochondrial outer membrane permeabilization (MOMP), permeability transition pore complex (PTPC) activation and the resulting mitochondrial permeability transition (MPT). By promoting the release of soluble mitochondrial membrane proteins and $\Delta\Psi$ dissipation, MOMP and MPT drive apoptotic and necrotic cell death [378, 380]. By removing dysfunctional mitochondria

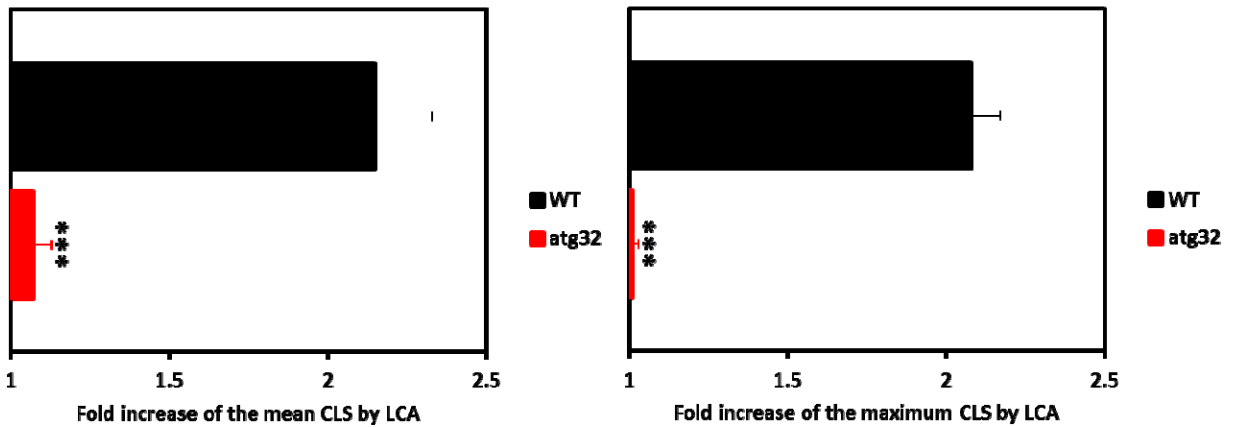
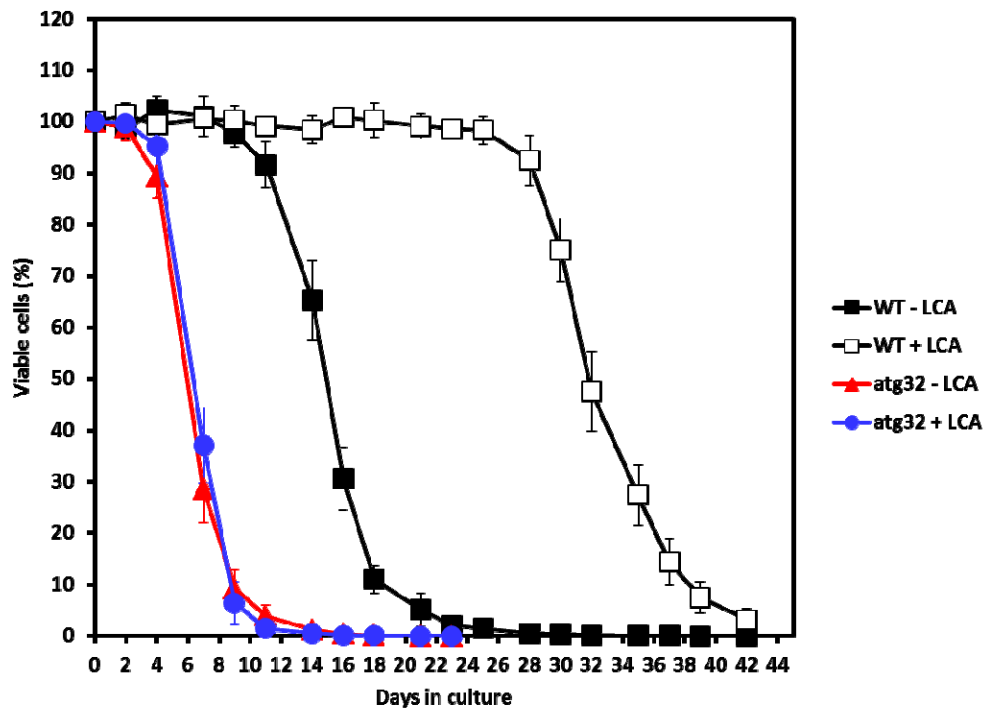


Figure 8.2. Under CR conditions, the *atg32Δ*-dependent mutational block of mitophagy abolishes the ability of LCA to increase both the mean and maximum chronological lifespans (CLS) of yeast. Wild-type (WT) and *atg32Δ* strains were cultured in YP medium initially containing 0.2% glucose in the presence or absence of 50 μ M LCA. Data are presented as means \pm SEM (n = 4; ***p < 0.001).

before this cycle of events can cause cell death, mitophagy has been hypothesized to function as a mitochondrial quality control mechanism having an essential cytoprotective

role that decelerates cellular and organismal aging [378, 381]. Our finding that mitophagy is a longevity assurance process provides the first, to our best knowledge, experimental confirmation of such a hypothesis. In addition, this our finding suggests that a deficiency in selective macroautophagic mitochondrial removal may result in accumulation of dysfunctional mitochondria displaying reduced respiration, declined $\Delta\Psi$ and excessive ROS production. To evaluate the validity of this suggestion, we compared the rate of oxygen consumption (a process of cellular respiration confined mainly to mitochondria) by prematurely aging *atg32Δ* cells to that by WT cells. We found that under both CR and non-CR conditions the rate of oxygen consumption by chronologically aging WT cells was 1) significantly increased when these cells entered diauxic (D) growth phase; and 2) gradually declined through the following post-diauxic (PD) and stationary (ST) growth phases (Figure 8.3; unpublished data for non-CR conditions are not shown [a personal communication from Alejandra Gomez-Perez in our laboratory]). Although prematurely aging *atg32Δ* cells exhibited a similar to WT cells amplitude of the increase in oxygen consumption by mitochondria upon entry into D growth phase, they displayed a greatly accelerated (as compared to WT cells) decline in the rate of mitochondrial oxygen consumption during the subsequent PD phase (Figure 8.3). This trend of the *atg32Δ* mutation has been observed under both CR (Figure 8.3) and non-CR (unpublished data; a personal communication from Alejandra Gomez-Perez in our laboratory) conditions. Thus, the *atg32Δ*-dependent mutational block of mitophagy indeed leads to accumulation of dysfunctional mitochondria displaying reduced respiration.

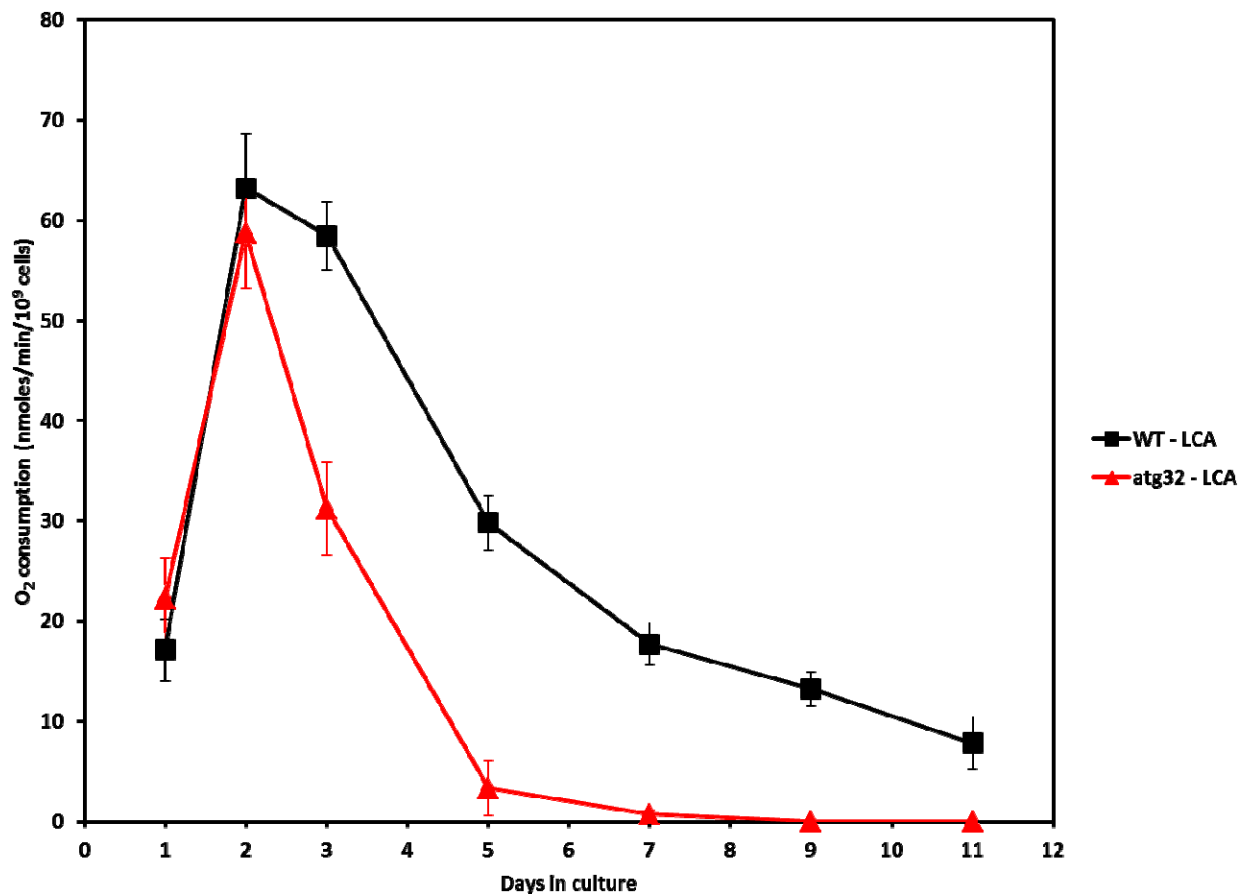


Figure 8.3. Under CR conditions, the *atg32Δ*-dependent mutational block of mitophagy leads to accumulation of dysfunctional mitochondria displaying reduced respiration. WT and *atg32Δ* strains were cultured in medium initially containing 0.2% glucose. Data are presented as means \pm SEM (n = 6).

Recent unpublished findings from our laboratory imply that mitochondria in prematurely aging *atg32Δ* cells also exhibit declined $\Delta\Psi$ and produce excessive levels of ROS (unpublished data; a personal communication from Alejandra Gomez-Perez in our laboratory). We therefore concluded that in chronologically aging yeast mitophagy is

essential for maintaining functional mitochondria both under lifespan-extending CR conditions and under lifespan-shortening non-CR conditions.

Furthermore, our finding that mitophagy is essential for the ability of LCA to extend longevity of chronologically aging yeast suggests that a deficiency in selective macroautophagic mitochondrial removal may alter the previously described effects of this bile acid [40] on mitochondrial respiration, $\Delta\Psi$ and/or ROS. We found that under both CR and non-CR conditions the rate of oxygen consumption by chronologically aging WT cells exposed to LCA 1) was increased to a much lesser extent during D growth phase than it was in WT cells not exposed to this bile acid; and 2) reached a plateau in late PD growth phase and remained mainly uncharged during the following ST growth phase (Figure 8.4; unpublished data for non-CR conditions are not shown [a personal communication from Alejandra Gomez-Perez in our laboratory]). In contrast, LCA had no significant effect on oxygen consumption by mitochondria in prematurely aging *atg32Δ* cells impaired in mitophagy (Figure 8.4). This trend of the *atg32Δ* mutation has been observed under both CR (Figure 8.4) and non-CR conditions. Recent unpublished findings from our laboratory imply that the *atg32Δ* mutation abolishes the ability of LCA to alter the age-related dynamics of changes in $\Delta\Psi$ and ROS (a personal communication from Alejandra Gomez-Perez). We therefore concluded that in chronologically aging yeast mitophagy is mandatory for the ability of LCA to cause longevity-increasing changes in mitochondrial respiration, $\Delta\Psi$ and ROS both under lifespan-extending CR conditions and under lifespan-shortening non-CR conditions.

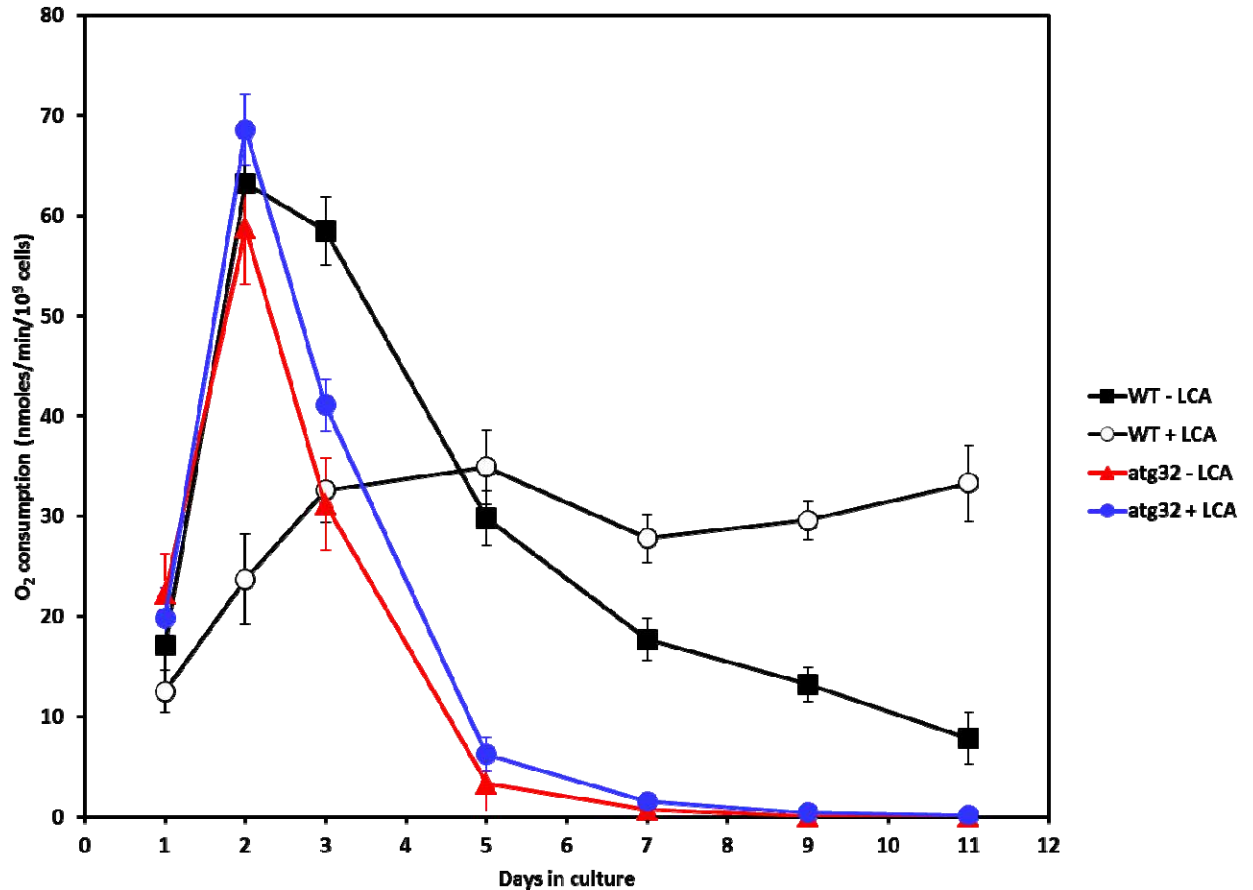


Figure 8.4. Under CR conditions, the *atg32Δ*-dependent mutational block of mitophagy abolishes the ability of LCA to cause longevity-increasing changes in mitochondrial respiration. Wild-type (WT) and *atg32Δ* strains were cultured in YP medium initially containing 0.2% glucose in the presence or absence of 50 μ M LCA. Data are presented as means \pm SEM (n = 6).

8.4.4 Mitophagy protects yeast cells from mitochondria-controlled apoptotic death caused by exogenous hydrogen peroxide

A short-term exposure to exogenous hydrogen peroxide has been shown to cause mitochondria-controlled apoptotic death of yeast cells [382 - 384]. As we mentioned above, by removing dysfunctional mitochondria before the “vicious cycle” of events accelerating a self-perpetuating decline in mitochondrial function can cause cell death,

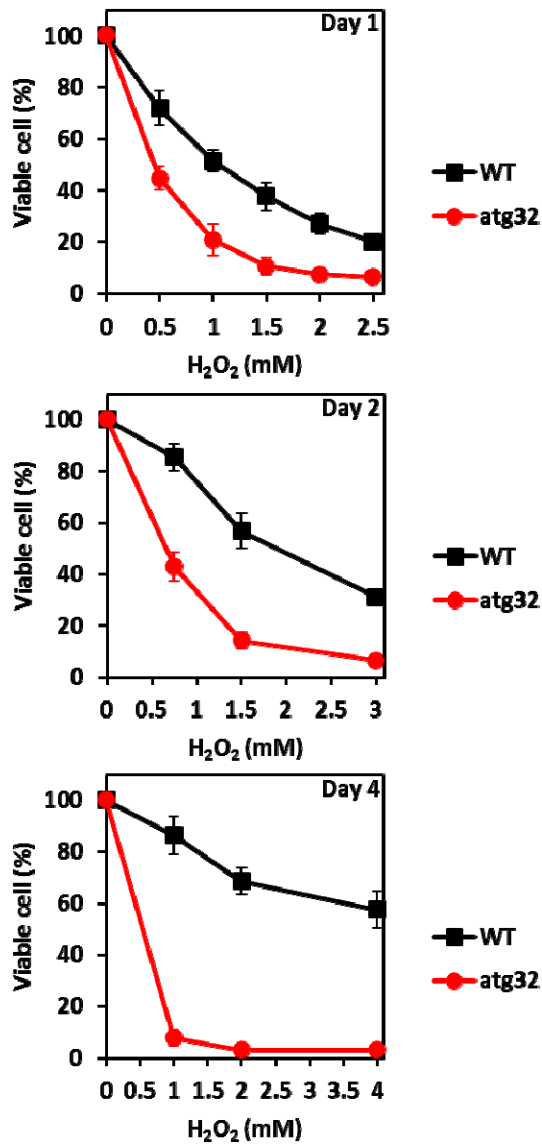


Figure 8.5. Under CR conditions, the *atg32Δ* mutation significantly enhances susceptibility of yeast to apoptotic cell death triggered by a brief exposure to exogenous hydrogen peroxide. Wild-type (WT) and *atg32Δ* strains were cultured in YP medium initially containing 0.2% glucose. Cells recovered at days 1, 2 and 4 were exposed for 2 h to various concentrations of exogenous hydrogen peroxide. Data are presented as means ± SEM (n = 3).

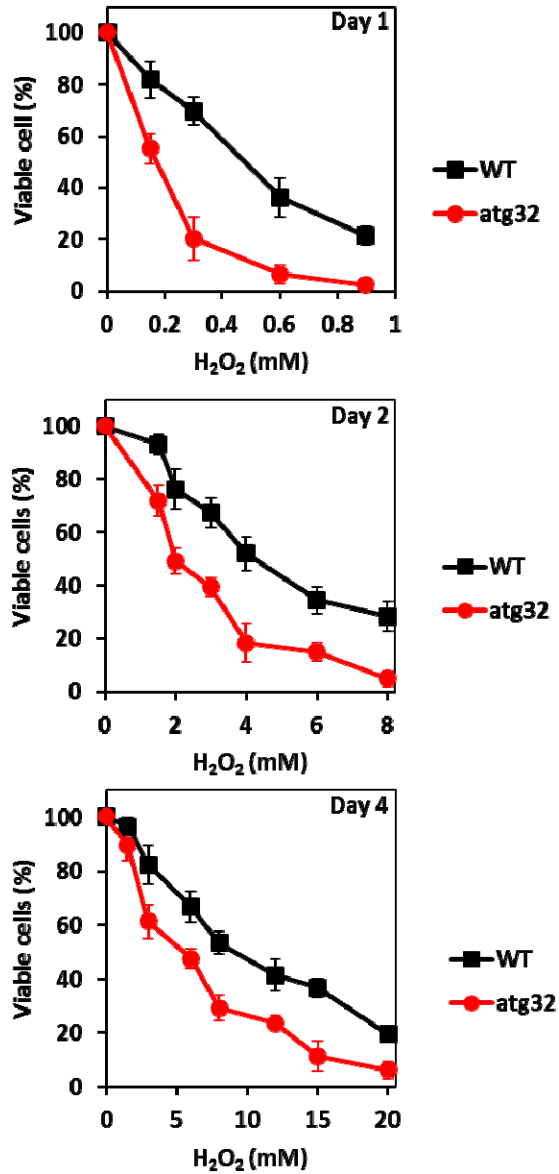


Figure 8.6. Under non-CR conditions, the *atg32Δ* mutation significantly enhances susceptibility of yeast to apoptotic cell death triggered by a brief exposure to exogenous hydrogen peroxide. Wild-type (WT) and *atg32Δ* strains were cultured in YP medium initially containing 2% glucose. Cells recovered at days 1, 2 and 4 were exposed for 2 h to various concentrations of exogenous hydrogen peroxide. Data are presented as means \pm SEM (n = 3).

mitophagy is believed to function as a mitochondrial quality control mechanism that decelerates cellular and organismal aging by preventing apoptotic and necrotic cell death [378, 381]. Our finding that in chronologically aging yeast mitophagy is essential for maintaining functional mitochondria prompted us to investigate if selective macroautophagic mitochondrial removal could protect yeast from mitochondria-controlled apoptotic death caused by exogenous hydrogen peroxide. We revealed that under both CR and non-CR conditions the *atg32Δ* mutation significantly enhances cell susceptibility to apoptotic cell death triggered by a short-term, 2-h exposure to exogenous hydrogen peroxide (Figures 8.5 and 8.6). Thus, by removing dysfunctional mitochondria, mitophagy protects yeast cells from mitochondria-controlled apoptotic death caused by exogenous hydrogen peroxide.

8.4.5 Mitophagy protects yeast from a mode of cell death triggered by exposure to palmitoleic fatty acid

A brief exposure of yeast cells to exogenous palmitoleic fatty acid has been shown to cause their death [40]. Noteworthy, the *pex5Δ* mutation previously known only for its ability to impair peroxisomal fatty acid oxidation [243] recently has been demonstrated not only to greatly reduce mitochondrial respiration and $\Delta\Psi$ but also to enhance the susceptibility of yeast to a mode of cell death elicited by a short-term exposure to exogenous palmitoleic acid [40]. We therefore decided to investigate if selective macroautophagic mitochondrial removal could protect yeast from this form of cell death. We found that under both CR and non-CR conditions the *atg32Δ* mutation significantly enhances cell susceptibility to cell death elicited by a brief, 2-h exposure to

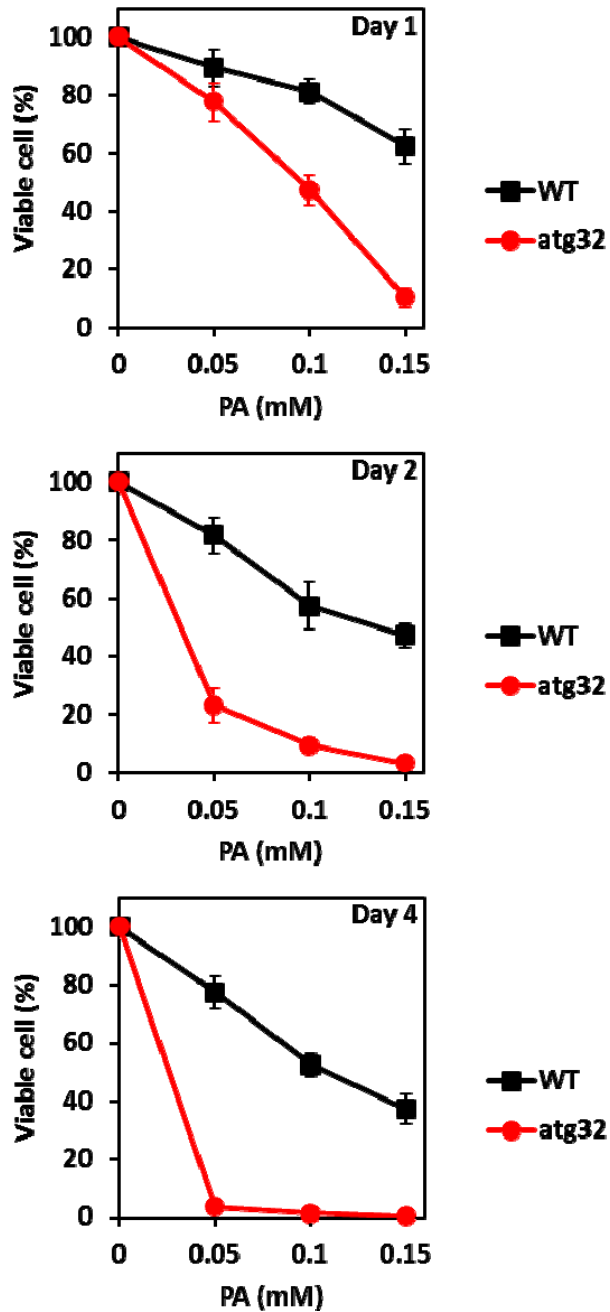


Figure 8.7. Under CR conditions, the *atg32Δ* mutation significantly enhances susceptibility of yeast to apoptotic cell death triggered by a brief exposure to exogenous palmitoleic fatty acid. Wild-type (WT) and *atg32Δ* strains were cultured in YP medium initially containing 0.2% glucose. Cells recovered at days 1, 2 and 4 were exposed for 2 h to various concentrations of exogenous palmitoleic acid. Data are presented as means \pm SEM (n = 4).

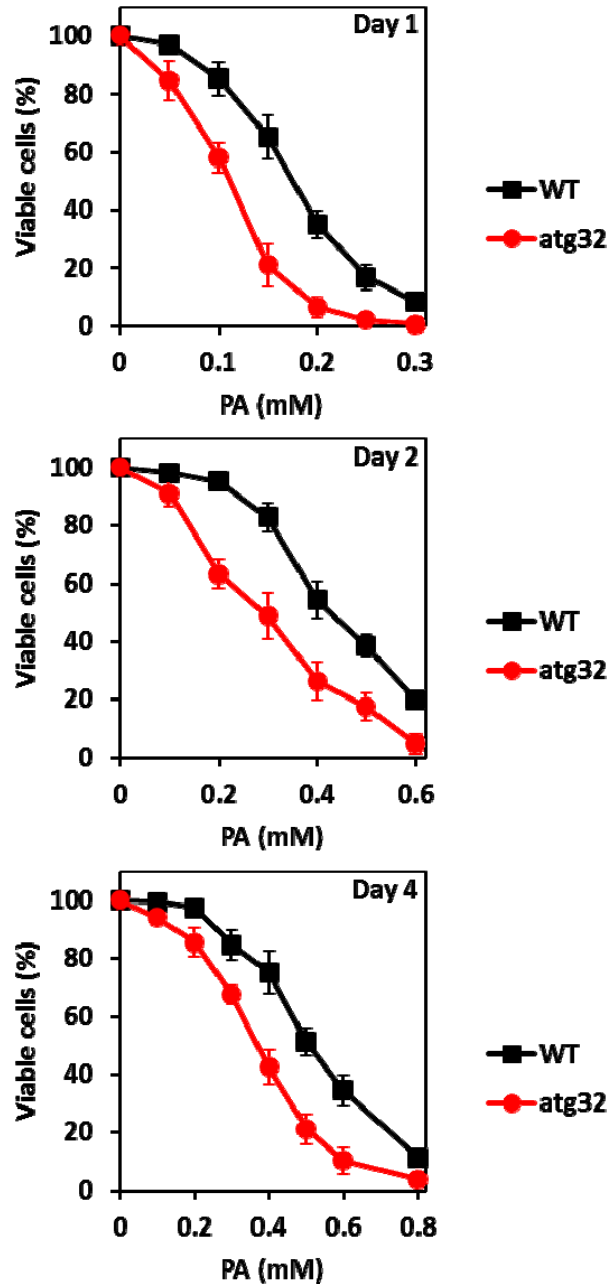


Figure 8.8. Under non-CR conditions, the *atg32Δ* mutation significantly enhances susceptibility of yeast to apoptotic cell death triggered by a brief exposure to exogenous palmitoleic fatty acid. Wild-type (WT) and *atg32Δ* strains were cultured in YP medium initially containing 2% glucose. Cells recovered at days 1, 2 and 4 were exposed for 2 h to various concentrations of exogenous palmitoleic acid. Data are presented as means \pm SEM (n = 4).

exogenous palmitoleic acid (Figures 8.7 and 8.8). Hence, by removing dysfunctional mitochondria, mitophagy protects yeast from a mode of cell death triggered by this fatty acid.

8.4.6 Microscopical analyses confirm the essential role of mitophagy in protecting yeast from mitochondria-controlled apoptotic cell death

Based on our finding that the *atg32Δ* mutation significantly enhances the susceptibility of yeast to apoptotic cell death triggered by a short-term exposure to exogenous hydrogen peroxide (see above), we concluded that selective macroautophagic mitochondrial removal protects yeast from this mitochondria-controlled mode of death. Our electron microscopical (EM) analysis of WT and *atg32Δ* cells treated with various concentration of exogenously added hydrogen peroxide confirmed the validity of this conclusion. Following their 2-h exposure to this oxidant, pre-grown under CR conditions and recovered at day 1 cells of both WT and *atg32Δ* exhibited nuclear fragmentation (Figure 8.9A), a characteristic marker of the mitochondria-controlled apoptotic mode of cell death [385, 386] (A similar trend was observed for WT and *atg32Δ* cells pre-grown under CR conditions and recovered at days 2 and 4 for a 2-h exposure to various concentrations of exogenous hydrogen peroxide; data not shown). It should be stressed that, although the percentage of cells displaying this hallmark of apoptotic death was proportional to the concentration of exogenous hydrogen peroxide for both strains, the *atg32Δ* mutation significantly increased the fraction of such cells (Figure 8.9B). Recent fluorescence microscopical analyses of pre-grown under CR conditions yeast exposed for 2 h to hydrogen peroxide revealed that the *atg32Δ* mutation also significantly increases

the percentage of cells exhibiting other characteristic markers of apoptosis, including phosphatidylserine translocation from the inner to the outer leaflet of the plasma membrane and cleavage of chromosomal DNA (unpublished data; a personal communication from Alejandra Gomez-Perez in our laboratory). In sum, these microscopical analyses provide further confirmation of the essential role of mitophagy in protecting yeast from mitochondria-controlled apoptotic cell death.

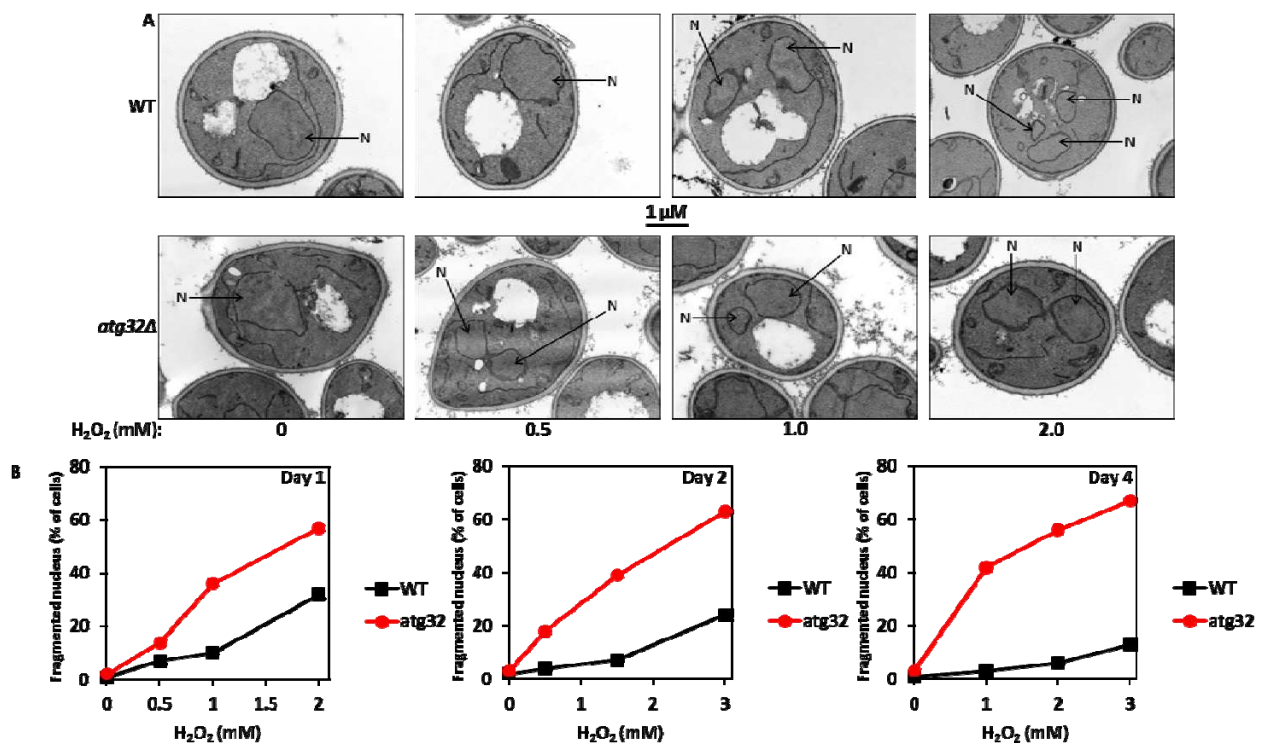


Figure 8.9. Under CR conditions, the *atg32Δ* mutation significantly increases the percentage of cells exhibiting nuclear fragmentation, a characteristic marker of the mitochondria-controlled apoptotic mode of cell death. (A) Transmission electron micrographs of wild-type (WT) and *atg32Δ* cells that were exposed to various concentrations of exogenously added hydrogen peroxide. WT and *atg32Δ* strains were cultured in YP medium initially containing 0.2% glucose. Cells recovered at day 1 were exposed for 2 h to various concentrations of exogenous hydrogen peroxide. (B) The percentage of cells displaying nuclear fragmentation, based on quantitation of transmission electron micrographs some of which are shown in

Figure 8.9A. WT and *atg32Δ* strains were cultured in medium initially containing 0.2% glucose. Cells recovered at days 1, 2 and 4 were exposed for 2 h to various concentrations of exogenous hydrogen peroxide. For each concentration of exogenously added hydrogen peroxide, at least 100 cells of each strain were used. Abbreviation: *N*, nucleus.

8.4.7 EM analysis implies that exogenous palmitoleic fatty acid triggers a necrosis-like “lipoptotic” cell death and confirms the essential role of mitophagy in protecting yeast from this previously unknown mode of death

As we found, the *atg32Δ* mutation significantly enhances the susceptibility of yeast to a mode of cell death elicited by a short-term exposure to exogenous palmitoleic acid (see above). Our finding implies that the macroautophagic removal of dysfunctional mitochondria is mandatory for protecting yeast from this cell death modality. As a first step towards understanding the molecular mechanisms underlying the essential role of mitophagy in enhancing yeast resistance to a cell death mode triggered by exogenous palmitoleic acid, we used EM analysis of WT and *atg32Δ* cells pre-grown under CR conditions and then treated with various concentration of this fatty acid to 1) define morphological traits characteristic of this cell death subroutine; 2) compare these traits to the well-established [385, 386] morphological features of several currently known cell death modalities; and 3) examine how the *atg32Δ*-dependent block of mitophagy affects these traits.

We found that, unlike significant portions of briefly exposed to exogenous hydrogen peroxide WT and *atg32Δ* cells that undergo a mitochondria-controlled apoptotic mode of cell death by displaying such characteristic marker of apoptosis as nuclear fragmentation, only minor fractions of WT and *atg32Δ* cells briefly treated with

various concentrations of palmitoleic acid exhibit this hallmark event of apoptotic cell death (Figure 8.10). Recent fluorescence microscopical analyses revealed that, unlike significant portions of WT and *atg32Δ* cells undergoing apoptosis in response to a short-term exposure to exogenous hydrogen peroxide, only minor fractions of WT and *atg32Δ*

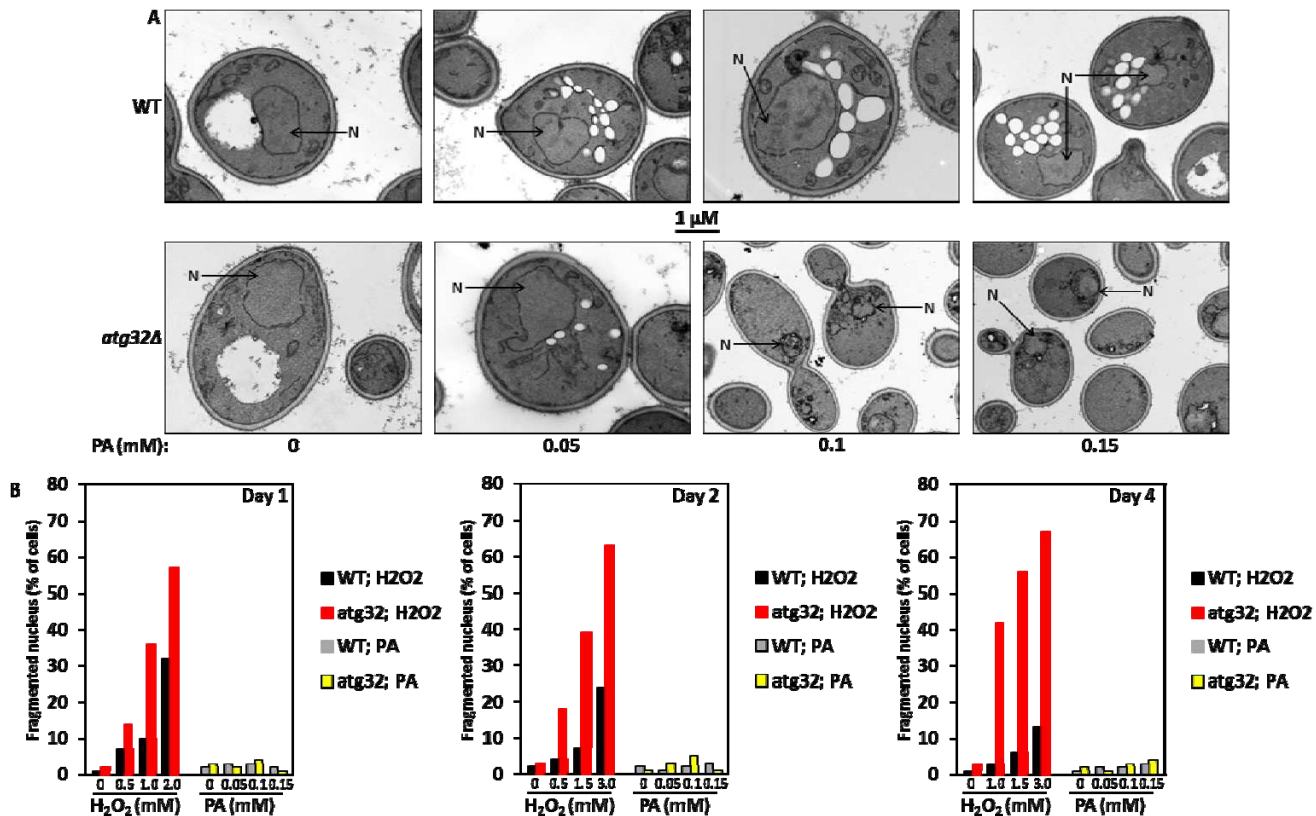


Figure 8.10. Unlike significant portions of briefly exposed to exogenous hydrogen peroxide wild-type (WT) and *atg32Δ* cells that display nuclear fragmentation (Figure 8.9), only minor fractions of WT and *atg32Δ* cells briefly treated with various concentrations of palmitoleic acid (PA) exhibit this hallmark event of apoptotic cell death. (A) Transmission electron micrographs of WT and *atg32Δ* cells that were exposed to various concentrations of exogenously added PA. WT and *atg32Δ* strains were cultured in YP medium initially containing 0.2% glucose. Cells recovered at day 1 were exposed for 2 h to various concentrations of exogenous PA. (B) The percentage of cells displaying nuclear fragmentation, based on quantitation of transmission electron micrographs some of which are shown in Figures 8.9A (for hydrogen peroxide-

treated cells) and 10A (for PA-treated cells). WT and *atg32Δ* strains were cultured in YP medium initially containing 0.2% glucose. Cells recovered at days 1, 2 and 4 were exposed for 2 h to various concentrations of exogenous hydrogen peroxide or PA. For each concentration of exogenously added hydrogen peroxide or PA, at least 100 cells of each strain were used. Abbreviation: *N*, nucleus.

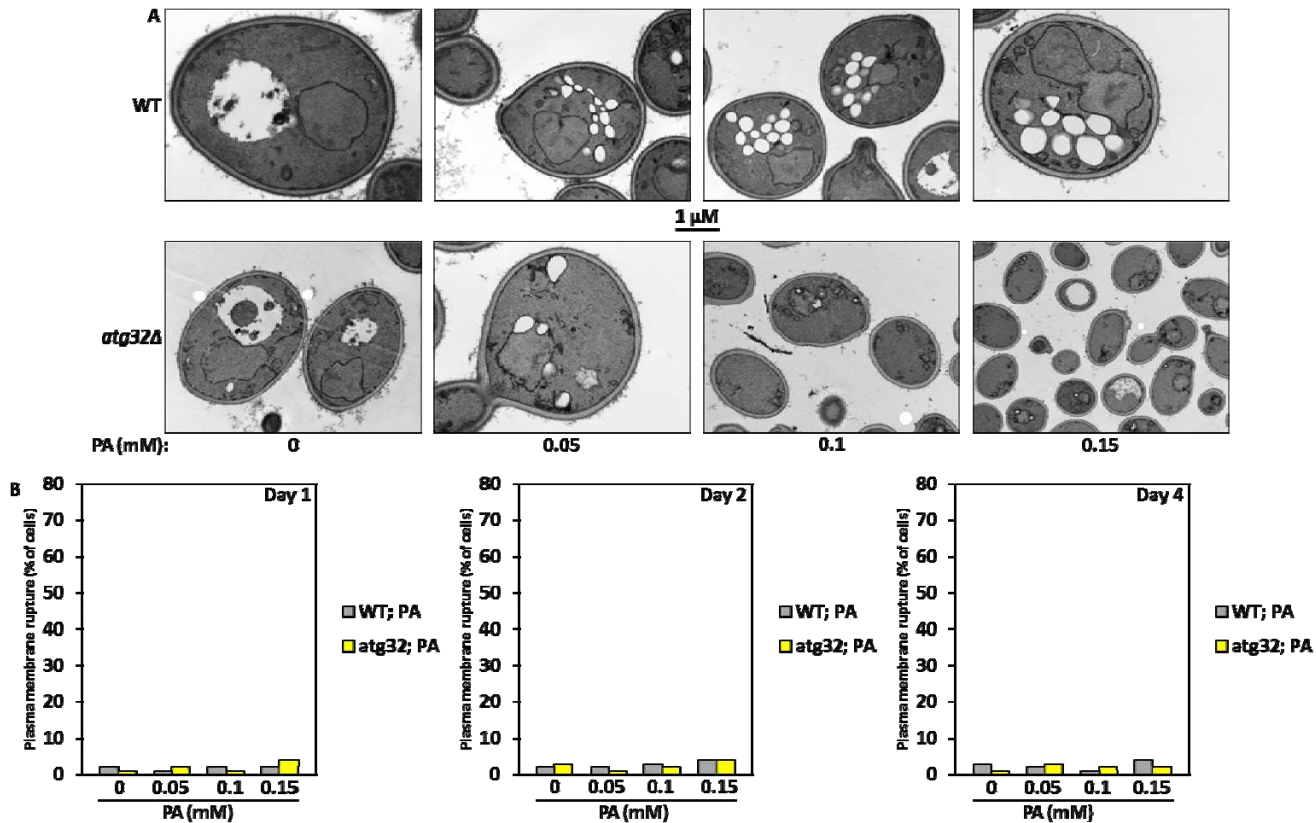


Figure 8.11. Under CR conditions, wild-type (WT) and *atg32Δ* cells briefly treated with various concentrations of palmitoleic acid (PA) do not exhibit such hallmark event of necrotic cell death as plasma membrane rupture. (A) Transmission electron micrographs of WT and *atg32Δ* cells that were exposed to various concentrations of exogenously added PA. WT and *atg32Δ* strains were cultured in YP medium initially containing 0.2% glucose. Cells recovered at day 1 were exposed for 2 h to various concentrations of exogenous PA. (B) The percentage of cells displaying plasma membrane rupture, based on quantitation of transmission electron micrographs some of which are shown in Figures 8.10A and 8.11A. WT and *atg32Δ* strains were cultured in YP medium initially containing 0.2% glucose. Cells recovered at days 1, 2

and 4 were exposed for 2 h to various concentrations of exogenous PA. For each concentration of exogenously added PA, at least 100 cells of each strain were used.

cells briefly treated with various concentrations of palmitoleic acid display such other characteristic markers of apoptotic cell death as phosphatidylserine translocation from the inner to the outer leaflet of the plasma membrane and cleavage of chromosomal DNA (unpublished data; a personal communication from Alejandra Gomez-Perez in our laboratory). Altogether, these microscopical analyses provide evidence that a mode of cell death elicited by a short-term exposure of both WT and *atg32Δ* yeast to exogenous palmitoleic acid is not an apoptotic cell death modality.

Furthermore, our EM analysis revealed that WT and *atg32Δ* cells briefly treated with various concentrations of palmitoleic acid do not exhibit such hallmark event of necrotic cell death [387 - 390] as plasma membrane rupture (Figure 8.11). Thus, a mode of cell death elicited by a short-term exposure of both WT and *atg32Δ* yeast to exogenous palmitoleic acid is not a necrotic cell death modality. However, it should be stressed that fluorescence microscopical analyses show that the vast majority of WT [40] and *atg32Δ* cells (unpublished data; a personal communication from Alejandra Gomez-Perez in our laboratory) briefly exposed to exogenous palmitoleic acid display propidium iodide positive staining. This staining pattern is characteristic of the loss of plasma membrane integrity and considered as a hallmark event of necrotic cell death in yeast [388, 389]. We therefore concluded that exogenously added palmitoleic acid triggers a previously unknown mode of cell death in yeast. We coin the name “lipoptosis” for this novel cell death modality. Although lipoptotic cell death elicited by exposure of yeast to exogenous palmitoleic acid does not lead to plasma membrane rupture (a hallmark event of necrotic

cell death), akin to necrotic cell death modality it results in compromised plasma membrane integrity.

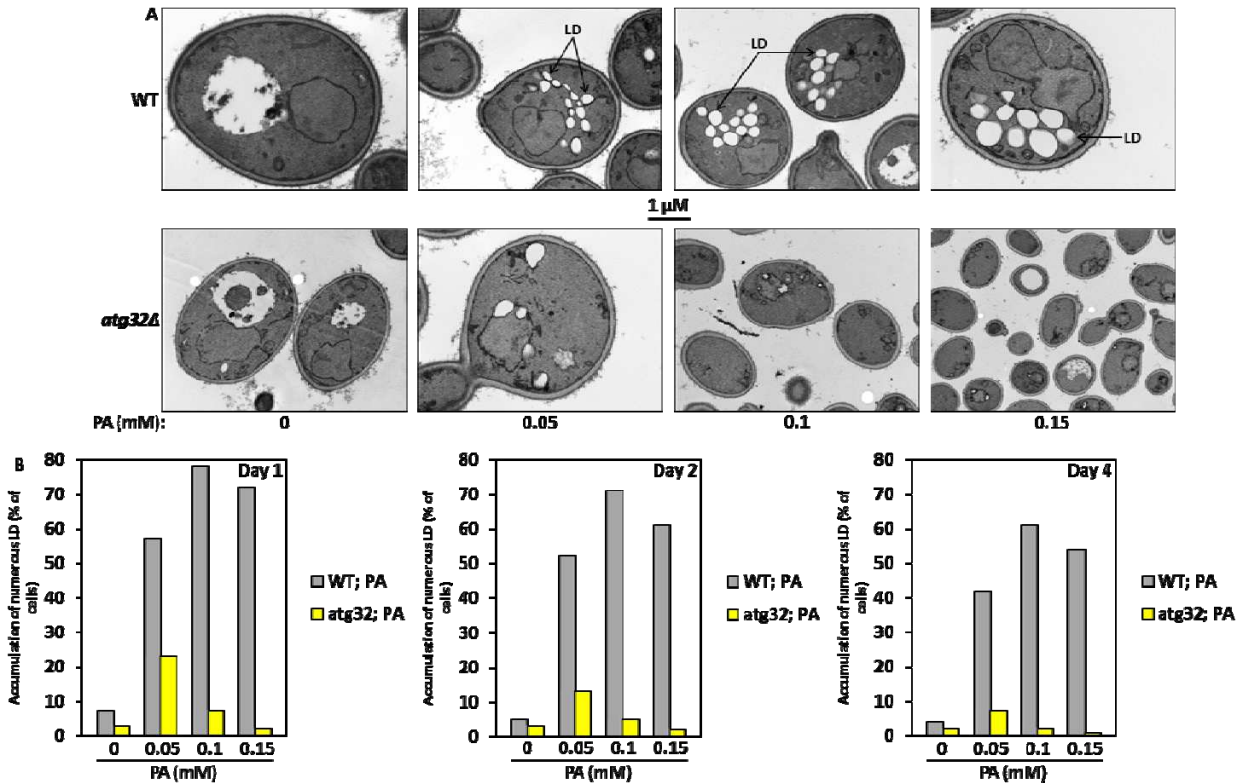


Figure 8.12. Under CR conditions, wild-type (WT) cells briefly treated with various concentrations of palmitoleic acid (PA) exhibit excessive accumulation of lipid droplets (LD), and the *atg32Δ* mutation significantly reduces the fraction of cells that display this feature following PA treatment. (A) Transmission electron micrographs of WT and *atg32Δ* cells that were exposed to various concentrations of exogenously added PA. WT and *atg32Δ* strains were cultured in YP medium initially containing 0.2% glucose. Cells recovered at day 1 were exposed for 2 h to various concentrations of exogenous PA. (B) The percentage of cells displaying excessive accumulation of LD, based on quantitation of transmission electron micrographs some of which are shown in Figures 8.10A and 8.11A. WT and *atg32Δ* strains were cultured in YP medium initially containing 0.2% glucose. Cells recovered at days 1, 2 and 4 were exposed for 2 h to various concentrations of exogenous PA. For each concentration of exogenously added PA, at least 100 cells of each strain were used.

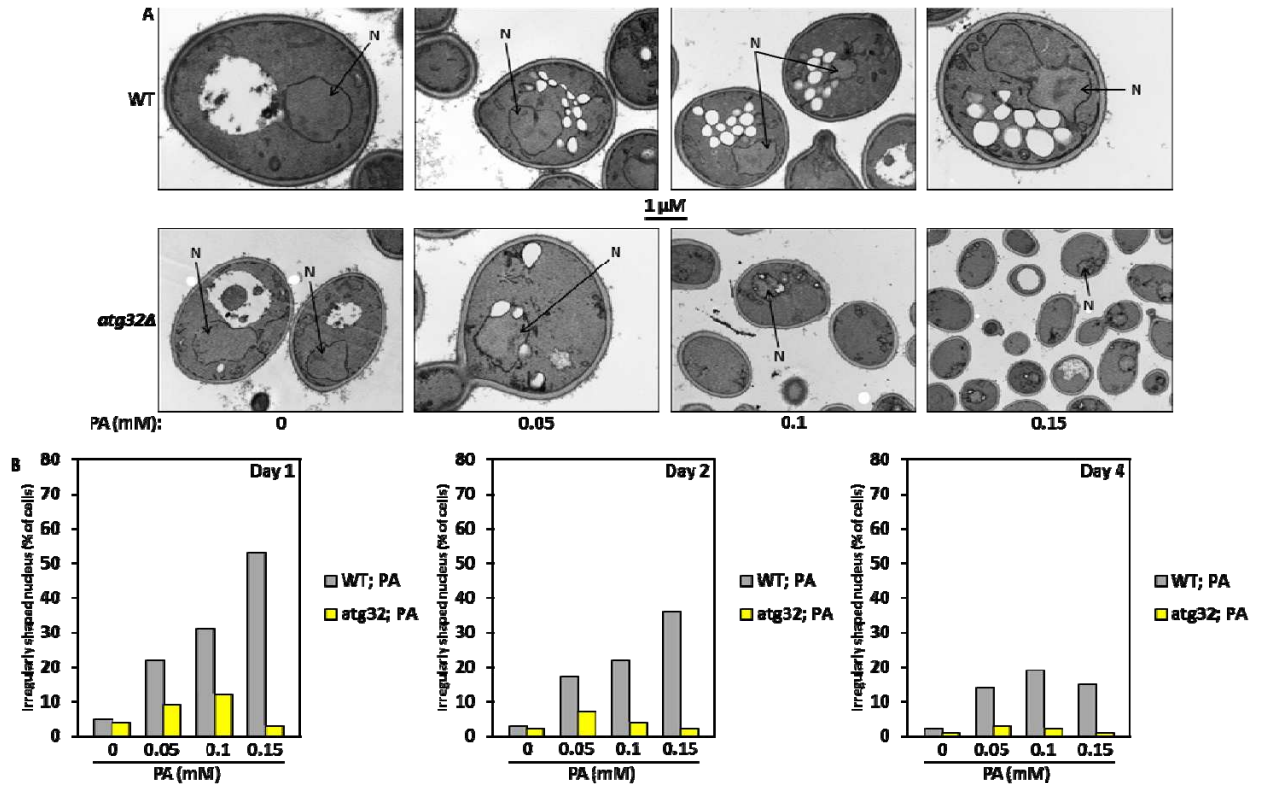


Figure 8.13. Under CR conditions, wild-type (WT) cells briefly treated with various concentrations of palmitoleic acid (PA) exhibit an irregularly shaped nucleus, and the *atg32Δ* mutation significantly reduces the fraction of cells that display this feature following PA treatment. (A) Transmission electron micrographs of WT and *atg32Δ* cells that were exposed to various concentrations of exogenously added PA. WT and *atg32Δ* strains were cultured in YP medium initially containing 0.2% glucose. Cells recovered at day 1 were exposed for 2 h to various concentrations of exogenous PA. (B) The percentage of cells displaying an irregularly shaped nucleus, based on quantitation of transmission electron micrographs some of which are shown in Figures 8.10A and 8.11A. WT and *atg32Δ* strains were cultured in medium initially containing 0.2% glucose. Cells recovered at days 1, 2 and 4 were exposed for 2 h to various concentrations of PA. For each concentration of exogenously added PA, at least 100 cells of each strain were used. Abbreviation: *N*, nucleus.

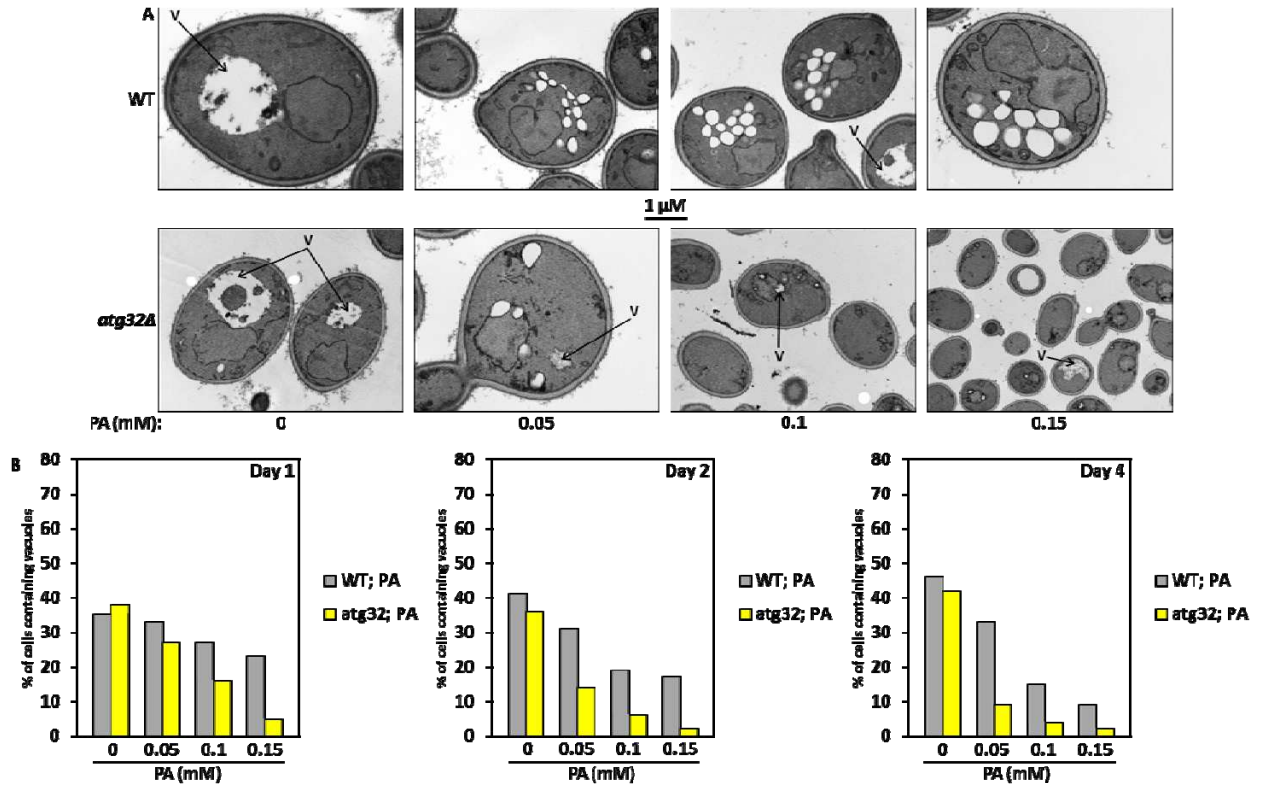


Figure 8.14. Under CR conditions, a short-term exposure of wild-type (WT) strain to various concentrations of palmitoleic acid (PA) reduces the fraction of cells that contain vacuoles, and the *atg32Δ* mutation further decreases the portion of such cells following PA treatment. (A) Transmission electron micrographs of WT and *atg32Δ* cells that were exposed to various concentrations of exogenously added PA. WT and *atg32Δ* strains were cultured in YP medium initially containing 0.2% glucose. Cells recovered at day 1 were exposed for 2 h to various concentrations of exogenous PA. (B) The percentage of cells containing vacuoles, based on quantitation of transmission electron micrographs some of which are shown in Figures 8.10A and 8.11A. WT and *atg32Δ* strains were cultured in YP medium initially containing 0.2% glucose. Cells recovered at days 1, 2 and 4 were exposed for 2 h to various concentrations of exogenous PA. For each concentration of exogenously added PA, at least 100 cells of each strain were used. Abbreviation: *V*, vacuole.

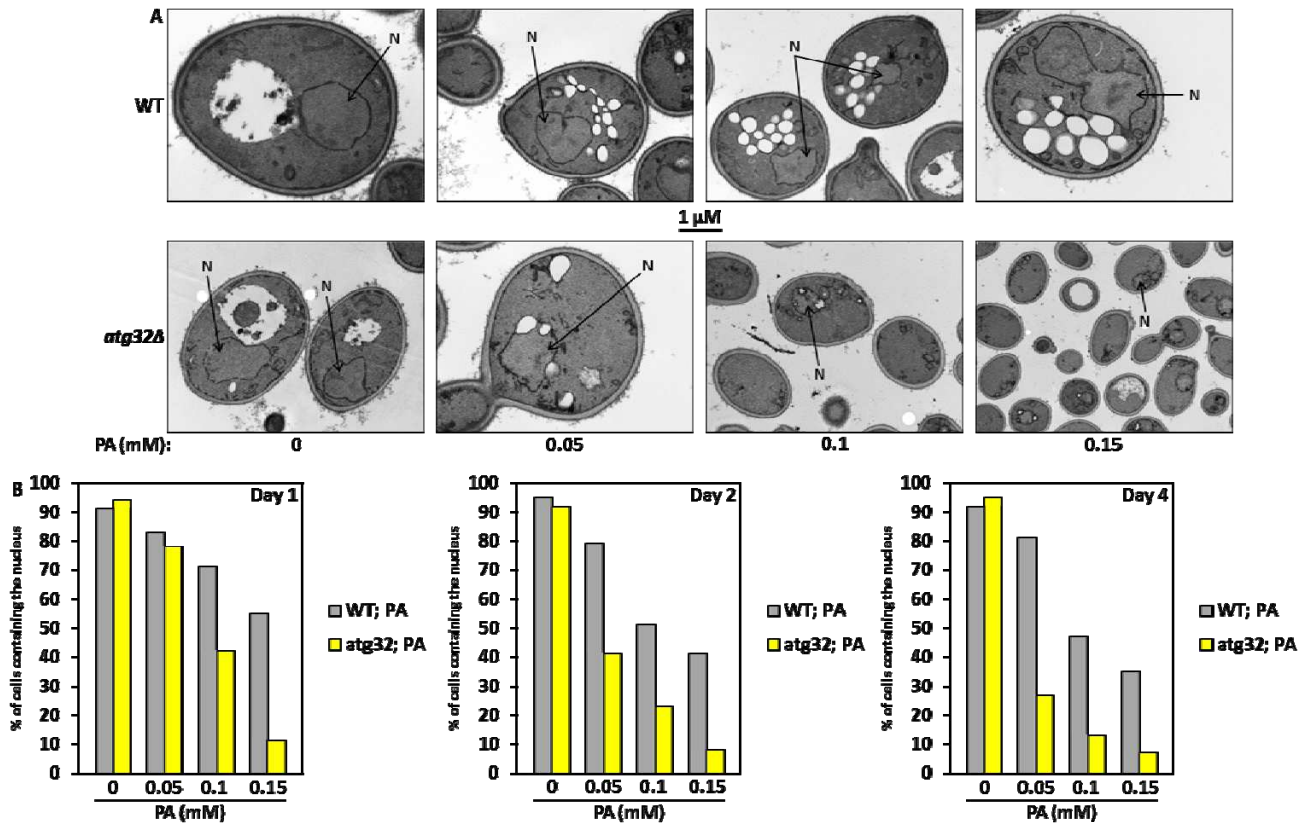


Figure 8.15. Under CR conditions, a short-term exposure of wild-type (WT) strain to various concentrations of palmitoleic acid (PA) reduces the fraction of cells that contain the nucleus, and the *atg32Δ* mutation further decreases the portion of such cells following PA treatment. (A) Transmission electron micrographs of WT and *atg32Δ* cells that were exposed to various concentrations of exogenously added PA. WT and *atg32Δ* strains were cultured in YP medium initially containing 0.2% glucose. Cells recovered at day 1 were exposed for 2 h to various concentrations of exogenous PA. (B) The percentage of cells containing the nucleus, based on quantitation of transmission electron micrographs some of which are shown in Figures 8.10A and 8.11A. WT and *atg32Δ* strains were cultured in medium initially containing 0.2% glucose. Cells recovered at days 1, 2 and 4 were exposed for 2 h to various concentrations of exogenous PA. For each concentration of exogenously added PA, at least 100 cells of each strain were used. Abbreviation: *N*, nucleus.

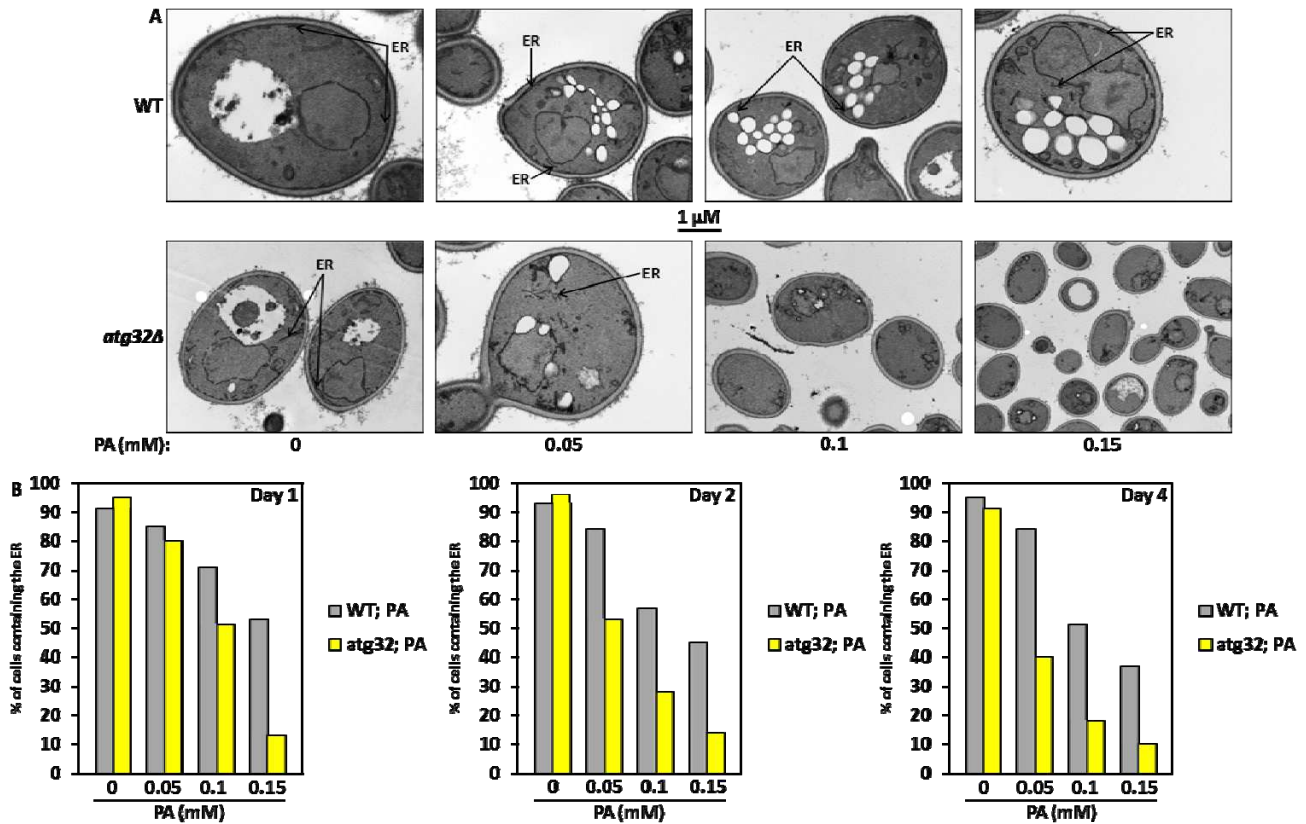


Figure 8.16. Under CR conditions, a short-term exposure of wild-type (WT) strain to various concentrations of palmitoleic acid (PA) reduces the fraction of cells that contain the ER, and the *atg32Δ* mutation further decreases the portion of such cells following PA treatment. (A) Transmission electron micrographs of WT and *atg32Δ* cells that were exposed to various concentrations of exogenously added PA. WT and *atg32Δ* strains were cultured in YP medium initially containing 0.2% glucose. Cells recovered at day 1 were exposed for 2 h to various concentrations of exogenous PA. (B) The percentage of cells containing the ER, based on quantitation of transmission electron micrographs some of which are shown in Figures 8.10A and 8.11A. WT and *atg32Δ* strains were cultured in YP medium initially containing 0.2% glucose. Cells recovered at days 1, 2 and 4 were exposed for 2 h to various concentrations of exogenous PA. For each concentration of exogenously added PA, at least 100 cells of each strain were used. Abbreviation: ER, the endoplasmic reticulum.

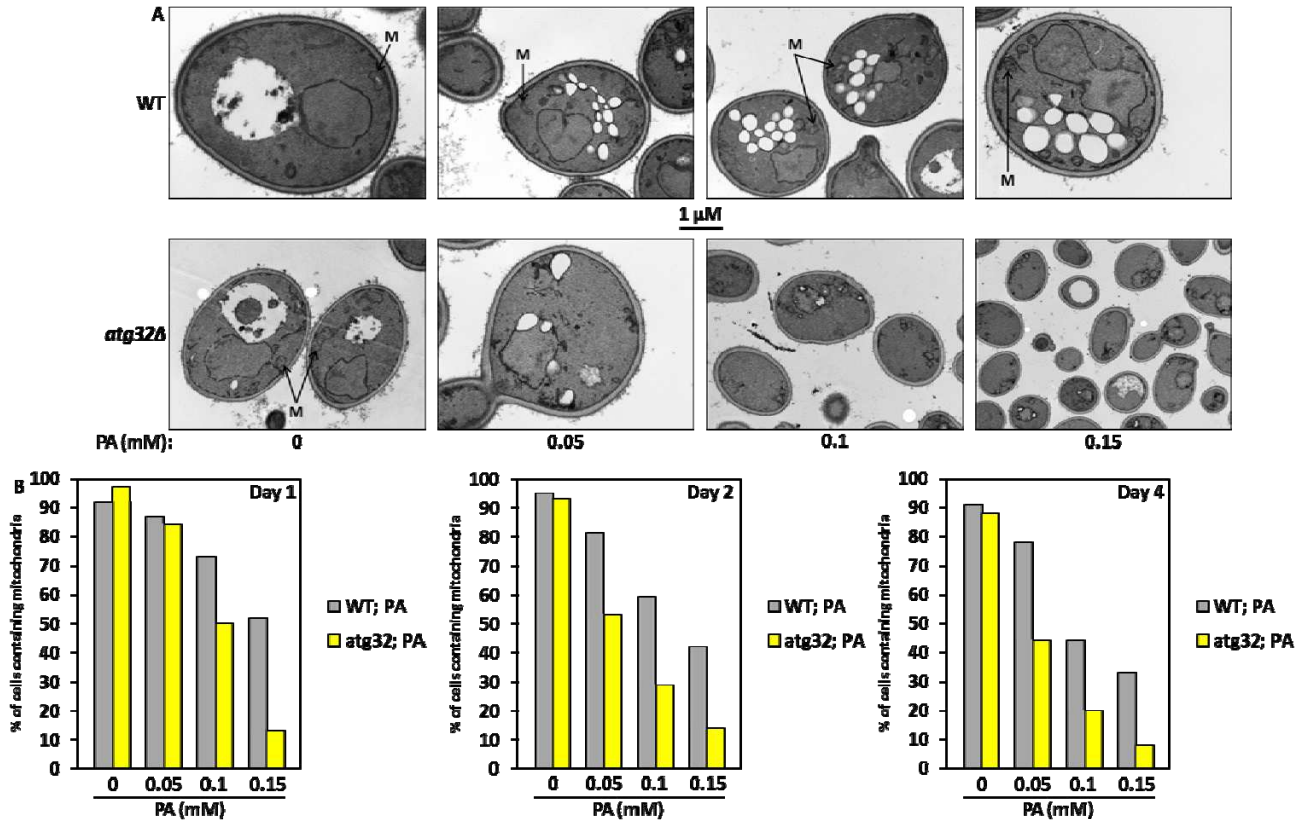


Figure 8.17. Under CR conditions, a short-term exposure of wild-type (WT) strain to various concentrations of palmitoleic acid (PA) reduces the fraction of cells that contain mitochondria, and the *atg32Δ* mutation further decreases the portion of such cells following PA treatment. (A) Transmission electron micrographs of WT and *atg32Δ* cells that were exposed to various concentrations of exogenously added PA. WT and *atg32Δ* strains were cultured in YP medium initially containing 0.2% glucose. Cells recovered at day 1 were exposed for 2 h to various concentrations of exogenous PA. (B) The percentage of cells containing mitochondria, based on quantitation of transmission electron micrographs some of which are shown in Figures 8.10A and 8.11A. WT and *atg32Δ* strains were cultured in YP medium initially containing 0.2% glucose. Cells recovered at days 1, 2 and 4 were exposed for 2 h to various concentrations of exogenous PA. For each concentration of exogenously added PA, at least 100 cells of each strain were used. Abbreviation: *M*, mitochondrion.

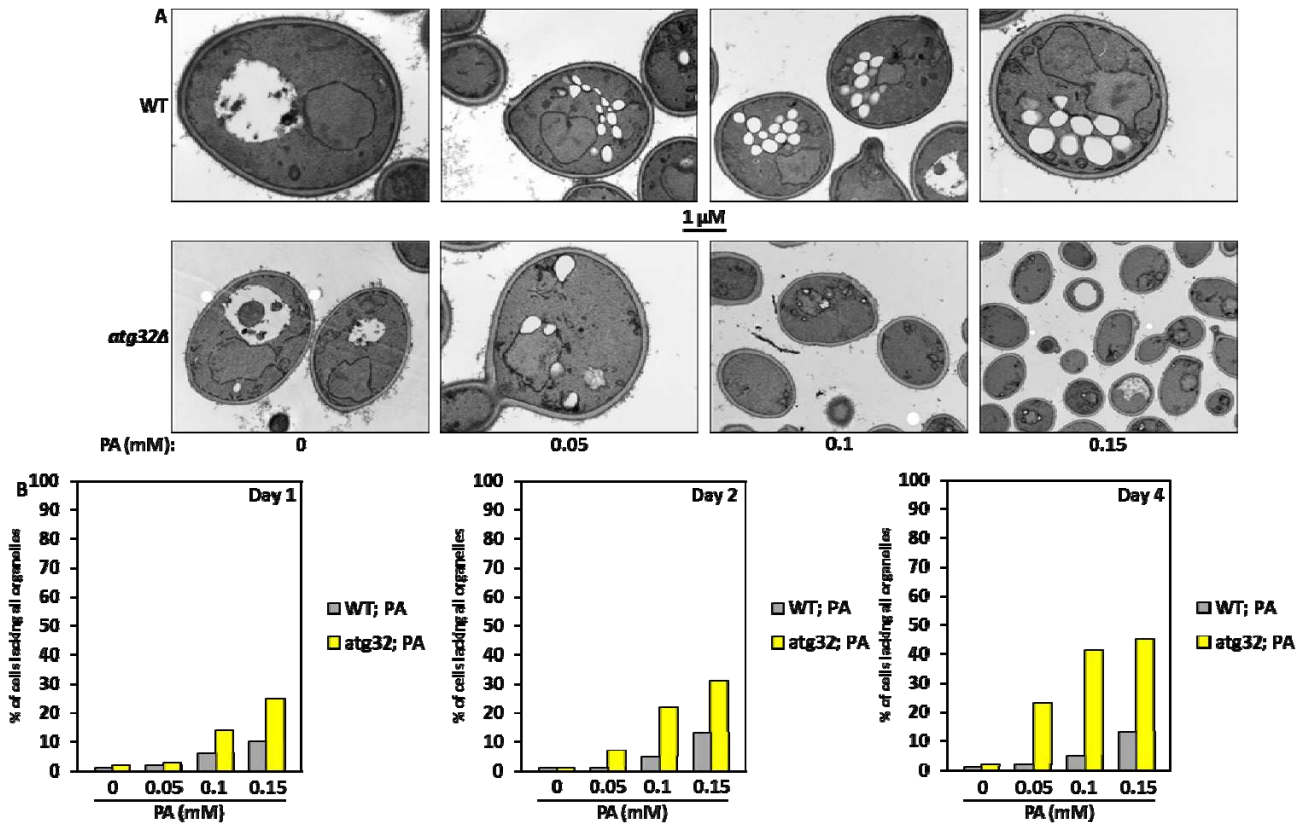


Figure 8.18. Under CR conditions, a short-term exposure of wild-type (WT) strain to various concentrations of palmitoleic acid (PA) increases the fraction of cells lacking all organelles, and the *atg32Δ* mutation further decreases the portion of such cells following PA treatment. (A) Transmission electron micrographs of WT and *atg32Δ* cells that were exposed to various concentrations of exogenously added PA. WT and *atg32Δ* strains were cultured in YP medium initially containing 0.2% glucose. Cells recovered at day 1 were exposed for 2 h to various concentrations of exogenous PA. (B) The percentage of cells lacking all organelles, based on quantitation of transmission electron micrographs some of which are shown in Figures 8.10A and 8.11A. WT and *atg32Δ* strains were cultured in YP medium initially containing 0.2% glucose. Cells recovered at days 1, 2 and 4 were exposed for 2 h to various concentrations of exogenous PA. For each concentration of exogenously added PA, at least 100 cells of each strain were used.

What combination of morphological traits is characteristic of the novel mode of cell death that we identified in yeast? Our EM analysis revealed the following hallmark events of the lipoptotic cell death triggered by a brief exposure of WT yeast to various concentrations of exogenous palmitoleic acid: 1) the excessive accumulation of lipid droplets, a deposition site for stockpiling non-esterified (“free”) fatty acids and sterols in the form of triacylglycerols and ergosteryl esters following their synthesis in the endoplasmic reticulum (ER) (Figure 8.12); 2) an irregularly shaped nucleus (Figure 8.13); 3) a reduced fraction of cells containing vacuoles (Figure 8.14), the nucleus (Figure 8.15), the ER (Figure 8.16) or mitochondria (Figure 8.17); and 4) an increased portion of cells lacking all these organelles (Figure 8.18).

Importantly, our EM analysis revealed that, although the percentage of cells displaying each of these hallmarks of the lipoptotic cell death triggered by a brief exposure of yeast to various concentrations of exogenous palmitoleic acid was proportional to the concentration of palmitoleic acid for both strains, the *atg32Δ* mutation 1) significantly reduced the fraction of cells that accumulate lipid droplets (Figure 8.12) or exhibit irregularly shaped nucleus (Figure 8.13); 2) considerably decreased the portion of cells containing vacuoles (Figure 8.14), the nucleus (Figure 8.15), the ER (Figure 8.16) or mitochondria (Figure 8.17); and 3) substantially increased the portion of cells lacking all these organelles (Figure 8.18).

In sum, the enhanced susceptibility of *atg32Δ* yeast to a mode of cell death elicited by a short-term exposure to exogenous palmitoleic acid and the observed effects of the *atg32Δ* mutation on the morphological traits characteristic of such previously

unknown cell death mode provide evidence of the essential role of mitophagy in protecting yeast from this cell death modality.

8.5 Discussion

Although recent findings in mammals suggest that mitophagy - a selective macroautophagic removal of dysfunctional mitochondria - may operate as an essential mechanism in ensuring quality control of mitochondria and suppressing pathologies caused by mitochondrial dysfunction, the physiological roles of mitophagy in yeast and underlying mechanisms remain to be established. We sought to explore the involvement of mitophagy in regulating yeast longevity, maintaining functional mitochondria, and protecting yeast from apoptotic and a recently discovered by our laboratory necrosis-like “lipoptotic” modes of age-related cell death. In studies described in this chapter of my thesis, we used a combination of functional genetic, chemical biological, cell biological and electron microscopical analyses to address this challenge and to elucidate the mechanisms by which mitophagy defines yeast longevity, enables lifespan extension by a novel anti-aging compound, sustains functional mitochondria and protects yeast from various cell death modalities. Our findings provide the first comprehensive evidence that mitophagy 1) is an essential longevity assurance process under both lifespan-extending CR conditions and lifespan-shortening non-CR conditions; 2) is mandatory for the ability of LCA - a recently discovered anti-aging and anti-cancer compound - to extend longevity of chronologically aging yeast; 3) is required for sustaining functional mitochondria by modulating mitochondrial respiration, mitochondrial membrane potential and mitochondrial reactive oxygen species; 4) protects yeast from a

mitochondria-controlled apoptotic cell death mode elicited by a short-term exposure to exogenous hydrogen peroxide; and 5) is essential for protecting yeast from a cell death modality that is triggered by a brief exposure to exogenous palmitoleic acid and differs from both apoptotic and necrotic cell death modes (we coined the name “lipoptosis” for this previously unknown cell death modality). We revealed a unique combination of morphological and biochemical traits characteristic of the lipoptotic cell death subroutine, and defined the spatiotemporal dynamics and molecular mechanisms underlying the progression of these traits.

8.6 Conclusions

Using a combination of functional genetic, chemical biological, cell biological and electron microscopical analyses, we provided the first evidence for the essential role of mitophagy - a selective macroautophagic removal of dysfunctional mitochondria - in defining yeast longevity, enabling lifespan extension by a recently discovered natural anti-aging compound, sustaining functional mitochondria and protecting yeast from various cell death modalities.

9 Conclusions and suggestions for future work

9.1 General conclusions

9.1.1 Caloric restriction (CR) modulates oxidation-reduction processes and ROS production in yeast mitochondria, reduces the frequency of mitochondrial DNA (mtDNA) mutations, and alters the abundance and mtDNA-binding activity of mitochondrial nucleoid-associated proteins

As a first step towards the use of high-throughput empirical data on cell metabolic history of chronologically aging yeast for defining the molecular causes of cellular aging, we recently conducted the mass spectrometry-based identification and quantitation of proteins recovered from purified mitochondria of CR and non-CR yeast [32]. Our comparative analysis of mitochondrial proteomes of these yeast revealed that CR altered the levels of numerous proteins that function in essential processes confined to mitochondria. In studies described in chapter 2, we established a spectrum of mitochondria-confined processes affected by CR. We found that CR modulates oxidation-reduction processes and ROS production in yeast mitochondria, reduces the frequency of mtDNA mutations, and alters the abundance and mtDNA-binding activity of mitochondrial nucleoid-associated proteins. Findings described in chapter 2 provide evidence that these mitochondrial processes play essential roles in regulating longevity of chronologically active yeast by defining their viability following cell entry into a quiescent state. Based on these findings, we propose a hypothesis that ROS, which are mostly generated as by-products of mitochondrial respiration, play a dual role in regulating longevity of chronologically aging yeast. On the one hand, if yeast mitochondria are unable (due to a dietary regimen) to maintain ROS concentration below

a toxic threshold, ROS promote aging by oxidatively damaging certain mitochondrial proteins and mtDNA. On the other hand, if yeast mitochondria can (due to a dietary regimen) maintain ROS concentration at a certain “optimal” level, ROS delay chronological aging. We propose that this “optimal” level of ROS is insufficient to damage cellular macromolecules but can activate certain signaling networks that extend lifespan by increasing the abundance or activity of stress-protecting and other anti-aging proteins. In addition, studies presented in chapter 2 of my thesis imply that mtDNA mutations do not contribute to longevity regulation in yeast grown under non-CR conditions but make important contribution to longevity regulation in yeast placed on a CR diet.

9.1.2 CR extends yeast chronological lifespan by altering a pattern of age-related changes in trehalose concentration

The nonreducing disaccharide trehalose has been long considered only as a reserve carbohydrate. However, recent studies in yeast suggested that this osmolyte can protect cells and cellular proteins from oxidative damage elicited by exogenously added reactive oxygen species (ROS). Trehalose has been also shown to affect stability, folding and aggregation of bacterial and firefly proteins heterologously expressed in heat-shocked yeast cells. Our recent investigation of how a lifespan-extending CR diet alters the metabolic history of chronologically aging yeast suggested that their longevity is programmed by the level of metabolic capacity - including trehalose biosynthesis and degradation - that yeast cells developed prior to entry into quiescence [32]. To investigate whether trehalose homeostasis in chronologically aging yeast may play a role in

longevity extension by CR, in studies described in chapter 3 we examined how single-gene-deletion mutations affecting trehalose biosynthesis and degradation impact 1) the age-related dynamics of changes in trehalose concentration; 2) yeast chronological lifespan under CR conditions; 3) the chronology of oxidative protein damage, intracellular ROS level and protein aggregation; and 4) the timeline of thermal inactivation of a protein in heat-shocked yeast cells and its subsequent reactivation in yeast returned to low temperature. Our data imply that CR extends yeast chronological lifespan in part by altering a pattern of age-related changes in trehalose concentration. We propose a model for molecular mechanisms underlying the essential role of trehalose in defining yeast longevity by modulating protein folding, misfolding, unfolding, refolding, oxidative damage, solubility and aggregation throughout lifespan.

9.1.3 A proper balance between the biosynthesis and degradation of glycogen is obligatory for lifespan extension by CR

Our recent comparative analysis of cellular proteomes of CR and non-CR yeast revealed that the administration of a low-calorie diet increased the levels of key enzymes involved in the biosynthesis of glycogen [32], known to be the major glucose store in yeast [169]. Moreover, CR reduced the levels of key enzymes catalyzing the degradation of glycogen in chronologically aging yeast [32]. To evaluate a potential role of glycogen metabolism in lifespan extension by CR, in studies described in chapter 4 we monitored the dynamics of age-related changes in its intracellular level. We also assessed how various single-gene-deletion mutations that differently alter glycogen concentrations in pre-quiescent and quiescent yeast cells affect longevity of chronologically aging yeast

under CR conditions. Our findings provide evidence that a proper balance between the biosynthesis and degradation of glycogen is obligatory for lifespan extension by CR.

9.1.4 CR extends yeast chronological lifespan by reducing ethanol concentration

In studies described in chapter 5, we monitored the dynamics of age-related changes in ethanol concentration in chronologically aging yeast cultured under CR and non-CR conditions. We also assessed how single-gene-deletion mutations eliminating Adh1p (an enzyme that is required for ethanol synthesis) or Adh2p (an enzyme that catalyzes ethanol degradation) affect longevity of chronologically aging yeast under CR and non-CR conditions. Furthermore, we examined the effects of the *adh1Δ* and *adh2Δ* mutations on the intracellular levels of trehalose, glycogen, neutral lipids, free fatty acids (FFA) and diacylglycerols (DAG) in chronologically aging yeast under non-CR conditions. Moreover, we monitored how single-gene-deletion mutations eliminating Adh1p or Adh2p influence the abundance of Fox1p, Fox2p and Fox3p, all of which are the core enzymes of fatty acid β -oxidation in peroxisomes. Our findings provide evidence that ethanol accumulated in yeast placed on a calorie-rich diet represses the synthesis of Fox1p, Fox2p and Fox3p, thereby suppressing peroxisomal oxidation of FFA that originate from triacylglycerols synthesized in the endoplasmic reticulum (ER) and deposited within LBs. The resulting build-up of arrays of FFA (so-called gnarls) within LBs of non-CR yeast initiates several negative feedback loops regulating the metabolism of triacylglycerols. Due to the action of these negative feedback loops, chronologically aging non-CR yeast not only amass triacylglycerols in LBs but also accumulate DAG and FFA in the ER. The resulting remodeling of lipid dynamics in chronologically aging non-

CR yeast shortens their lifespan by causing their premature death due to 1) necrosis triggered by the inability of their peroxisomes to oxidize FFA; 2) lipopoptosis initiated in response to the accumulation of DAG and FFA; and 3) the DAG-induced reorganization of the protein kinase C-dependent signal transduction network affecting multiple longevity-related cellular targets.

9.1.5 LCA, a novel anti-aging compound, alters mitochondrial structure and function, reduces cell susceptibility to mitochondria-controlled apoptosis, and increases cell resistance to oxidative and thermal stresses

We sought to identify small molecules that increase the chronological lifespan of yeast under CR conditions by targeting lipid metabolism and modulating “housekeeping” longevity assurance pathways. We predicted that such housekeeping pathways 1) modulate longevity irrespective of the organismal and intracellular nutrient and energy status; and 2) do not overlap (or only partially overlap) with the “adaptable” longevity pathways that are under the stringent control of calorie and/or nutrient availability. In studies presented in this chapter of my thesis, we found that in yeast grown under CR conditions the *pex5Δ* mutation not only remodels lipid metabolism but also causes the profound changes in longevity-defining processes in mitochondria, resistance to chronic (long-term) stresses, susceptibility to mitochondria-controlled apoptosis, and frequencies of mutations in mitochondrial and nuclear DNA. We therefore chose the single-gene-deletion mutant strain *pex5Δ* as a short-lived strain for carrying out a chemical genetic screen aimed at the identification of novel anti-aging compounds targeting housekeeping longevity assurance pathways. By screening the total of approximately 19,000

representative compounds from seven commercial libraries, our laboratory recently identified 24 small molecules that greatly extend the chronological lifespan of *pex5Δ* under CR conditions and belong to 5 chemical groups. One of these groups consisted of 6 bile acids, including LCA. Findings presented in chapter 6 imply that LCA modulates housekeeping longevity assurance pathways by 1) attenuating the pro-aging process of mitochondrial fragmentation, a hallmark event of age-related cell death; 2) altering oxidation-reduction processes in mitochondria - such as oxygen consumption, the maintenance of membrane potential and ROS production - known to be essential for longevity regulation; 3) enhancing cell resistance to oxidative and thermal stresses, thereby activating the anti-aging process of stress response; 4) suppressing the pro-aging process of mitochondria-controlled apoptosis; and 5) enhancing stability of nuclear and mitochondrial DNA, thus activating the anti-aging process of genome maintenance. The observed pleiotropic effect of LCA on a compendium of housekeeping longevity assurance processes implies that this bile acid is a multi-target life-extending compound that increases chronological lifespan in yeast by modulating a network of the highly integrated cellular events that are not controlled by the adaptable AMP-activated protein kinase/target of rapamycin (AMPK/TOR) and cAMP/protein kinase A (cAMP/PKA) pathways.

9.1.6 LCA extends longevity of chronologically aging yeast only if added at certain critical periods of their lifespan

Findings described in chapter 7 provide evidence that in yeast grown under CR conditions on 0.2% glucose, there are two critical periods when the addition of LCA to

growth medium can increase both their mean and maximum chronological lifespans. One of these two critical periods includes logarithmic and diauxic growth phases, whereas the other period exists in the early stationary (ST) phase of growth. In contrast, LCA does not cause a significant extension of the mean or maximum chronological lifespan of CR yeast if it is added in post-diauxic or late ST growth phases. Because aging of multicellular and unicellular eukaryotic organisms affects numerous anti- and pro-aging processes within cells [2, 3, 7, 9, 14, 17 - 21, 27 - 36], we hypothesized that the observed ability of LCA to delay chronological aging of yeast grown under CR conditions only if added at certain critical periods (checkpoints) of their lifespan could be due to its differential effects on certain anti- and pro-aging processes at different checkpoints. To test the validity of our hypothesis, in studies described in chapter 7 we examined how the addition of LCA at different periods of chronological lifespan in yeast grown under CR conditions influences anti- and pro-aging processes taking place during each of these periods. Our empirical validation of this hypothesis suggests a mechanism linking the ability of LCA to delay chronological aging of yeast only if added at certain periods (checkpoints) of their lifespan to the differential effects of this natural anti-aging compound on certain anti- and pro-aging processes at each of these checkpoints.

9.1.7 Mitophagy is a longevity assurance process that in yeast sustains functional mitochondria and protects cells from apoptotic and necrosis-like “lipoptotic” modes of cell death

Recent findings in mammals suggest that mitophagy, a selective macroautophagic removal of dysfunctional mitochondria, is an essential cellular process aimed at

maintaining mitochondrial functionality and suppressing cellular and organismal pathologies that arise due to dysfunction of mitochondria. However, the physiological roles of mitophagy in yeast and underlying mechanisms remained to be discovered. Chapter 8 describes studies aimed at exploring possible roles of mitophagy in regulating yeast longevity, maintaining functional mitochondria, and protecting yeast from apoptotic and a recently discovered by our laboratory necrosis-like “lipoptotic” modes of age-related cell death. In studies described in chapter 8, we used a combination of functional genetic, chemical biological, cell biological and electron microscopical analyses to carry out comparative analyses of the single-gene-deletion mutant strain *atg32Δ*, which is impaired only in the mitophagic pathway of selective macroautophagy, and wild-type (WT) strain. *atg32Δ* is known to lack a mitochondrial outer membrane protein Atg32p whose binding to an adaptor protein Atg11p drives the recruitment of mitochondria to the phagophore assembly site, thereby initiating the mitophagy process. Our findings imply that mitophagy defines yeast longevity, facilitates yeast chronological lifespan extension by a recently discovered anti-aging natural compound, sustains functional mitochondria, and protects yeast from apoptotic and necrosis-like “lipoptotic” forms of cell death.

9.2 Suggestions for future work

As the reported in chapter 2 investigation of a spectrum of mitochondrial processes affected by CR revealed, the low-calorie diet modulates oxidation-reduction processes and ROS production in yeast mitochondria, reduces the frequency of mtDNA mutations, and alters the abundance and mtDNA-binding activity of mitochondrial nucleoid-associated proteins. These findings provide evidence that these mitochondria-

confined processes play essential roles in regulating longevity of chronologically active yeast by defining cell viability following entry into a quiescent state. A challenge for the future will be to examine whether the pattern established in yeast cells grown under CR conditions can be reversed upon their transfer to calorie-rich medium. Another challenge for the future will be to test the validity of the proposed here hypothesis that chronologically aging CR yeast protect their mitochondrial nucleoids from oxidative damage by turning on the RTG signaling pathway, which then activates transcription of *ACO1* and other genes encoding bifunctional mtDNA-binding proteins known to maintain the integrity of mtDNA under respiratory conditions. It is conceivable that this knowledge will be instrumental for designing high-throughput screens aimed at discovering novel anti-aging drugs and natural compounds that can increase lifespan by modulating the longevity-defining processes confined to mitochondria.

Findings presented in chapter 3 of my thesis provide evidence that CR extends yeast chronological lifespan in part by altering a pattern of age-related changes in trehalose concentration. Based on these findings, we propose a model for molecular mechanisms underlying the essential role of trehalose in defining yeast longevity by modulating cellular proteostasis throughout lifespan. A challenge now is to get a greater insight into these mechanisms. To address this challenge, many important questions need to be answered. What are the identities of oxidatively damaged proteins whose accumulation in pre-quiescent WT cells proliferating under CR conditions is reduced by genetic manipulations that elevate trehalose concentration prior to entry into quiescence? Are these proteins known for their essential role in defining longevity? Will genetic manipulations eliminating any of these proteins or altering their levels affect the

chronological lifespan of yeast? What kind of proteins form insoluble aggregates that accumulate, in a trehalose-dependent fashion, in WT cells prior to and/or following entry into a quiescent state? Are they known to be modifiers of lifespan in yeast? How will genetic manipulations eliminating any of these proteins or altering their levels influence longevity of chronologically aging yeast? Do oxidatively damaged and/or aggregated protein species concentrate in certain protein quality control compartments, such as the juxtannuclear quality control compartment, the insoluble protein deposit compartment and/or aggresome [195, 200, 201], or are they randomly distributed throughout a cell prior to and/or following entry into quiescence? Does trehalose reside, permanently or temporarily, in any of these protein quality control compartments or is this osmolyte dispersed within a cell before and/or after it enters a quiescent state? What molecular chaperones constitute the proteostasis machinery whose ability to refold aberrantly folded proteins is compromised by trehalose in quiescent cells? We shall have to answer these important questions if we want to understand the complexity of the proteostasis network that defines longevity by sensing the dynamics of age-related changes in trehalose concentration.

Along with other data from our laboratory on the molecular mechanism underlying the ability of CR to extend longevity of chronologically aging yeast [32, 40, 110, 114], findings presented in chapter 4 imply that, by activating the synthesis of enzymes catalyzing the biosynthesis of glycogen and by suppressing the synthesis of enzymes required for its degradation, CR promotes the accumulation of this major reserve carbohydrate. Our functional analysis of the role for age-dependent glycogen dynamics in lifespan extension by CR with the help of a collection of mutants, each

lacking a single protein that functions in glycogen biosynthesis or degradation, provides evidence that lifespan extension by CR relies in part on the establishment of a proper balance between the biosynthesis and degradation of glycogen. A challenge now is to get a greater insight into the molecular mechanisms underlying the longevity-defining role of such balance in chronologically aging yeast.

Findings described in this chapter 6, together with some recently published data from our laboratory [40, 114], identify a compendium of processes that compose LCA-targeted housekeeping longevity assurance pathways. These findings imply that LCA modulates such pathways by 1) suppressing the pro-aging process [32, 110, 114, 244] of lipid-induced necrotic cell death, perhaps due to its observed ability to reduce the intracellular levels of FFA and DAG that trigger such death; 2) attenuating the pro-aging process [32, 251, 252] of mitochondrial fragmentation, a hallmark event of age-related cell death; 3) altering oxidation-reduction processes in mitochondria - such as oxygen consumption, the maintenance of membrane potential and ROS production - known to be essential for longevity regulation [32, 245, 253 - 255]; 4) enhancing cell resistance to oxidative and thermal stresses, thereby activating the anti-aging process [32, 110, 255 - 257] of stress response; 5) suppressing the pro-aging process [32, 251, 252] of mitochondria-controlled apoptosis; and 6) enhancing stability of nuclear and mitochondrial DNA, thus activating the anti-aging process [32, 258, 259] of genome maintenance. The observed pleiotropic effect of LCA on a compendium of housekeeping longevity assurance processes implies that this bile acid is a multi-target life-extending compound that increases chronological lifespan in yeast by modulating a network of the highly integrated cellular events not controlled by the adaptable TOR and cAMP/PKA

pathways. The major challenge now is to define the molecular mechanisms by which LCA modulates each of these pro- and anti-aging housekeeping processes and integrates them in chronologically aging yeast.

10 References

1. Kirkwood, T.B.L. (2005). Understanding the odd science of aging. *Cell* 120:437-447.
2. Guarente, L.P., Partridge, L. and Wallace, D.C. (Editors) (2008). *Molecular Biology of Aging*. Cold Spring Harbor Laboratory Press, Cold Spring Harbor, New York, 610 pages.
3. Fontana, L., Partridge, L. and Longo, V.D. (2010). Extending healthy life span - from yeast to humans. *Science* 328:321-326.
4. Partridge, L. (2010). The new biology of ageing. *Philos. Trans. R. Soc. Lond. B Biol. Sci.* 365:147-154
5. Tavernarkis, N. (Editor) (2010). *Protein Metabolism and Homeostasis in Aging*. Landes Bioscience and Springer Science+Business Media, New York, 249 pages.
6. Kirkwood, T.B.L. (2011). Systems biology of ageing and longevity. *Philos. Trans. R. Soc. Lond. B Biol. Sci.* 366:64-70.
7. Masoro, E.J. and Austad, S.N. (Editors) (2011). *Handbook of the Biology of Aging*. 7th Edition. Academic Press (an imprint of Elsevier), Amsterdam, 572 pages.
8. Kirkwood, T.B.L. (2008). Understanding ageing from an evolutionary perspective. *J.*

Intern. Med. 263:117-127.

9. Mair, W. and Dillin, A. (2008). Aging and survival: the genetics of life span extension by dietary restriction. *Annu. Rev. Biochem.* 77:727-754.

10. Kirkwood, T.B.L. (2011). Systems biology of ageing and longevity. *Philos. Trans. R. Soc. Lond. B Biol. Sci.* 366:64-70.

11. Masoro, E.J. and Austad, S.N. (Editors) (2011). *Handbook of the Biology of Aging*. 7th Edition. Academic Press (an imprint of Elsevier), Amsterdam, 572 pages.

12. Wheeler, H.E. and Kim, S.K. (2011). Genetics and genomics of human ageing. *Philos. Trans. R. Soc. Lond. B Biol. Sci.* 366:43-50.

13. Longo, V.D. and Kennedy, B.K. (2006). Sirtuins in aging and age-related disease. *Cell* 126:257-268.

14. Kaerberlein, M., Burtner, C.R. and Kennedy, B.K. (2007). Recent developments in yeast aging. *PLoS Genet.* 3:e84.

15. Lin, S.-J., and Sinclair, D. (2008). Molecular mechanisms of aging: insights from budding yeast. In: Guarente, L.P., Partridge, L., Wallace, D.C. (Eds.), *Molecular Biology of Aging*. Cold Spring Harbor Laboratory Press, Cold Spring Harbor, New York, pp. 483-

516.

16. Kaerberlein, M. (2010). Lessons on longevity from budding yeast. *Nature* 464:513-519.

17. Kenyon, C. (2001). A conserved regulatory system for aging. *Cell* 105:165-168.

18. Kenyon, C. (2005). The plasticity of aging: insights from long-lived mutants. *Cell* 120:449-460.

19. Longo, V.D., and Finch, C.E. (2003). Evolutionary medicine: from dwarf model systems to healthy centenarians? *Science* 299:1342-1346.

20. Russell, S.J., and Kahn, C.R. (2007). Endocrine regulation of ageing. *Nat. Rev. Mol. Cell Biol.* 8:681-691.

21. Bitterman, K.J., Medvedik, O. and Sinclair, D.A. (2003). Longevity regulation in *Saccharomyces cerevisiae*: linking metabolism, genome stability, and heterochromatin. *Microbiol. Mol. Biol. Rev.* 67:376-399.

22. Fabrizio, P. and Longo, V.D. (2003). The chronological life span of *Saccharomyces cerevisiae*. *Aging Cell* 2:73-81.

23. Bordone, L., and Guarente, L. (2005). Calorie restriction, SIRT1 and metabolism: understanding longevity. *Nat. Rev. Mol. Cell Biol.* 6, 298-305.
24. Sinclair, D.A. (2005). Toward a unified theory of caloric restriction and longevity regulation. *Mech. Ageing Dev.* 126, 987-1002.
25. Masoro, E.J. (2005). Overview of caloric restriction and ageing. *Mech. Ageing Dev.* 126, 913-922.
26. Masoro, E.J. (2006). Caloric restriction and aging: controversial issues. *J. Gerontol. Biol. Sci.* 61A, 14-19.
27. Wei, M., Fabrizio, P., Hu, J., Ge, H., Cheng, C., Li, L. and Longo, V.D. (2008). Life span extension by calorie restriction depends on Rim15 and transcription factors downstream of Ras/PKA, Tor, and Sch9. *PLoS Genet.* 4:e13.
28. Eisenberg, T., Knauer, H., Schauer, A., Büttner, S., Ruckenstuhl, C., Carmona-Gutierrez, D., Ring, J., Schroeder, S., Magnes, C., Antonacci, L., Fussi, H., Deszcz, L., Hartl, R., Schraml, E., Criollo, A., Megalou, E., Weiskopf, D., Laun, P., Heeren, G., Breitenbach, M., Grubeck-Loebenstein, B., Herker, E., Fahrenkrog, B., Fröhlich, K.U., Sinner, F., Tavernarakis, N., Minois, N., Kroemer, G. and Madeo, F. (2009). Induction of autophagy by spermidine promotes longevity. *Nat. Cell Biol.* 11:1305-1314.

29. Guarente, L. (2006). Sirtuins as potential targets for metabolic syndrome. *Nature* 444:868-874.
30. Greer, E.L. and Brunet, A. (2008). Signaling networks in aging. *J. Cell Sci.* 121:407-412.
31. Murphy, M.P. and Partridge, L. (2008). Toward a control theory analysis of aging. *Annu. Rev. Biochem.* 77:777-798.
32. Goldberg, A.A., Bourque, S.D., Kyryakov, P., Gregg, C., Boukh-Viner, T., Beach, A., Burstein, M.T., Machkalyan, G., Richard, V., Rampersad, S., Cyr, D., Milijevic, S. and Titorenko, V.I. (2009). Effect of calorie restriction on the metabolic history of chronologically aging yeast. *Exp. Gerontol.* 44:555-571.
33. Kenyon, C. (2010). The genetics of ageing. *Nature* 464:504-512.
34. Kenyon, C. (2010). A pathway that links reproductive status to lifespan in *Caenorhabditis elegans*. *Ann. N. Y. Acad. Sci.* 1204:156-162.
35. Kenyon, C. (2011). The first long-lived mutants: discovery of the insulin/IGF-1 pathway for ageing. *Philos. Trans. R. Soc. Lond. B Biol. Sci.* 366:9-16.

36. Narasimhan, S.D., Yen, K. and Tissenbaum, H.A. (2009). Converging pathways in lifespan regulation. *Curr. Biol.* 19:R657-R666.
37. Kaeberlein, M., Burtner, C.R., and Kennedy, B.K. (2007). Recent developments in yeast aging. *PLoS Genet.* 3:e84.
38. Haigis, M.C., and Guarente, L.P. (2006). Mammalian sirtuins - emerging roles in physiology, aging, and calorie restriction. *Genes Dev.* 20:2913-2921.
39. Wolff, S., and Dillin, A. (2006). The trifecta of aging in *Caenorhabditis elegans*. *Exp. Gerontol.* 41:894-903.
40. Goldberg, A.A., Richard, V.R., Kyryakov, P., Bourque, S.D., Beach, A., Burstein, M.T., Glebov, A., Koupaki, O., Boukh-Viner, T., Gregg, C., Juneau, M., English, A.M., Thomas, D.Y., and Titorenko, V.I. (2010). Chemical genetic screen identifies lithocholic acid as an anti-aging compound that extends yeast chronological life span in a TOR-independent manner, by modulating housekeeping longevity assurance processes. *Aging* 2:393-414.
41. Jazwinski, S.M. (2005). Yeast longevity and aging - the mitochondrial connection. *Mech. Ageing Dev.* 126:243-248.

42. Jazwinski, S.M. (2005). The retrograde response links metabolism with stress responses, chromatin-dependent gene activation, and genome stability in yeast aging. *Gene* 354:22-27.
43. Jazwinski, S.M. (2012). The retrograde response and other pathways of interorganelle communication in yeast replicative aging. *Subcell. Biochem.* 57:79-100.
44. Titorenko, V.I., and Terlecky, S.R. (2011). Peroxisome metabolism and cellular aging. *Traffic* 12:252-259.
45. Panowski, S.H., Wolff, S., Aguilaniu, H., Durieux, J., and Dillin, A. (2007). PHA-4/Foxa mediates diet-restriction-induced longevity of *C. elegans*. *Nature* 447:550-555.
46. Giannakou, M.E., and Partridge, L. (2004). The interaction between FOXO and SIRT1: tipping the balance towards survival. *Trends Cell Biol.* 14:408-412.
47. Weindruch, R. and Walford, R.L. (1988). *The Retardation of Aging and Disease by Dietary Restriction*. Thomas, Springfield.
48. Masoro, E.J. (2002). *Caloric Restriction: A Key to Understanding and Modulating Aging*. Elsevier, Amsterdam.
49. Colman, R.J., Anderson, R.M., Johnson, S.C., Kastman, E.K., Kosmatka, K.J.,

Beasley, T.M., Allison, D.B., Cruzen, C., Simmons, H.A., Kemnitz, J.W. and Weindruch, R. (2009). Caloric restriction delays disease onset and mortality in rhesus monkeys. *Science* 325:201-204.

50. Min, K.J., Flatt, T., Kulaots, I. and Tatar, M. (2007). Counting calories in *Drosophila* diet restriction. *Exp. Gerontol.* 42:247-251.

51. Zimmerman, J.A., Malloy, V., Krajcik, R. and Orentreich, N. (2003). Nutritional control of aging. *Exp. Gerontol.* 38:47-52.

52. Mair, W., Piper, M.D. and Partridge, L. (2005). Calories do not explain extension of life span by dietary restriction in *Drosophila*. *PLoS Biol.* 3:e223.

53. Piper, M.D., Mair, W. and Partridge, L. (2005). Counting the calories: the role of specific nutrients in extension of life span by food restriction. *J. Gerontol. A Biol. Sci. Med. Sci.* 60:549-555.

54. Richardson, A. (1985). The effect of age and nutrition on protein synthesis by cells and tissues from mammals. In *Handbook of nutrition in the aged* (ed. W.R. Watson), pp. 31-48. CRC Press, Boca Raton, FL.

55. Weindruch, R., Walford, R.L., Fligiel, S., and Guthrie, D. (1986). The retardation of aging in mice by dietary restriction: Longevity, cancer, immunity and lifetime energy

intake. *J. Nutr.* 116:641-654.

56. Sohal, R.S. and Weindruch, R. (1996). Oxidative stress, caloric restriction, and aging. *Science* 273:59-63.

57. Lane, M.A., Black, A., Handy, A., Tilmont, E.M., Ingram, D.K., and Roth, G.S. (2001). Caloric restriction in primates. *Ann. NY Acad. Sci.* 928:287-295.

58. Jazwinski, S.M. (2002). Biological aging research today: potential, peeves, and problems. *Exp. Gerontol.* 37:1141-1146.

59. Duan, W. and Mattson, M.P. (1999). Dietary restriction and 2-deoxyglucose administration improve behavioral outcome and reduce degeneration of dopaminergic neurons in models of Parkinson's disease. *J. Neurosci. Res.* 57:195-206.

60. Zhu, H., Guo, Q., and Mattson, M.P. (1999). Dietary restriction protects hippocampal neurons against the death-promoting action of presenilin-1 mutation. *Brain Res.* 842:224-229.

61. Ingram, D.K., Weindruch, R., Spangler, E.L., Freeman, J.R., and Walford, R.L. (1987). Dietary restriction benefits learning and motor performance of aged mice. *J. Gerontol.* 42:78-81.

62. Moroi-Fetters, S.E., Mervis, R.F., London, E.D., and Ingram, D.K. (1989). Dietary restriction suppresses age-related changes in dendritic spines. *Neurobiol. Aging* 10:317-322.
63. Mattson, M.P. (2000). Neuroprotective signaling and the aging brain: Take away my food and let me run. *Brain Res.* 886, 47-53.
64. Lin, S.J., Defossez, P.A., and Guarente, L. (2000). Requirement of NAD and SIR2 for life-span extension by calorie restriction in *Saccharomyces cerevisiae*. *Science* 289:2126-2128.
65. Jiang, J., Wawryn, J., Shantha Kumara, H., and Jazwinski, S. (2002). Distinct roles of processes modulated by histone deacetylases Rpd3p, Hda1p, and Sir2p in life extension by caloric restriction in yeast. *Exp. Gerontol.* 37:1023-1030.
66. Jiang, J.C., Jaruga, E., Repnevskaya, M.V., and Jazwinski, S.M. (2000). An intervention resembling caloric restriction prolongs life span and retards aging in yeast. *FASEB J.* 14:2135-2137.
67. Guarente, L. and Picard, F. (2005). Calorie restriction - the SIR2 connection. *Cell* 120:473-482.
68. Harman, D. (1956). Aging: a theory based on free radical and radiation chemistry. *J.*

Gerontol. 11:298-300.

69. Harman, D. (1972). The biologic clock: the mitochondria? *J. Am. Geriatr. Soc.* 20:145-147.

70. Fraga, C.G., Shigenaga, M.K., Park, J.W., Degan, P., and Ames, B.N. (1990). Oxidative damage to DNA during aging: 8-Hydroxy-2'-deoxyguanosine in rat organ DNA and urine. *Proc. Natl. Acad. Sci. USA* 87:4533-4537.

71. Stadtman, E.R. (1992). Protein oxidation and aging. *Science* 257:1220-1224.

72. Head, E., Liu, J., Hagen, T.M., Muggenburg, B.A., Milgram, N.W., Ames, B.N., and Cotman, C.W. (2002). Oxidative damage increases with age in a canine model of human brain aging. *J. Neurochem.* 82:375-381.

73. Liu, J., Head, E., Gharib, A.M., Yuan, W., Ingersoll, R.T., Hagen, T.M., Cotman, C.W., and Ames, B.N. (2002). Memory loss in old rats is associated with brain mitochondrial decay and RNA/DNA oxidation: Partial reversal by feeding acetyl-L-carnitine and/or R- -lipoic acid. *Proc. Natl. Acad. Sci. USA* 99:2356-2361.

74. Parkes, T.L., Elia, A.J., Dickinson, D., Hilliker, A.J., Phillips, J.P., and Boulianne, G.L. (1998). Extension of *Drosophila* lifespan by overexpression of human SOD1 in motorneurons. *Nat. Genet.* 19:171-174.

75. Longo, V.D., Liou, L.L., Valentine, J.S., and Gralla, E.B. (1999). Mitochondrial superoxide decreases yeast survival in stationary phase. *Arch. Biochem. Biophys.* 365:131-142.
76. Nicholls, D. (2002). Mitochondrial bioenergetics, aging, and aging-related disease. *Sci. Aging Knowledge Environ.* 31:pe12.
77. Newmeyer, D.D., and Ferguson-Miller, S. (2003). Mitochondria: releasing power for life and unleashing the machineries of death. *Cell* 112:481-490.
78. Balaban, R.S., Nemoto, S., and Finkel, T. (2005). Mitochondria, oxidants, and aging. *Cell* 120:483-495.
79. Storz, P. (2007). Mitochondrial ROS - radical detoxification, mediated by protein kinase D. *Trends Cell Biol.* 17:13-18.
80. Titorenko, V.I., and Rachubinski, R.A. (2001). Dynamics of peroxisome assembly and function. *Trends Cell Biol.* 11:22-29.
81. Titorenko, V.I. and Rachubinski, R.A. (2001). The life cycle of the peroxisome. *Nat. Rev. Mol. Cell Biol.* 2:357-368.
82. Finley, L.W., and Haigis, M.C. (2009). The coordination of nuclear and

mitochondrial communication during aging and calorie restriction. *Ageing Res. Rev.* 8:173-188.

83. Rea, S.L., Ventura, N., and Johnson, T.E. (2007). Relationship between mitochondrial electron transport chain dysfunction, development, and life extension in *Caenorhabditis elegans*. *PLoS Biol.* 5:e259.

84. Schulz, T.J., Zarse, K., Voigt, A., Urban, N., Birringer, M., and Ristow, M. (2007). Glucose restriction extends *Caenorhabditis elegans* life span by inducing mitochondrial respiration and increasing oxidative stress. *Cell Metab.* 6:280-293.

85. Gems, D., and Partridge, L. (2008). Stress-response hormesis and aging: "that which does not kill us makes us stronger". *Cell Metab.* 7:200-203.

86. Rattan, S.I. (2008). Hormesis in aging. *Ageing Res. Rev.* 7:63-78.

87. Van Raamsdonk, J.M., and Hekimi, S. (2009). Deletion of the mitochondrial superoxide dismutase *sod-2* extends lifespan in *Caenorhabditis elegans*. *PLoS Genet.* 5:e1000361.

88. Ventura, N., Rea, S.L., Schiavi, A., Torgovnick, A., Testi, R., and Johnson, T.E. (2009). p53/CEP-1 increases or decreases lifespan, depending on level of mitochondrial bioenergetic stress. *Aging Cell* 8:380-393.

89. Lapointe, J., and Hekimi S. (2010). When a theory of aging ages badly. *Cell Mol. Life Sci.* 67:1-8.
90. Balaban, R.S., Nemoto, S., and Finkel, T. (2005). Mitochondria, oxidants, and aging. *Cell* 120:483-495.
91. D'Autréaux, B., and Toledano, M.B. (2007). ROS as signalling molecules: mechanisms that generate specificity in ROS homeostasis. *Nat. Rev. Mol. Cell Biol.* 8:813-824.
92. Giorgio, M., Trinei, M., Migliaccio, E., and Pelicci, P.G. (2007). Hydrogen peroxide: a metabolic by-product or a common mediator of ageing signals? *Nat. Rev. Mol. Cell Biol.* 8:722-728.
93. Veal, E.A., Day, A.M., and Morgan, B.A. (2007). Hydrogen peroxide sensing and signaling. *Mol. Cell* 26:1-14.
94. Madeo, F., Herker, E., Wissing, S., Jungwirth, H., Eisenberg, T., and Frohlich, K.U. (2004). Apoptosis in yeast. *Curr. Opin. Microbiol.* 7:655-660.
95. Eisenberg, T., Büttner, S., Kroemer, G., and Madeo, F. (2007). The mitochondrial pathway in yeast apoptosis. *Apoptosis* 12:1011-1023.

96. Balaban, R.S., Nemoto, S., and Finkel, T. (2005). Mitochondria, oxidants, and aging. *Cell* 120:483-495.
97. Bredesen, D.E., Rao, R.V., and Mehlen, P. (2006). Cell death in the nervous system. *Nature* 443:796-802.
98. Lin, M.T., and Beal, M.F. (2006). Mitochondrial dysfunction and oxidative stress in neurodegenerative diseases. *Nature* 443:787-795.
99. Newmeyer, D.D., and Ferguson-Miller, S. (2003). Mitochondria: releasing power for life and unleashing the machineries of death. *Cell* 112:481-490.
100. Steller, H. (1995). Mechanisms and genes of cellular suicide. *Science* 267:1445-1449.
101. Green, D. (2011). *Means to an end: apoptosis and other cell death mechanisms*. Cold Spring Harbor Laboratory Press, Cold Spring Harbor, New York, 220 pages.
102. Madeo, F., Herker, E., Wissing, S., Jungwirth, H., Eisenberg, T., and Frohlich, K.U. (2004). Apoptosis in yeast. *Current Option in Microbiology*. 7:655-660.
103. Madeo, F., Herker, E., Maldener, C., Wissing, S., Lächelt, S., Herlan, M., Fehr, M., Lauber, K., Sigrist, S.J., Wesselborg, S., and Fröhlich, K.U. (2002). A caspase-related

protease regulates apoptosis in yeast. *Mol. Cell* 9:911-917.

104. Madeo, F., Fröhlich, E., Ligr, M., Grey, M., Sigrist, S.J., Wolf, D.H. and Fröhlich, K.U. (1999). Oxygen stress: a regulator of apoptosis in yeast. *J. Cell Biol.* 145:757-767.

105. Fahrenkrog, B., Sauder, U., and Aebi, U. (2004). The *S. cerevisiae* HtrA-like protein Nma111p is a nuclear serine protease that mediates yeast apoptosis. *J. Cell Sci.* 117:115-126.

106. Wissing, S., Ludovico, P., Herker, E., Büttner, S., Engelhardt, S.M., Decker, T., Link, A., Proksch, A., Rodrigues, F., Corte-Real, M., Fröhlich, K.U., Manns, J., Candé, C., Sigrist, S.J., Kroemer, G., and Madeo, F. (2004). An AIF orthologue regulates apoptosis in yeast. *J. Cell Biol.* 166:969-974.

107. Yamaki, M., Umehara, T., Chimura, T. and Horikoshi, M. (2001). Cell death with predominant apoptotic features in *Saccharomyces cerevisiae* mediated by deletion of the histone chaperone ASF1/CIA1. *Genes Cells* 6:1043-1054.

108. Fannjiang, Y., Cheng, W.C., Lee, S.J., Qi, B., Pevsner, J., McCaffery, J.M., Hill, R.B., Basañez, G. and Hardwick, J.M. (2004). Mitochondrial fission proteins regulate programmed cell death in yeast. *Genes Dev.* 18:2785-2797.

109. Herker, E., Jungwirth, H., Lehmann, K.A., Maldener, C., Fröhlich, K.U., Wissing,

S., Buttner, B., Markus, F., Sigrist, S., and Madeo, F. (2004). Chronological aging leads to apoptosis in yeast. *J. Cell. Biol.* 164:501-507.

110. Goldberg, A.A., Bourque, S.D., Kyryakov, P., Boukh-Viner, T., Gregg, C., Beach, A., Burstein, M.T., Machkalyan, G., Richard, V., Rampersad, S. and Titorenko, V.I. (2009). A novel function of lipid droplets in regulating longevity. *Biochem. Soc. Trans.* 37:1050-1055.

111. Allen, C., Büttner, S., Aragon, A.D., Thomas, J.A., Meirelles, O., Jaetao, J.E., Benn, D., Ruby, S.W., Veenhuis, M., Madeo, F., and Werner-Washburne, M. (2006). Isolation of quiescent and nonquiescent cells from yeast stationary-phase cultures. *J. Cell Biol.* 174:89-100.

112. Aragon, A.D., Rodriguez, A.L., Meirelles, O., Roy, S., Davidson, G.S., Tapia, P.H., Allen, C., Joe, R., Benn, D., and Werner-Washburne, M. (2008). Characterization of differentiated quiescent and nonquiescent cells in yeast stationary-phase cultures. *Mol. Biol. Cell* 19:1271-1280.

113. Bonawitz, N.D., Chatenay-Lapointe, M., Pan, Y., and Shadel, G.S. (2007). Reduced TOR signaling extends chronological life span via increased respiration and upregulation of mitochondrial gene expression. *Cell Metab.* 5:265-277.

114. Beach, A., and Titorenko, V.I. (2011). In search of housekeeping pathways that

regulate longevity. *Cell Cycle* 10:3042-3044.

115. Howitz, K.T., Bitterman, K.J., Cohen, H.Y., Lamming, D.W., Lavu, S., Wood, J.G., Zipkin, R.E., Chung, P., Kisielewski, A., Zhang, L.L., Scherer, B., and Sinclair, D.A. (2003). Small molecule activators of sirtuins extend *Saccharomyces cerevisiae* lifespan. *Nature* 425:191-196.

116. Viswanathan, M., Kim, S.K., Berdichevsky, A., and Guarente, L. (2005). A role for SIR-2.1 regulation of ER stress response genes in determining *C. elegans* life span. *Dev. Cell* 9:605-615.

117. Wood, J.G., Rogina, B., Lavu, S., Howitz, K., Helfand, S.L., Tatar, M., and Sinclair, D. (2004). Sirtuin activators mimic caloric restriction and delay ageing in metazoans. *Nature* 430:686-689.

118. Viswanathan, M., Kim, S.K., Berdichevsky, A., and Guarente, L. (2005). A role for SIR-2.1 regulation of ER stress response genes in determining *C. elegans* life span. *Dev. Cell* 9:605-615.

119. Baur, J.A., Pearson, K.J., Price, N.L., Jamieson, H.A., Lerin, C., Kalra, A., Prabhu, V.V., Allard, J.S., Lopez-Lluch, G., Lewis, K., Pistell, P.J., Poosala, S., Becker, K.G., Boss, O., Gwinn, D., Wang, M., Ramaswamy, S., Fishbein, K.W., Spencer, R.G., Lakatta, E.G., Le Couteur, D., Shaw, R.J., Navas, P., Puigserver, P., Ingram, D.K., de

Cabo, R., and Sinclair, D.A. (2006). Resveratrol improves health and survival of mice on a high-calorie diet. *Nature* 444:337-342.

120. Valenzano, D.R., Terzibasi, E., Genade, T., Cattaneo, A., Domenici, L., and Cellarino, A. (2006). Resveratrol prolongs lifespan and retards the onset of age-related markers in a short-lived vertebrate. *Curr. Biol.* 16:296-300.

121. Chen, D., and Guarente, L. (2007). SIR2: a potential target for calorie restriction mimetics. *Trends Mol. Med.* 13:64-71.

122. Curtis, R., Geesaman, B.J., and DiStefano, P.S. (2005). Ageing and metabolism: drug discovery opportunities. *Nat. Rev. Drug Discov.* 4:569-580.

123. Milne, J.C., Lambert, P.D., Schenk, S., Carney, D.P., Smith, J.J., Gagne, D.J., Jin, L., Boss, O., Perini, R.B., Vu, C.B., Bemis, J.E., Xie, R., Disch, J.S., Ng, P.Y., Nunes, J.J., Lynch, A.V., Yang, H., Galonek, H., Israelian, K., Choy, W., Iffland, A., Lavu, S., Medvedik, O., Sinclair, D.A., Olefsky, J.M., Jirousek, M.R., Elliott, P.J., and Westphal, C.H. (2007). Small molecule activators of SIRT1 as therapeutics for the treatment of type 2 diabetes. *Nature* 450:712-716.

124. Yang, H., Ren, Q., and Zhang, Z. (2008). Cleavage of Mcd1 by caspase-like protease Esp1 promotes apoptosis in budding yeast. *Mol. Biol. Cell* 19:2127-2134.

125. Goldberg, A.A., Beach, A., Davies, G.F., Harkness, T.A.A., LeBlanc, A. and Titorenko, V.I. (2011). Lithocholic bile acid selectively kills neuroblastoma cells, while sparing normal neuronal cells. *Oncotarget* 2:761-782.
126. Yen, W.L., and Klionsky, D.J. (2008). How to Live Long and Prosper: Autophagy, Mitochondria, and Aging. *Physiology* 23:248-262.
127. Morselli, E., Galluzzi, L., Kepp, O., Criollo, A., Maiuri, M.C., Tavernarakis, N., Madeo, F., and Kroemer, G. (2009). Autophagy mediates pharmacological lifespan extension by spermidine and resveratrol. *Aging* 1:961-970.
128. Levine, B., and Kroemer, G. (2008). Autophagy in the pathogenesis of disease. *Cell* 132:27-42.
129. Mizushima, N., Levine, B., Cuervo, A.M., and Klionsky, D.J. (2008). Autophagy fights disease through cellular self-digestion. *Nature* 451:1069-1075.
130. Vellai, T., Takacs-Vellai, K., Sass, M., and Klionsky, D.J. (2009). The regulation of aging: does autophagy underlie longevity? *Trends Cell Biol.* 19:487-494.
131. Chan, E.Y., Tooze, S.A. (2009). Evolution of Atg1 function and regulation. *Autophagy* 5:758-765.

132. Stephan, J.S., Yeh, Y.Y., Ramachandran, V., Deminoff, S.J., and Herman, P.K. (2009). The Tor and PKA signalling pathways independently target the Atg1/Atg13 protein kinase complex to control autophagy. *Proc. Natl. Acad. Sci. USA* 106:17049-17054.
133. Chan, EY. and Tooze, SA. (2009). Evolution of Atg1 function and regulation. *Autophagy* 5:758-765.
134. Markaki, M., and Tavernarakis. N. (2011). The role of autophagy in genetic pathways influencing ageing. *Biogerontology* 12:377-386.
135. Deminoff, S.J., and Herman, P.K. (2007). Identifying Atg1 Substrates: Four Means to an End. *Autophagy* 3:667-673.
136. Gao, W., Shen, Z., Shang, L., and Wang, X. (2011). Upregulation of human autophagy-initiation kinase ULK1 by tumor suppressor p53 contributes to DNA-damage-induced cell death. *Cell Death Differ.* 18:1598-1607.
137. Yorimitsu, T., and Klionsky, DK. (2005). Atg11 Links Cargo to the Vesicle-forming Machinery in the Cytoplasm to Vacuole Targeting Pathway *Mol. Biol. Cell* 16:1593–1605.
138. Monastyrska, I., Shintani, T., Klionsky, D.J., and Reggiori, F. (2006). Atg11 directs

autophagosome cargoes to the PAS along actin cables. *Autophagy* 2:119-121.

139. Reggiori, F., Monastyrska, I., Shintani, T., and Klionsky, D.J. (2005). The actin cytoskeleton is required for selective types of autophagy, but not nonspecific autophagy, in the yeast *Saccharomyces cerevisiae*. *Mol. Biol. Cell* 16:5843-5856.

140. Sherman, F. (2002). Getting started with yeast. *Methods Enzymol.* 350:3-41.

141. Doudican, N.A., Song, B., Shadel, G.S. and Doetsch, P.W. (2005). Oxidative DNA damage causes mitochondrial genomic instability in *Saccharomyces cerevisiae*. *Mol. Cell. Biol.* 25:5196-5204.

142. Chi, N.W. and Kolodner, R.D. (1994). Purification and characterization of MSH1, a yeast mitochondrial protein that binds to DNA mismatches. *J. Biol. Chem.* 269:29984-29992.

143. Cui, Z. and Mason, T.L. (1989). A single nucleotide substitution at the *rib2* locus of the yeast mitochondrial gene for 21S rRNA confers resistance to erythromycin and cold-sensitive ribosome assembly. *Curr. Genet.* 16:273-279.

144. Gregg, C., Kyryakov, P., and Titorenko, V.I. (2009). Purification of mitochondria from yeast cells. *J. Vis. Exp.* 30:1-2, doi: 10.3791/1417.

145. Kaufman, B.A., Newman, S.M., Perlman, P.S. and Butow, R.A. (2002). Crosslinking of proteins to mtDNA. *Methods Mol. Biol.* 197:377-389.
146. Kaufman, B.A., Newman, S.M., Hallberg, R.L., Slaughter, C.A., Perlman, P.S., and Butow, R.A. (2000). *In organello* formaldehyde crosslinking of proteins to mtDNA: identification of bifunctional proteins. *Proc. Natl. Acad. Sci. USA* 97:7772-7777.
147. Titorenko, V.I., Smith, J.J., Szilard, R.K. and Rachubinski, R.A. (1998). Pex20p of the yeast *Yarrowia lipolytica* is required for the oligomerization of thiolase in the cytosol and for its targeting to the peroxisome. *J. Cell Biol.* 142:403-420.
148. Szilard, R.K., Titorenko, V.I., Veenhuis, M. and Rachubinski, R.A. (1995). Pay32p of the yeast *Yarrowia lipolytica* is an intraperoxisomal component of the matrix protein translocation machinery. *J. Cell Biol.* 131:1453-1469.
149. Graham, J.M. (1999). Purification of a crude mitochondrial fraction by density-gradient centrifugation. In: *Current Protocols in Cell Biology*. Bonifacino, J.S., Dasso, M., Harford, J.B., Lippincott-Schwartz, J., Yamada, K.M. (Eds.). John Wiley & Sons, Inc., pp. 3.4.1-3.4.22.
150. Fabrizio, P., Liou, L.L., Moy, V.N., Diaspro, A., Valentine, J.S., Gralla, E.B. and Longo, V.D. (2003). SOD2 functions downstream of Sch9 to extend longevity in yeast. *Genetics* 163:35-46.

151. Kirkwood, T.B.L., Boys, R.J., Gillespie, C.S., Proctor, C.J., Shanley, D.P., and Wilkinson, D.J. (2003). Towards an e-biology of ageing: integrating theory and data. *Nat. Rev. Mol. Cell Biol.* 4:243-249.
152. D'Autréaux, B. and Toledano, M.B. (2007). ROS as signalling molecules: mechanisms that generate specificity in ROS homeostasis. *Nat. Rev. Mol. Cell Biol.* 8:813-824.
153. Giorgio, M., Trinei, M., Migliaccio, E. and Pelicci, P.G. (2007). Hydrogen peroxide: a metabolic by-product or a common mediator of ageing signals? *Nat. Rev. Mol. Cell Biol.* 8:722-728.
154. Titorenko, V.I. and Terlecky, S.R. (2011). Peroxisome metabolism and cellular aging. *Traffic* 12:252-259.
155. Fabrizio, P., Pozza, F., Pletcher, S.D., Gendron, C.M. and Longo, V.D. (2001). Regulation of longevity and stress resistance by Sch9 in yeast. *Science* 292:288-290.
156. Sherman, F. (2002). Getting started with yeast. *Methods Enzymol.* 350:3-41.
157. Chen, X.J. and Butow, R.A. (2005). The organization and inheritance of the mitochondrial genome. *Nat. Rev. Genet.* 6:815-825.

158. Doudican, N.A., Song, B., Shadel, G.S. and Doetsch, P.W. (2005). Oxidative DNA damage causes mitochondrial genomic instability in *Saccharomyces cerevisiae*. *Mol. Cell. Biol.* 25:5196-5204.
159. Chi, N.W. and Kolodner, R.D. (1994). Purification and characterization of MSH1, a yeast mitochondrial protein that binds to DNA mismatches. *J. Biol. Chem.* 269:29984-29992.
160. Cui, Z. and Mason, T.L. (1989). A single nucleotide substitution at the *rib2* locus of the yeast mitochondrial gene for 21S rRNA confers resistance to erythromycin and cold-sensitive ribosome assembly. *Curr. Genet.* 16:273-279.
161. Chen, X.J., Wang, X., Kaufman, B.A. and Butow, R.A. (2005). Aconitase couples metabolic regulation to mitochondrial DNA maintenance. *Science* 307:714-717.
162. Butow, R.A. and Avadhani, N.G. (2004). Mitochondrial signaling: the retrograde response. *Mol. Cell* 14:1-15.
163. Liu, Z. and Butow, R.A. (2006). Mitochondrial retrograde signaling. *Annu. Rev. Genet.* 40:159-185.
164. Veal, E.A., Day, A.M. and Morgan, B.A. (2007). Hydrogen peroxide sensing and signaling. *Mol. Cell* 26:1-14.

165. Schulz, T.J., Zarse, K., Voigt, A., Urban, N., Birringer, M. and Ristow, M. (2007). Glucose restriction extends *Caenorhabditis elegans* life span by inducing mitochondrial respiration and increasing oxidative stress. *Cell Metab.* 6:280-293.
166. Kaeberlein, M., Hu, D., Kerr, E.O., Tsuchiya, M., Westman, E.A., Dang, N., Fields, S. and Kennedy, B.K. (2005). Increased life span due to calorie restriction in respiratory-deficient yeast. *PLoS Genet.* 1:e69.
167. Wei, M., Fabrizio, P., Hu, J., Ge, H., Cheng, C., Li, L. and Longo, V.D. (2008). Life span extension by calorie restriction depends on Rim15 and transcription factors downstream of Ras/PKA, Tor, and Sch9. *PLoS Genet.* 4:e13.
168. Anderson, R.M., and Weindruch, R. (2010). Metabolic reprogramming, caloric restriction and aging. *Trends Endocrinol. Metab.* 21:134-141.
169. François J., and Parrou, J.L. (2001). Reserve carbohydrates metabolism in the yeast *Saccharomyces cerevisiae*. *FEMS Microbiol. Rev.* 25:125-145.
170. Benaroudj, N., Lee, D.H., and Goldberg, A.L. (2001). Trehalose accumulation during cellular stress protects cells and cellular proteins from damage by oxygen radicals. *J. Biol. Chem.* 276:24261-24267.

171. Singer, M.A., and Lindquist, S. (1998a). Multiple effects of trehalose on protein folding *in vitro* and *in vivo*. *Mol. Cell* 1:639-648.
172. Singer, M.A., and Lindquist, S. (1998b). Thermotolerance in *Saccharomyces cerevisiae*: the Yin and Yang of trehalose. *Trends Biotechnol.* 16:460-468.
173. Jain, N.K., and Roy, I. (2009). Effect of trehalose on protein structure. *Protein Sci.* 18:24-36.
174. Jain, N.K., and Roy I. (2010). Trehalose and protein stability. *Curr. Protoc. Protein Sci.* 59:4.9.1-4.9.12.
175. Tavernarakis, N. (2010). *Protein Metabolism and Homeostasis in Aging*. Austin: Landes Bioscience.
176. Morimoto, R.I., Selkoe, D.J., and Kelly, J.W. (2012). *Protein Homeostasis*. Cold Spring Harbor: Cold Spring Harbor Laboratory Press.
177. Lin, S.S., Manchester, J.K., and Gordon, J.I. (2001). Enhanced gluconeogenesis and increased energy storage as hallmarks of aging in *Saccharomyces cerevisiae*. *J. Biol. Chem.* 276:36000-36007.

178. Titorenko, V.I., Smith, J.J., Szilard, R.K., and Rachubinski, R.A. (1998). Pex20p of the yeast *Yarrowia lipolytica* is required for the oligomerization of thiolase in the cytosol and for its targeting to the peroxisome. *J. Cell Biol.* 142:403-420.
179. Madeo, F., Fröhlich, E., and Fröhlich, K.-U. (1997). A yeast mutant showing diagnostic markers of early and late apoptosis. *J. Cell Biol.* 139:729-734.
180. Parsell, D.A., Kowal, A.S., Singer, M.A., and Lindquist, S. (1994). Protein disaggregation mediated by heat-shock protein Hsp104. *Nature* 372:475-478.
181. Boukh-Viner, T., Guo, T., Alexandrian, A., Cerracchio, A., Gregg, C., Haile, S., Kyskan, R., Milijevic, S., Oren, D., Solomon, J., Wong, V., Nicaud, J.-M., Rachubinski, R.A., English, A.M. and Titorenko, V.I. (2005). Dynamic ergosterol- and ceramide-rich domains in the peroxisomal membrane serve as an organizing platform for peroxisome fusion. *J. Cell Biol.* 168:761-773.
182. Chow, T., and Zukin, R.S. (1983). Solubilization and preliminary characterization of mu and kappa opiate receptor subtypes from rat brain. *Mol. Pharmacol.* 24:203-212.
183. Evans, E.A., Gilmore, R., and Blobel, G. (1986). Purification of microsomal signal peptidase as a complex. *Proc. Natl. Acad. Sci. USA* 83:581-585.

184. Tao, H., Liu, W., Simmons, B.N., Harris, H.K., Cox, T.C., and Massiah, M.A. (2010). Purifying natively folded proteins from inclusion bodies using sarkosyl, Triton X-100, and CHAPS. *Biotechniques* 48:61-64.
185. Harman, D. (1956). Aging: a theory based on free radical and radiation chemistry. *J. Gerontol.* 11:298-300.
186. Harman, D. (1972). The biologic clock: the mitochondria? *J. Am. Geriatr. Soc.* 20:145-147.
187. Gems, D., and Doonan, R. (2009). Antioxidant defense and aging in *C. elegans*: is the oxidative damage theory of aging wrong? *Cell Cycle* 8:1681-1687.
188. Pérez, V.I., Bokov, A., Van Remmen, H., Mele, J., Ran, Q., Ikeno, Y., and Richardson, A. (2009) Is the oxidative stress theory of aging dead? *Biochim. Biophys. Acta* 1790:1005-1014.
189. Lapointe, J., and Hekimi, S. (2010). When a theory of aging ages badly. *Cell. Mol. Life Sci.* 67:1-8.
190. Ristow, M., and Zarse K. (2010). How increased oxidative stress promotes longevity and metabolic health: The concept of mitochondrial hormesis (mitohormesis). *Exp. Gerontol.* 45:410-418.

191. Sanz, A., Fernández-Ayala, D.J., Stefanatos, R.K., and Jacobs, H.T. (2010). Mitochondrial ROS production correlates with, but does not directly regulate lifespan in *Drosophila*. *Aging* 2:200-223.
192. Hekimi, S., Lapointe, J., and Wen, Y. (2011). Taking a “good” look at free radicals in the aging process. *Trends Cell Biol.* 21:569-576.
193. Nyström, T. (2005). Role of oxidative carbonylation in protein quality control and senescence. *EMBO J.* 24:1311-1317.
194. Hipkiss, A.R. (2006). Accumulation of altered proteins and ageing: causes and effects. *Exp. Gerontol.* 41:464-473.
195. Chen, B., Retzlaff, M., Roos, T., and Frydman, J. (2011). Cellular strategies of protein quality control. *Cold Spring Harb. Perspect. Biol.* 3:a004374.
196. Gidalevitz, T., Prahlaad, V., and Morimoto, R.I. (2011). The stress of protein misfolding: from single cells to multicellular organisms. *Cold Spring Harb Perspect Biol.* 3:a009704.
197. Lindquist, S.L., and Kelly, J.W. (2011). Chemical and biological approaches for adapting proteostasis to ameliorate protein misfolding and aggregation diseases: progress and prognosis. *Cold Spring Harb. Perspect. Biol.* 3:a004507.

198. Taylor, R.C., and Dillin, A. (2011). Aging as an event of proteostasis collapse. *Cold Spring Harb. Perspect Biol.* 3:a004440.
199. Kikis, E.A., Gidalevitz, T., and Morimoto, R.I. (2010). Protein homeostasis in models of aging and age-related conformational disease. *Adv. Exp. Med. Biol.* 694:138-159.
200. Ben-Gedalya, T., Lyakhovetsky, R., Yedidia, Y., Bejerano-Sagie, M., Kogan, N.M., Karpuj, M.V., Kaganovich, D., and Cohen, E. (2011). Cyclosporin-A-induced prion protein aggregates are dynamic quality-control cellular compartments. *J. Cell Sci.* 124:1891-1902.
201. Ben-Gedalya, T., and Cohen, E. (2012). Quality control compartments coming of age. *Traffic* 13:635-642.
202. Titorenko, V.I., Smith, J.J., Szilard, R.K. and Rachubinski, R.A. (1998). Pex20p of the yeast *Yarrowia lipolytica* is required for the oligomerization of thiolase in the cytosol and for its targeting to the peroxisome. *J. Cell Biol.* 142:403-420.
203. Guo, T., Gregg, C., Boukh-Viner, T., Kyryakov, P., Goldberg, A., Bourque, S., Banu, F., Haile, S., Milijevic, S., San, K.H., Solomon, J., Wong, V. and Titorenko, V.I. (2007). A signal from inside the peroxisome initiates its division by promoting the remodeling of the peroxisomal membrane. *J. Cell Biol.* 177:289-303.

204. Czabany, T., Athenstaedt, K. and Daum, G. (2007). Synthesis, storage and degradation of neutral lipids in yeast. *Biochim. Biophys. Acta* 1771:299-309.
205. Hiltunen, J.K., Mursula, A.M., Rottensteiner, H., Wierenga, R.K., Kastaniotis, A.J. and Gurvitz, A. (2003). The biochemistry of peroxisomal β -oxidation in the yeast *Saccharomyces cerevisiae*. *FEMS Microbiol. Rev.* 27:35-64.
206. van der Klei, I.J., Yurimoto, H., Sakai, Y. and Veenhuis, M. (2006). The significance of peroxisomes in methanol metabolism in methylotrophic yeast. *Biochim. Biophys. Acta* 1763:1453-1462.
207. Binns, D., Januszewski, T., Chen, Y., Hill, J., Markin, V.S., Zhao, Y., Gilpin, C., Chapman, K.D., Anderson, R.G., and Goodman, J.M. (2006). An intimate collaboration between peroxisomes and lipid bodies. *J. Cell Biol.* 173:719-731.
208. Bener Aksam, E., Jungwirth, H., Kohlwein, S.D., Ring, J., Madeo, F., Veenhuis, M., and van der Klei, I.J. (2008). Absence of the peroxiredoxin Pmp20 causes peroxisomal protein leakage and necrotic cell death. *Free Radic. Biol. Med.* 45:1115-1124.
209. Jungwirth, H., Ring, J., Mayer, T., Schauer, A., Büttner, S., Eisenberg, T., Carmona-Gutierrez, D., Kuchler, K., and Madeo, F. (2008). Loss of peroxisome function triggers necrosis. *FEBS Lett.* 582:2882-2886.

210. Low, C.P., Liew, L.P., Pervaiz, S., and Yang, H. (2005). Apoptosis and lipoapoptosis in the fission yeast *Schizosaccharomyces pombe*. *FEMS Yeast Res.* 5:1199-1206.
211. Spitaler, M., and Cantrell, D.A. (2004). Protein kinase C and beyond. *Nat. Immunol.* 5:785-790.
212. Feng, H., Ren, M., Chen, L., and Rubin, C.S. (2007). Properties, regulation and *in vivo* functions of a novel protein kinase D: *C. elegans* DKF-2 links diacylglycerol second messenger to the regulation of stress responses and lifespan. *J. Biol. Chem.* 282:31273-31288.
213. Weindruch, R. and Walford, R.L. (1988). *The Retardation of Aging and Disease by Dietary Restriction*. Thomas, Springfield.
214. Masoro, E.J. (2002). *Caloric Restriction: A Key to Understanding and Modulating Aging*. Elsevier, Amsterdam.
215. Min, K.J., Flatt, T., Kulaots, I. and Tatar, M. (2007). Counting calories in *Drosophila* diet restriction. *Exp. Gerontol.* 42:247-251.
216. Colman, R.J., Anderson, R.M., Johnson, S.C., Kastman, E.K., Kosmatka, K.J., Beasley, T.M., Allison, D.B., Cruzen, C., Simmons, H.A., Kemnitz, J.W. and Weindruch,

- R. (2009). Caloric restriction delays disease onset and mortality in rhesus monkeys. *Science* 325:201-204.
217. Piper, M.D., Selman, C., McElwee, J.J. and Partridge, L. (2008). Separating cause from effect: how does insulin/IGF signalling control lifespan in worms, flies and mice? *J. Intern. Med.* 263:179-191.
218. Zimmerman, J.A., Malloy, V., Krajcik, R. and Orentreich, N. (2003). Nutritional control of aging. *Exp. Gerontol.* 38:47-52.
219. Mair, W., Piper, M.D. and Partridge, L. (2005). Calories do not explain extension of life span by dietary restriction in *Drosophila*. *PLoS Biol.* 3:e223.
220. Piper, M.D., Mair, W. and Partridge, L. (2005). Counting the calories: the role of specific nutrients in extension of life span by food restriction. *J. Gerontol. A Biol. Sci. Med. Sci.* 60:549-555.
221. Bartke, A., Masternak, M.M., Al-Regaiey, K.A. and Bonkowski, M.S. (2007). Effects of dietary restriction on the expression of insulin-signaling-related genes in long-lived mutant mice. *Interdiscip. Top. Gerontol.* 35:69-82.

222. Wanke, V., Cameroni, E., Uotila, A., Piccolis, M., Urban, J., Loewith, R. and De Virgilio, C. (2008). Caffeine extends yeast lifespan by targeting TORC1. *Mol. Microbiol.* 69:277-285.
223. Powers, R.W. 3rd, Kaeberlein, M., Caldwell, S.D., Kennedy, B.K. and Fields, S. (2006). Extension of chronological life span in yeast by decreased TOR pathway signaling. *Genes Dev.* 20:174-184.
224. Bonawitz ND, Chatenay-Lapointe M, Pan Y, Shadel GS. Reduced TOR signaling extends chronological life span via increased respiration and upregulation of mitochondrial gene expression. *Cell Metab.* 2007; 5: 265-277.
225. Ingram, D.K., Zhu, M., Mamczarz, J., Zou, S., Lane, M.A., Roth, G.S., and deCabo, R. (2006). Calorie restriction mimetics: an emerging research field. *Aging Cell* 5:97-108.
226. Lane, M.A., Roth, G.S., and Ingram, D.K. (2007). Caloric restriction mimetics: a novel approach for biogerontology. *Methods Mol. Biol.* 371:143-149.
227. Howitz, K.T., Bitterman, K.J., Cohen, H.Y., Lamming, D.W., Lavu, S., Wood, J.G., Zipkin, R.E., Chung, P., Kisielewski, A., Zhang, L.L., Scherer, B., and Sinclair, D.A. (2003). Small molecule activators of sirtuins extend *Saccharomyces cerevisiae* lifespan. *Nature* 425:191-196.

228. Wood, J.G., Rogina, B., Lavu, S., Howitz, K., Helfand, S.L., Tatar, M., and Sinclair, D. (2004). Sirtuin activators mimic caloric restriction and delay ageing in metazoans. *Nature* 430:686-689.
229. Baur, J.A., Pearson, K.J., Price, N.L., Jamieson, H.A., Lerin, C., Kalra, A., Prabhu, V.V., Allard, J.S., Lopez-Lluch, G., Lewis, K., Pistell, P.J., Poosala, S., Becker, K.G. et al. (2006). Resveratrol improves health and survival of mice on a high-calorie diet. *Nature* 444:337-342.
230. Petrascheck, M., Ye, X., and Buck, L.B. (2007). An antidepressant that extends lifespan in adult *Caenorhabditis elegans*. *Nature* 450:553-556.
231. Onken, B., and Driscoll, M. (2010). Metformin induces a dietary restriction-like state and the oxidative stress response to extend *C. elegans* healthspan via AMPK, LKB1, and SKN-1. *PLoS ONE* 5:e8758.
232. McColl, G., Killilea, D.W., Hubbard, A.E., Vantipalli, M.C., Melov, S. and Lithgow, G.J. (2008). Pharmacogenetic analysis of lithium-induced delayed aging in *Caenorhabditis elegans*. *J. Biol. Chem.* 283:350-357.
233. Bjedov I, Toivonen JM, Kerr F, Slack C, Jacobson J, Foley A, Partridge L. Mechanisms of life span extension by rapamycin in the fruit fly *Drosophila melanogaster*. *Cell Metab.* 2010; 11: 35-46.

234. Narbonne, P. and Roy, R. (2009). *Caenorhabditis elegans* dauers need LKB1/AMPK to ration lipid reserves and ensure long-term survival. *Nature* 457:210-214.
235. Soukas, A.A., Kane, E.A., Carr, C.E., Melo, J.A. and Ruvkun, G. (2009). Rictor/TORC2 regulates fat metabolism, feeding, growth, and life span in *Caenorhabditis elegans*. *Genes Dev.* 23:496-511.
236. Wang, M.C., O'Rourke, E.J. and Ruvkun, G. (2008). Fat metabolism links germline stem cells and longevity in *C. elegans*. *Science* 322:957-960.
237. Grönke, S., Mildner, A., Fellert, S., Tennagels, N., Petry, S., Müller, G., Jäckle, H. and Kühnlein, R.P. (2005). Brummer lipase is an evolutionary conserved fat storage regulator in *Drosophila*. *Cell Metab.* 1:323-330.
238. Picard, F., Kurtev, M., Chung, N., Topark-Ngarm, A., Senawong, T., Machado De Oliveira, R., Leid, M., McBurney, M.W. and Guarente, L. (2004). Sirt1 promotes fat mobilization in white adipocytes by repressing PPAR- γ . *Nature* 429:771-776.
239. Blüher, M., Kahn, B.B. and Kahn, C.R. (2003). Extended longevity in mice lacking the insulin receptor in adipose tissue. *Science* 299:572-574.
240. Chiu, C.H., Lin, W.D., Huang, S.Y. and Lee, Y.H. (2004). Effect of a C/EBP gene replacement on mitochondrial biogenesis in fat cells. *Genes Dev.* 18:1970-1975.

241. Haemmerle, G., Lass, A., Zimmermann, R., Gorkiewicz, G., Meyer, C., Rozman, J., Heldmaier, G., Maier, R., Theussl, C., Eder, S., Kratky, D., Wagner, E.F. and Klingenspor, M. (2006). Defective lipolysis and altered energy metabolism in mice lacking adipose triglyceride lipase. *Science* 312:734-737.
242. Gerhart-Hines, Z., Rodgers, J.T., Bare, O., Lerin, C., Kim, S.H., Mostoslavsky, R., Alt, F.W., Wu, Z. and Puigserver, P. (2007). Metabolic control of muscle mitochondrial function and fatty acid oxidation through SIRT1/PGC-1 α . *EMBO J.* 26:1913-1923.
243. Léon, S., Goodman, J.M. and Subramani, S. (2006). Uniqueness of the mechanism of protein import into the peroxisome matrix: transport of folded, co-factor-bound and oligomeric proteins by shuttling receptors. *Biochim. Biophys. Acta* 1763:1552-1264.
244. Low, C.P., Liew, L.P., Pervaiz, S. and Yang, H. (2005). Apoptosis and lipoapoptosis in the fission yeast *Schizosaccharomyces pombe*. *FEMS Yeast Res.* 5:1199-1206.
245. Giorgio, M., Trinei, M., Migliaccio, E. and Pelicci, P.G. (2007). Hydrogen peroxide: a metabolic by-product or a common mediator of ageing signals? *Nat. Rev. Mol. Cell Biol.* 8:722-728.

246. D'Autréaux, B. and Toledano, M.B. (2007). ROS as signalling molecules: mechanisms that generate specificity in ROS homeostasis. *Nat. Rev. Mol. Cell Biol.* 8:813-824.
247. Dirkx, R., Vanhorebeek, I., Martens, K., Schad, A., Grabenbauer, M., Fahimi, D., Declercq, P., Van Veldhoven, P.P. and Baes, M. (2005). Absence of peroxisomes in mouse hepatocytes causes mitochondrial and ER abnormalities. *Hepatology* 41:868-878.
248. Eisenberg, T., Büttner, S., Kroemer, G. and Madeo, F. (2007). The mitochondrial pathway in yeast apoptosis. *Apoptosis* 12:1011-1023.
249. Pereira, C., Silva, R.D., Saraiva, L., Johansson, B., Sousa, M.J. and Côte-Real, M. (2008). Mitochondria-dependent apoptosis in yeast. *Biochim. Biophys. Acta* 1783:1286-1302.
250. Pereira, C., Camougrand, N., Manon, S., Sousa, M.J. and Côte-Real, M. (2007). ADP/ATP carrier is required for mitochondrial outer membrane permeabilization and cytochrome c release in yeast apoptosis. *Mol. Microbiol.* 66:571-582.
251. Fabrizio, P. and Longo, V.D. (2008). Chronological aging-induced apoptosis in yeast. *Biochim. Biophys. Acta* 1783:1280-1285.

252. Hamann, A., Brust, D. and Osiewacz, H.D. (2008). Apoptosis pathways in fungal growth, development and ageing. *Trends Microbiol.* 16:276-283.
253. Finley, L.W. and Haigis, M.C. (2009). The coordination of nuclear and mitochondrial communication during aging and calorie restriction. *Ageing Res. Rev.* 8:173-188.
254. Skulachev, V.P., Anisimov, V.N., Antonenko, Y.N., Bakeeva, L.E., Chernyak, B.V., Elichev, V.P., Filenko, O.F., Kalinina, N.I., Kapelko, V.I., Kolosova, N.G., Kopnin, B.P., Korshunova, G.A., Lichinitser, M.R., Obukhova, L.A., Pasyukova, E.G., Pisarenko, O.I., Roginsky, V.A., Ruuge, E.K., Senin, I.I., Severina, I.I., Skulachev, M.V., Spivak, I.M., Tashlitsky, V.N., Tkachuk, V.A., Vyssokikh, M.Y., Yaguzhinsky, L.S. and Zorov, D.B. (2009). An attempt to prevent senescence: a mitochondrial approach. *Biochim. Biophys. Acta* 1787:437-461.
255. Lapointe, J. and Hekimi, S. (2010). When a theory of aging ages badly. *Cell Mol. Life Sci.* 67:1-8.
256. Schulz, T.J., Zarse, K., Voigt, A., Urban, N., Birringer, M. and Ristow, M. (2007). Glucose restriction extends *Caenorhabditis elegans* life span by inducing mitochondrial respiration and increasing oxidative stress. *Cell Metab.* 6:280-293.

257. Gems, D. and Partridge, L. (2008). Stress-response hormesis and aging: "that which does not kill us makes us stronger". *Cell Metab.* 7:200-203.
258. Pang, C.Y., Ma, Y.S. and Wei, Y.U. (2008). MtDNA mutations, functional decline and turnover of mitochondria in aging. *Front. Biosci.* 13:3661-3675.
259. Sinclair, D.A. and Oberdoerffer, P. (2009). The ageing epigenome: damaged beyond repair? *Ageing Res. Rev.* 8:189-198.
260. Sherman, F. (2002). Getting started with yeast. *Methods Enzymol.* 350:3-41.
261. Dillin, A., Hsu, A.L., Arantes-Oliveira, N., Lehrer-Graiwer, J., Hsin, H., Fraser, A.G., Kamath, R.S., Ahringer, J., and Kenyon, C. (2002). Rates of behavior and aging specified by mitochondrial function during development. *Science* 298:2398-2401.
262. Tsang, W.Y., and Lemire, B.D. (2002). Mitochondrial genome content is regulated during nematode development. *Biochem. Biophys. Res. Commun.* 291:8-16.
263. Rea, S.L., Ventura, N., and Johnson, T.E. (2007). Relationship between mitochondrial electron transport chain dysfunction, development, and life extension in *Caenorhabditis elegans*. *PLoS Biol.* 5:e259.

264. Durieux, J., and Dillin, A. (2007). Mitochondria and aging: dilution is the solution. *Cell Metab.* 6:427-429.
265. Butler, J.A., Ventura, N., Johnson, T.E., and Rea, S.L. (2010). Long-lived mitochondrial (Mit) mutants of *Caenorhabditis elegans* utilize a novel metabolism. *FASEB J.* 24:4977-4988.
266. Gallo, M., Park, D., and Riddle, D.L. (2011). Increased longevity of some *C. elegans* mitochondrial mutants explained by activation of an alternative energy-producing pathway. *Mech. Ageing Dev.* 132:515-518.
267. Durieux, J., Wolff, S., and Dillin, A. (2011). The cell-non-autonomous nature of electron transport chain-mediated longevity. *Cell* 144:79-91.
268. Woo, D.K., and Shadel, G.S. (2011). Mitochondrial stress signals revise an old aging theory. *Cell* 144:11-12.
269. Dillin, A., Crawford, D.K., and Kenyon, C. (2002). Timing requirements for insulin/IGF-1 signaling in *C. elegans*. *Science* 298:830-834.
270. Mukhopadhyay, A., and Tissenbaum, H.A. (2007). Reproduction and longevity: secrets revealed by *C. elegans*. *Trends Cell Biol.* 17:65-71.

271. Panowski, S.H., and Dillin, A. (2009). Signals of youth: endocrine regulation of aging in *Caenorhabditis elegans*. *Trends Endocrinol. Metab.* 20:259-264.
272. Panowski, S.H., Wolff, S., Aguilaniu, H., Durieux, J. and Dillin, A. (2007). PHA-4/Foxa mediates diet-restriction-induced longevity of *C. elegans*. *Nature* 447: 550-555.
273. Weindruch, R., and Walford, R.L. (1982). Dietary restriction in mice beginning at 1 year of age: effects on lifespan and spontaneous cancer incidence. *Science* 215:1415-1418.
274. Yu, B.P., Masoro, E.J., and McMahan, C.A. (1985). Life span study of SPF Fischer 344 male rats. I. Physical, metabolic, and longevity characteristics. *J. Gerontol.* 40:657-670.
275. Masoro, E.J. (2005). Overview of caloric restriction and ageing. *Mech. Ageing Dev.* 126:913-922.
276. Blagosklonny, M.V., and Hall, M.N. (2009). Growth and aging: a common molecular mechanism. *Aging* 1:357-362.
277. Hands, S.L., Proud, C.G., and Wytenbach, A. (2009). mTOR's role in ageing: protein synthesis or autophagy? *Aging* 1:586-597.

278. Goldberg, A.A., Kyryakov, P., Bourque, S.D., and Titorenko, V.I. (2010). Xenohormetic, hormetic and cytostatic selective forces driving longevity at the ecosystemic level. *Aging* 2:361-370.
279. Chen, C., Liu, Y., Liu, Y., and Zheng, P. (2009). mTOR regulation and therapeutic rejuvenation of aging hematopoietic stem cells. *Sci. Signal.* 2:ra75.
280. Harrison, D.E., Strong, R., Sharp, Z.D., Nelson, J.F., Astle, C.M., Flurkey, K., Nadon, N.L., Wilkinson, J.E., Frenkel, K., Carter, C.S., Pahor, M., Javors, M.A., Fernandez, E., and Miller, R.A. (2009). Rapamycin fed late in life extends lifespan in genetically heterogeneous mice. *Nature* 460:392-395.
281. Anisimov, V.N., Zabezhinski, M.A., Popovich, I.G., Piskunova, T.S., Semenchko, A.V., Tyndyk, M.L., Yurova, M.N., Antoch, M.P., and Blagosklonny, M.V. (2010). Rapamycin extends maximal lifespan in cancer-prone mice. *Am. J. Pathol.* 176:2092-2097.
282. Anisimov, V.N., Zabezhinski, M.A., Popovich, I.G., Piskunova, T.S., Semenchko, A.V., Tyndyk, M.L., Yurova, M.N., Rosenfeld, S.V., and Blagosklonny, M.V. (2011). Rapamycin increases lifespan and inhibits spontaneous tumorigenesis in inbred female mice. *Cell Cycle* 10:12-15.

283. Miller, R.A., Harrison, D.E., Astle, C.M., Baur, J.A., Boyd, A.R., de Cabo, R., Fernandez, E., Flurkey, K., Javors, M.A., Nelson, J.F., Orihuela, C.J., Pletcher, S., Sharp, Z.D., Sinclair, D., Starnes, J.W., Wilkinson, J.E., Nadon, N.L., and Strong, R. (2011). Rapamycin, but not resveratrol or simvastatin, extends life span of genetically heterogeneous mice. *J. Gerontol. A Biol. Sci. Med. Sci.* 66:191-201.
284. Wilkinson, J.E., Burmeister, L., Brooks, S.V., Chan, C.C., Friedline, S., Harrison, D.E., Hejtmancik, J.F., Nadon, N., Strong, R., Wood, L.K., Woodward, M.A., and Miller, R.A. (2012). Rapamycin slows aging in mice. *Aging Cell* doi: 10.1111/j.1474-9726.2012.00832.x. [Epub ahead of print].
285. Wanke, V., Cameroni, E., Uotila, A., Piccolis, M., Urban, J., Loewith, R. and De Virgilio, C. (2008). Caffeine extends yeast lifespan by targeting TORC1. *Mol. Microbiol.* 69:277-285.
286. Laplante, M. and Sabatini, D.M. (2009). mTOR signaling at a glance. *J. Cell Sci.* 122:3589-3594.
287. Wullschleger, S., Loewith, R. and Hall, M.N. (2006). TOR signaling in growth and metabolism. *Cell* 124:471-484.

288. McColl, G., Killilea, D.W., Hubbard, A.E., Vantipalli, M.C., Melov, S. and Lithgow, G.J. (2008). Pharmacogenetic analysis of lithium-induced delayed aging in *Caenorhabditis elegans*. *J. Biol. Chem.* 283:350-357.
289. Sinclair, D.A. and Oberdoerffer, P. (2009). The ageing epigenome: damaged beyond repair? *Ageing Res. Rev.* 8:189-198.
290. Benedetti, M.G., Foster, A.L., Vantipalli, M.C., White, M.P., Sampayo, J.N., Gill, M.S., Olsen, A. and Lithgow, G.J. (2008). Compounds that confer thermal stress resistance and extended lifespan. *Exp. Gerontol.* 43:882-891.
291. Bauer, J.H., Goupil, S., Garber, G.B. and Helfand, S.L. (2004). An accelerated assay for the identification of lifespan-extending interventions in *Drosophila melanogaster*. *Proc. Natl. Acad. Sci. USA* 101:12980-12985.
292. Onken, B. and Driscoll, M. (2010). Metformin induces a dietary restriction-like state and the oxidative stress response to extend *C. elegans* healthspan via AMPK, LKB1, and SKN-1. *PLoS ONE* 5:e8758.
293. Anisimov, V.N., Berstein, L.M., Egormin, P.A., Piskunova, T.S., Popovich, I.G., Zabezhinski, M.A., Tyndyk, M.L., Yurova, M.V., Kovalenko, I.G., Poroshina, T.E. and Semchenko, A.V. (2008). Metformin slows down aging and extends life span of female SHR mice. *Cell Cycle* 7:2769-2773.

294. Shaw, R.J., Lamia, K.A., Vasquez, D., Koo, S.H., Bardeesy, N., Depinho, R.A., Montminy, M. and Cantley, L.C. (2005). The kinase LKB1 mediates glucose homeostasis in liver and therapeutic effects of metformin. *Science* 310:1642-1646.
295. Shaw, R.J. (2009). LKB1 and AMP-activated protein kinase control of mTOR signalling and growth. *Acta Physiol.* 196:65-80.
296. Powers, R.W. 3rd, Kaeberlein, M., Caldwell, S.D., Kennedy, B.K. and Fields, S. (2006). Extension of chronological life span in yeast by decreased TOR pathway signaling. *Genes Dev.* 20:174-184.
297. Crespo, J.L, Powers, T., Fowler, B. and Hall, M.N. (2002). The TOR-controlled transcription activators *GLN3*, *RTG1*, and *RTG3* are regulated in response to intracellular levels of glutamine. *Proc. Natl. Acad. Sci. USA* 99:6784-6789.
298. Petrascheck, M., Ye, X. and Buck, LB. (2007). An antidepressant that extends lifespan in adult *Caenorhabditis elegans*. *Nature* 450:553-556.
299. Bjedov I, Toivonen JM, Kerr F, Slack C, Jacobson J, Foley A, Partridge L. Mechanisms of life span extension by rapamycin in the fruit fly *Drosophila melanogaster*. *Cell Metab.* 2010; 11: 35-46.

300. Bonawitz ND, Chatenay-Lapointe M, Pan Y, Shadel GS. Reduced TOR signaling extends chronological life span via increased respiration and upregulation of mitochondrial gene expression. *Cell Metab.* 2007; 5: 265-277.
301. Medvedik O, Lamming DW, Kim KD, Sinclair DA. MSN2 and MSN4 link calorie restriction and TOR to sirtuin-mediated lifespan extension in *Saccharomyces cerevisiae*. *PLoS Biol.* 2007; 5: e261.
302. Harrison DE, Strong R, Sharp ZD, Nelson JF, Astle CM, Flurkey K, Nadon NL, Wilkinson JE, Frenkel K, Carter CS, Pahor M, Javors MA, Fernandez E, Miller RA. Rapamycin fed late in life extends lifespan in genetically heterogeneous mice. *Nature* 2009; 460: 392-395.
303. Alvers AL, Wood MS, Hu D, Kaywell AC, Dunn WA Jr, Aris JP. Autophagy is required for extension of yeast chronological life span by rapamycin. *Autophagy* 2009; 5: 847-849.
304. Howitz, K.T., Bitterman, K.J., Cohen, H.Y., Lamming, D.W., Lavu, S., Wood, J.G., Zipkin, R.E., Chung, P., Kisielewski, A., Zhang, L.L., Scherer, B. and Sinclair, D.A. (2003). Small molecule activators of sirtuins extend *Saccharomyces cerevisiae* lifespan. *Nature* 425:191-196.

305. Wood, J.G., Rogina, B., Lavu, S., Howitz, K., Helfand, S.L., Tatar, M. and Sinclair, D. (2004). Sirtuin activators mimic caloric restriction and delay ageing in metazoans. *Nature* 430:686-689.

306. Baur, J.A., Pearson, K.J., Price, N.L., Jamieson, H.A., Lerin, C., Kalra, A., Prabhu, V.V., Allard, J.S., Lopez-Lluch, G., Lewis, K., Pistell, P.J., Poosala, S., Becker, K.G., Boss, O., Gwinn, D., Wang, M., Ramaswamy, S., Fishbein, K.W., Spencer, R.G., Lakatta, E.G., Le Couteur, D., Shaw, R.J., Navas, P., Puigserver, P., Ingram, D.K., de Cabo, R. and Sinclair, D.A. (2006). Resveratrol improves health and survival of mice on a high-calorie diet. *Nature* 444:337-342.

307. Valenzano, D.R., Terzibasi, E., Genade, T., Cattaneo, A., Domenici, L. and Cellierino, A. (2006). Resveratrol prolongs lifespan and retards the onset of age-related markers in a short-lived vertebrate. *Curr. Biol.* 16:296-300.

308. Demidenko, Z.N. and Blagosklonny, M.V. (2009). At concentrations that inhibit mTOR, resveratrol suppresses cellular senescence. *Cell Cycle* 8:1901-1904.

309. Pearson, K.J., Baur, J.A., Lewis, K.N., Peshkin, L., Price, N.L., Labinsky, N., Swindell, W.R., Kamara, D., Minor, R.K., Perez, E., Jamieson, H.A., Zhang, Y., Dunn, S.R., Sharma, K., Pleshko, N., Woollett, L.A., Csiszar, A., Ikeno, Y., Le Couteur, D., Elliott, P.J., Becker, K.G., Navas, P., Ingram, D.K., Wolf, N.S., Ungvari, Z., Sinclair, D.A. and de Cabo, R. (2008). Resveratrol delays age-related deterioration and mimics

transcriptional aspects of dietary restriction without extending life span. *Cell Metab.* 8:157-168.

310. Viswanathan, M., Kim, S.K., Berdichevsky, A. and Guarente, L. (2005). A role for SIR-2.1 regulation of ER stress response genes in determining *C. elegans* life span. *Dev. Cell* 9:605-615.

311. Lagouge, M., Argmann, C., Gerhart-Hines, Z., Meziane, H., Lerin, C., Daussin, F., Messadeq, N., Milne, J., Lambert, P., Elliott, P., Geny, B., Laakso, M., Puigserver, P. and Auwerx, J. (2006). Resveratrol improves mitochondrial function and protects against metabolic disease by activating SIRT1 and PGC-1 α . *Cell* 127:1109-1122.

312. Picard, F., Kurtev, M., Chung, N., Topark-Ngarm, A., Senawong, T., Machado De Oliveira, R., Leid, M., McBurney, M.W. and Guarente, L. (2004). Sirt1 promotes fat mobilization in white adipocytes by repressing PPAR- γ . *Nature* 429:771-776.

313. Blagosklonny, MV. (2009). TOR-driven aging: speeding car without brakes. *Cell Cycle* 8:4055-4059.

314. Morselli, E., Maiuri, M.C., Markaki, M., Megalou, E., Pasparaki, A., Palikaras, K., Criollo, A., Galluzzi, L., Malik, S.A., Vitale, I., Michaud, M., Madeo, F., Tavernarakis, N. and Kroemer, G. (2010). Caloric restriction and resveratrol promote longevity through the Sirtuin-1-dependent induction of autophagy. *Cell Death Dis.* 1:e10.

315. Morselli, E., Maiuri, M.C., Markaki, M., Megalou, E., Pasparaki, A., Palikaras, K., Criollo, A., Galluzzi, L., Malik, S.A., Vitale, I., Michaud, M., Madeo, F., Tavernarakis, N. and Kroemer, G. (2010). The life span-prolonging effect of sirtuin-1 is mediated by autophagy. *Autophagy* 6:186-188.
316. Morselli, E., Galluzzi, L., Kepp, O., Criollo, A., Maiuri, M.C., Tavernarakis, N., Madeo, F. and Kroemer, G. (2009). Autophagy mediates pharmacological lifespan extension by spermidine and resveratrol. *Aging* 1:961-970.
317. Skulachev, V.P., Anisimov, V.N., Antonenko, Y.N., Bakeeva, L.E., Chernyak, B.V., Elichev, V.P., Filenko, O.F., Kalinina, N.I., Kapelko, V.I., Kolosova, N.G., Kopnin, B.P., Korshunova, G.A., Lichinitser, M.R., Obukhova, L.A., Pasyukova, E.G., Pisarenko, O.I., Roginsky, V.A., Ruuge, E.K., Senin, I.I., Severina, I.I., Skulachev, M.V., Spivak, I.M., Tashlitsky, V.N., Tkachuk, V.A., Vyssokikh, M.Y., Yaguzhinsky, L.S. and Zorov, D.B. (2009). An attempt to prevent senescence: a mitochondrial approach. *Biochim. Biophys. Acta* 1787:437-461.
318. Engel, N. and Mahlknecht, U. (2008). Aging and anti-aging: unexpected side effects of everyday medication through sirtuin1 modulation. *Int. J. Mol. Med.* 21:223-232.
319. Eisenberg, T., Knauer, H., Schauer, A., Büttner, S., Ruckenstein, C., Carmona-Gutierrez, D., Ring, J., Schroeder, S., Magnes, C., Antonacci, L., Fussi, H., Deszcz, L., Hartl, R., Schraml, E., Criollo, A., Megalou, E., Weiskopf, D., Laun, P., Heeren, G.,

Breitenbach, M., Grubeck-Loebenstein, B., Herker, E., Fahrenkrog, B., Fröhlich, K.U., Sinner, F., Tavernarakis, N., Minois, N., Kroemer, G. and Madeo, F. (2009). Induction of autophagy by spermidine promotes longevity. *Nat. Cell Biol.* 11:1305-1314.

320. Evason, K., Collins, J.J., Huang, C., Hughes, S. and Kornfeld, K. (2008). Valproic acid extends *Caenorhabditis elegans* lifespan. *Aging Cell* 7:305-317.

321. Demidenko, Z.N., Shtutman, M. and Blagosklonny, M.V. (2009). Pharmacologic inhibition of MEK and PI-3K converges on the mTOR/S6 pathway to decelerate cellular senescence. *Cell Cycle* 8:1896-1900.

322. Zarse, K. and Ristow, M. (2008). Antidepressants of the serotonin-antagonist type increase body fat and decrease lifespan of adult *Caenorhabditis elegans*. *PLoS ONE* 3:e4062.

323. Kaeberlein, M., McDonagh, T., Heltweg, B., Hixon, J., Westman, E.A., Caldwell, S.D., Napper, A., Curtis, R., DiStefano, P.S., Fields, S., Bedalov, A. and Kennedy, B.K. (2005). Substrate-specific activation of sirtuins by resveratrol. *J. Biol. Chem.* 280:17038-17045.

324. Bass, T.M., Weinkove, D., Houthoofd, K., Gems, D. and Partridge, L. (2007). Effects of resveratrol on lifespan in *Drosophila melanogaster* and *Caenorhabditis elegans*. *Mech. Ageing Dev.* 128:546-552.

325. Borra, M.T., Smith, B.C. and Denu, J.M. (2005). Mechanism of human SIRT1 activation by resveratrol. *J. Biol. Chem.* 280:17187-17195.
326. Denu, J.M. (2005). The Sir 2 family of protein deacetylases. *Curr. Opin. Chem. Biol.* 9:431-440.
327. Kaeberlein, M. and Kennedy, B.K. (2007). Does resveratrol activate yeast Sir2 in vivo? *Aging Cell* 6:415-416.
328. Harikumar, K.B. and Aggarwal, B.B. (2008). Resveratrol: a multitargeted agent for age-associated chronic diseases. *Cell Cycle* 7:1020-1035.
329. Shakibaei, M., Harikumar, K.B. and Aggarwal, B.B. (2009). Resveratrol addiction: to die or not to die. *Mol. Nutr. Food Res.* 53:115-128.
330. Strong, R., Miller, R.A., Astle, C.M., Floyd, R.A., Flurkey, K., Hensley, K.L., Javors, M.A., Leeuwenburgh, C., Nelson, J.F., Ongini, E., Nadon, N.L., Warner, H.R., and Harrison, D.E. (2008). Nordihydroguaiaretic acid and aspirin increase lifespan of genetically heterogeneous male mice. *Aging Cell* 7:641-650.
331. Weissmann, G. (1991). Aspirin. *Sci. Am.* 264:84-90.

332. Shi, X., Ding, M., Dong, Z., Chen, F., Ye, J., Wang, S., Leonard, S.S., Castranova, V., and Vallyathan, V. (1999). Antioxidant properties of aspirin: characterization of the ability of aspirin to inhibit silica-induced lipid peroxidation, DNA damage, NF-kappaB activation, and TNF-alpha production. *Mol. Cell. Biochem.* 199:93-102.
333. Vane, S.J. (2000). Aspirin and other anti-inflammatory drugs. *Thorax* 55:3-9.
334. Mitchell, J.A., Akarasereenont, P., Thiemermann, C., Flower, R.J., and Vane, J.R. (1993). Selectivity of nonsteroidal antiinflammatory drugs as inhibitors of constitutive and inducible cyclooxygenase. *Proc. Natl. Acad. Sci. USA* 90:11693-11697.
335. Stark, L.A., Reid, K., Sansom, O.J., Din, F.V., Guichard, S., Mayer, I., Jodrell, D.I., Clarke, A.R., and Dunlop, M.G. (2007). Aspirin activates the NF- κ B signalling pathway and induces apoptosis in intestinal neoplasia in two in vivo models of human colorectal cancer. *Carcinogenesis* 28:968-976.
336. Tuttle, R.S., Yager, J., and Northrup, N. (1988). Age and the antihypertensive effect of aspirin in rats. *Br. J. Pharmacol.* 94:755-758.
337. Miquel, J., Fleming, J., and Economos, A.C. (1982). Antioxidants, metabolic rate and aging in *Drosophila*. *Arch. Gerontol. Geriatr.* 1:159-165.

338. Richie, J.P. Jr., Mills, B.J., and Lang, C.A. (1986). Dietary nordihydroguaiaretic acid increases the life span of the mosquito. *Proc. Soc. Exp. Biol. Med.* 183:81-85.
339. Buu-Hoi, N.P., and Ratsimamanga, A.R. (1959). Retarding action of nordihydroguaiaretic acid on aging in the rat. *CR Seances Soc. Biol. Fil.* 153:1180-1182.
340. Reed, M.J., Meszaros, K., Entes, L.J., Claypool, M.D., Pinkett, J.G., Brignetti, D., Luo, J., Khandwala, A., and Reaven, G.M. (1999). Effect of masoprocol on carbohydrate and lipid metabolism in a rat model of type II diabetes. *Diabetologia* 42:102-106.
341. Park, Y., and Pariza, M.W. (2001). Lipoxygenase inhibitors inhibit heparin-releasable lipoprotein lipase activity in 3T3-L1 adipocytes and enhance body fat reduction in mice by conjugated linoleic acid. *Biochim. Biophys. Acta* 1534:27-33.
342. Li, B.H., Ma, X.F., Wang, Y., Tian, W.X. (2005). Structure-activity relationship of polyphenols that inhibit Fatty Acid synthase. *J. Biochem. (Tokyo)* 138:679-685.
343. McDonald, R.W., Bunjobpon, W., Liu, T., Fessler, S., Pardo, O.E., Freer, I.K., Glaser, M., Seckl, M.J., and Robins, D.J. (2001). Synthesis and anticancer activity of nordihydroguaiaretic acid (NDGA) and analogues. *Anticancer Drug Des.* 16:261-270.
344. Hoferova, Z., Soucek, K., Hofmanova, J., Hofer, M., Chramostova, K., Fedorocko, P., and Kozubik, A. (2004). In vitro proliferation of fibrosarcoma cells depends on intact

functions of lipoxygenases and cytochrome P-450-monoxygenase. *Cancer Invest.* 22:234-247.

345. Nony, P.A., Kennett, S.B., Glasgow, W.C., Olden, K., and Roberts, J.D. (2005). 15S-Lipoxygenase-2 mediates arachidonic acid-stimulated adhesion of human breast carcinoma cells through the activation of TAK1, MKK6, and p38 MAPK. *J. Biol. Chem.* 280:31413-31419.

346. Youngren, J.F., Gable, K., Penaranda, C., Maddux, B.A., Zavodovskaya, M., Lobo, M., Campbell, M., Kerner, J., and Goldfine, I.D. (2005). Nordihydroguaiaretic acid (NDGA) inhibits the IGF-1 and c-erbB2/HER2/neu receptors and suppresses growth in breast cancer cells. *Breast Cancer Res. Treat.* 94:37-46.

347. Harper, A., Kerr, D.J., Gescher, A., and Chipman, J.K. (1999). Antioxidant effects of isoflavonoids and lignans, and protection against DNA oxidation. *Free Radic. Res.* 31:149-160.

348. Büttner, S., Eisenberg, T., Herker, E., Carmona-Gutierrez, D., Kroemer, G., and Madeo, F. (2006). Why yeast cells can undergo apoptosis: death in times of peace, love, and war. *J. Cell Biol.* 175:521-525.

349. Eisenberg, T., Büttner, S., Kroemer, G., and Madeo, F. (2007). The mitochondrial pathway in yeast apoptosis. *Apoptosis* 12:1011-1023.

350. Mazzoni, C., and Falcone, C. (2008). Caspase-dependent apoptosis in yeast. *Biochim. Biophys. Acta* 1783:1320-1327.
351. Pereira, C., Silva, R.D., Saraiva, L., Johansson, B., Sousa, M.J., and Côte-Real, M. (2008). Mitochondria-dependent apoptosis in yeast. *Biochim. Biophys. Acta* 1783:1286-1302.
352. Ludovico, P., Rodrigues, F., Almeida, A., Silva, M.T., Barrientos, A., and Côte-Real, M. (2004). Cytochrome c release and mitochondria involvement in programmed cell death induced by acetic acid in *Saccharomyces cerevisiae*. *Mol. Biol. Cell* 13:2598-2606.
353. Fannjiang, Y., Cheng, W.C., Lee, S.J., Qi, B., Pevsner, J., McCaffery, J.M., Hill, R.B., Basañez, G., and Hardwick, J.M. (2004). Mitochondrial fission proteins regulate programmed cell death in yeast. *Genes Dev.* 18:2785-2797.
354. Wissing, S., Ludovico, P., Herker, E., Büttner, S., Engelhardt, S.M., Decker, T., Link, A., Proksch, A., Rodrigues, F., Corte-Real, M., Fröhlich, K.U., Manns, J., Candé, C., Sigrist, S.J., Kroemer, G., and Madeo, F. (2004). An AIF orthologue regulates apoptosis in yeast. *J. Cell Biol.* 166:969-974.

355. Pozniakovsky, A.I., Knorre, D.A., Markova, O.V., Hyman, A.A., Skulachev, V.P., and Severin, F.F. (2005). Role of mitochondria in the pheromone- and amiodarone-induced programmed death of yeast. *J. Cell Biol.* 168:257-269.
356. Sokolov, S., Knorre, D., Smirnova, E., Markova, O., Pozniakovsky, A., Skulachev, V., and Severin, F.F. (2006). Ysp2 mediates death of yeast induced by amiodarone or intracellular acidification. *Biochim. Biophys. Acta* 1757:1366-1370.
357. Büttner, S., Eisenberg, T., Carmona-Gutierrez, D., Ruli, D., Knauer, H., Ruckenstuhl, C., Sigrist, C., Wissing, S., Kollroser, M., Fröhlich, K.U., Sigrist, S., and Madeo, F. (2007). Endonuclease G regulates budding yeast life and death. *Mol. Cell* 25:233-246.
358. Kitagaki, H., Araki, Y., Funato, K., and Shimoi, H. (2007). Ethanol-induced death in yeast exhibits features of apoptosis mediated by mitochondrial fission pathway. *FEBS Lett.* 581:2935-2942.
359. Pereira, C., Camougrand, N., Manon, S., Sousa, M.J., and Côte-Real, M. (2007). ADP/ATP carrier is required for mitochondrial outer membrane permeabilization and cytochrome c release in yeast apoptosis. *Mol. Microbiol.* 66:571-582.

360. Taylor, R.C., Cullen, S.P., and Martin, S.J. (2008). Apoptosis: controlled demolition at the cellular level. *Nat. Rev. Mol. Cell Biol.* 9:231-241.
361. Li, P., Nijhawan, D., Budihardjo, I., Srinivasula, S.M., Ahmad, M., Alnemri, E.S. and Wang, X. (1997). Cytochrome *c* and dATP-dependent formation of Apaf-1/caspase-9 complex initiates an apoptotic protease cascade. *Cell* 91:479-489.
362. Ludovico, P., Rodrigues, F., Almeida, A., Silva, M.T., Barrientos, A., and Côrte-Real, M. (2002). Cytochrome *c* release and mitochondria involvement in programmed cell death induced by acetic acid in *Saccharomyces cerevisiae*. *Mol. Biol. Cell* 13:2598-2606.
363. Severin, F.F., and Hyman, A.A. (2002). Pheromone induces programmed cell death in *S. cerevisiae*. *Curr. Biol.* 12:R233-R235.
364. Silva, R.D., Sotoca, R., Johansson, B., Ludovico, P., Sansonetty, F., Silva, M.T., Peinado, J.M., and Côrte-Real, M. (2005). Hyperosmotic stress induces metacaspase- and mitochondria-dependent apoptosis in *Saccharomyces cerevisiae*. *Mol. Microbiol.* 58:824-834.
365. Yang, H., Ren, Q., and Zhang, Z. (2008). Cleavage of Mcd1 by caspase-like protease Esp1 promotes apoptosis in budding yeast. *Mol. Biol. Cell* 19:2127-2134.

366. Roucou, X., Prescott, M., Devenish, R.J., and Nagley, P. (2000). A cytochrome c-GFP fusion is not released from mitochondria into the cytoplasm upon expression of Bax in yeast cells. *FEBS Lett.* 471:235-239.
367. Madeo, F., Herker, E., Maldener, C., Wissing, S., Lächelt, S., Herlan, M., Fehr, M., Lauber, K., Sigrist, S.J., Wesselborg, S., and Fröhlich, K.U. (2002). A caspase-related protease regulates apoptosis in yeast. *Mol. Cell* 9:911-917.
368. Fabrizio, P., Battistella, L., Vardavas, R., Gattazzo, C., Liou, L.L., Diaspro, A., Dossen, J.W., Gralla, E.B., and Longo, V.D. (2004). Superoxide is a mediator of an altruistic aging program in *Saccharomyces cerevisiae*. *J. Cell Biol.* 166:1055-1067.
369. Herker, E., Jungwirth, H., Lehmann, K.A., Maldener, C., Fröhlich, K.U., Wissing, S., Buttner, S., Fehr, M., Sigrist, S., and Madeo, F. (2004). Chronological aging leads to apoptosis in yeast. *J. Cell Biol.* 164:501-507.
370. Mazzoni, C., Herker, E., Palermo, V., Jungwirth, H., Eisenberg, T., Madeo, F., and Falcone, C. (2005). Yeast caspase 1 links messenger RNA stability to apoptosis in yeast. *EMBO Rep.* 6:1076-1081.
371. Allen, C., Büttner, S., Aragon, A.D., Thomas, J.A., Meirelles, O., Jaetao, J.E., Benn, D., Ruby, S.W., Veenhuis, M., Madeo, F., and Werner-Washburne, M. (2006). Isolation

of quiescent and nonquiescent cells from yeast stationary-phase cultures. *J. Cell Biol.* 174:89-100.

372. Li, W., Sun, L., Liang, Q., Wang, J., Mo, W., and Zhou, B. (2006). Yeast AMID homologue Ndi1p displays respiration-restricted apoptotic activity and is involved in chronological aging. *Mol. Biol. Cell* 17:1802-1811.

373. Aragon, A.D., Rodriguez, A.L., Meirelles, O., Roy, S., Davidson, G.S., Tapia, P.H., Allen, C., Joe, R., Benn, D., and Werner-Washburne, M. (2008). Characterization of differentiated quiescent and nonquiescent cells in yeast stationary-phase cultures. *Mol. Biol. Cell* 19:1271-1280.

374. Fabrizio, P., and Longo, V.D. (2008). Chronological aging-induced apoptosis in yeast. *Biochim. Biophys. Acta* 1783:1280-1285.

375. Laun, P., Heeren, G., Rinnerthaler, M., Rid, R., Kössler, S., Koller, L., and Breitenbach, M. (2008). Senescence and apoptosis in yeast mother cell-specific aging and in higher cells: A short review. *Biochim. Biophys. Acta* 1783:1328-1334.

376. Okamoto, K., Kondo-Okamoto, N., and Ohsumi, Y. (2009). Mitochondria-anchored receptor Atg32 mediates degradation of mitochondria via selective autophagy. *Dev. Cell* 17:87-97.

377. Kanki, T., Wang, K., Cao, Y., Baba, M., and Klionsky, D.J. (2009). Atg32 is a mitochondrial protein that confers selectivity during mitophagy. *Dev. Cell* 17:98-109.
378. Green, D.R., Galluzzi, L., and Kroemer, G. (2011). Mitochondria and the autophagy-inflammation-cell death axis in organismal aging. *Science* 333:1109-1112.
379. Yen, W.L., and Klionsky, D.J. (2008). How to live long and prosper: autophagy, mitochondria, and aging. *Physiology* 23:248-262.
380. Bhatia-Kiššová, I., and Camougrand, N. (2010). Mitophagy in yeast: actors and physiological roles. *FEMS Yeast Res.* 10:1023-1034.
381. Kanki, T., and Klionsky, D.J. (2010). The molecular mechanism of mitochondria autophagy in yeast. *Mol. Microbiol.* 75:795-800.
382. Eisenberg, T., Büttner, S., Kroemer, G., and Madeo, F. (2007). The mitochondrial pathway in yeast apoptosis. *Apoptosis* 12:1011-1023.
383. Pereira, C., Silva, R.D., Saraiva, L., Johansson, B., Sousa, M.J., and Côrte-Real, M. (2008). Mitochondria-dependent apoptosis in yeast. *Biochim. Biophys. Acta* 1783:1286-1302.

384. Carmona-Gutierrez, D., Eisenberg, T., Büttner, S., Meisinger, C., Kroemer, G., and Madeo, F. (2010). Apoptosis in yeast: triggers, pathways, subroutines. *Cell Death Differ.* 17:763-773.

385. Carmona-Gutierrez, D., Eisenberg, T., Büttner, S., Meisinger, C., Kroemer, G., and Madeo F. (2010). Apoptosis in yeast: triggers, pathways, subroutines. *Cell Death Differ.* 17:763-773.

386. Galluzzi, L., Vitale, I., Abrams, J.M., Alnemri, E.S., Baehrecke, E.H., Blagosklonny, M.V., Dawson, T.M., Dawson, V.L., El-Deiry, W.S., Fulda, S., Gottlieb, E., Green, D.R., Hengartner, M.O., Kepp, O., Knight, R.A., Kumar, S., Lipton, S.A., Lu, X., Madeo, F., Malorni, W., Mehlen, P., Nuñez, G., Peter, M.E., Piacentini, M., Rubinsztein, D.C., Shi, Y., Simon, H.U., Vandenabeele, P., White, E., Yuan, J., Zhivotovsky, B., Melino, G., and Kroemer, G. (2012). Molecular definitions of cell death subroutines: recommendations of the Nomenclature Committee on Cell Death 2012. *Cell Death Differ.* 19:107-120.

387. Kroemer, G., Galluzzi, L., Vandenabeele, P., Abrams, J., Alnemri, E.S., Baehrecke, E.H., Blagosklonny, M.V., El-Deiry, W.S., Golstein, P., Green, D.R., Hengartner, M., Knight, R.A., Kumar, S., Lipton, S.A., Malorni, W., Nuñez, G., Peter, M.E., Tschopp, J., Yuan, J., Piacentini, M., Zhivotovsky, B., and Melino, G. (2009). Classification of cell death: recommendations of the Nomenclature Committee on Cell Death 2009. *Cell Death Differ.* 16, 3-11.

388. Eisenberg, T., Knauer, H., Schauer, A., Büttner, S., Ruckenstuhl, C., Carmona-Gutierrez, D., Ring, J., Schroeder, S., Magnes, C., Antonacci, L., Fussi, H., Deszcz, L., Hartl, R., Schraml, E., Criollo, A., Megalou, E., Weiskopf, D., Laun, P., Heeren, G., Breitenbach, M., Grubeck-Loebenstein, B., Herker, E., Fahrenkrog, B., Fröhlich, K.U., Sinner, F., Tavernarakis, N., Minois, N., Kroemer, G., and Madeo, F. (2009). Induction of autophagy by spermidine promotes longevity. *Nat. Cell Biol.* 11:1305-1314.

389. Eisenberg, T., Carmona-Gutierrez, D., Büttner, S., Tavernarakis, N., and Madeo F. (2010). Necrosis in yeast. *Apoptosis* 15:257-268.

390. McCall, K. (2010). Genetic control of necrosis - another type of programmed cell death. *Curr. Opin. Cell Biol.* 22:882-888.

11 List of my publications and manuscripts in preparation

Published papers

1. Guo, T., Gregg, C., Boukh-Viner, T., **Kyryakov, P.**, Goldberg, A., Bourque, S., Banu, F., Haile, S., Milijevic, S., Hung Yeung San, K., Solomon, J., Wong, V. and Titorenko, V.I. A signal from inside the peroxisome initiates its division by promoting the remodeling of the peroxisomal membrane. *J. Cell Biol.* (2007) 177:289-303.

This article was an Editors' Choice article in *Science* (2007) 316:801.

2. Goldberg, A.A.* , Bourque, S.D.* , **Kyryakov, P.***, Boukh-Viner, T., Gregg, C., Beach, A., Burstein, M.T., Machkalyan, G., Richard, V., Rampersad, S. and Titorenko, V.I. A novel function of lipid droplets in regulating longevity. *Biochem. Soc. Trans.* (2009) 37:1050-1055.

** Equally contributed first co-authors*

3. Goldberg, A.A.* , Bourque, S.D.* , **Kyryakov, P.***, Gregg, C., Boukh-Viner, T., Beach, A., Burstein, M.T., Machkalyan, G., Richard, V., Rampersad, S., Cyr, D., Milijevic, S. and Titorenko, V.I. Effect of calorie restriction on the metabolic history of chronologically aging yeast. *Exp. Gerontol.* (2009) **44**:555-571.

** Equally contributed first co-authors*

4. Goldberg, A.A.* , Richard, V.R.* , **Kyryakov, P.***, Bourque, S.D., Beach, A., Burstein, M.T., Glebov, A., Koupaki, O., Boukh-Viner, T., Gregg, C., Juneau, M., English, A.M., Thomas, D.Y. and Titorenko, V.I. Chemical genetic screen identifies lithocholic acid as an anti-aging compound that extends yeast chronological life span in a TOR-independent manner, by modulating housekeeping longevity assurance processes. *Aging* (2010) 2:393-414.

** Equally contributed first co-authors*

This article was highlighted in the news media, including Radio-Canada (<http://www.radio-canada.ca/nouvelles/science/2010/09/16/002-longevite-bile.shtml>); **TFI News France** (<http://lci.tf1.fr/science/sante/2010-09/la-bile-un-espoir-contre-le-veillissement-6071272.html>); **The McGill Daily** (http://hotink.theorem.ca/system/mcgilldaily/issues/000/004/689/vol100iss7_screen_quality.pdf?1285709690); **Science Daily** (<http://www.sciencedaily.com/releases/2010/09/100915100935.htm>); **EurekAlert!** (http://www.eurekalert.org/pub_releases/2010-09/cu-foy091510.php); **Now Concordia** (<http://now.concordia.ca/what-we-do/research/20100921/fountain-of-youth-in-bile-longevity-molecule-identified.php>); **Media Relations Concordia** (http://mediarelations.concordia.ca/pressreleases/archives/2010/09/fountain_of_youth_in_bile_long.php?&print=1); **Bio Ethics Hawaii** (<http://www.bioethicshawaii.org/s-science/the-key-to-human-longevity-in-yeast-could-be/>); **Fight Aging!** (<http://www.fightaging.org/archives/2010/09/bile-acids-and-yeast-longevity.php>); **Xenophilia** (<https://xenophilus.wordpress.com/2010/09/16/fountain-of-youth-in-bile-longevity-molecule-identified/>); **Thaindian** (http://www.thaindian.com/newsportal/health/bile-may-harbour-human-fountain-of-youth_100429315.html); **DNA India** (http://www.dnaindia.com/scitech/report_bile-may-harbour-human-fountain-of-youth_1438869); **India Vision** (<http://www.indiavision.com/news/article/scitech/103189/>); **REVLET** (<http://www.revleft.com/vb/fountain-youth-bilei-t141779/index.html?s=1294a5663f51df1055ad3ff2b53db082&p=1865643>); **Stop Aging Solutions** (<http://stopagingsolutions.com/?p=704>); **Longevity Medicine** (<http://www.longevitymedicine.tv/longevity-as-housekeeping-and-a-role-for-bile-acids/>); **News Guide US** (<http://newsguide.us/education/science/Fountain-of-youth-in-bile-Longevity-molecule-identified/?date=2010-03-26>); **Dallas News** (<http://topics.dallasnews.com/quote/06AP1cA3HLa9j?q=Diabetes>); **e! Science News** (<http://esciencenews.com/articles/2010/09/15/fountain.youth.bile.longevity.molecule.identified>); **TENDENCIAS CIENTIFICAS** (http://www.tendencias21.net/La-clave-de-la-longevidad-humana-podria-estar-en-la-levadura-a4848.html?utm_source=feedburner&utm_medium=feed); **Canadian Health Reference Guide** (http://www.chrgonline.com/news_detail.asp?ID=140067); **Techno-Science** (http://www.chrgonline.com/news_detail.asp?ID=140067); **METRO** (<http://www.journalmetro.com/plus/article/672613--la-bile-fontaine-de-jouvence>) **and others.**

5. Goldberg, A.A.*, **Kyryakov, P.***, Bourque, S.D.* and Titorenko, V.I. Xenohormetic, hormetic and cytostatic selective forces driving longevity at the ecosystemic level. *Aging* (2010) 2:361-370.

* *Equally contributed first co-authors*

6. Burstein, M.T., Beach, A., Richard, V.R., Koupaki, O., Gomez-Perez, A., Goldberg, A.A., **Kyryakov, P.**, Bourque, S.D., Glebov, A. and Titorenko, V.I. Interspecies chemical signals released into the environment may create

xenohormetic, hormetic and cytostatic selective forces that drive the ecosystemic evolution of longevity regulation mechanisms. *Dose-Response* (2012) 10:75-82.

7. **Kyryakov, P.**, Beach, A., Richard, V.R., Burstein, M.T., Leonov, A., Levy, S. and Titorenko, V.I. Caloric restriction extends yeast chronological lifespan by altering a pattern of age-related changes in trehalose concentration. *Front. Physiol.* (2012), in press.

Manuscripts in preparation

1. **Kyryakov, P.**, Beach, A., Burstein, M.T., Richard, V.R. and Titorenko, V.I. The maintenance of a proper balance between the biosynthesis and degradation of glycogen in chronologically aging yeast is mandatory for lifespan extension by caloric restriction. In preparation for submission to *Aging Cell*.
2. **Kyryakov, P.**, Beach, A., Burstein, M.T., Richard, V.R. and Titorenko, V.I. Lipid droplets function as a hub in a regulatory network that defines the chronological lifespan of yeast by modulating lipid metabolism in the endoplasmic reticulum and peroxisomes. In preparation for submission to *Cell Metabolism*.
3. **Kyryakov, P.**, Beach, A., Burstein, M.T., Richard, V.R., Gomez-Perez, A. and Titorenko, V.I. Lithocholic acid, a natural anti-aging compound, extends longevity of chronologically aging yeast only if added at certain critical periods of their lifespan. In preparation for submission to *Cell Cycle*.
4. **Kyryakov, P.**, Gomez-Perez, A., Koupaki, O., Beach, A., Burstein, M.T., Richard, V.R., Leonov, A. and Titorenko, V.I. Mitophagy is a longevity assurance process that in chronologically aging yeast sustains functional mitochondria and maintains lipid homeostasis. In preparation for submission to *Autophagy*.

5. **Kyryakov, P.**, Sheibani, S., Mattie, S., Gomez-Perez, A., Beach, A., Burstein, M.T., Richard, V.R., Leonov, A., Vali, H. and Titorenko, V.I. Mitophagy protects yeast from a necrosis-like “lipoptotic” mode of cell death triggered by exposure to palmitoleic fatty acid. In preparation for submission to *Cell Death and Differentiation*.